INFORMATION TO USERS

This manuscript has been reproduced from the microfilm master. UMI films the text directly from the original or copy submitted. Thus, some thesis and dissertation copies are in typewriter face, while others may be from any type of computer printer.

The quality of this reproduction is dependent upon the quality of the copy submitted. Broken or indistinct print, colored or poor quality illustrations and photographs, print bleedthrough, substandard margins, and improper alignment can adversely affect reproduction.

In the unlikely event that the author did not send UMI a complete manuscript and there are missing pages, these will be noted. Also, if unauthorized copyright material had to be removed, a note will indicate the deletion.

Oversize materials (e.g., maps, drawings, charts) are reproduced by sectioning the original, beginning at the upper left-hand corner and continuing from left to right in equal sections with small overlaps. Each original is also photographed in one exposure and is included in reduced form at the back of the book.

Photographs included in the original manuscript have been reproduced xerographically in this copy. Higher quality 6" x 9" black and white photographic prints are available for any photographs or illustrations appearing in this copy for an additional charge. Contact UMI directly to order.

UMI

A Bell & Howell Information Company
300 North Zeeb Road, Ann Arbor MI 48106-1346 USA
313/761-4700 800/521-0600

A

Adaptive Signal Processing with Weyl-Heisenberg Expansions

By

E. Anthony Joseph

A dissertation submitted to the Graduate Faculty in Engineering in partial fulfillment of the requirements for the degree of Doctor of Philosophy.
The City University of New York

1999

This manuscript has been read and accepted for the Graduate Faculty in Engineering in satisfaction of the dissertation requirement for the degree of Doctor of Philosophy.

December 23, 1998
Date

Richard Tolimieri
Chair of Examining Committee

January 4, 1999
Date

Mumtaz K. Kassir
Executive Officer

Dean Joseph Barber

Professor Michael Conner

Professor Barry Gross

Dr. Myoung An
Supervisory Committee

THE CITY UNIVERSITY OF NEW YORK

Abstract
Adaptive Signal Processing with Weyl-Heisenberg Expansions
by
E. Anthony Joseph

Adviser: Professor Richard Tolimieri

A sufficiently large class of signals exists whose information content is inadequately described in either the time or the frequency domain. These signals, which include speech and music, are nonstationary in nature. Nonstationary signals are best described in a time-frequency representation. However, a time-frequency signal representation must adhere to the lower bound established by the Heisenberg uncertainty principle. In particular, the powerful and robust Zak transform, which preserves many properties of Fourier analysis, has a peculiar property in the zero theorem imposed by the uncertainty principle. The Zak transform resides at the crossroad of Fourier analysis and Fourier synthesis; it is coarsely sampled at the Nyquist rate; and it is inherent in the structure of the Cooley-Tukey algorithm. The Zak transform is included in theory and application of Cohen's class of bilinear distributions, ambiguity functions, wavelet transforms, and Weyl-Heisenberg expansions. Moreover, it is recognized as the most suitable tool for the study of Weyl-Heisenberg expansions. Both Zak transform and Weyl-Heisenberg expansions are adaptive forms of Fourier representations. A Weyl-Heisenberg expansion is a nonorthogonal series expansion whose basis signals usually constitute a redundant and nonorthogonal set.

The main results of this research are the development of an orthogonal projection algorithm for

Weyl-Heisenberg expansions in Zak space and an extension of Zak transform theory to cover non-critical sampling situations. This orthogonal projection algorithm projects Weyl-Heisenberg expansions from a critically sampled subspace onto an undersampled subspace. The projection signal on the undersampled subspace is synthesized with a subset of the original signal's coefficient set; the orthogonality of the projection caused an intrinsic change in the subset values. The orthogonal projection algorithm has potential application in data compression; it is adaptable to a multiresolutional decomposition.

The restriction of the Nyquist rate is removed from the definition of the Zak transform. The result is a generalization which is more consistent with Fourier analysis in terms of undersampling, critical sampling, and oversampling. At the critical sampling rate, its operation is identical to the standard Zak transform. This generalized Zak transform is suitable for Weyl-Heisenberg expansions over any Weyl-Heisenberg system.

Contents

List of Figures

Adaptive Signal Processing with Weyl-Heisenberg Expansions

Chapter 1

Introduction

What is time-frequency signal[1] representation? There are some signals that are better described as a function of time, while others are more appropriately described as a function of frequency. However, a sufficiently large class of signals exists whose information content is inadequately described in either the time or the frequency domain. Two well-known examples of this class of signals are human speech and music. Signals such as speech and music are nonstationary in nature. This means that the information content of these signals fluctuates simultaneously in both time and frequency. To adequately describe a nonstationary signal, a time-frequency representation is needed to show the time localization of the signal's spectral content in the relevant time-frequency space. In this formulation of a signal, a 'breakdown of causality' exists.

Oftentimes, a signal analyst may need to study the detailed characteristics of a signal. To thoroughly investigate the signal, the analyst may have to study it in at least one other domain. Traditionally, the choice alternate domain of signal representation is the frequency domain. In the frequency representation of a signal, the analyst can often analyze its physical subtleties in

---

[1] A function that usually conveys information about the properties of a physical, social, or psychological system

a descriptively simpler form and in a mathematically more convenient way [1, 2]. Whenever time analysis of a signal is forsaken for its spectral analysis, the central aim is to decompose the signal into a continuous or discrete set of frequency components so that the relative strength of the individual components can be made evident. The set of frequencies, which are constituents of the signal, may be of finite or infinite duration, depending on the nature of the signal. If it becomes necessary to retrieve the signal from its frequency representation, then the signal can be reconstructed from a weighted continuous or discrete sum of elementary signals, namely complex exponentials, that are representative of the signal's frequency components. The analysis and synthesis of a signal are usually done through the instrument of Fourier transformation and representation. The Fourier representation of a signal constitutes a dual operational process, consisting of an analysis and a synthesis operation. These two operations establish a one-to-one relationship between the time and the frequency description of a signal, and are therefore two different ways of viewing a signal. Of the many advantages of Fourier analysis, one of the most significant lies in the elegance and simplicity of the mathematics it affords the signal analyst who has encountered mathematically troublesome signal operations in the time analysis. A typical example is the time domain convolution of a signal contrasted with its equivalent spectral domain multiplication.

The elementary signals, which form the basic building blocks of a signal in Fourier representation, are time-frequency signals. That is, in the analysis and/or the synthesis statement of a signal in Fourier representation, the elementary signals, in terms of complex exponentials and without regard for sign, can be written as $\chi(\nu, t) = \exp(2\pi i \nu t)$.

Nonetheless, in the usual approach to Fourier analysis, this time-frequency composition of a signal is not fully utilized in the general sense. In fact, the Fourier representational definition of a signal restricts either the time or the frequency variable to a parameter depending upon the form of the representation, thereby making the Fourier representation of a signal a description in either time or frequency. For example, whenever the Fourier representation of a signal is the Fourier transform, the elementary signals assume the notational form $X_\nu(t) = X(\nu, t)$ where for each value of the parameter ν, the weighted sum of the product of the signal and the elementary signals is computed over all available time. The resulting Fourier transform usually provides unintelligible time localization information about the relative strength of any frequency component, ν, contained in the signal. In spite of the frequency variable being a parameter in the Fourier transformation of a signal, for a limited class of complex-valued signals slowly changing in time and in frequency, the time-frequency property inherent in the Fourier description of a signal can be exploited from the phase, which carries the time-frequency localization information of the signal. To obtain the time localization information of the frequencies in a signal, each frequency component is extracted from the derivative of its instantaneous phase. Homologously, to obtain the frequency localization information of the time instants in a signal each time instant is extracted from the derivative of the instantaneous phase of the Fourier transform. The frequency components and the time instants obtained in the preceding manner are known respectively as the instantaneous frequency and the group delay. The instantaneous frequency and the group delay are incapable of resolving multiple frequencies at any time instant and multiple time instants at any frequency component respectively. Therefore, because the usual Fourier analysis only permits the description of a signal in one

domain at a time, the exploitation of the time-frequency feature of a signal is severely hampered.

Although in the classical sense, the theory of Fourier Analysis has very limited use in the arena of nonstationary signals, it is mature and rich in applications in the sphere of stationary signals and linear time-invariant systems. In fact, its role is pivotal in the areas which include signal representation, spectrum estimation, system identification, noise removal, filtering techniques, signal detection and classification, and digital signal processing algorithms (e.g., Cooley-Tukey fast Fourier transform (FFT)).

As mentioned earlier, in classical Fourier analysis, the Fourier representations of a signal do not make good simultaneous use of the time and frequency aspects of the complex exponentials which are its basis functions. Furthermore, Fourier analysis is powerful and robust because not only is it supported by a mature and well-understood theory but also it is an insightful and invaluable analytical tool supported by a healthy reserve of powerful FFT algorithms. Thus, it is intuitive to realize that it may be possible to modify the classical Fourier analysis methods to accommodate nonstationary signals in a time-frequency atmosphere, while hoping to retain its chief advantages. Conceptually, a direct way in which this can be done would require a redefinition of the Fourier analysis methods so as to employ local concepts of the range of observation of a signal, in terms of time and frequency, rather than global ones which result in a global picture of a signal in either the time or the frequency domain. That is, the definitions for Fourier methods need to exploit the local time-frequency properties of the basis functions in the signal representation. This is equivalent to defining the Fourier methods to exhibit the local

behavior of a signal with respect to changes experienced in time and in frequency. This means that if the signal under study has a duration that is longer than will necessitate a description showing its local time and frequency dependency, a partitioning of the signal duration is needed and the relevant classical Fourier techniques can be applied to each partition of the signal in a sequential manner until the total signal is analyzed or synthesized. This alternative definition of Fourier analysis methods is an inductive one, wherein Fourier analysis of a signal is accomplished in terms of partial Fourier analysis of the signal. The concept of partial Fourier analysis is the central idea giving impetus to the short-time Fourier transform, Gabor transform, and Zak transform. In the same sense that in the classical Fourier analysis, the Fourier transform and the Fourier series are related, in the general Fourier analysis, the short-time Fourier transform and the Gabor transform, which is a series representation of a signal, are related. The short-time Fourier transform, Gabor transform, and Zak transform are linear time-frequency techniques. That is, each of these transforms takes a time or frequency signal and converts it into a signal dependent on both time and frequency. There are several types of time-frequency representations. They can be broadly classified as linear and nonlinear. The linear approach to time-frequency representation of a signal mainly involves the manipulation of the signal content in the time-frequency space, whereas the nonlinear approach involves the manipulation of the signal energy density distribution in the time-frequency space. Some examples of premier nonlinear time-frequency representations are Wigner distribution, ambiguity function, Rihaczek distribution, and Page distribution, with Wigner distribution and the ambiguity function being the most common. These examples of time-frequency techniques are bilinear. Of all the time-frequency transformations, the Gabor transform and the short-time Fourier transform are the

most commonly used. In general, time-frequency analysis is a variation of the classical Fourier analysis. In fact, practically all time-frequency methods are a form of Fourier analysis methods at least in the context of group theory. In this sense, even affine wavelets are an example of Fourier analysis on the group [3]. The fact that time-frequency analysis is subsumed in the generalization of Fourier analysis should come as no surprise because it is widely known that the classical Fourier analysis has a straightforward generalization in group theory.

As previously mentioned, there are several time-frequency transformation techniques available. Each one has desirable properties as well as some inherent limitations. Besides, the Heisenberg uncertainty principle limits the time-frequency resolution of any signal in the sense that the resolvable content of a signal or its energy in time-frequency space cannot be arbitrarily highly concentrated but must adhere to the lower bound established by the product of the time concentration and the frequency concentration for the signal. Therefore, it may be unreasonable to expect to find a panacea among time-frequency analysis methods that is most suitable in all situations of signal investigation. However, if the Fourier transform[2] of classical Fourier analysis is used as a yardstick for selecting a powerful and robust time-frequency tool with many of its significant properties, then Zak transform [4] is perhaps the most likely candidate because it retains many of the significant features of the Fourier transform. The Zak transform stands at center stage in the theory and application of Wigner distribution, Rihaczek distribution, ambiguity function, and Gabor expansions. In addition, the Zak transform is quite useful in

---

[2] In this context of the word, all variations of Fourier representation are included.

displaying a signal's time-frequency characteristics. Moreover, like the Fourier transform, the true power of the Zak transform lies in its analytical capability wherein it has the ability to make certain troublesome linear equations more tractable.

The application of the Zak transform to the Gabor transform constitutes a powerful alliance with the embedment of the ambiguity function in it being a desirable outcome. Apart from human speech and music, the class of nonstationary signals covers a wide range. Some of these signals are associated with the following application fields: medical imaging, image processing, seismology, communications, biological and machine vision, sonar and radar, and artificial intelligence. These types of signals can be investigated using Gabor expansion[3] in the framework of Zak space. Gabor representations depend on the choice of an analyzing signal and the choice of a two-dimensional lattice which act on the time-frequency translates to construct a Gabor-wavelet system. Gabor methods have been used in computer vision, edge detection, feature analysis, and image reconstruction. In fact, in the framework of Zak space fast and numerically stable algorithms, constraint by the uncertainty principle, have been designed for the determination of Gabor coefficients of a signal representation. In spite of the uncertainty constraint manifesting as the zero theorem in Zak space, more stable and computably faster efficient algorithms can be developed to ascertain the Gabor coefficients in Zak space. One way to accomplish this task is to skilfully exploit the imposition of the uncertainty constraint. Furthermore, the theater of Zak space may prove to be significant in the design of joint time-

---

[3] The expansion of a signal as a linear combination of functions from the Gabor-wavelet system

frequency signals having desirable properties. In addition, there exists a strong urgency to develop a deeper understanding of the Zak transform in terms of both its numerics of signal representation and its generalization. In general, the desire to develop an alternative to the classical Fourier theory of signals and to develop this alternate theory so that time-frequency (or time-scale) representation of nonstationary signals is at center stage, may well lead to Zak transform theory being the structure of support.

The main focus of this research is to develop a better understanding of the discrete Zak transform theory with its application to Gabor (Weyl-Heisenberg) expansions as well as to generalize this theory so that it includes the capacity to vary the coarse and fine sample values to accommodate different sampling conditions, and to demonstrate that under appropriate sampling conditions the discrete Zak transform is a more realistic replica of its continuous counterpart. Chapter two will introduce the relevant mathematical notation as well as some concepts in the form of definitions, assertions, theorems, and corollaries that will be used throughout this treatise. The subsequent chapter will present an overview of several prominent time-frequency representational techniques. First, the nonlinear time-frequency techniques will be discussed followed by the linear time-frequency techniques with special emphasis on the Zak transform. Moreover, the intra-relationship as well as the interrelationship among nonlinear and linear time-frequency representations will be developed in a consistent manner. It will be shown that some of these representations only differ in interpretation and that seemingly disparate representations are linked by means of the ambiguity function, which acts as a bridge. For example, any bilinear distribution can be expressed in the framework of Zak transform through

the instrumentality of the conventional ambiguity function. The chapter will conclude with the Zak transform and its roles in the use of and its relationship to Fourier techniques and other time-frequency methods. Chapter four presents a general overview of discrete Weyl-Heisenberg expansions and the discrete Zak transform with Weyl-Heisenberg expansions, while chapter five builds on this foundation. Chapter five presents the results of the research undertaken. It is highlighted with the development of an orthogonal projection algorithm with its application to Weyl-Heisenberg expansions in Zak space, and a broadened concept of the Zak transform to allow it to accommodate other than the critical sampling rate. Chapter six will summarize the main aspects of this discourse and suggest some potential areas for furture research.

Chapter 2

Mathematical Concepts

This chapter establishes the mathematical foundation for this treatise. It will introduce some notations and diverse mathematical concepts in mathematical formalism without much regard for engineering clarity. These concepts, which include basic definitions and assertions as well as theorems and corollaries without proofs, will be presented in a clear, coherent, narrative form. The ideas presented here will again be encountered mainly in an engineering context, either directly or indirectly, throughout the body of this work. Notably, it must be borne in mind that, in general, the mathematical models used in electrical engineering cannot be adequately exploited [5]. Thus, the realization of a relevant mathematical model in an engineering context is highly constraint in terms of the engineers' understanding and interpretation of the model together with the technological tools available to exploit it.

2.1 Set Theory

A set is any well defined collection of objects called elements. An element x that is a member of a set X is denoted by $x \in X$ whereas an element x that is not a member of this set is denoted by $x \notin X$. A set X with no elements is called an empty set which is denoted by the symbol $\varnothing$ and it is written as $X = \varnothing$. If X and Y are sets, Y is a subset of X if and only if every element of Y is an element of X. This relationship between X and Y is written as $Y \subseteq X$;

however, if Y is a subset of X and Y is not equal to X, the immediately preceded relationship becomes $Y \subset X$. If in a given situation X encompasses all the objects under consideration, X is the universal set. Further, If A is a subset of a set X, the complement of A (written as A^{-}) with respect to X is the set of elements of X that are not members of A. This statement in symbolic form is

$$A^{-} = \{x \in X: x \notin A\}.$$

In addition, if a set A contains either no element or a limited number of distinct elements, it is finite and the number of elements in it is its order; the order of A is zero when it is empty. The cardinal number of A is equal to its order. In the cases where A is not finite, it is infinite. If A has a one-to-one correspondence with the natural numbers, it is countable and may be countably finite or countably infinite; otherwise, it is uncountable. Moreover, if a set X is decomposed into subsets such that every element of X is in one and only one of the subsets, X is said to be partitioned into subsets with each subset being a cell. Suppose A and B are subsets of X, the union of A and B, denoted by $A \cup B$, is the set of all elements that are contained in A or B; that is,

$$A \cup B = \{x \in X: x \in A \text{ or } x \in B\}.$$

Conversely, the intersection of A and B, denoted by $A \cap B$, is the set of all elements that are contained in both A and B. Symbolically,

$$A \cap B = \{x \in X: x \in A \text{ and } x \in B\}.$$

If it turns out that the intersection of A and B is empty, A and B are disjoint.

The direct product $X \times Y$ of two sets X and Y is the set of all ordered pairs (x, y) where $x \in X$ and $y \in Y$. In symbolic form

$$X \times Y = \{(x, y): x \in X \text{ and } y \in Y\}.$$

Now, suppose I and X are two sets such that for each $i \in I$ there is a unique element $x_i \in X$, the set $\{x_i: i \in I\}$ is the indexed set and I is the index set. If I is equal to the set of all integers, the indexed set is a sequence. Suppose further that the set X is acquired from subsets by forming an exact number of countable unions, intersections, and complements, then X is a Borel set in the classical sense.

2.2 Basic Symbols

The set of all real numbers and the set of all positive real numbers are denoted by $\mathbb{R}$ and $\mathbb{R}^+$ respectively while the set of all integers and the set of all positive integers are denoted by $\mathbb{Z}$ and $\mathbb{Z}^+$ respectively. The set of all complex numbers is denoted by $\mathbb{C}$. If for $x, y \in \mathbb{R}$, $z = x + iy$ is a complex number, its complex conjugate is $z^* = x - iy$ and its modulus is indicated by $|z| = |z^*|$. The phrase almost everywhere is abbreviated by a.e. and the phrases for all, if and

only if, and implies are designated by the respective symbols $\forall$, $\Leftrightarrow$, and $\Rightarrow$. The functions that will be encountered, are defined over $\mathbb{R}$, which is also referred to as the real number line. They may be real or complex-valued depending on the context. Integrals with undefined limits should be understood to be taken over $\mathbb{R}$ while series with undefined limits are taken over Z.

2.3 Special Concepts

Function: Assign X and Y to be sets. A function[4] f, which is a mapping of X into Y, is a rule that associates each element $x \in X$, a unique element $f(x) \in Y$. $f(x)$ is the image of x under f. The set X is the domain of definition of f and the set of all $f(x)$ of elements of X is the range of f. If the elements in X are negative, then the function f becomes a time-reversed function f_- defined on X such that $f_-(x) \in Y$, $f_-(x) = f(-x)$.

Mapping: Suppose X and Y are sets and f is a function from X into Y, designated by $f: X \rightarrow Y$, and Y is the range of f, if at least one element of X is mapped into each element of Y, f maps X onto Y and it is therefore surjective; however, if for every $x_1, x_2 \in X$, $f(x_1) = f(x_2)$ implies that $x_1 = x_2$, then each $x \in X$ maps into at most one unique $y \in Y$ such that $y = f(x)$, which means that f is injective or has a one-to-one mapping. Moreover, if f is both surjective and injective, it is bijective.

---

[4] A multivalued function is a relation.

Relation: Suppose X is a set. A binary relation R on X is a set of ordered pairs in X. Some of the properties of R include it being reflexive if

$$xRx \quad \forall x \in X,$$[5]

symmetric if

$$xRy \Rightarrow yRx \quad \forall x, y \in X,$$

and transitive if

$$(xRy \wedge yRz) \Rightarrow xRz \quad \forall x, y, z \in X$$[6]

Whenever R is a reflexive, symmetric, and transitive binary relation on the set X, it is an equivalence relation. If in addition to the equivalence relation R on X, there are $x \in X$ that correspond to an equivalent class Y, a subset of X, relative to R which is defined as

$$Y = \{y \mid xRy\}.$$

---

[5] An expression of the form xRy stands for x bears R to y whenever the ordered pair $(x, y) \in R$.

[6] The notation $\wedge$ stands for logical **and.**

Extension and Restriction: Suppose X and Y are sets and f is a mapping from a subset $A \subset X$ into Y, the mapping g of X into Y is an extension of f provided

$$g(x) = f(x) \quad \forall x \in A.$$

Conversely, suppose h is a mapping of the subset $A \subset X$ into Y, h induced by the mapping $f: X \rightarrow Y$ is the restriction of f to the set A and

$$h(x) = f(x) \quad \forall x \in A.$$

Topology: A collection τ of subsets of any set X is a topology on X provided τ is closed under the creation of finite intersections and arbitrary unions of its members and it contains X as well as $\varnothing$ as members.

2.4 Arithmetical Concepts

Euclid's Division Lemma: suppose k is any integer and m is any positive integer. There exist integers q and r such that

$$k = qm + r \quad \text{and } 0 \leq r < m.$$

Fundamental Theorem of Arithmetic: Suppose there exist primes $p_1 \leq p_2 \leq \cdots \leq p_n$ for a positive integer $p > 1$ such that

$$p = p_1 p_2 \cdots p_n,$$

n is a unique factorization of p in terms of primes.

Greatest Common Divisor (gcd): If a and b are integers that are both nonzero, there exists a unique c that is the gcd of a and b expressible as $c = \gcd(a, b)$ provided $c > 0$, c divides both a and b, and each integer n that divides both a and b also divides c. Moreover, there exist integers k and m such that $c = ak + bm$. In terms of the least common multiple (lcm) of a and b, $\gcd(a, b) = ab(lcm(a, b))$.

Linear Congruence: suppose k, m, and n are integers and $a = \gcd(k, n)$, the congruence

$$ks \equiv m \pmod{n}$$

for an integer s has no solution if a does not divide m, and it has a mutually incongruent solutions if a divides m. The abbreviation mod stands for modulo.

Primitive Root: An integer a is a primitive root modulo n if a belongs to the exponent $p(n)$ modulo n, where $p(n)$ denotes the number of positive integers equal to or less than n that are relatively prime to n. In particular, $a^{p(n)} \equiv 1 \pmod{n}$ whenever $\gcd(a, n) = 1$.

Chinese Remainder Theorem: Suppose a set of integers $S = \{n_1, n_2, \ldots, n_s\}$ are pairwise relatively prime and $N = n_1 n_2 \ldots n_s$. If another set of integers $A = \{a_1, a_2, \ldots, a_s\}$ exists satisfying the condition $\gcd(a_i, n_i) = 1$ for each i, then the system of linear congruences

$$\begin{aligned} a_1 x &\equiv b_1 \pmod{n_1} \\ a_2 x &\equiv b_2 \pmod{n_2} \\ &\ldots \\ a_s x &\equiv b_s \pmod{n_s} \end{aligned}$$

has a unique solution modulo N.

2.5 Algebraic Structures

The structures reviewed in this section are groups, fields, linear spaces, operators, and topological space.

2.5.1 Groups

A group $(G, *)$ is a set G together with an associative binary operation $*$ on G and an unique

identity element e for $*$ satisfying the conditions:

1. $\forall a \in G,\ a * e = e * a = a.$

2. For every $a \in G,$ there exists a unique inverse $b \in G$ such that

$a * b = b * a = e.$

3. $\forall a, b \in G,\ (a * b) \in G.$

Depending on the group theoretic context, the binary operation $*$ may adopt the arithmetic operations addition, $+$, or multiplication, $\bullet$, but not in the usual arithmetical sense. The addition symbol is used whenever it is certain that the binary operation on the group is commutative; otherwise, the multiplication symbol is used. Under addition, the group identity element $e = 0$ and the inverse element $b = -a$; while under multiplication, the group identity element $e = 1$ and the inverse element $b = a^{-1}$.

A subgroup is a group that is a subset of another group under whose binary operation it is closed. For example, if A is a group, but it is a subset of another group G, and $\forall a_1, a_2 \in A,$ $a_1 * a_2 \in A$ although it is computed in G, and A is a subgroup of G. A group (or subgroup) may be of infinite or finite order. A group of infinite order contains an infinite number of elements. A group of finite order contains a finite number of elements. The order of a finite group is equal to the number of elements in it. In particular, a subgroup of a finite group has an order that divides the order of the group. It turns out that if the order of the group is a prime number, the group is cyclic. That is, G is a cyclic group if it contains at least one element a satisfying the condition

$G = \{a^n \mid n \in Z\}$. Besides, if G is a finite group with generator element $a \in G$, there exists a smallest positive integer n, the order of a, which satisfies the condition $a^n = 1$. This implies that G consists of only n distinct elements: $1, a, \ldots, a^{n-1}$.

A homomorphism is a mapping ψ of a group G into a group H that satisfies the condition

$$\psi(a_1 a_2) = \psi(a_1)\psi(a_2) \quad \forall a_1, a_2 \in G.$$

In particular, if the mapping ψ of G into H is a bijective homomorphism, ψ is an isomorphism, which means that the groups G and H are structurally the same. Specifically, if G is a cyclic group of prime order n, G is isomorphic to Z modulo n. More generally, if two cyclic groups have the same finite order, they are isomorphic but if a cyclic group has infinite order, it is isomorphic to the group Z under addition. Besides, for the homomorphism ψ from G into H, if the subgroup $\psi(G)$ of H has identity element u, $u \in H$, the subgroup K_ψ of G is the kernel of ψ defined by

$$K_\psi = \{a \in G \mid \psi(a) = u\}.$$

Sometimes, it becomes necessary to partition a group into cells. Suppose an arbitrary group G has a subgroup K, the subsets $aK = \{ab \mid b \in K\}$ of G and $Ka = \{ba \mid b \in K\}$ of G are the respective left and right cosets of K containing a. These cosets of K are the cells of the

partition of G and each coset contains the same number of elements as K. Furthermore, if $K = K_{\psi}$ and the mapping $\psi: G \rightarrowtail H$ with $a \in G$ is a group homomorphism, the set

$$\psi^{-1}\{\psi(a)\} \equiv \{x \in G \mid \psi(x) = \psi(a)\}$$

is the left coset aK of K as well as the right coset Ka. Thus $aK = Ka \ \forall a \in G$. This is the condition for K to be a normal subgroup of G. Moreover, if K is the kernel of the group homomorphism $\psi: G \rightarrowtail H$, the cosets of K form a quotient group of G modulo K, written as G/K. The binary operation on G/K defines the product $(aK)(bK)$ of two cosets such that $(aK)(bK) = (ab)K$ for $a \in aK$ and $b \in bK$. In addition, the map ρ is an isomorphism from the quotient group G/K into the group $\psi(G)$ defined by $\rho(aK) = \psi(a)$.

A group is decomposable into a subnormal or normal series. This series consists of a finite sequence of subgroups of the group. Specifically, a subnormal series of group G is a finite sequence $K_0, K_1, \ldots, K_n$ of subgroups of G such that K_i is a proper and normal subgroup of K_{i-1} with $K_0 = \{e\}$ and $K_n = G$, whereas a normal series of G is a finite sequence $K_0, K_1, \ldots, K_n$ of normal subgroups of G such that K_i is a proper subgroup K_{i-1}, $K_0 = \{e\}$, and $K_n = G$. The subnormal (or normal) can be further decomposed through the process of refinement. That is, a subnormal (or normal) series $\{A_i\}$ is a refinement of subnormal (or normal) series $\{K_j\}$ of a group G if $\{K_j\}$ is contained in $\{A_i\}$.

A set X is a G-set, if the action of a group G on X is the binary operation $\bullet$ with the mapping: $G \times X \mapsto X$ provided that $1x = x$, $\forall x \in X$ and $(g_1 g_2)(x) = g_1(g_2 x)$, $\forall x \in X$ and $\forall g_1, g_2 \in G$. If X is a G-set, then each cell in the partition of the equivalence relation described by $x_1 \sim x_2$, $\forall x_1, x_2 \in X$ for the existence of $g \in G$ such that $gx_1 = x_2$ is an orbit in X under G with the property that the cell containing x is the G-orbit of x or simply orbit of x so long as x is in X. Besides, if X is a G-set, the condition $gx = x$ for each x in X and each g in G in the subsets $G_x = \{x \in G \mid gx = x\}$ and $X_g = \{x \in X \mid gx = x\}$ is such that the subset G_x is not only a subgroup of G but it is also an isotropic subgroup of x and when G and X are finite, the number of orbits n in X under G is given by

$$n|G| = \sum_{g \in G} |X_g|.$$

A discrete group G may be defined as a group of isometries with the property that for any point x and any bounded set S, S contains a finite number of points in the G-orbit of x. A discrete group is countable. A discrete group with every element being a translation is a lattice group having each G-orbit as a lattice. Additionally, a lattice group or one of its lattices is k-dimensional if the maximum number of independent points in any orbit is $k+1$. Specifically, a group of translations generated by k-translations, such that any point and its k-images under these translations are independent, is a k-dimensional lattice group. That is, if $t_1, t_2, \ldots, t_k$ are k independent translations and $G = \{a_1 t_1 + \cdots + a_k t_k \mid a_i \in Z\}$, then G is a lattice group and $t_1, t_2, \ldots, t_k$ constitute one of its integral basis. Nonetheless, the set of linearly independent translations $t_1, t_2, \ldots, t_k$ that form an integral basis is not unique. Moreover, the ordered

integral bases for a k-dimensional lattice group G are in a one-to-one correspondence with the extended group of k by k integral unimodular matrices. In other words, these nonunique matrices containing integer elements and having determinant is ± 1.

There are numerous examples of groups. Some have already been mentioned. Other examples include the set of integers under addition, the set of positive rationals under multiplication, the set of real numbers under addition, and the n th roots of unity of nonzero complex numbers under multiplication. Groups of special interest in this treatise are abelian, affine, and Heisenberg. In general, groups are either abelian or nonabelian.

Abelian Groups: A group is Abelian if it is commutative under its binary operation $*$. Like cyclic groups, abelian groups can be generated from elements in the group. In fact, cyclic groups are fundamental entities in all sufficiently small and all finite order abelian groups that are finitely generated [10]. Specifically, an abelian group G that is finitely generated is isomorphic to a direct product

$$Z_{p_1^{s_1}} \times Z_{p_2^{s_2}} \times \ldots \times Z_{p_n^{s_n}} \times Z \times Z \times \ldots \times Z$$

of cyclic groups, where the number of factors of Z is unique and the primes p_i have unique prime powers $p_i^{s_i}$. However, if $s_1 = 1$ for $1 \le i \le n$ and p_i are not primes but p_i divides p_{i-1} for $1 \le i \le n-1$, the finitely generated abelian group is isomorphic to a group of the form

of the above direct product. Moreover, an abelian group G is generable from a subgroup G_1 which constitutes a basis and which satisfies the two equivalent conditions

$$a = \sum_{i=0}^{n-1} k_i x_i \quad a \in G,\ k_i \in Z/\{0\},\ \text{and}\ x_i \in G_1$$

as well as G_1 is a generator G and

$$\sum_{i=0}^{n-1} k_i x_i = 0 \quad k_i \in Z,\ x_i \in G_1 \text{ whenever } k_i = 0,\ 0 \le i \le n-1,$$

is a free abelian group. In fact, there exists a basis that can be used to express each element of G in a unique linear manner in cases where "the coefficients are residues modulo the orders of the basis elements." G may have several bases of different orders. Whenever G is finite and its order is divisible by some integer constant, say s, G has subgroup of order s. Suppose H and K are two subgroups of G. All the elements in G that are orthogonal[7] to all the elements in H for a specific basis are contained in the subgroup K. Resultantly, H and K are mutually orthogonal. If it happens that H is orthogonal to itself, it is isotropic. Specifically,

$$\sum_{l \in H} \omega^{lm} = |H|, \quad (\omega = e^{2\pi i/N} \text{ and } 0 \le l, m \le N)$$

if $m \in K$, and is equal to zero otherwise. $|H|$ is the order of H.

---

[7] See subsection **2.5.3** for the definition of orthogonal.

Affine Group [11, 12]: An affine group is a two-dimensional matrix group G of the form

$$G = \begin{bmatrix} a & b \\ 0 & 1 \end{bmatrix}, \quad a \geq 1$$

with the multiplicative rule

$$(a, b)(x, y) = (ax, ay + b).$$

The expression (a, b) denotes the matrix G. In particular, on the space of square integrable functions, reducible operators $\Psi(a, b)$ define a unitary representation of G such that

$$(\Psi(a, b)f)(t) = a^{-1/2} f\left(\frac{t + b}{a}\right),$$

where f is square integrable and Ψ "decomposes into a direct sum of two irreducible" unitary representations over the positive real line and the negative real line respectively.

Heisenberg Group[11, 13, 14, 15, 16, 17, 18]: The Heisenberg group "is not in fact one object, but a collection of similar objects, rather like a functor, or a scheme in algebraic geometry, or even a combination of several overlapping functors." In exact terms, the Heisenberg group H is defined as a $(2n + 1)$-dimensional Lie group [19] whose underlying manifold is $\mathbb{R}^{2n} \times \mathbb{R}$ and whose group multiplication rule is

$$(\zeta, z)(\eta, w) = \left(\zeta + \eta, z + w + 0.5J_{2n}(\zeta, \eta)\right)$$

where $\zeta, \eta, \in \mathbb{R}^{2n}$, $z, w \in \mathbb{R}$, $n \in Z$, and J_{2n} is $(2n \times 2n)$-dimensional matrix

$$J_{2n} = \begin{bmatrix} 0 & D_n \\ -D_n & 0 \end{bmatrix}$$

with D_n being the $n \times n$ identity matrix. Generally, a typical element $a \in H$ is denoted by $a = (\zeta, z)$ with $\zeta \in \mathbb{R}^{2n}$ and $z \in \mathbb{R}$. The Heisenberg group is decomposable in lattices defined as discrete subgroups Γ of H such that the homogeneous spaces of right cosets $\Gamma \backslash H = \{\Gamma_a : a \in H\}$ are compact. These lattices can be characterized as the collection of all nonabelian subgroups of H on $2n$-generators. In specific and explicit terms, the 3-dimensional real H is a group of all matrices of the form

$$(a, b, c) = \begin{bmatrix} 1 & b & c \\ 0 & 1 & a \\ 0 & 0 & 1 \end{bmatrix}, \quad a, b, c \in \mathbb{R}$$

where the multiplication rule becomes

$$(a, b, c)(x, y, z) = (a + x, b + y, c + z + ay).$$

In this instance, there exists a unitary irreducible representation U such that its right quasi-regular representation of H on the space of square integrable functions on $\Gamma \backslash H$ is given by

$$\left(U_a f\right)(b) = f(ba), \quad a, b \in \mathrm{H},$$

and f is defined on the space of square integrable functions on $\Gamma \backslash \mathrm{H}$. Furthermore, the space of square integrable functions on $\Gamma \backslash \mathrm{H}$ decomposes into a direct sum of U-invariant subspaces wherein for f as previously defined

$$\left(U_{(0,0,z)} f\right) = e^{2\pi i m z} f, \quad z \in \mathbb{R}$$

and subspaces can be found that are U-invariant and irreducible.

2.5.2 Fields

A field K is a commutative division ring [9, 10, 20, 21], which is sometimes called an integral domain. In K, both the additive identity and inverse as well as the multiplicative identity and inverse are denoted in the arithmetical sense. Some typical examples of fields include the set of complex numbers, the set of real numbers, and the set of rational numbers. Fields aid and abet in the definition of linear spaces [21, 22, 24]. They are the instrument used to experience multiplication by a scalar in a linear space.

2.5.3 Linear Spaces

A linear space is defined on a set X over the field K with elements of the set being referred to

as vectors. Thus, linear space and vector space are synonymous concepts. A linear space (or vector space) is formed if the set X over the field K is an abelian group under addition where the additive identity and the additive inverse uniquely represent the zero vector and the additive inverse vector respectively and the multiplication of the vectors of X by the real or complex scalars of K satisfies the conditions

$$\begin{aligned} a(x+y) &= ax+ay, \\ (a+b)y &= ax+by, \\ a(bx) &= (ab)x, \\ 1x = x, \quad 0x &= 0, \quad \forall x, y \in X, \ \forall a, b \in K. \end{aligned}$$

A subspace of X over K is a subset A of X which is also a complete linear space over K with the operations of vector addition and scalar multiplication on X. Moreover, if Δ is a subset of X, the span of a subspace A of X is the set of all linear combinations of $x_i \in \Delta$, $i \in Z$. In particular, if $\Delta = \{x_i\}$ for $1 \le i \le n$, it is said that the finite sequence of vectors $\{x_i\}$ spans A. For vectors $x_i \in X$, $1 \le i \le n$ and scalars $a_i \in K$, $1 \le i \le n$, if the linear combination of x_i s such that

$$\sum_{i=1}^{n} a_i x_i = \begin{cases} 0, & a_i = 0 \\ K \neq 0, & \text{otherwise,} \end{cases}$$

the sequence of vectors $\{x_i\}$ is linearly independent; otherwise, it is linearly dependent. A linear independent set of vectors in X that spans X is a Hamel basis (or simply basis) for X. In particular, if the sequence of vectors $\{x_1, x_2, \ldots, x_n\}$ in X is a basis for X, there is a unique sequence of scalars $\{a_1, a_2, \ldots, a_n\}$ in K such that each $x \in X$ can be written as

$$x = \sum_{i=1}^{n} a_i x_i.$$

Moreover, if the basis is finite, X is finite-dimensional with the number of vectors in the basis being its dimension. If X is not finite-dimensional, it is infinite-dimensional.

Metric Space: A metric space is a set X with a symmetric, real-valued, positive definite distance function ϕ defined on $X \times X$. For all $x, y, z \in X$, the metric ϕ has the following properties between every two points of X:

$$\begin{aligned} 0 \le \phi(x, y) < \infty, \\ \phi(x, y) = 0 \text{ if and only if } x = y, \\ \phi(x, y) = \phi(y, x), \\ \phi(x, y) \le \phi(x, z) + \phi(z, y). \end{aligned}$$

A sequence $\{x_i\}$ that converges in a metric space is a Cauchy sequence. That is, a Cauchy sequence is a sequence $x_i \in X$, if for every element $\varepsilon > 0$, there exists a positive integer N such that the condition $\phi(x_i, x_j) < \varepsilon$, $\forall i, j \ge N$ is satisfied. A metric space X is complete if every Cauchy sequence $\{x_i\}$ in it converges to a point x in X. In addition, if a metric space is linear, it becomes a linear space (or vector space) X with the metric ϕ defined upon it having the additional property which states that the metric spaces $X \times X$ and $K \times X$ continuously map into X in that $(x, y) \Rightarrow x + y$ and $(a, x) \Rightarrow ax$ for x and y in X and a in K. That is, the linearity condition holds for a convergent Cauchy sequence in X; namely, if $a_i \Rightarrow a$, $b_i \Rightarrow b$, $x_i \Rightarrow x$, and $y_i \Rightarrow y$, $a_i x_i + b_i y_i \Rightarrow ax + by$. Also, if X contains a subset A that is countable

and dense[8] throughout X, X is separable. Sometimes, two distinctly different metric spaces are isometric. To be specific, two metric spaces X and A with metric functions ϕ_1 and ϕ_2 respectively, and for which there exists a bijective mapping ψ from X onto A, are isometric if

$$\phi_1(x, y) = \phi_2(\psi(x), \psi(y)) \quad \forall x, y \in X$$

implying that the mapping ψ is an existing isometry. The fact that ψ is an isometry implies it is a homeomorphism.

Normed Space: A norm space is a linear space X over the field K (K = $\mathbb{R}$ or $\mathbb{C}$) on which is defined a norm $\|\cdot\|$ that maps X into $\mathbb{R}$ and the norm for all $x, y \in X$ and $a \in K$ satisfies the following conditions:

$\|x\| \geq 0$, and only with equality when $x = 0$;
$\|ax\| = |a| \, \|x\|$; and
$\|x + y\| \leq \|x\| + \|y\|$.

From the properties of the norm of a normed space, it is clear that a normed space is a metric space, because the metric function ϕ defined on X has the form

$$\phi(x, y) = \|x - y\|, \quad \forall x, y \in X.$$

When a normed space is complete in the metric ϕ defined by its norm, it is called a Banach

---

[8] Subset A of metric space X is dense if the closure of A is equal to X.

space. As a consequence, every Cauchy sequence ought to converge. There are several examples of Banach space. Some include Lesbesgue space L_p of Lesbesgue measurable functions f, space of continuous functions on a compact space C(X), and Hilbert space H. In general, a Banach space X over a field K possesses a Hamel basis. Except for finite-dimensional Banach spaces, it is usually impossible to construct a Hamel basis for an infinite-dimensional Banach space. In many of these cases, it is possible to construct a Schauder basis[9]. Schauder basis for an infinite-dimensional Banach space X is an infinite sequence of vectors $\{x_i\}$ in X to which there exists a corresponding unique infinite sequence of scalars $\{a_i\}$ in K such that for every vector $x \in X$,

$$x = \sum_{i=1}^{\infty} a_i x_i$$

with convergence in the norm

$$\| x - \sum_{i=1}^{\infty} a_i x_i \| \to 0 \quad \text{as} \quad n \to \infty.$$

The basis $\{x_i\}$ for X is unconditional if every convergent series of the form of (the just mentioned) infinite series representation of x converges unconditionally [10]. In general, every

---

[9] For an infinite-dimensional Banach space, the term basis will be understood to mean Schauder basis.

[10] If every possible arrangement of the terms of an infinite series $\sum x_i$ in a Banach space converges to the same element, the series converges unconditionally.

Banach space X with a basis is separable but the converse is not necessarily true.

Lesbesgue Space: For any real number $p \geq 1$, the Lesbesgue space written as $L_p(X)$[11] is a normed linear space over the field K consisting of real- or complex-valued functions f, defined on the Lesbesgue measurable set X such that

$$\| f \|_p = \left(\int_X | f(x) |^p dx \right)^{1/p} < \infty, \quad x \in X \text{ and } p \geq 1$$

and if $f, g \in L_p(X)$, $(f+g) \in L_p(X)$ follows from Minkowski's inequality, $\| f + g \|_p = \| f \|_p + \| g \|_p$. In addition, if $f \in L_p(X)$ and $a \in K$, $af \in L_p(X)$. In particular, when $p = \infty$, $f \in L_p(X)$ there is a smallest constant c satisfying $| f(x) | \leq c$ a.e., for $x \in X$ and the norm of f is equal to its essential supremum. That is

$$\| f \|_\infty = \operatorname*{ess\ sup}_X | f |.$$

Furthermore, for every $x \in X$ and $a, b \in K$ the norms $\| \|_1$ and $\| \|_2$ are equivalent if

$$a \| x \|_1 \leq \| x \|_2 \leq b \| x \|_1.$$

Moreover, Hölder's equality states that if $f \in L_p(X)$ and $g \in L_q(X)$, $fg \in L_1(X)$ and

---

[11] L_p is the space of all equivalence classes $\mathfrak{F}$ of Lesbesgue space functions $f \in \mathfrak{L}_p$ modulo the null functions such that for a sequence of functions $\{f_i\} \in L_p$ and any for function $f \in \mathfrak{L}_p$ there exists a subsequence f_i of $\{f_i\}$ in $\mathfrak{L}_p$ satisfying the condition $\| f - f_i \| = 0$ or $f_i = f$ a.e.

$$\|fg\|_1 \leq \|f\|_p \|g\|_q, \quad p,q \geq 1 \text{ and } \frac{1}{p} + \frac{1}{q} = 1.$$

In a manner similar to L_p function space, Lesbesgue space l_p of sequences, with real- or complex-valued components, is defined in terms of summation. Both spaces share similar properties and satisfy equivalent conditions. For example, Minkowski and Hölder's inequalities in L_p have corollaries in l_p.

Space of Continuous Functions: Space C(X) is the normed space with field K consisting of all continuous real- and complex-valued functions f defined on the compact metric space[12] X having norm

$$\|f\| = \max\{\,|f(x)|\;\big|\; x \in X\}.$$

Additionally, there is a sequence $\{f_i\}$ of functions in C(X), which is defined on X, that contains a subsequence f_i. f_i converges to f in C(X) while equivalently it converges to f in X. That is, for every $\varepsilon > 0$ there exists an N such that $\|f_i - f\| < \varepsilon$ whenever $i \geq N$ and equivalently $|f_i(x) - f(x)| < \varepsilon$ whenever $\geq N$ and $x \in X$. Furthermore, if X denotes the set of all continuous functions defined on a closed finite interval, Weierstrass approximation theorem [23, 43] affirms that polynomials can be used to approximate functions on X because

[12] A metric space is compact if and only if it is complete and totally bounded.

polynomials are dense in C(X). That is, for each function f on X, there exists a polynomial p such that the norm

$$\|f - p\| < \varepsilon \quad \forall \varepsilon > 0.$$

Besides, C(X) has a basis and each f in C(X) has at least one unique infinite series representation of the form

$$f = \sum_{i=0}^{\infty} a_i f_i.$$

Hilbert Space: If an inner product space[13] H over the field K is complete relative to the norm $\|x\| = \sqrt{\langle x, x \rangle}$[14], it is called the Hilbert space. A Hilbert space H may be real or complex relative to K[15] while being finite or infinite dimensional. A finite dimensional H is called a unitary space $\mathbb{C}^n$ if it is complex; otherwise, it is called a Euclidean space $\mathbb{R}^n$. Two other typical examples of Hilbert space H are Lesbesgue spaces L_2 and l_2. For every $x, y, z \in H$ and any $a, b \in K$, the properties of the Hilbert space are:

---

[13] An inner product space is a type of normed space.

[14] The symbol $\langle\ \rangle$ denotes inner product.

[15] If K is real, the Hilbert space is real and if K is complex, the Hilbert space is complex.

$$\begin{aligned} \langle ax + by, z\rangle &= a\langle x, z\rangle + b\langle y, z\rangle, \\ \langle x, y\rangle &= \langle y, x\rangle^*, \\ \langle x, x\rangle &\geq 0 \quad \text{equality occurs only for } x = 0. \end{aligned}$$

Some consequences of Hilbert space:

1. Cauchy-Schwarz Inequality states that

$$|\langle x, y\rangle| \leq \|x\|\|y\|, \quad x, y \in H,$$

with

$$|\langle x, y\rangle| = \|x\|\|y\|$$

if and only if x and y are linearly dependent.

2. In the space of $L_2(X)$ functions, the general form of the inner product of $f, g \in L_2(X)$ is defined as

$$\langle f, g\rangle = \int_X f(x)g^*(x)dx.$$

A similar formula is definable for l_2 sequences.

3. For Two Hilbert spaces H_1 and H_2, if there exists a linear isomorphism T from H_1 to H_2 that preserves the norm,

$$\|Tw\| = \|w\| \quad \forall w \in H_1,$$

H_1 and H_2 are isometrically isomorphic and T is an isometric isomorphism with isometry:

$$\psi(T(w), T(x)) = \|T(w - x)\| = \|w - x\| = \psi(w, x) \quad \forall w, x \in H_1.$$

4. Triangle inequality states that

$$\|x + y\| \leq \|x\| + \|y\|, \quad x, y \in H,$$

with equality in terms of its square expansion whenever x is orthogonal to y. That is

$$\|x + y\|^2 = \|x\|^2 + \|y\|^2, \quad x \perp y.$$

5. If $\langle x, y \rangle = 0$ for $x, y \in H$, x and y are orthogonal to each other. Furthermore, if X and Y are subsets of H and $\langle x, y \rangle = 0$ for each $x \in X$ and $y \in Y$, X and Y

are orthogonal to each other. Besides, the set of all elements in H that is orthogonal to X is a closed subspace of H, which is called the orthogonal complement of X and is denoted by $X^{\perp}$. Clearly, $Y \subseteq X^{\perp}$ if and only if $X \subseteq Y^{\perp}$, and if $x \in X \cap X^{\perp}$, $\langle x, x \rangle = 0$ and $X \cap X^{\perp} = \{0\}$.

6. In a Hilbert space H with closed subspace X, each element $z \in H$ can be uniquely written as $z = x + y$ for $x \in X$ and $y \in X^{\perp}$. Importantly, x is the unique element in X that is closest to z.

7. If $X = \{x_i \mid i \in I\}$ is a subset of Hilbert space H, X is an orthogonal set if any two of its distinct elements are mutually orthogonal. Furthermore, if X is an orthogonal subset of H, it is linearly independent and it is complete for the condition $X^{\perp} = \{0\}$. When X is a complete orthogonal set, it is an orthogonal basis. Whenever each of the elements $x_i \in X$ has norm $\|x_i\| = 1$, X is, instead, an orthonormal basis consisting of an orthonormal set. An orthonormal basis is a characteristic of each Hillbert space H.

8. In the Hilbert space $H = l_2$, a sequence of elements $\{e_i\}$ is an orthonormal basis if it has the property that

$$\langle e_i, e_j \rangle = \delta_{ij},$$

where

$$\delta_{ij} = \begin{cases} 1, & i = j \\ 0, & i \neq j \end{cases}$$

is the Kronecker delta sequence.

9. In a Hilbert space H with an orthonormal set X, the conditions:

   (a) X is complete;

   (b) X is an orthonormal basis;

   (c) X spans a closed subspace that is equal to H;

   (d) $\langle y, z \rangle = \sum_{x \in X} \langle y, x \rangle \langle x, z \rangle \quad \forall y, z \in H$;

   (e) $\|y\|^2 = \sum_{x \in X} |\langle y, x \rangle|^2 \quad \forall y \in H$; and

   (f) $y = \sum_{x \in X} \langle y, x \rangle x \quad \forall y \in H$

   are equivalent.

10. In a Hilbert space H, an unconditional basis $\{x_i\}$ for H is a Reisz basis. A Reisz basis $\{x_i\}$ for H is equivalent to an orthonormal basis $\{e_i\}$ for H in that the basis $\{x_i\}$ is an image of the basis $\{e_i\}$ through the operation of a bounded invertible[16] operator. A Reisz basis $\{x_i\}$ for H is bounded,

[16] Invertible means bijective.

$$0 < \inf_i \|x_i\| \leq \sup_i \|x_i\| < \infty.$$

Moreover, a Reisz basis $\{x_i\}$ is complete in a separable H and for positive constants A and B, $B < \infty$, an equivalent characterization for $\{x_i\}$ is the following condition:

$$A\sum_{n=1}^{i} |a_n|^2 \leq \left\|\sum_{n=1}^{i} a_n x_n\right\|^2 \leq B\sum_{n=1}^{i} |a_n|^2$$

where i is an arbitrary positive integer and $\{a_n\}$ is an arbitrary sequence of scalars. The inequality

$$\left\|\sum_{n=1}^{i} a_n x_n\right\|^2 \leq B\sum_{n=1}^{i} |a_n|^2$$

guarantees that the sequence of vectors $\{x_n\}$ is a Bessel sequence. Thus a Bessel sequence is a key constituent of every Reisz basis. In general, a Bessel sequence is a sequence of vectors $\{x_n\}$ in H satisfying the condition:

$$\sum_{n=1}^{\infty} |\langle x, x_n\rangle|^2 < \infty.$$

Additionally, there is a positive constant B such that

$$\sum_{n=1}^{\infty} |\langle x, x_n\rangle|^2 \leq B\|x\|^2.$$

11. A sequence $\{x_n\}$ in a Hilbert space H is a Hilbert sequence if it satisfies the condition

$$A\|x\|^2 \leq \sum_{n=1}^{\infty} |\langle x, x_n \rangle|^2,$$

for every sequence x in H where A is a positive constant.

12. Any two sequences $\{x_i\}$ and $\{y_j\}$ of a Hilbert space H are biorthogonal provided that

$$\langle x_i, y_j \rangle = \delta_{ij} \quad \forall i, j.$$

If the sequence $\{x_i\}$ is a basis for H, it possesses a unique biorthogonal sequence $\{y_j\}$ that is also a basis for H. As a result, each vector $x \in H$ has a unique infinite series representation of dual form

$$x = \sum_{i=1}^{\infty} \langle x, y_i \rangle x_i \text{ as well as } x = \sum_{i=1}^{\infty} \langle x, x_i \rangle y_i.$$

13. Any two Hilbert spaces H_1 and H_2 of the same finite or infinite dimension are isometrically isomorphic. In particular, each Hilbert space H is isometrically isomorphic to one of form l_2 but if H is infinite-dimensional and separable, it is isometrically isomorphic to $L_2(0, 1)$. However, if H has finite dimension n, it is isometrically isomorphic to the unitary space $\mathbb{C}^n$.

2.5.4 Operators

An operator is a function[17]. Suppose X and A are linear spaces over the field K of real- or complex-valued numbers, the function T from X into A is an operator. If, however, the space A corresponds to the field K, the function T is, instead, a functional on X.

Linear: An operator T from X into A is linear if it satisfies the property:

$$T(ax + by) = aT(x) + bT(y) \quad \forall x, y \in X \text{ and } a, b \in K.$$

If in addition to T satisfying the linearity property, X and A are normed linear spaces, the linear mapping from X into A is bounded provided there exist a real positive constant α such that

$$\|Tx\|_A \leq \alpha \|x\|_X \quad \forall x \in X.$$

The boundedness condition on T is sufficient to make T continuous.

Unitary: In terms of Hilbert spaces H_1 and H_2, if for $T \in B_{H_{12}}$, the Hilbert space of all linear operators from H_1 into H_2, there exists a unique operator $T^\circ \in B_{H_{21}}$ such that

---

[17] Functions may be subdivided into scalar functions, which associate elements of a space to elements of the real- or complex-valued field and vector functions associated, which associate elements of one space to elements of another or the same space.

$$\langle T^{\circ}x, y\rangle = \langle x, Ty\rangle \quad \forall\, x \in H_1 \text{ and } y \in H_2,$$

T° is the adjoint of T and additionally, $(T^{\circ})^{\circ} = T$, $\|T^{\circ}T\| = \|T\|^2$, and $\|T^{\circ}\| = \|T\|$. Moreover, when T is a bounded linear operator from H_1 into H_2 and it is norm-preserving and invertible ($T^{-1} = T^{\circ}$), T is an isometric isomorphism from H_1 onto H_2. In particular, for the case where $H_1 = H_2$ and $H = H_1$, the action of T on H is such that T is self-adjoint when $T^{\circ} = T$ and unitary when

$$TT^{\circ} = T^{\circ}T = I.$$

I, in this sense, is the identity operator. The unitary condition is a consequence of the norm-preserving property of T acting on H.

Orthogonal Projection: A Hilbert space H with a closed linear subspace X can be expressed in terms of the direct sum $H = X \oplus X^{\perp}$ so that each element *z* in H is a sum of respective unique elements x in X and y in $X^{\perp}$. The function P_X that linearly maps H onto itself and defines the projection $x = P_X(z)$ on X along $X^{\perp}$ is the orthogonal projection on X. In fact, $P_X(z)$, which can be stated as the orthogonal projection of *z* on X, represents the unique element in X closest to *z*. The element $y \in X^{\perp}$ is equal to $z - P_X(z)$. Moreover, P_X is a self-adjoint positive operator with $\|P_X\| = 1$ provided P_X is nonzero and idempotent, $P_X^2 = P_X$. The subspaces X and $X^{\perp}$ can be respectively written as

$$X = \{P_X(z) \mid z \in H\} = \{x \in H \mid x = P_X(x)\}$$

and

$$X^{\perp} = \{y \in H \mid P_X(z - P_X(z)) = 0\}.$$

Because $(X^{\perp})^{\perp} = X$, there is another orthogonal projection; namely, $P_{X^{\perp}} = I - P_X$ acting on H. $P_{X^{\perp}}$ is the orthogonal projection of H onto $X^{\perp}$ with the property

$$y = P_{X^{\perp}}(z) = P_{X^{\perp}}(y), \quad y \in X^{\perp} \text{ and } z \in H.$$

The functions f defined on $\mathbb{R}$ have norm equal to the norms of the action of the following operators on it.

Translation:

$$(T_a f)(t) = f(t - a), \quad a \in \mathbb{R};$$

Modulation:

$$(R_b f)(t) = f(t)e^{2\pi i b t}, \quad b \in \mathbb{R}; \text{ and}$$

Dilation:

$$(D_c f)(t) = \sqrt{c} f(ct), \quad c \in \mathbb{R}\backslash\{0\}.$$

The equality among the norms is:

$$\|f\| = \|T_a f\| = \|R_b f\| = \|D_c f\|.$$

Interestingly, the operators R_b and T_a do not compute because $R_b T_a = e^{2\pi i ab} T_a R_b$. The operations $R_b T_a$ on a function f may be written as $(R_b T_a f) = f_{a,b}$.

2.5.5 Topological Space

A topological space is a set X with an associated topology T. A topological space X becomes a Hausdorff space whenever any two distinct elements x and y of X are contained in separate open sets S and T having empty intersection. Importantly, Hausdorff spaces include all metric spaces. The space X with an element $x \in X$ within a neighborhood S wherein lies a compact set A satisfying $x \in A^\circ \subset A \subset S$ is locally compact. A° is the interior of A. The Euclidean space is locally compact. The space $C_c(X)$ is the set of all functions $f \in C(X)$ with compact support[18] and the space $C_0(X)$ is the set of all $f \in C(X)$ that vanishes at infinity.

---

[18] The support of a function f defined on X is the closure of the set of points x where $f(x) \neq 0$.

A topological abelian group G is a Hausdorff space. It becomes a locally compact abelian (*LCA*) group when the continuous map from the cartesian product $G \times G$ onto G is the map $(x, y) = x + y$, $x, y \in G$, and when G is a locally compact topology τ. Each *LCA* group G has a Haar measure m, which is a translation-invariant positive regular measure [25, 44]. That is

$$m(B + x) = m(B), \quad \forall x \in G \text{ and } B \subset G,$$

where B is the Borel set. Additionally, since G is compact, $m(G) < \infty$ and normalizable. Any two functions f and g on the *LCA* group G has an associated convolution defined by

$$(f * g)(x) = \int_G f(x - y)g(y)dy, \quad x \in G,$$

whenever

$$\int_G |f(x - y)g(y)|dy < \infty.$$

Furthermore, it can be proven that whenever f and g are in $L_1(G)$

$$f * g \in L_1(G) \text{ and } \|f * g\|_1 \leq \|f\|_1 \|g\|_1.$$

A complex function χ defined on a *LCA* group G with absolute value $|\chi(x)| = 1, \forall x \in G,$ and functional equation

$$\chi(x + y) = \chi(x)\chi(y), \quad x, y \in G,$$

is a character of G. In other words, a character χ on G is a continuous homomorphism of G into the multiplicative group of complex numbers having absolute value equal to 1. The set of all continuous characters of G with addition taking the form

$$(\chi_1 + \chi_2)(x) = \chi_1(x)\chi_2(x), \quad x \in G \text{ and } \chi_1, \chi_2 \in \hat{G},$$

constitute the dual group $\hat{G}$ of G. Like G, $\hat{G}$ is a *LCA* group. From Pontryagin duality theorem, a *LCA* group G is the dual of its dual group $\hat{G}$. A consequence of this theorem states that relating to each compact (discrete) G is a discrete (compact) dual $\hat{G}$. The set of all functions $\hat{f} \in \hat{G}$ is the space $A(\hat{G})$, which is dense in $C_0(\hat{G})$, invariant under translation as well as under multiplication by $\chi(x)$, $x \in G$, and the convolution $(f * \chi)(x) = \chi(x)\hat{f}(\chi)$ for all $f \in L_1(G)$ and $\chi \in \hat{G}$. The dual group $\hat{G}$ has a special relationship to the Banach space $L_1(G)$.

2.5.6 Fourier Transform

Suppose G[19] is a *LCA* group with the corresponding dual group $\hat{G}$ such that for any $f \in L_1(G)$, there is a function $\hat{f} \in A(\hat{G})$ given by

$$\hat{f}(\chi) = \int_G f(x)\chi(-x)dx, \quad \chi \in \hat{G},$$

which is called the Fourier transform of f. This Fourier transform is norm-decreasing and continuous with the property $\|\hat{f}\|_\infty \leq \|f\|_1$. Moreover, the Fourier transform of the convolution $f * g$ is described by the product $\hat{f}\hat{g}$. Conversely, it is possible to extract the function f from its Fourier transform $\hat{f}$ provided $f \in L_1(G) \cap D(G)$[20] and Haar measure m of G is fixed. The inversion of the Fourier transform is possible under these conditions because the respective implications are $\hat{f} \in L_1(G)$ and Haar measure $\hat{m}$ of $\hat{G}$ is normalizable to effect the inverse Fourier transform of $\hat{f} \in L_1(\hat{G})$:

$$f(x) = \int_{\hat{G}} \hat{f}(\chi)\chi(x)d\chi, \quad x \in G.$$

Plancherel Theorem [27, 29]: The Fourier transform, restricted to the dense subspace $(L_1 \cap L_2)(G)$ of $L_2(G)$, is an isometry, relative to L_2-norms, onto a dense linear subspace of $L_2(\hat{G})$. Thus, it may be uniquely extended to an isometry of $L_2(G)$ onto $L_2(\hat{G})$.

---

[19] Note if $G = \mathbb{R}$, it turns out that the dual group $\hat{G} = \mathbb{R}$.

[20] $D(G)$ is the space of all positive-definite f on G.

In the L_2-sense, the Fourier transform is a unitary operator on $L_2(G)$ and each function $\hat{f}$ in $L_2(\hat{G})$ is the Fourier transform of some function f in $L_2(G)$. Besides, for all $f \in (L_1 \cap L_2)(G)$, $\|\hat{f}\|_2 = \|f\|_2$.

Discrete Poisson's Summation Formula [31, 32]: For a finite abelian group G of order N having mutually orthogonal subgroups H and K, for a given basis, of orders of M and L respectively, the generalized discrete version of Poisson's summation formula in terms of any sequence a, with elements in G, and its discrete Fourier transform $\hat{a}$ can be written as follows:

$$\sum_{m=0}^{M-1} a_{n-mL} e^{2\pi imk/M} = \frac{1}{L} \sum_{l=0}^{L-1} \hat{a}_{-k-lM} e^{2\pi il(-k-lM)n/N},$$

where $n, k \in G$ and $ML = N$. It will become obvious in a later chapter that this definition of the discrete Poisson's summation formula is commonly referred to nowadays as the discrete Zak transform duality relationship. An alternative but less general form of the discrete Poisson's summation formula can be obtained by setting n and k to zero. This version of Poisson's formula takes the form:

$$L \sum_{m=0}^{M-1} a_{mL} = \sum_{l=0}^{L-1} \hat{a}_{lM}.$$

It can be concluded that Poisson's summation formula, which is of critical importance in engineering and mathematics, describes the fundamental duality between periodization and decimation operators under Fourier transformtion.

Pauli-Weyl-Heisenberg Uncertainty Relation [1, 34, 35, 36, 37, 38, 39, 40]: The classical uncertainty principle of quantum mechanics, adopted to signal processing by Gabor in 1946, is a consequence of the inequality

$$\frac{\|(x-x_0)f\|_p \|(v-v_0)\hat{f}\|_p}{\|f\|_2^2} \geq \frac{1}{4\pi}, \quad 1 \leq p \leq 2, \ f \in L_2, \text{ and } f \neq 0,$$

whenever $p = 2$. The arbitrary real constants x_0 and v_0 are the means of the squared absolute value of f and $\hat{f}$ respectively. In signal processing, it is only at $p = 2$ that this equation attains equality for functions f of the form $f(x) = ke^{-\alpha x^2}$ with k and α being constants and $\alpha > 0$. The conceptual meaning of the uncertainty relation in signal processing bear no resemblance to its quantum mechanical meaning. In fact, the uncertainty relation of quantum theory is only formally analogous to its meaning in signal theory. The main reason being that in quantum mechanics the uncertainty relation is intrinsically probabilistic and is therefore written in terms of standard deviations whereas in signal processing the uncertainty relation is not probabilistic. In signal processing, the uncertainty relation, commonly referred to as the time-bandwidth product theorem, which estabishes a lower limit on the product on the time and frequency concentration of a function f that decreases relatively quickly to zero at infinity, essentially states that f and its Fourier transform $\hat{f}$ cannot be simultaneously highly concentrated. That is, if f is concentrated on a time interval $\Delta x = \|(x-x_0)f\| / \|f\|$, then $\hat{f}$ must be concentrated on a spectral interval $\Delta v = \|(v-v_0)\hat{f}\| / \|f\|$ in such a way that $\Delta x \Delta v \geq (4\pi)^{-1}$. The unadulterated adoption of the quantum mechanical uncertainy principle to signal processing suffers from several other drawbacks according to Lerner, Landau and

Pollak, and Slepian [41]. Because of the many pitfalls in the use of the Heisenberg uncertainty principle in signal processing, other more relevant and convenient ways of establishing the reciprocity relationship of the simultaneous time and frequency concentration of a function have been developed. One of these methods, which is a useful device in signal recovery (Donoho and Stark), is a generalization of the aforementioned uncertainty relation defined over the measurable sets $|\Delta x|$ and $|\Delta v|$ respectively outside of which f and $\hat{f}$ are correspondingly virtually zero.

Continuous-Time Uncertainty Relation: An L_2-function f with Fourier transform $\hat{f}$ satisfies the L_2-norm equality $\|f\|_2 = \|\hat{f}\|_2$. If f is normalized so that $\|f\|_2 = 1$ and $\varepsilon = \varepsilon_x + \varepsilon_v$ is a small real number equivalent to the phrase "essentially zero", then f ε_x-concentrated on a measurable set $|\Delta x|$ to a function g that is zero outside $|\Delta x|$ satisfies the inequality of the norm $\|f - g\|_2 \leq \varepsilon_x$ and $\hat{f}$ ε_v-concentrated on a measurable set $|\Delta v|$ to a function $\hat{h}$ that is zero outside $|\Delta v|$ satisfies the inequality of the norm $\|\hat{f} - \hat{h}\|_2 \leq \varepsilon_v$ result in the condition

$$|\Delta x|\,|\Delta v| \geq (4\pi)^{-1}(1 - \varepsilon)^2.$$

Discrete-Time Uncertainty Relation: For a finite-duration sequence a of order N consisting of M nonzero elements and its discrete Fourier transform $\hat{a}$ consisting of L nonzero elements and no M consecutive zeros,

$$ML \geq N \text{ and consequentially } (M + L)^2 \geq 4N.$$

Like in the continuous case, the discrete-time uncertainty relation can be generalized in terms of sets with concentration being understood in the framework of Euclidean norm on the vector space $\mathbb{R}^N$. In other words, for the discrete Fourier transform pair a and $\hat{a}$ of unit norm, having a ε_x-concentrated on the index set $|\Delta x|$ consisting of M elements and $\hat{a}$ ε_v-concentrated on the index set $|\Delta v|$ consisting of L elements,

$$ML \geq N(1 - \varepsilon)^2.$$

2.5.7 Frames

A frame is the generalization of a Reisz basis. A frame is defined as an infinite sequence of distinct vectors $\{x_i\}$ in a separable Hilbert space H satisfying the condition:

$$A\|x\|^2 \leq \sum_{i=1}^{\infty} |\langle x, x_i \rangle|^2 \leq B\|x\|, \quad \forall x \in H, \quad A > 0, \quad \text{and} \quad A \leq B < \infty.$$

The positive numbers A and B are the frame bounds. A is the lower bound which is usually difficult to obtain and B is the upper bound whose existence is evident from the fact that $\{x_i\}$ is also a Bessel sequence with bound B. If $A = B$, $\{x_i\}$ is a tight frame but it becomes a snug frame if $A \approx B$, with the degree of snugness measured by the value of the number

$(B/A - 1)^{-1}$. A frame is a complete set and so any finite linear combination of it is everywhere dense. A frame may be exact or inexact. An exact frame fails to be a frame whenever anyone of its vectors is removed by becoming an incomplete set. An inexact frame remains a frame with the removal of any finite number of its vectors. In other words, a linearly independent set of vectors is an exact frame. Thus, an inexact frame is redundant. Both exact and inexact frames may be tight. Because of the redundancy of an inexact frame, it cannot constitute a linearly independent set and therefore, it cannot form a basis. However, an exact frame is a Reisz basis. Of significant importance is the fact that a tight frame of unity norm with $A = 1$ is an orthonormal basis and an orthonormal basis is a tight exact frame with $A = 1$.

For a frame $\{x_i\}$, a bounded, invertible, linear, self-adjoint operator S on H defined by the relation

$$Sx = \sum_{i=1}^{\infty} \langle x, x_i \rangle x_i$$

is called a frame operator. Because S is invertible, it has a unique inverse S^{-1}. This leads to the definition of a new frame, $\{S^{-1}x_i\}$, called the dual frame of $\{x_i\}$, with lower and upper frame bounds B^{-1} and A^{-1} respectively. Now every vector $x \in \mathsf{H}$ can be written in terms of not only a series expansion with respect to the frame but also a series expansion with respect to the dual frame; namely,

$$x = \sum_{i=1}^{\infty} \langle x, S^{-1}x_i \rangle x_i = \sum_{i=1}^{\infty} \langle x, x_i \rangle S^{-1}x_i.$$

Furthermore, when $\{x_i\}$ is an exact frame it is a Riesz basis and $\{x_i\}$ and $\{S^{-1}x_i\}$ are biorthogonal. When $\{x_i\}$ is simply a tight frame, the series expansion of any $x \in H$ becomes

$$x = A^{-1}\sum_{i=1}^{\infty} \langle x, x_i \rangle x_i$$

implying that the frame operator S is restricted to $S = AI$ with inverse $S^{-1} = A^{-1}I$; I is the identity operator. A is the redundancy measure of the representation. Although the expansion of x with respect to tight frames is quite similar to an orthonormal series expansion of x, it is only orthonormal-like because the tight frame, $\{x_i\}$, is generally nonorthogonal and redundant. Nevertheless, this non-unique series representation of x has strong convergence and orthonormality advantages.

Chapter 3

Overview of Time-Frequency Methodologies

The discussion in this chapter will focus on the different methods used to represent a signal or its energy density in the joint time-frequency space. This discussion will be inexhaustive. It will be illustrative in the choice and number of the nonlinear as well as linear time-frequency methods described and compared. The time-frequency signal (or signal energy) description will be typically general. However, some of the different time-frequency signal representations that will be explored in this and subsequent chapters have more than one definition. For example, the Zak transform can be defined in at least four standard equivalent ways while the short-time Fourier transform and ambiguity functions can each be defined in many more standard equivalent ways. Usually, the definition adopted for a time-frequency signal representation is consistent with the intended outcome in theory or application. Therefore, emphasis will be placed on time-frequency representation definitions that are easily related to each other functionally and formally. The relatedness of time-frequency analysis to the classical Fourier analysis as well as the interrelationship among time-frequency representations will be explained. Moreover, it will be shown that distributions are not true transforms [3]. Additionally, it will be shown that the Zak transform is intimately related to the ambiguity function, which is at least the cornerstone of a large class of time-frequency and time-scale signal representations [49, 50]. Furthermore, the mathematical basis for time-frequency representations will be explored, and some of the current areas of application of the more widely used time-frequency techniques will be outlined.

3.1 Nonlinear Time-Frequency Methods

In the 1940s, the quantum mechanics mathematical concept of dual space representation of a wave function [51, 52] was formally introduced into signal processing in the form of the joint time-frequency representation of a nonstationary signal devoid of equivalent interpretative meaning. Although there is much correspondence in the form of the mathematics of quantum mechanics and signal processing, the physical meaning of the properties of the functions and variables involved are quite different. In fact, time in quantum mechanics has no analogy in signal processing. The most basic difference between the two disciplines lies in the inherent nondeterministic theory [53, 54] of quantum mechanics contrasted to the general deterministic theory of signal processing. In 1946, Gabor adopted the paradigm of coherent states in quantum mechanics [47, 55, 56, 57] into signal processing to facilitate his pioneering work on voice and image analysis and transmission in terms of a simultaneous time and frequency description of a single signal [38]. Gabor's work set forth the theoretical foundation for joint time-frequency signal analysis and synthesis which contains classical Fourier analysis and synthesis theories as degenerative special cases. Gabor derived a synthesis equation for the joint time-frequency space, which constitutes a series expansion whose coefficients correspond to the sample values of the short-time Fourier transform [1, 38, 58, 59]. In putting his new theory to viable practical use on voice signals, Gabor proposed a mechanical method and an electrical method for the purpose of voice compression suitable for transmission and voice interpolation to recover the original voice signal from the compressed version. The mechanical method utilized the concept of the short-time Fourier transform in an existing patented

kinematical frequency converter, which is a special type of sound spectrograph, to produce a spectrogram of intensities corresponding to Gabor's series expansion coefficients. The electrical method was devised to be mathematically equivalent to the mechanical method. The sound spectrograph, which models the short-time Fourier transform to produce a spectrogram of the signal energy distribution in the time-frequency space, was invented at Bell Telephone Laboratories prior to 1945 for the purpose of sound reproduction and analysis [38, 60, 61, 62]. The spectrogram "is the prototype of a time-frequency distribution." This energy distribution is not a probabilistic one [2] but is merely the spread of the signal energy density [63, 64] in the joint time-frequency space.

Because the theory of time-frequency distributions assumes the form of the general theory of two-dimensional joint probability density functions [53, 54], some of the desired properties correspond identically. For example, both nonnegativity and existence of the marginals are necessary properties in joint probability density functions and their equivalence are desirable properties in time-frequency distributions. Moreover, the quantum physics formalism in signal processing has led to some conceptual confusion regarding the uncertainty principle [1, 51]. In signal processing, the uncertainty principle concept is non-probabilistic and it establishes the minimum bound on the time-bandwidth product of a signal. The time-bandwidth product essentially states that a signal cannot be highly concentrated in both time and frequency. This statement implies the inherent inverse relationship between a signal's time and frequency description, which further suggests that the existence of an impulse in the time-frequency space may be violation of the lower limit of the time-bandwidth product depending on its definition [1].

However, more significantly, the time-bandwidth product gives a useful quantitative estimate of the amount of coefficients needed to accurately describe a bandlimited or otherwise "nice" signal within acceptable error [1].

In 1948, Ville [65] formally introduced the quantum mechanical Wigner distribution [66] into signal processing. Ville's Wigner distribution is the first time-frequency distribution to evolve formally from axioms. It is bilinear and has many desirable mathematical properties including high signal concentration in the time-frequency space [3, 62, 67, 68, 69, 70, 71, 72, 73]. It is a basis for all time-frequency distributions and at least some time-scale distributions [51, 74, 75], but it is the model of all distributions except those characteristically adaptive in the sense of the spectrogram [51,67]. Although the Wigner distribution is conceptually elegant, generally versatile, comprehensively researched, and widely used in practice, it suffers from some serious drawbacks. These include local negativity, cross-terms, and noncompliance to easy implementation [67]. Following the introduction of the Wigner distribution into signal processing, several researchers have developed time-frequency distributions to supplement it [62]. Few of these reseachers established the general relationship that exists amongst at least some of the then current distributions [76]. Nonetheless, even among the related distributions, there are unique behaviors and properties characteristic of each. In 1966, Cohen [77] formulated an equivalent generalized class of time-frequency distributions, which is a generalization of Ville's method to derive the Wigner distribution, containing existing distributions as special cases. Cohen's formula consists of an arbitrary two-dimensional kernel function, which is "sufficiently well behaved" and that may be dependent on time, frequency, and the signal, and an arbitrary

distribution function. Also, Cohen's formula can be interpreted as a two-dimensional Fourier transform of a generalized ambiguity function, which consists of the aforementioned kernel and a regular ambiguity function. There are other interpretations for Cohen's generalized distribution function [62, 69, 78, 79]. The kernel function determines and controls the type of distribution. Because Cohen's generalized distribution function kernel is arbitrary and each unique kernel corresponds to a different distribution, Cohen's distribution class can be used to generate not only an infinite number of unique time-frequency[21] distributions, but also an infinite number of unique time-scale distributions [51, 75]. This is evidenced by the fact that the most general form of Cohen's generalized distribution function is a two-dimensional Fourier transform of an arbitrary generalized "special"[22] function of arbitrary variables. It is therefore claimed that this distribution is an abstract description of the sum of all possible distributions [80].

In the time-frequency framework, when the kernel function is independent of the signal, the corresponding signal energy distribution is bilinear [51,75]. The set of all bilinear time-frequency energy distributions include most of the known distributions [51,69, 70 79]. The characteristic properties of these distributions are detemined by the design constraints imposed upon the kernel function. A desirable property of bilinear distributions is invariance to both time and frequency shifts. This invariance property results from the imposition of time and frequerncy shift invariance on the kernel function. Apart from invariance, bilinear time-frequency energy

---

[21] Frequency can be interpreted to include inverse normalized frequency in its meaning.

[22] Special is used to avoid confusion with the usage of characteristic function of probability theory.

distributions have many other desirable properties [69, 81, 82]. However, it is not possible for any particular bilinear energy distribution to satisfy all the desirable properties because some of these properties can only be inherited at the exclusion of others. For example, adaptive bilinear distributions such as the spectrogram satisfy the positivity condition, at the expense of being able to satisfy the signal's instantaneous power and energy spectral density conditions. Sometimes it may not be necessary to design a new kernel function to obtain a new bilinear distribution, it may be preferable to approximate the needed distribution and its corresponding kernel in terms of others having the desired properties [83].

As earlier stated, the Wigner distribution is bilinear; its drawbacks are more or less characteristic of all bilinear time-frequency energy distributions. The single most significant undesirability of bilinear time-frequency analysis relates to the existence of crossterms in the energy distribution of sophisticated signals like multicomponent signals [84] and nonlinear frequency modulated signals at locations where they are intuitively unexpected [70]. Crossterms result from the interactions of the composite mixture of components that make up the multicomponent signal during processing. They are relatively high difference frequency (time) oscillations constituting the two-dimensional Fourier transform of the kernel function as a function of the difference frequency (time) and the shifted average of the signal frequencies (time duration). Depending on the closeness of the auto-terms (individual components) in the time-frequency space, it may be impossible to resolve the crossterms and interpret the signal energy distribution even if the auto-terms are highly concentrated. Thus, in some instances, the existence of crossterms interfering with auto-terms can even frustrate and render useless the

interpretive abilities of a skilled signal analyst. Because crossterms are inherent in bilinear time-frequency energy distributions, they can never be totally eliminated. Their reduction can only be accomplished at the expense of losing some auto-terms' energy concentration. Therefore, it may be argued that crossterms contain useful information reflective of the multicomponent nature of the signal and that the real issue is not crossterms, which is caused by the method used to analyze the signal, but rather the method (bilinear time-frequency energy distribution) used and its appropriateness. Perhaps the two most widely used bilinear time-frequency distributions are the spectrogram and Wigner distribution. Although the spectrogram orients the expectant crossterms only in the region where the auto-terms overlap, it must ordinarily experience an inherent trade-off between time and frequency resolution of the signal energy concentration in single window use. While the Wigner distribution has highly concentrated auto-terms, its crossterms are a serious problem. Thus, the main challenge facing signal analysts using bilinear time-frequency distribution method as a signal processing tool is how to gain significant crossterms suppression and/or reorientation to satisfactorily improve auto-terms resolution at relatively high signal energy concentration, while retaining as much desirable properties as possible.

Within the last ten years, the knowledge gained from crossterms research [70] has been put to design kernel functions that yield corresponding bilinear time-frequency distributions having highly concentrated auto-terms and other desirable properties of the Wigner distribution as well as the positivity property of the spectrogram. These distributions are intended to suppressed the crossterms and/or reorient them in local isolated regions. The objective is to get highly

concentrated and resolved signal energy distribution with minimal crossterms in the time-frequency space. As previously mentioned, the existence of some desirable properties in a time-frequency distribution mutually exclude the existence of others. Since the choice of the kernel function is responsible for the properties of the corresponding time-frequency distribution and its crossterms, crossterms manipulation is an imposition on the kernel as well as the properties of the distribution. Therefore trade-offs must be made between the level of crossterms suppression and/or reorientation and the desired properties of the distribution during the kernel design phase. In addition, any attempt to manipulate the crossterms patterns in a time-frequency distribution will force trade-offs between the finite support properties, instantaneous signal power and energy density spectrum properties, instantaneous frequency and group delay properties, and crossterms concentration and attenuation properties because it is impossible to simultaneously satisfy these properties in a single distribution. Some of the time-frequency distributions that have been developed to utilize the advantages of the Wigner distribution and the spectrogram while avoiding their disadvantages are : Choi-Williams distribution [85, 86], Cone-kernel distributions [87, 88, 89], reduced interference distributions [90, 91], and bessel distribution [92]. It can be said that these bilinear time-frequency distributions have fulfilled their design objectives in terms of crossterms suppression and/or reorientation and resolution of auto-terms concentration. Each of these distributions performs exceptionally well for certain signals. A distribution with exceptionally good performance on a specific set of signals will usually outperforms other time-frequency distributions on those signals. However, this quality performance is only attainable for a small class of signals. This performance deficiency is characteristic of all bilinear time-frequency distributions because of their signal independence

[93]. Thus, the desire to obtain a bilinear time-frequency distribution with the advantages of the spectrogram and the Wigner distribution for a sufficiently large class of signals, has only led to the development of several distributions of more or less limited capability. A solution to this problem involves giving up bilinearity for kernels that are signal dependent [93, 94, 95, 96].

Although a signal can be uniquely recovered from its bilinear time-frequency energy distribution within a constant factor provided the relevant kernel function or ambiguity function is either well-behaved or has isolated zeros, the synthesis problem of signal design is a delicate issue [51]. This is the case because it is exceedingly difficult to construct a worthwhile time-frequency distribution from an arbitrary signal except in the least squares sense under restricted circumstances.

The following subsections provide illustrative examples of some bilinear time-frequency representations. They are page distribution, Rihaczek distribution, Wigner distribution, and ambiguity function. These time-frequency representations will give some insight into the possible representations and their orientations of a signal's energy. In addition, connection will be made between Wigner distribution and Rihaczek distribution; their relationship to the ambiguity function will be established.

3.1.1 Page Distribution

In 1952, Page [97] published a paper on time-frequency energy distribution in which he devised the mathematical formula for the concept of a changing spectrum relative to time. He referred to this time-frequency formulation as the instantaneous power spectrum. Page developed his time-frequency representation of a signal's energy based upon the assumption that only the past history of a signal is relevant. Page's formula states that the energy density distribution, $\rho(t,\nu)$, of a signal $f(t)$, with Fourier transform $\hat{f}(\nu)$, that is describable by a nonstationary auxiliary signal of the form

$$f_t(\tau) = \begin{cases} f(\tau), & \tau < t \\ 0, & \tau > t \end{cases}$$

is the instantaneous power spectrum of $f_t(\tau)$, expressible as

$$\rho(t,\nu) = \frac{\partial}{\partial t}\left|\hat{f}_t(\nu)\right|^2. \tag{3.1}$$

This formula for the instantaneous power spectrum is commonly called Page distribution. It describes the rate of change of a signal segment energy density spectrum with respect to increases in time t over the interval $(-\infty, t)$. The function $\hat{f}_t(\nu)$, which is central to Page distribution, is the 'running transform' of $f(t)$ or the Fourier transform of the auxiliary signal $f_t(\tau)$. Page distribution, $\rho(t,\nu)$, must satisfy the frequency marginal condition:

$$\int_{-\infty}^{t} \rho(\tau, \nu) d\tau = |\tilde{f}_t(\nu)|^2,$$

which describes the energy density spectrum at frequency ν for all times t. From Plancherel's theorem equating a signal's energy with the energy in its spectrum, $\rho(\tau, \nu)$ must also satisfy the time marginal condition,

$$\int_{-\infty}^{\infty} \rho(t, \nu) d\nu = |f(t)|^2,$$

which describes the instantaneous power at time t for all frequencies ν. Thus, it is obvious that the marginal conditions are crucial to the existence of Page distribution. These conditions can be easily obtained from the signal's total energy (E) distribution, extended up to the current time t, in the time-frequency plane. This total energy is expressible as

$$\int_{-\infty}^{t} \int_{-\infty}^{\infty} \rho(\tau, \nu) d\nu d\tau = E.$$

There are more convenient ways to express Page distribution than equation (3.1), but they are derivable from it. Two of these other expressions are:

$$\rho(t, \nu) = 2\,\mathrm{Re}\, f^*(t) \tilde{f}_t(\nu) e^{2\pi i \nu t} \tag{3.2}$$

and

$$\rho(t,\nu) = 2\int_0^{\infty} f^*(t)f(t-\tau)\cos(2\pi\nu\tau)\,d\tau \qquad (3.3)$$

The product $f^*(t)f(t-\tau)$ is a time-dependent autocorrelation[23] function, $R_t(\tau)$, with the property $R_t(\tau) = R_t^*(-\tau)$ [62, 76]. Therefore equation (3.3) can be rewritten as

$$\rho(t,\nu) = 2\int_0^{\infty} R_t(\tau)\cos(2\pi\nu\tau)\,d\tau.$$

An important feature of Page distribution is the observation duration of a given frequency. The longer any given frequency ν is observed, the more intense the energy distribution becomes at ν. However, Page distribution is not unique [76]. Turner argued that the assumption which led to Page distribution is unnecessarily restrictive. In other words, it is irrelevant to have the complete history of a signal's past because any signal that is continuously observed for any given finite duration will produce a nonunique instantaneous power spectrum. If a signal observed for different finite time durations had different initial times, the corresponding instantaneous power spectrums will be different. Thus, there is a class of instantaneous power spectrums and Page distribution is a member it. These instantaneous power spectrums or

---

[23] the phrase "time-dependent autocorrelation" is synonymous to the phrases "local autocorrelation." and "instantaneous autocorrelation." Autocorrelation is a special case of autoconvolution.

distributions are related to each other by a complementary distribution, $\rho_c(t,v)$, satisfying the conditions

$$\int_{-\infty}^{\infty} \rho_c(t,v)dv = 0 \quad \text{and} \quad \int_{-\infty}^{\infty} \rho_c(t,v)dt = 0.$$

For example, the sum of Page distribution and the complementary distribution is a new distribution in the class. That is, $\rho(t,v) + \rho_c(t,v) = \rho_n(t,v)$. The introduction of the complementary distribution does not affect the original signal.

Levin [98] generalized Page distribution to include all times. First, he used a contrary assumption to Page but the same argument to derive the complement of Page distribution; namely,

$$\rho_1(t,v) = 2\mathrm{Re}\, g^*(t)\hat{g}_t(v)e^{2\pi ivt}, \tag{3.4}$$

using a future running transform defined on the interval $[t, \infty)$. Considering the distributions based upon the past and future behaviors of a signal as partial distributions of equal weight, Levin defined a generalized Page distribution as the average of the two distributions, $0.5[\rho(t,v) + \rho_1(t,v)]$. If this sum is set to $P(t,v)$ and it is recognized that f and g are complemenary segments of the same signal such that

$$f_t(\tau) = \begin{cases} f(\tau) & \tau < t \\ g(\tau) & \tau \geq t \end{cases},$$

Levin's generalization of Page distribution may be written as

$$P(t,\nu) = \mathrm{Re}\, f^{*}(t)\,\hat{f}(\nu)e^{2\pi i\nu t}. \tag{3.5}$$

This distribution may also be called Page-Levin distribution.

3.1.2 Rihaczek Distribution

Rihaczek distribution [99] was first formulated and introduced into the quantum physics community by Kirkwood [100]. Prior to Rihaczek, many other investigators used this same formula and its variations in the area of time-frequency nonstationary signal processing. However, it was Rihaczek who, aware of the work of several investigators and the seeming interrelationship of their work, reintroduced this time-frequency energy distribution into signal processing under the alias of complex energy density function to shed new light on its meaning in terms of other well-known time-frequency methods, like Page-Levin distribution and ambiguity functions. Rihaczek derived the complex energy spectrum using more than one technique. First, he used the method of Page, wherein a signal is investigated under physical circuit conditions with respect to the signal energy delivered by the source to a complex load. Substituting signal for voltage and the corresponding signal spectrum for current in the energy expression and evaluating, Rihaczek was able to come up with the complex energy density distribution; namely,

$$R(t,\nu) = f(t)\hat{f}^{*}(\nu)e^{-2\pi i\nu t}. \tag{3.6}$$

In a similar manner to Page distribution, the complex energy density distribution, which is usually called Rihaczek distribution, satisfies the conditions for the signal's instantaneous power and energy density spectrum in the time-frequency space, while the sum of the signal energy distribution over the entire time-frequency space yields the total energy. Rihaczek distribution is a general form of Page-Levin distribution. In fact, Page-Levin distribution is the real part of the complex conjugate of Rihaczek distribution.

Another approach that Rihaczek used to obtain equation (3.6) utilized the concept of the autocorrelation function extended into the time-frequency space to get an ambiguity function. From the two-dimensional Fourier transform of the ambiguity function, he, again, derived equation (3.6) via the Fourier transform of the local correlation function. That is

$$\int_{-\infty}^{\infty} f(t)f^{*}(t-\tau)e^{-2\pi j\nu\tau}d\tau = f(t)\hat{f}^{*}(\nu)e^{-2\pi j\nu t}. \qquad (3.7)$$

Comparing equations (3.3) and (3.7), it can be readily seen that equation (3.3) is a special case of equation (3.7). Equation (3.3) can be interpreted as the real even part of the complex conjugate of equation (3.7).

With Rihaczek distribution, $R(t, \nu)$, the signal energy is concentrated in time-frequency space at a location specified by the instantaneous frequency $\nu_i(t) = d\varphi(t)/dt$ and the group delay $\tau(\nu) = -0.5\pi d\theta(\nu)/d\nu$. The variables and are the respective phases of $f(t)$ and its spectrum. The region over which the energy is concentrated in time and frequency at any given instant is

determined by the product of the signal's relaxation time and dynamic bandwidth while the degree of the energy distribution depends on $|f(t)|$ and $|\hat{f}(v)|$ within this area. This product defines each cell size in the time-frequency space. Each cell has an area of one. However, the shape of each cell changes with $dv_i(t)/dt$.

3.1.3 Wigner Distribution

As previously stated in section 3.1, Wigner distribution is the first proposed axiomatic time-frequency distribution, which is bilinear and highly concentrated with many desirable properties and a few significant shortcomings in crossterms, local negativity, and troublesome implementation. In spite of its defects, it is the most investigated and widely used axiomatic time-frequency distribution. The definition of the Wigner distribution of two signals can be expressed in either their time or frequency descriptions because the Wigner distribution of two time signals is symmetrical to the Wigner distribution of their spectrums. That is, for two reasonable well-behaved signals f and g, the Wigner distribution W is such that $W_{f,g}(t,v) = W_{\hat{f},\hat{g}}(v,-t)$. Thus, the definition of the Wigner distribution of two time signals can be easily and equivalently described in terms of their spectrums. The Wigner distribution of two sufficiently well behaved signals f and g is defined as follows:

$$W_{f,g}(t,v) = \int_{-\infty}^{\infty} f(t+\tau/2)g^{*}(t-\tau/2)e^{-2\pi iv\tau}d\tau. \qquad (3.8)$$

This definition of Wigner distribution is usually called the cross-Wigner distribution. A commonly encountered special case of equation (3.8) occurs when f and g are the same signal. This specialized Wigner distribution is usually called the auto-Wigner distribution. Some of the desirable properties Wigner distribution possesses [67, 68] are realness for the auto-Wigner distribution of any signal and realness as well as evenness in frequency for the auto-Wigner distribution of a real signal, shift-invariance in both time and frequency corresponding to an equivalent shift-invariance in the signals, preservation of the time-limitedness and band-limitedness of the signals, satisfaction of the conditions for a signal's instantaneous power and energy density spectrum, existence of the average frequency at a given time and the average time at a given frequency respectively yielding the instantaneous frequency $v_f(t)$ and the group delay $\tau_g(\nu)$ of the signal, and satisfaction of Parseval's relation counterpart in Moyal's formula.

The Wigner distribution is highly concentrated in the time-frequency space. It is amongst the most concentrated time-frequency distribution of any distribution that satisfies the conditions for the instantaneous signal power and the energy density spectrum of the signal [73]. For some signals, the concentration of Wigner distribution is along the instantaneous frequency. This fact is particularly evident in cases where the signals are either purely frequency modulated or slightly amplitude modulated. For example, the concentration of the Wigner distribution of the chirp is totally along $v_f(t)$.

From the definition of Wigner distribution in equation (3.8), the Wigner distribution can be viewed as the Fourier transform of the product signal $f(t + \tau/2)g^*(t - \tau/2)$ with respect to τ; t is a

fixed parameter. This product signal can be interpreted as the local cross-correlation function $R_{f,g}(t, \tau)$. To recover the product signal from the Wigner distribution, the inverse Fourier transform must be taken of the Wigner distribution with respect to the frequency variable v. This inverse Fourier transform of $W_{f,g}(t,v)$ is $f(t + \tau/2)g^*(t - \tau/2)$ and it is defined as follows,

$$f(t + \tau/2)g^*(t - \tau/2) = \int_{-\infty}^{\infty} W_{f,g}(t,v)e^{2\pi iv\tau}\,dv. \tag{3.9}$$

Suppose it is desired to recover the signal f from $W_{f,g}$ independent of the signal g, then by setting $t - \tau/2 = 0$,

$$f(\tau) = \frac{1}{g^*(0)}\int_{-\infty}^{\infty} W_{f,g}(\tau/2,v)e^{2\pi iv\tau}\,dv. \tag{3.10}$$

This means that $f(t)$ is recoverable from the Wigner distribution to within a constant factor $g^*(0)$ at time $t/2$. The signal $g(t)$ can be similarly obtained from the Wigner distribution. Equation (3.9) has other implications. They include instantaneous signal power of $f(t)$ or $g(t)$ and inner product of $f(t)$ and $g(t)$, g may or may not equal to f. An interesting relationship connected to how the inner product relates to Wigner distribution is established in Moyal formula. Moyal's formula expresses the relationship between two sets of inner products and the product of two cross-Wigner distributions. It states that

$$\langle f_1, f_2\rangle\langle g_1, g_2\rangle^* = \int_{-\infty}^{\infty}\int_{-\infty}^{\infty} W_{f_1,g_1}(t,v)\,W^*_{f_2,g_2}(t,v)\,dt\,dv. \tag{3.11}$$

$$\langle f_1, f_2\rangle\langle g_1, g_2\rangle^* = \int\int W_{f_1,g_1}(t,v)\,W^*_{f_2,g_2}(t,v)\,dt\,dv.$$

A significant special case of Moyal's formula occurs when the signals f_1, f_2, g_1, and g_2 are all equal to f. This special case is

$$\|f\|^4 = \int_{-\infty}^{\infty}\int_{-\infty}^{\infty} W^2{}_f(t,v)\,dt\,dv. \tag{3.12}$$

The Wigner distribution of a linear signal space [101] is quite similar to the Wigner distribution of a signal. They share many of the same desirable and undesirable properties. The Wigner distribution of a linear signal space essentially describes the energy distribution of the signal space in the framework of the time-frequency space. It can be expressed in terms of both the projection operator and the bases of the space. To illustrate, a linear signal space X, which is a subspace of $L_2(\mathbb{R})$, is a set of signals and their linear combinations. Now suppose P is a self-adjoint idempotent orthogonal projection operator, Wigner distribution of X, W_X, is expressible in terms the projection operator P of X in the following way:

$$W_X(t,v) = \int_{-\infty}^{\infty} P(t + \tau/2, t - \tau/2)\,e^{-2\pi i v\tau}\,d\tau. \tag{3.13}$$

P is completely recoverable from $W_X(t,v)$ by means of the inverse Fourier transform.

Because Wigner distribution of a signal is bilinear and satisfies the conditions for instantaneous signal power and energy spectral density, it must satisfy the condition for the total energy. In addition, the Wigner distribution must attain local negativity somewhere in the time-frequency space. However, this statement is not always true. There is at least one signal for which the Wigner distribution is positive throughout the time-frequency space. This signal is the gaussian modulated chirp,

$$f(t) = \left(\frac{a}{\pi} \right)^{1/4} e^{-(a/2)t^2 - i(2\pi\nu_0 t - (b/2)t^2)}.$$

For this signal, the Wigner distribution may be considered as a positive distribution [51] rather than a bilinear one.

As aforementioned, crossterms are the most significant drawback of Wigner distribution. They are amplitude modulated oscillatory terms that may be twice as high as the signal terms. Therefore, they can result in misleading analysis of multicomponent signals. A multicomponent signal is the sum of at least two different signals. It possesses the property that allows for multiple (two or more) clearly delineated regions of concentration in the time-frequency space. The Wigner distribution of the sum of two signals does not equal the sum of the Wigner distributions of the individual signals. The cross-Wigner distribution of two multicomponent signals $f_1(t) + f_2(t)$ and $g_1(t) + g_2(t)$ can be described as follows:

$$W_{f_1 - f_2, g_1 - g_2}(t,\nu) = W_{f_1,g_1}(t,\nu) + W_{f_2,g_2}(t,\nu) + W_{f_1,g_2}(t,\nu) + W_{f_2,g_1}(t,\nu) \qquad (3.14)$$

with the result that

$$W_{f-g}(t,\nu) = W_f(t,\nu) + W_g(t,\nu) + 2\mathrm{Re}\,W_{f,g}(t,\nu) \tag{3.15}$$

whenever $f_1 = g_1$ and $f_2 = g_2$ because the realness property of the Wigner distribution states that $W_{f,g}(t,\nu) = W^*_{g,f}(t,\nu)$. While Wigner distribution is an excellent tool for the determination of multicomponent signals, the evidence of the term $2\mathrm{Re}\,W_{f,g}(t,\nu)$ in equation (3.14) leads to the undesired crossterms that may sometimes mar efficient and worthwhile signal analysis to the point of uselessness. These unattenuated high-frequency oscillatory crossterms are located in the time-frequency space midway between the autocomponents of $W_{f-g}(t,\nu)$ with amplitude that may be twice as high. Their frequency of oscillation increases as the time-frequency distance between the autocomponents increases and their direction of oscillation is orthogonal to the imaginary line joining the autocomponent terms. Because of Wigner distribution sensitivity to crossterms resulting from multicomponent signal analysis, Wigner distribution is also particularly sensitive to any break or noise in a signal that masquerades as signal components at unexpected time-frequency locations. To facilitate easy interpretation of Wigner distribution, suppressing the crossterms is almost mandatory. A straightforward approach to crossterms suppression involves lowpass filtering of the Wigner distribution to remove the high-frequency components in the crossterms. However, lowpass filtering of the Wigner distribution comes at the price of broadening of the autocomponent signal terms. Two forms of Wigner distribution that does smoothing are the pseudo-Wigner distribution and the smoothed Wigner distribution.

The pseudo-Wigner distribution of a signal $f(t)$ is defined as follows:

$$PW_f(t,\nu) = \int_{-\infty}^{\infty} f(t + \tau/2) f^*(t - \tau/2) g(\tau) e^{-2\pi i \nu \tau} d\tau. \tag{3.16}$$

The window function $g(\tau)$ brings with it convolution in frequency in the time-frequency space such that

$$PW_f(t,\nu) = W_f(t,\nu) *_\nu g(\nu).$$

On the other hand, the smoothed Wigner distribution performs two-dimensional lowpass filtering so as to reduce the crossterms' oscillation in both time and frequency. The smoothed Wigner distribution can be defined as a two-dimensional convolution of the Wigner distribution W_f and a two-dimensional filter $G(t,\nu)$ in the time-frequency space. Its definition is

$$SW_f(t,\nu) = (W_f * G)(t,\nu) = \int_{-\infty}^{\infty}\int_{-\infty}^{\infty} W_f(\tau,\xi) G(t - \tau, \nu - \xi) d\tau d\xi. \tag{3.17}$$

Usually, physical realization of the Wigner distribution as a time-frequency analysis tool may require some degree of windowing of the signals because a signal's total existence must be known in time before the application of Wigner distribution. Moreover, fast and efficient evaluation of the Wigner distribution employs the process of discretization and the instrument of the DFT, especially in the use of FFT algorithms.

The transition from the continuous Wigner distribution to an alias-free discrete-time or discrete Wigner distribution with the good properties preserved is a difficult task [67, 68, 102]. In fact, the discrete-time Wigner distribution is generally aliased while preserving most of the properties of the continuous case whereas the discrete Wigner distribution is always aliased while sharing all of the properties of the continuous case [102]. However, significant progress has been made with the discrete-time and discrete Wigner distributions in terms of obtaining acceptable solutions to the continuous version. For the discrete-time Wigner distribution, an alias-free version is obtainable for signals that are either oversampled, by at least a factor of two, or analytic. The original idea of the discrete-time Wigner distribution was introduced in [67] and developed in [68]. Claasen and Mecklenbräker used bandlimited signals to introduce the idea of discrete-time Wigner distribution of a sampled bandlimited signal:

$$W_f(nt_s, \nu) = 2t_s \sum_{k=-\infty}^{\infty} f((n+k)t_s) f^*((n-k)t_s) e^{-4\pi i \nu k t_s}, \quad t_s \le (4\nu_{max})^{-1}. \qquad (3.18)$$

They developed this definition of the Wigner distribution for all discrete-time signals. Although the discrete-time Wigner distribution and the discrete-time signal are sampled at the same rate in equation (3.18), at least twice the Nyquist rate of the signal, the signal may be sampled at any rate equal to or exceeding the Nyquist rate. The discrete-time Wigner distribution of Equation (3.18) is alias-free for band-limited and analytic signals.

An alternative approach to the discrete-time Wigner distribution was developed in [102]. Here, Peyrin and Prost derived a discrete-time Wigner distribution that is closely related to the

continuous one whose samples can be obtained from it. They defined the discrete-time Wigner distribution of a discrete-time signal as

$$W_f(n,v) = \sum_{k=-\infty}^{\infty} f(kt_s)f^*((n-k)t_s)e^{-2\pi iv(2k-nt_s}, \tag{3.19}$$

where

$$f = \sum_{n=\infty}^{\infty} g(nt_s)\delta(t-nt_s).$$

The discrete-time Wigner distribution of equation (3.19) can be rewritten in terms of the continuous one, W_g, as

$$W_f(n,v) = \frac{1}{2t_s}\sum_{k=-\infty}^{\infty}(-1)^{nk}W_g\left(\frac{nt_s}{2}, v-\frac{k}{2t_s}\right), \tag{3.20}$$

wherein $W_f(n,v)$ is alias-free for $|v| \le (4t_s)^{-1}$ when g is a bandlimited signal sampled by at least twice the Nyquist rate and for $0 < v \le (2t_s)^{-1}$ when g is an analytic signal sampled at Nyquist rate. Additionally, Peyrin and Prost derived a discrete Wigner distribution of the form,

$$W_f(n,k) = \frac{1}{2N}\sum_{m=0}^{N-1} f(m)f^*(n-m)e^{-2\pi ik/N(m-0.5n)}, \quad 0 \le n,k < 2N \tag{3.21}$$

and

$$f(m) = \sum_{l=-\infty}^{\infty} f(mt_s - lNt_s).$$

Regardless of the type of signal and the nature of sampling, $W_f(n,m)$ will contain aliasing because a signal cannot be simultaneously limited in time and in frequency. However, practically alias-free $W_f(n,m)$ is achievable.

Although the Wigner distribution is symmetrical and Rihaczek distribution is asymmetrical, they are related through the asymmetrical narrow-band ambiguity function. The Wigner distribution is the two-dimensional time-frequency convolution of Rihaczek distribution and a complex exponential. This convolution can be described as

$$\begin{aligned} W(t,\nu) &= (R * \chi_2)(t,\nu) \\ &= \int_{-\infty}^{\infty}\int_{-\infty}^{\infty} \chi_2(\tau,\xi) R(t-\tau,\nu-\xi)\,d\tau\,d\xi, \quad \chi_2(t,\nu) = e^{4\pi i\nu t}. \end{aligned} \tag{3.22}$$

Moreover, Wigner distribution and Rihaczek distribution can be generalized into one distribution that assimilates both distributions. This distribution [50, 79] has the form

$$G_{f,g}(t,\nu) = \int_{-\infty}^{\infty} f(t + (1/2 - \alpha)\tau) g^*(t - (1/2 + \alpha)\tau) e^{-2\pi i\nu\tau}\,d\tau, \quad \alpha \in \mathbb{R}. \tag{3.23}$$

From equation (3.22), Wigner distribution $W_{f,g}$ results when $\alpha = 0$ while Rihaczek distribution $R_{f,g}$ results at $\alpha = 0.5$. Nonetheless, some investigators believe that compared with Rihaczek distribution, the unaltered symmetrical nature of Wigner distribution makes it unsuitable for

revealing simple physical relationships among distributions through its dual, the symmetrical ambiguity function [99].

3.1.4 Ambiguity Function

In general, the ambiguity function is essentially an application-oriented two-dimensional correlation function [59, 69, 99, 103, 104, 105, 106] of two necessarily related signals. Each signal is usually a fixed frequency harmonic carrier signal modulated with a slowly varying complex envelope signal. The correlation function is a special instance of convolution. Generally, correlation is the convolution of a signal and the complex conjugate of a time-reversed signal. The correlation function has properties that are not generally consistent with convolution. If the correlated signals are real, the correlation function is even and achieves its maximum at the origin. In addition, the correlation function does not commute. In the L_2 – sense of square integrable functions (signals), this correlation operation can also be interpreted as an inner product [11, 59, 104, 105, 107] between two related signals of interest wherein the ambiguity function is a reality of the matched filter response. In fact, a central purpose of the ambiguity function is to estimate the delay-doppler (or range-velocity) coordinates of point objects and, more generally, to estimate the object (target) density function[24] as well as, perhaps, determine estimates of the delay-doppler coordinates that maximize it so that recognition can be made of objects in the environment. In other words, the ambiguity function

---

[24] In this sense, density function is also referred to by other names. They include spread function, spreading function, reflectivity function, reflectivity process, and reflectivity density.

does not uniquely determine the number of objects, their range or doppler coordinates, except in the limiting case of theoretical idealism [106]. Thus, the ambiguity function is a measure of the ambiguous resolution of an object and its coordinates in a dense environment. The object density function describes the distribution of objects in the environment under study. It may be viewed as either deterministic or probabilistic depending on the accuracy required in its computation. Sometimes, using the ambiguity surface (magnitude squared of the ambiguity function) is preferable to the ambiguity function. The ambiguity surface gives a more intense presence of a resolved object. Moreover, in a distributed object environment, its expected value, which is called the object scattering function, provides a better estimate of the resolved object(s) than the density function [106, 108, 109]. The scattering function is the probabilistic expected intensity[25] of the density function viewed from the perspective of a random process. It may be considered an image of the resolved object. The expected value of the ambiguity surface is the second-order statistic of the ambiguity function. Overall, the ambiguity function is the filtered version of the object density function and its second-order statistic is the filtered version of the object scattering function.

The ambiguity function is subdivided in two general classes of functions. One class is called the wide-band ambiguity function and the other is called the narrow-band ambiguity function. In each class, the ambiguity function is defined in several equivalent mathematical ways as indicated in [62, 69, 103, 104, 105, 106, 110, 111, 112]. Each definition has its advantages

---

[25] The phrase "probability expected intensity" is used to mean the expected value of the magnitude squared of the density function.

regarding its application to a particular problem. Some differences in the related forms of the definition of the ambiguity function are minor; they include use of signs, placement of complex conjugation, compression of delay, and relationship between the transmitted and received signals. However, at least in the narrow-band class, there is a seemingly significant difference in the appearance of the asymmetrical form and the symmetrical form of the ambiguity function [104]. Although the classes of ambiguity functions are distinctively different in form and supporting mathematics, they are functionally alike and are mathematically equivalent under appropriate but special parametric conditions [11, 106]. Two important requirements for the wide-band ambiguity function to become the narrow-band ambiguity function relate to the relative difference between the velocity (v)[26] of the object and the velocity (c) of the emitted signal in the transmission medium, and to the value of the fractional bandwidth, B_{v_0}, of the emitted signal. The emitted signal is targeted to the object and it is assumed to have a fixed time-bandwidth product. In general, the narrow-band ambiguity function is an approximation of the wide-band ambiguity function when either or both of the following two conditions hold:

- B_{v_0} is relatively small -- usually less than 0.1;
- For an emitted signal of fixed time-bandwidth product TB, $2 \mid TBv \mid \ll c$.

Of the several equivalent definitions for the wide-band and narrow-band ambiguity functions, the definitions used in this research will be chosen for their consistency with each other and with linear time-frequency (scale) representations while retaining the appropriate relationships with bilinear distributions.

---

[26] This symbol "v" is also used to mean frequency; its exact usage will be made clear by the context.

Suppose f and g are finite energy signals in that they are contained in $L_2(\mathbb{R})$ and consequently satisfy the inner product condition, if $f(t)$ is the received (or input) signal and $g(t)$ is the emitted signal that generates the basis signals, then for $f(t)$, the wide-band ambiguity function can be defined as follows,

$$\tilde{A}_{f,g}(\tau, u) = \sqrt{u}\int_{-\infty}^{\infty} f(t)g^{*}(u(t-\tau))dt, \quad u > 0, \tag{3.24}$$

where for a point object

$$f(t) = \sqrt{\gamma}g(\gamma(t-x)), \quad x, \gamma \in \mathbb{R} \text{ with } \gamma > 0, \tag{3.25}$$

and for a distributed object or distributed objects in an environment

$$f(t) = \int_{0}^{\infty}\int_{-\infty}^{\infty} D(x,\gamma)\sqrt{\gamma}\, g^{*}(\gamma(t-x))dxd\gamma. \tag{3.26}$$

The scale factor $\sqrt{u}$ is used to ensure that the energy in the emitted signal is conserved in the received signal and the density function $D(x,\gamma)$ is the density of the object(s) at distance x and velocity γ. When the object(s) in the environment are moving relatively slowly ($|v| \ll c$) and/or the fractional bandwidth of the emitted signal is relatively small ($B_{\nu_0} < 0.1$), the wide-band ambiguity function can be approximated by the narrow-band ambiguity function. This is because the stated conditions of the doppler effect, which previously resulted in dilation of the return signal in the wide-band model approximation, now results in a doppler frequency shift in the return signal through an approximation of the wide-band model [11]. As a consequence, the

narrow-band model approximation of the return signal is created from the wide-band model. In other words, $f(t) = \sqrt{\gamma} g(\gamma(t - x)) \approx g(t - s)e^{2\pi i z t}$. Accordingly, the narrow-band ambiguity function derived from an approximation of the wide-band version can be written in the following form,

$$A_{f,g}(\tau, u) = \int_{-\infty}^{\infty} f(t) g^{*}(t - \tau) e^{-2\pi i u t} dt, \tag{3.27}$$

where for a point object

$$f(t) = g(t - s)e^{2\pi i z t} \tag{3.28}$$

and for a distributed object or distributed objects in an environment

$$f(t) = \int_{-\infty}^{\infty} \int_{-\infty}^{\infty} D(s, z) g(t - s) e^{2\pi i z t} ds dz. \tag{3.29}$$

In general, the emitted signal $g(t) = h(t)X_{\nu_0}(t)$ with $h(t)$ being a slowly varying complex envelope of the harmonic carrier signal $X_{\nu_0}(t) = e^{2\pi i \nu_0 t}$. When the equations describing $f(t)$ are substituted into the equations for the wide-band and narrow-band ambiguity functions, these ambiguity functions result in forms that are dependent on their respective related auto-ambiguity functions [105, 106, 108, 109]. For point objects, these forms are merely

$$\tilde{A}_{f,g}(\tau, u) = \tilde{A}_{g}(\gamma(\tau - x), u/\gamma)$$

and

$$A_{f,g}(\tau, u) = e^{-2\pi i(u-z)\tau} A_g(\tau - s, u - z)$$

for the respective wide-band and narrow-band models of the received signal $f(t)$, where $\tilde{A}_g = \tilde{A}_{g,g}$ and $A_g = A_{g,g}$ are the wide-band and narrow-band auto-ambiguity functions of the signal $g(t)$. In the general case of distributed objects,

$$\tilde{A}_{f,g}(\tau, u) = \int_0^{\infty} \int_{-\infty}^{\infty} D(x, y) \tilde{A}_{g,g}(y(\tau - x), u/y) dx dy \tag{3.30}$$

and

$$A_{f,g}(\tau, u) = \int_{-\infty}^{\infty} \int_{-\infty}^{\infty} D(s, z) A_{g,g}(\tau - s, u - z) e^{-2\pi i(u-z)s} ds dz, \tag{3.31}$$

where equation (3.30) represents wide-band convolution on the affine group and equation (3.31) represents twisted convolution (or convolution on the Heisenberg group) [106]. One can, therefore, deduce from the analysis and synthesis equations relating to the ambiguity functions that the ambiguity function is the smoothed density function and as such, it is an image of the target. It is of course possible to express the narrow-band ambiguity function as the regular two-dimensional convolution, but this can only be done probabilistically with second-order statistics, which require the scattering function be used in place of the density function. Therefore, equation (3.31) can be reformulated as

$$E[|A_{f,g}(\tau, u)|^2] = \int_{-\infty}^{\infty}\int_{-\infty}^{\infty} S(s,z)\,|A_{g,g}(\tau - s, u - z)|^2\,ds\,dz,$$
$$S(s,z) = E[|D(s,z)|^2]. \tag{3.32}$$

When the density functions of equations (3.30) and (3.31) represent point objects, they are expressible as delta functions, and the cross-ambiguity functions of equations (3.30) and (3.31) degenerate into the corresponding wide-band and narrow-band auto-ambiguity functions. That is, if $D(x,y) = \delta(x-a)\delta(y-b)$, for any $a \in \mathbb{R}$ and any $b \in \mathbb{R}^+$, and if $D(s,z) = \delta(s-c)\delta(z-d)$, for any $c, d \in \mathbb{R}$, the wide-band and narrow-band cross-ambiguity functions of equations (3.30) and (3.31) become

$$\tilde{A}_{f,g}(\tau, u) = \tilde{A}_g(b(\tau - a), u/b)$$
$$\text{and} \tag{3.33}$$
$$A_{f,g}(\tau, u) = e^{-2\pi i(u-d)c} A_g(\tau - c, u - d)$$

respectively. The equations of equation (3.33) agree with those obtained under the assumption that a point object is being studied. The auto-ambiguity functions in equation (3.33) are not in their usual forms. The usual form of the wide-band auto-ambiguity function is obtained when $a = 0$ and $b = 1$. It is formulated as

$$\tilde{A}_g(\tau, u) = \sqrt{u}\int_{-\infty}^{\infty} g(t)g^*(u(t-\tau))\,dt, \quad u > 0. \tag{3.34}$$

Similarly, the usual form of the narrow-band auto-ambiguity function is obtained when $c = 0$ and $d = 0$. It has the form

$$A_g(\tau, u) = \int_{-\infty}^{\infty} g(t)g^*(t-\tau)e^{-2\pi i u t}dt. \tag{3.35}$$

It can be easily seen from equations (3.34) and (3.35) that they correspond to equations (3.24) and (3.27) exactly whenever $f(t) = g(t)$.

Many properties of the wide-band and the narrow-band ambiguity functions are similar [111]. Some of these properties are even identical. For example, both types of auto-ambiguity functions are unique in that the auto-ambiguity of one signal[27] is equal to the auto-ambiguity of another signal if and only if the two signals are linearly dependent almost everywhere and differ by ± 1. The wide-band ambiguity function achieves its maximum value at $(\tau, u) = (0, 1)$. For the auto-ambiguity function, it is obvious from equation (3.34) that $\bar{A}_g(0, 1) = \int |g(t)|^2 dt$ is this maximum. While for most practical purposes the volume under the wide-band ambiguity surface is approximately equal to the signal energy, the signal energy is, indeed, only a lower bound [112, 113]. In fact, the volume under the wide-band ambiguity surface may not converge. For example, it does not converge for the gaussian envelope pulse. In addition, the signal can be recovered from the wide-band ambiguity function using at least two methods. One method involves the interpretation and reformulation of the wide-band ambiguity function as a wavelet

---

[27] Reminder: all signals are assumed to represent functions that belong to Hilbert space.

transform prior to the inversion process [106]. The second method brings to bear the expression of the wide-band ambiguity function as the Fourier transform of the product of the signals' spectrums, from which inversion follows [111].

The narrow-band ambiguity function is usually called the conventional ambiguity function. It is sometimes called Woodward's ambiguity function. It has an asymmetrical form. The theory of the ambiguity function[28] is mature and its properties are reasonably well understood. Moreover, it is widely used in several applications. Much of the theory and many properties of the conventional ambiguity function can be found in [49, 103, 104, 114, 115]. The conventional ambiguity function

$$A_{f,g}(\tau, u) = \int_{-\infty}^{\infty} f(t) g^{*}(t - \tau) e^{-2\pi i u t} dt$$

is expressible in an equivalent but symmetrical form to within a phase factor. That is,

$$A_{f,g}(\tau, u) = e^{-\pi i u \tau} B_{f,g}(\tau, u),$$

where

[28] From this point, the phrase "ambiguity function" means "narrow-band ambiguity function."

$$B_{f,g}(\tau, u) = \int_{-\infty}^{\infty} f(t + \tau/2) g^{*}(t - \tau/2) e^{-2\pi i u t} dt \qquad (3.36)$$

is the symmetrical ambiguity function [13, 51, 69, 81, 110, 116, 117, 118]. The theory of symmetrical ambiguity function is consistent with that of the conventional ambiguity function. These two types of ambiguity functions have properties that are equivalent and sometimes identical. Depending on the definition of the ambiguity function, it can be shown that the conventional ambiguity function is the characteristic function of Rihaczek distribution and that the symmetrical ambiguity function is the characteristic function of the Wigner distribution. Because distributions are dependent on time and frequency, the conventional and the symmetrical ambiguity functions can be interpreted as the two-dimensional Fourier transforms [53][29] of the Rihaczek and the Wigner distributions respectively. Using the above definitions of the ambiguity functions, it can be said that the conventional ambiguity function is related to the Rihaczek distribution by the two-dimensional Fourier transform of the form

$$A_{f,g}(-\tau, u) = \int_{-\infty}^{\infty} \int_{-\infty}^{\infty} R_{f,g}(t, v) e^{-2\pi i (ut - v\tau)} dt\, dv, \qquad (3.37)$$

while the symmetrical ambiguity function is similarly related to the Wigner distribution with the form

---

[29] Of course, it is equally valid to use the interpretation of the inverse two-dimensional Fourier transform.

$$B(-\tau, u) = \int_{-\infty}^{\infty}\int_{-\infty}^{\infty} W_{f,g}(t, v)e^{-2\pi j(ut - v\tau)}dt\,dv. \qquad (3.38)$$

The ambiguity function can be generalized in the same way that the Rihaczek and the Wigner distributions are folded into one distribution. The generalized ambiguity function [110] is defined as follows:

$$H_{f,g}(\tau, u) = \int_{-\infty}^{\infty} f(t + (1/2 - \alpha)\tau)g^{*}(t - (1/2 + \alpha)\tau)e^{-2\pi jut}dt, \quad \alpha \in \mathbb{R}. \qquad (3.39)$$

This ambiguity function degenerates into the conventional ambiguity function whenever $\alpha = 0.5$ and into the symmetrical ambiguity function when $\alpha = 0$. From equations (3.37) and (3.38), it is obvious that equation (3.23) and equation (3.39) constitute a Fourier transform pair. Besides representing ambiguity functions in terms of the time description of the pertinent signals, they may be equally represented as the Fourier spectrums of these signals. Moreover, the relationship between ambiguity functions and distributions clearly suggests that the ambiguity functions are bilinear functions with crossterms as an inherent property. Nevertheless, the duality relationship between ambiguity functions and other bilinear time-frequency representations such as Wigner and Rihaczek distributions can be useful in the analysis of highly complicated signals. With a highly complicated signal, crossterms may obscure worthwhile analysis of the relevant time-frequency distribution. In these situations, putting the signal in the appropriate ambiguity space may make it analyzable because the auto-

terms of the ambiguity function are centrally concentrated at the origin while the crossterms are concentrated away from the origin.

As previously mentioned, the ambiguity function is a two-dimensional correlation function in time and frequency. Two other equally important interpretations of the ambiguity function are possible from viewing the expressions of the ambiguity function as a Fourier transform and as an inner product [104]. Each interpretation readily leads to a different set of properties. In addition, properties obtained for the conventional and the symmetrical versions of the ambiguity function, under each interpretation, may be seemingly different. Thus, it follows that $A_{f,g}$ is naturally more workable in situations where $B_{f,g}$ may not be, and vice versa. An important property of the symmetrical auto-ambiguity function B_f relates to its surface being generable by the surface of another ambiguity function B_g, f and g are not necessarily unrelated signals, through the operation of elliptical rotation about the origin. From now on in this section, the focus will be on the conventional ambiguity function.

From the viewpoint of the Fourier transform, the product signal $f(t)g^*(t-\tau)$, which may additionally be viewed as a local cross-correlation, is recoverable from the ambiguity function $A_{f,g}$ by means of inverse Fourier transformation; namely,

$$f(t)g^*(t-\tau) = \int_{-\infty}^{\infty} A_{f,g}(\tau, u)e^{2\pi iut}\,du. \tag{3.40}$$

If the signal to be recovered from the ambiguity function, $A_{f,g}(\tau, u)$, is $f(t)$, then for $\tau = t$

$$f(t) = [g^*(0)]^{-1} \int_{-\infty}^{\infty} A_{f,g}(\tau, u) e^{2\pi i u t} dt.$$

By applying the Fourier transform to equation (3.40), the inverse relationship of equation (3.37) is obtained. Many properties of the ambiguity function can be deduced from equations (3.27) and (3.40). For example, the auto-ambiguity function attained its maximum value at the origin where it equals the signal's energy and thereafter tapers off. That is,

$$|A_f(\tau, u)| \leq A_f(0, 0) = \int_{-\infty}^{\infty} |f(t)|^2 dt.$$

Besides, Woodward's condition on the auto-ambiguity function, as described in

$$\int_{-\infty}^{\infty} \int_{-\infty}^{\infty} |A_f(\tau, u)|^2 d\tau du = \int_{-\infty}^{\infty} |f(t)|^2 dt,$$

states that the concentration of an auto-ambiguity function cannot be arbitrarily close to the origin. This condition is commonly referred to as the radar uncertainty principle. The expression $|A_f(\tau, u)|^2$ is the ambiguity surface.

In the framework of inner products, the ambiguity function can be written in compact form as

$$A_{f,g}(\tau, u) = \langle f, g_{\tau,u} \rangle, \quad g_{\tau,u} = g(t - \tau) e^{2\pi i u t}, \tag{3.41}$$

but from Plancheral theorem, which relates the inner product of two signals to the inner product of their Fourier spectrums,

$$A_{f,g}(\tau, u) = \langle \hat{f}, (g_{\tau,u})\hat{} \rangle, \quad \hat{f}(v) = \int f(t) e^{-2\pi i v t} dt.$$

and

$$\langle \hat{f}, (g_{\tau,u})\hat{} \rangle = e^{-2\pi i u \tau} A_{\hat{f},\hat{g}}(u, -\tau), \quad (g_{\tau,u})\hat{}(v) = e^{2\pi i u \tau} \hat{g}_{u,-\tau}(v). \tag{3.42}$$

Apart from expressing the ambiguity function as the inner product of two signals, the inner product of the two ambiguity functions can be established to show the relationship of the relating signals. This relationship is the essence of Moyal's formula. It states

$$\langle A_{f_1,g_1}, A_{f_2,g_2} \rangle = \langle f_1, f_2 \rangle \langle g_1, g_2 \rangle^*. \tag{3.43}$$

An important special case of this formula occurs when the two ambiguity functions are auto-ambiguity functions of the same signal. This special case may be expressed as $\| A_f \|^2 = \| f \|^4$.

The aforementioned method of recovering a signal $f(t)$ from its associated ambiguity function makes use of inverse Fourier transformation in the Fourier interpretation, but a more straightforward and elegant approach brings to bear the inner product interpretation. It states that

$$f(t) = \int_{-\infty}^{\infty}\int_{-\infty}^{\infty} A_{f,g}(\tau,u)g(t-\tau)e^{2\pi iut}d\tau\,du. \tag{3.44}$$

Observe that this equation is the same as equation (3.29) with the ambiguity function and density function interchanged.

Previously it was stated that the volume under the auto-ambiguity surface has a total ambiguity equal to the signal's energy. In general, the product of two ambiguity functions is equal to the two-dimensional Fourier transform of a related product of two ambiguity functions. The Fourier relationship that states

$$\begin{aligned} &A_{f_1,g_1}(-t,v)A^{*}_{f_2,g_2}(-t,v) \\ &\quad = \int_{-\infty}^{\infty}\int_{-\infty}^{\infty} A_{f_1,f_2}(\tau,u)A^{*}_{g_1,g_2}(\tau,u)e^{-2\pi i(ut-v\tau)}du\,d\tau, \end{aligned} \tag{3.45}$$

leads to a very significant result if the signals are identical. This result shows that not only an auto-ambiguity surface is its own Fourier transform but its rotation by $90°$ is invariant under two-dimensional Fourier transformation. Within the integral, the product

$e^{-2\pi iut}A^{*}_{f,g}(\tau,u) = A_{g,f}(-\tau,-u)$.

The discrete ambiguity function is obtainable from the ambiguity function through the process of sampling over the points of a lattice in the time-frequency plane. Different lattices usually lead

to discrete ambiguity functions with different norm-square energy. There are many ways to sample the ambiguity function. If the signals f and g of the ambiguity function are members of Schwartz space, Poisson summation formula is an elegant and useful procedure in getting the samples. The details of the discretization procedure and the implementation issues of the discrete ambiguity function can be found in [114, 120, 121, 122].

3.2 Linear Time-Frequency Methods

Any linear signal representation may take the form of a continuous or discrete weighted sum of kernel signal. The kernel signal may be as simple as an unit impulse or a complex exponential, or may be an arbitrary elementary signal as sophisticated as a gaussian pulse or gaussian enveloped chirp. A kernel signal may or may not generate a basis in the strict mathematical sense because the generated basis signals may form a redundant set. The basis signals may not even be an orthogonal set because they generally form a nonorthogonal set. However, they must constitute a complete set, at least, in the mean-square sense. Moreover, it is often desirable for the kernel signal to be carefully chosen to induce a convergent signal representation whose computation is amenable to easy implementation with efficient algorithms that lead to clear visualization and unencumbered signal analysis. This linear signal representation can be described abstractly with Fredholm integral equation of the first type or its discrete counterpart. Furthermore, all linear signal representations satisfy the superposition principle. Thus, they do not suffer from the crossterms problem of bilinear signal representations in the time-frequency space. Because of the lack of crossterms resulting from

the processing of multicomponent signals in the time-frequency space, linear time-frequency techniques are efficient tools in the computation, visualization and analysis of multicomponent signals. These linear time-frequency methods convert a one-dimensional time (or frequency) signal into a two-dimensional mixed time-frequency signal. However, each method has its own way of accomplishing the dimension conversion task and describing the signal in the new domain. Examples of linear time-frequency techniques include phi-transform [123], wavelet transform, fractional Fourier transform [124], short-time Fourier transform, Weyl-Heisenberg expansion, and Zak transform (Weil-Brezin map Gel'fand mapping, or *kq*-representation). Actually, psi-transform and wavelet transform are not true time-frequency techniques, but instead they are time-scale techniques. Nonetheless, the psi-transform and wavelet transform can be adapted to time-frequency operations. With the wavelet transform, the scale parameter is interpretable as inverse frequency normalized to the center frequency of the analyzing wavelet. A significant difference between psi-transform and wavelet transform lies in the fact that the sets of kernel signals used in the analysis and synthesis forms of psi-transform are always nonorthogonal and generally different.

The short-time Fourier transform is a natural extension of the Fourier transform. It is intimately related to the Zak transform and Weyl-Heisenberg expansion, and is functionally related to the wavelet transform. The short-time Fourier transform overcomes the lack of time localization of the frequency components in the Fourier transform and the lack of frequency localization of the time instants in the inverse Fourier transform. This time and frequency localization of the signal components by the short-time Fourier transform is accomplished through the means of

progressive windowing operations of the signal and correspondingly performing successive Fourier operations on the windowed portion of the signal over the window duration. Since the Fourier operations are only partial, they can be viewed as partial transforms. When the window signal[30] of the short-time Fourier transform is the impulse train, the short-time Fourier transform becomes the Zak transform to within a phase factor. The synthesis form of the short-time Fourier transform is the continuous version of Weyl-Heisenberg expansion. When this synthesis formula is approximated by its sampled version wherein the time-frequency sample values of the short-time Fourier transform are the expansion coefficients, Weyl-Heisenberg expansion is obtained [1, 38, 58, 110]. Because the short-time Fourier transform is an adaptive form of the Fourier transform, it follows that Zak transform and Weyl-Heisenberg expansion are also adaptive forms of Fourier analysis and synthesis respectively. In fact, the short-time Fourier transform and the Zak transform preserve many properties of the Fourier transform [50, 64, 125, 126]. They efficiently use available powerful FFT algorithms. The short-time Fourier transform is functionally equivalent to the wavelet transform. However, they have different group representations. In terms of group theory interpretation, the short-time Fourier transform is the matrix elements of unitary irreducible representations of the three-dimensional Heisenberg group and the wavelet transform is the matrix elements of unitary irreducible representations of the two-dimensional affine group. More interestingly, in the limit, the short-time Fourier transform is obtainable from the wavelet transform by a contraction process because the

---

[30] The window signal goes by several names. They include analysis (synthesis) signal, analysis (synthesis) window, analyzing (synthesizing) signal, kernel, kernel function, reference signal, elementary signal, and fiducial vector.

Heisenberg group is a contraction of the product group consisting of the affine group and the additive real numbers group [11]. Therefore, it can be inferred that the short-time Fourier transform and the wavelet transform are in some sense complementary transforms. Further, the efficacy of either transform over the other in signal analysis and synthesis is application dependent. While the short-time Fourier transform or the wavelet transform is perhaps more meritorious in a particular application, over a class of applications neither one may have a decided advantage in describing the details in a signal.

In Gabor's seminal work on Weyl-Heisenberg expansion of a signal, he laid the foundation for the theoretical basis for time-frequency signal processing. One main factor that motivated Gabor's signal expansion is the practical concern for real signals in analysis, synthesis, and transmission by voice and image. These signals are either time-limited or bandlimited. Their dual representations can be made essentially limited over the inverse duration. The physically imposed requirement of time and frequency limitation on a signal is the philosophy behind time-frequency representation and processing of most real signals. Further, the simultaneous existence of time-limitedness and bandlimitedness of a signal results in its description over an effective time-frequency area of finite extent, equivalent to the signal's time-bandwidth product[31]. This suggests that the actual number of expansion coefficients must be finite. The effective time-frequency domain is subdivided into data cells of unit area with each cell occupying one coefficient. As in any new exercise, Gabor's endeavor had some inherent flaws.

---

[31] Time-bandwidth product is the product of the signal's time duration and spectral duration.

Lerner in [1] introduced improvements into Gabor's Weyl-Heisenberg expansion theory with regard to the Weyl-Heisenberg (Gabor-wavelet) system and its degrees of freedom. He raised three objections to Gabor's definition of a signal's duration and then showed that the definition of duration (or bandwidth) is arbitrary, sometimes leading to a time-bandwidth product with a lower bound of zero [37]. Lerner generalized the concept of the elementary signal of the Weyl-Heisenberg system from the gaussian to any arbitrary finite energy signal of desired properties having no strict obedience to any particular arbitrary definition of a time-bandwidth product[32] and stressed that the choice of the time translate sample interval should be carefully decided because the selection of this sample interval is as important as the choice of the elementary signal in determining the values of the Weyl-Heisenberg expansion coefficients and the least number of coefficients needed to represent the signal adequately. With proper choice of the time translate sample interval of the window signal, an apparently sophisticated signal may have practically all its signal energy concentrated in a small number of expansion coefficients that are less than the time-bandwidth product of concern, thereby seemingly violating any strict reliance on Weyl-Heisenberg (or any equivalent) uncertainty relationship which is used to specify the time-bandwidth product as a measure of the number of samples required accurately to represent a signal within acceptable error. Generally, the time-bandwidth product is a meritorious estimate of the number of expansion coefficients that may be needed to represent a signal but its quantitative value depends on the adopted definition of duration and the analyzed signal.

---

[32] It may be said, nonetheless, that signals having reasonably high time-bandwidth product can be readily assumed to be time and band limited because the relevant estimation error is quite small.

Lerner, further, pointed out that these expansion coefficients are the time-frequency sample values of the short-time Fourier transform characterized by the time-frequency space lattice constants, which are the respective time and frequency sample intervals of the Weyl-Heisenberg system.

Weyl-Heisenberg systems are generally nonorthogonal "overcomplete" sets [127, 128]. They may generate Weyl-Heisenberg frames provided that their associating lattice parameters have products equal to or less than one with time parameters not greater than the windows' duration regardless of the frequency parameter values, the window signals have finite support of length equal to the inverse of the frequency parameter of the lattice constants and the infinite sum of the modulus squared of the time translated window signals are bounded below and above by positive constants, almost everywhere, or the modulus squared of the Zak transform of the window signals are bounded below and above by the frame bounds, which are positive constants. Whenever a Weyl-Heisenberg system constitutes a frame (Weyl-Heisenberg frame), the corresponding Weyl-Heisenberg expansion over it not only reliably reconstructs the relevant signal from the expansion coefficients but, in principle, the reconstruction can be done using numerically stable algorithms. This expansion includes in it the use of the dual window signal from the dual Weyl-Heisenberg frame. The dual window is in essence a multiple of the window signal [47]. Although, computation of the dual window, which is defined in terms of the window, is highly constraint by frame[33] bounds, its expression in terms of Zak transform is

---

[33] The Weyl-Heisenberg frame bounds and the dual Weyl-Heisenberg frame bounds are inversely related.

simple and elegant [49]. The Zak transform of the dual window is equal to the inverse of the conjugated Zak transform of the window. The frame bounds are generally difficult to find, even to within good approximation. However, finding good estimates of the Weyl-Heisenberg frame bounds for the cases of tight and snug frames may be elementary and determining the nature of the dual window becomes a simple matter. When a Weyl-Heisenberg frame is tight with bounds equal to one, its dual frame is equivalent to it, correspondingly the inherent dual window is just the same as the window, and resultingly the Weyl-Heisenberg frame is an orthonormal basis under the assumption of a normalized window signal. More generally, a tight Weyl-Heisenberg frame may or may not be orthogonal [128, 129], but more accurately, tightness of a Weyl-Heisenberg frame only occurs under the conditions of orthogonality of the Weyl-Heisenberg system defined on the complementary lattice parameters. Furthermore, a Weyl-Heisenberg system whose linear span is dense in Hilbert space of finite energy signals guarantees that the Weyl-Heisenberg system of complementary lattice parameters is weakly linearly independent. Whenever a tight Weyl-Heisenberg frame exists, the frame bounds equal to the product of two factors [47] of the corresponding Weyl-Heisenberg system: the inverse of the product of the lattice parameters and the energy of the window signal. Clearly, when the window signal is normalized to unit energy and the lattice parameters are both equal to unity, the Weyl-Heisenberg frame is an orthonormal basis with restrictions on the behavior of the window signal in time and frequency. These restrictions, which are a consequence of Balian-Low theorem and its derivatives [47, 129, 130], can be summarized as the window signal cannot be well-localized simultaneously in time and frequency. They extend beyond orthonormality and tightness of the Weyl-Heisenberg frame. They are conditioned on the simple fact of the lattice parameters being

equal with product equal to one. In this context, the related Balian-Low theorems also prohibit a window signal that shares smooth and rapid decay properties with its dual from being a Weyl-Heisenberg frame. These inhibitive theorems are a reflection of the inverse time frequency relationship in the time-bandwidth product, which in terms of the Heisenberg uncertainty relation is essentially lower bounded by the inverse of four pi $(4\pi)^{-1}$. In spite of the imposed constraints on a Weyl-Heisenberg system that constitutes a Weyl-Heisenberg frame, it is still possible to find window signals with tight Weyl-Heisenberg frames having good time and frequency localization properties [131]. These window signals, instead of having one peak, are bimodal.

While the idea of Weyl-Heisenberg frames is an efficient means to determine the conditions under which the degrees of freedom of a Weyl-Heisenberg system result in numerically stable Weyl-Heisenberg expansions, it is not explicitly essential. It was previously stated that Zak transform can be used to establish the existence of Weyl-Heisenberg frames and to determine a simple expression of the dual window. In fact, without any knowledge of the concept of frames, Zak transform can be used to determine necessary and sufficient conditions for viable Weyl-Heisenberg expansions over a Weyl-Heisenberg system [1, 125, 132, 133, 134]. *Essentially, numerically stable Weyl-Heisenberg expansions are possible over "a complete and* orthogonal" Weyl-Heisenberg system when the modulus of Zak transform of the window signal is a constant almost everywhere. However, these expansions become generally impossible or quite numerically unstable when Zak transform of the window signal is continuous in time and frequency as a consequence of a smooth and rapidly decaying signal. A continuous Zak

transform guarantees at least one zero in Zak space forced upon it by the time and frequency periodicity conditions. This statement is the gist of the zero theorem [132], which is related to Balian-Low theorem. Weyl-Heisenberg systems consisting of window signals like the gaussian pulse and the sinc lead to unreliable Weyl-Heisenberg expansions whenever they are forced to become orthonormal bases because they will experience zeros in Zak space.

In the subsections that follow illustrative examples of linear time-frequency representations will be expounded. These examples are wavelet transform, short-time Fourier transform, Weyl-Heisenberg expansion, and Zak transform. They will be described in terms of time signals, but each has a dual representation in frequency. They will provide some insightful clues as to the general character of all linear time-frequency techniques, their relatedness, and their relationship to bilinear distributions. Furthermore, Zak transform will be put at a center stage of linear time frequency representations as a representational tool similar to the Fourier analysis in the study of stationary signals.

3.2.1 Wavelet Transform

The wavelet transform is essentially the wide-band ambiguity function with an expanded interpretation. To illustrate, the wide-band ambiguity function was defined as

$$\tilde{A}_{f,g}(\tau, u) = \sqrt{u}\int_{-\infty}^{\infty} f(t)g^{*}(u(t-\tau))dt, \quad u > 0;$$

with $u = a^{-1}$, the structural definition of the wavelet transform is obtained; namely,

$$\tilde{A}_{f,g}(\tau, a^{-1}) = \sqrt{a^{-1}} \int_{-\infty}^{\infty} f(t) g^{*}(a^{-1}(t-\tau)) dt, \quad a \neq 0. \tag{3.46}$$

In this definition, the scale (dilation[34]) factor a is free to assume any real value except zero. The signal $f(t)$ is still the one being investigated and it is now simply referred to as the analyzed signal. The signal $g(t)$ remains the essence of the basis signals but it now assumes the role of the analyzing wavelet while the basis signals assume the role of the corresponding wavelets. Furthermore, the relationship between $f(t)$ and $g(t)$ in the transform is different. Instead of maintaining nonlinearity of the wide-band ambiguity function, the wavelet transform of a signal is interpreted as being linear with respect to the analyzing wavelet. In essence, the wavelet transform is a special interpretative generalization of the wide-band ambiguity function with the analyzing wavelet constituting the set of fixed shape wavelets produced from it through the process of time translations and dilations. However, there is restriction on the class of finite energy signals that makes up valid analyzing wavelets suitable for the analysis and synthesis of a finite energy signal of concern. The signals that are acceptable analyzing wavelets must satisfy the finite affine energy condition, which is commonly known as the admissibility condition. This means that only certain types of signals are admissible for analyzing wavelets. Signals that are notable exceptions include the complex exponential and the chirp. In a unique

---

[34] Because the dilation parameter assumes both negative and positive values, dilation corresponds to expansion and compression.

general interpretation of the wide-band ambiguity function, the wavelet transform is defined as an inner product formulation in the following,

$$L_f(\tau, a) = \int_{-\infty}^{\infty} f(t) g^*_{\tau,a}(t)\,dt, \quad \forall \tau \in \mathbb{R} \text{ and } \forall a \in \mathbb{R}\backslash\{0\}, \tag{3.47}$$

where the wavelets

$$g_{\tau,a}(t) = |a|^{-1/2} g(a^{-1}(t-\tau)) \text{ satisfies } \alpha_g = \int_{-\infty}^{\infty} |\nu|^{-1} |\hat{g}(\nu)|^2 d\nu < \infty,$$

the admissibility condition[35]. The admissibility (finite affine energy) condition of the analyzing wavelet is crucial for the recovery of the signal from the wavelet transform [106, 135, 136]. The admissibility condition is a consequence of the nonunimodularity of the affine group [129, 137] to which the wavelet transform belongs.

The Wavelet transform has many properties, some are included in [69, 106]. They include the cross wavelet transform and its relationship to affine group convolution and correlation, and preservation of time translation and dilation. In the context of time-frequency analysis and synthesis, the wavelet transform retains, under relaxed conditions, the usual bandpass characteristics of the wide-band ambiguity function [11,136, 138,138]. This means that the analyzing wavelet, $g(t)$, is assumed to be a bandpass signal with center frequency, $\nu_0 = a\nu$,

---

[35] This condition corresponds to $\int g(t)dt = 0$.

showing an inverse relationship between the dilation parameter and local frequency. With this adjustment to the wavelets, the wavelet transform emerges as a time-frequency representation of the form

$$L_f(\tau, \nu) = \sqrt{|\nu_0^{-1}\nu|}\int_{-\infty}^{\infty} f(t)g^*(\nu_0^{-1}\nu(t-\tau))dt. \qquad (3.48)$$

Since the analyzing wavelet, $g(t)$, is referenced in time at $t = 0$ and frequency at $\nu = \nu_0$, it is clear that $L_f(0, 1) = \int f(t)g^*(t)dt$ and that the dilation parameter, $a = 1$. In addition, the bandwidth of $g(t)$ is constraint to be proportional to frequency. Thus, the Weyl-Heisenberg related (RMS[36]) bandwidth, $\Delta\nu = c\nu$, where c is the proportionality constant. This implies that the related time duration must be inversely proportional to frequency. Moreover, the bandwidth and the duration change with the center frequency, which is obvious from $\Delta\nu = a^{-1}(c\nu_0)$. The above modifications on the dilation parameter of wavelets, allows the wavelet transform to perform time-frequency analysis as a constant-Q filter-bank analysis [59]. In this context, time resolution is improved with increases in frequency while sacrificing good frequency resolution, whereas frequency resolution is improved with decreases in time while losing good time resolution. This diverging tendency of time and frequency resolutions suggests that there is a general tradeoff in the time-frequency resolution of the wavelet transform using a single wavelet analyzing signal. By making use of more than one analyzing signal to generate

[36] RMS is the acronym for root-mean-square.

the wavelets, the wavelet transform emerges as a multiwavelet [139] transform with improved resolution quality.

Since any arbitrary signal that satisfies the admissibility condition is a suitable analyzing wavelet, wavelets are generally nonorthogonal and redundant [138]. Nonetheless, for two finite energy signals f_1 and f_2 the condition [47]

$$\int_{-\infty}^{\infty}\int_{-\infty}^{\infty} a^{-2} L_{f_1}(\tau, a)(L_{f_2})^*(\tau, a)\,d\tau\,da = \alpha_g \langle f_1, f_2 \rangle, \quad a = v_0^{-1} v \neq 0 \tag{3.49}$$

holds with the implication that a signal f can be easily recovered from the wavelet transform in the following manner,

$$f(t) = \alpha_g^{-1} \int_{-\infty}^{\infty}\int_{-\infty}^{\infty} a^{-2} L_f(\tau, a)\,|a|^{-1/2} g(a^{-1}(t-\tau))\,d\tau\,da, \quad a = v_0^{-1} v \neq 0, \tag{3.50}$$

and with the special case

$$\alpha_g^{-1} \int_{-\infty}^{\infty}\int_{-\infty}^{\infty} a^{-2} |L_f(\tau, a)|^2\,d\tau\,da = \|f\|^2 \tag{3.51}$$

showing that the preservation of the signal's energy in the wavelet transform is a reflection of the isometry from the inner product space of finite energy signals onto the inner product space of valid square integrable wavelet transforms. This energy conservation property of the wavelet transform has led to the development of affine energy distribution [74, 78, 140], which is

modulus squared of the wavelet transform expressible as the signal and the analyzing wavelet Wigner distributions[37],

$$|L_f(\tau, a)|^2 = \int_{-\infty}^{\infty}\int_{-\infty}^{\infty} W_f(t, s) W_g(a^{-1}(t-\tau), as)\,dt\,ds, \quad a = v_0^{-1}v \neq 0. \tag{3.52}$$

This positive bilinear energy distribution is called a scalogram. It performs affine correlation that results in smoothing of the Wigner distribution. Scalograms constitute a subset of the extended Cohen class. In comparison to Wigner distribution, they are quite flexible in balancing time-frequency resolution and crossterms reduction.

In synthesizing a signal using wavelets, it is often more desirable to use a wavelet series with wavelet coefficients that are sample values of the wavelet transform. A wavelet series is a discrete subset of the synthesis, equation (3.50), with the wavelet parameters defined on the lattice points of the time-frequency plane. Usually, the wavelet parameters are discretized so that the wavelets decompose into

$$g_{m,n}(t) = a_0^{-m/2} g(a_0^{-m} t - n\tau_0),$$

where $m, n \in Z$ and $a_0 > 1$ and $\tau_0 > 0$ are fixed, with the objective that the structural behavior and expected performance of the previous wavelet synthesis are maintained. However,

---

[37] Any member of Cohen's class of bilinear distributions is a suitable replacement for Wigner distribution.

these requirements are only met under proper choices of the analyzing wavelet[38] with appropriate values assigned to the translation and dilation constants. When this isdone, the set of wavelets, $\{g_{m,n}(t)\}$, constitute a frame. The frame embraces the inherent nonorthogonality and redundancy preserved in the discrete set of wavelets to its character as a generalized basis. Under these conditions, the wavelet series and its dual are valid approximations of their continuous counterparts. The wavelet series can be defined as follows [136],

$$f(t) = 2(A+B)^{-1} \sum_{m=-\infty}^{\infty} \sum_{n=-\infty}^{\infty} c_{m,n} g_{m,n}(t) + R, \tag{3.53}$$

where

$$\|R\| \leq O(B/A - 1)\|f\|$$

and A and B are the respective lower and upper frame bounds, $c_{m,n} = \langle f, g_{m,n} \rangle$ are the coefficients relating the wavelet series to the wavelet transform, and O is the acronym for order. If the wavelet frame, $\{g_{m,n}(t)\}$, is exact, or more preferably, tight and exact, it correspondingly forms a biorthogonal basis or an orthogonal basis. If $\{g_{m,n}(t)\}$ is simply tight, it has a definitive estimate of the equal frame bounds [47] and it forms an orthogonal-like basis. Under these frame conditions, the wavelet series is expressible in a relatively simple, elegant

[38] Bandlimited signals make good analyzing wavelets.

manner. For example, wavelet series expansion of $f(t)$ with respect to a tight exact wavelet frame, $\{g_{m,n}(t)\}$, is

$$f(t) = \sum_{m=-\infty}^{\infty} \sum_{n=-\infty}^{\infty} c_{m,n} g_{m,n}(t), \tag{3.54}$$

where the coefficients, $c_{m,n} = \langle f, g_{m,n} \rangle$, are exactly equal to the sample values of the wavelet transform. The number of coefficients in the synthesis of $f(t)$, is recoverable by means of the inversion formula,

$$c_{m,n} = \int_{-\infty}^{\infty} f(t) g^{*}_{m,n}(t) dt. \tag{3.55}$$

Because wavelet orthogonal bases are not constraint in the sense of a Balian-Low theorem, it is possible to generate them from analyzing wavelets that are well-localized in time and frequency simultaneously.

There are methodical ways to build orthogonal wavelet bases. One technique uses the concept of multiresolution analysis [141, 142, 143, 144] to construct a hierarchical signal approximation within a set of nested subspaces.

The efficient implementation of the wavelet transform or wavelet series requires both the discretization of all variables to get the discrete wavelet transform and the use of recursion [145]. Using the discrete wavelet transform to approximate the wavelet transform and wavelet

series is often subtle, since there is an initialization issue [146]. The discrete Wavelet transform may be implemented using either multiresolution pyramid algorithms or subband coding schemes [139]. Pyramid algorithms and subband coding are realizable using tree-structured multirate filter banks [147].

3.2.2 Short-Time Fourier Transform

The short-time Fourier transform is the classical Fourier transform of a signal viewed through a running window signal meant to continuously and sufficiently localize the stationary behavior of the analyzed signal within it. It is the conventional ambiguity function with a broadened interpretation. For example, the received signal and emitted signal assume the role of analyzed signal and window signal respectively. Thus, the arguments expounded for the conventional ambiguity function apply to the short-time Fourier transform. In fact, the analysis and synthesis equations of the ambiguity function are those of the short-time Fourier transforms, written as

$$S_f(\tau, u) = \int_{-\infty}^{\infty} f(t) g^*(t-\tau) e^{-2\pi i u t}\, dt \tag{3.56}$$

and

$$f(t) = \int_{-\infty}^{\infty}\int_{-\infty}^{\infty} S_f(\tau, u) g(t-u) e^{2\pi i u t}\, d\tau\, du, \quad \|g\|^2 = 1, \tag{3.57}$$

respectively. Recalling equations (3.27) and (3.44), $S_f = A_{f,g}$, but S_f is linear and $A_{f,g}$ is bilinear. This means that the short-time Fourier transform is also a restriction on the ambiguity function's ability to process the analyzed signal relative to a reference signal. The admissibility condition [110,129] that necessitates the easy and exact recovery of the analyzed signal from S_f is the finite value of $\|g\|^2$, the window's energy[39]. This finite energy criterion of the window signal allows admission of a very large class of signals. Besides, the synthesis formula holds even if $f(t)$ is just an integrable ($L_1(\mathbb{R})$) signal and $g(t)$ is either essentially bounded ($L_\infty(\mathbb{R})$) or is in the nonzero intersection of the space of finite energy and essentially bounded signals. In general, $g(t)$ generates a set of basis signals that are nonorthogonal and redundant (linearly dependent) [133], $\{g_{\tau,a}(t)\}$. Because the wide-band and the conventional ambiguity function are related in the limiting sense, and the wavelet transform is, in essence, the wide-band ambiguity function, the short-time Fourier transform is not only formally the wavelet transform [59], but these transforms also share many properties [47]. For example, concerning Moyal's formula for the ambiguity function, the unique recovery of the analyzed signal from the short-time Fourier transform is a result of the isometry that exists from the inner product space of finite energy signals onto the inner product space of square integrable short-time Fourier transforms [47, 148]. That is,

$$\|S_f\|^2 = \lambda_g \|f\|^2, \ \forall f \in L_2(\mathbb{R})$$

---

[39] Henceforth, it will be assumed that the window signal's energy is unity unless otherwise suggested from the context.

and $\lambda_g = \|g\|^2$. The short-time Fourier transform may be formally written as

$$S_f(\tau, u) = \int_{-\infty}^{\infty} f(t) g^*_{\tau,u}(t) dt, \quad \forall \tau, u \in \mathbb{R} \tag{3.58}$$

with $g_{\tau,u}(t) = g(t - \tau) e^{2\pi i u t}$. This equation is identical to equation (3.47) except that the second parameter of the analyzing wavelet is not defined on zero. The character of the second parameter of the analyzing signal determines its structure. The second parameter is responsible for dilating the analyzing wavelet and modulating the window signal. It is at the heart of the structural difference between the wavelet transform and the short-time Fourier transform.

Since the short-time Fourier transform is synonymous to the ambiguity function, the ambiguity surface is the modulus squared of the short-time Fourier transform. It naturally follows that the short-time Fourier transform conserves the signal energy. In an analogous manner to the ambiguity surface in radar analysis, the modulus squared of the short-time Fourier transform, $|S_f|^2$, is commonly used in time-frequency analysis. It is referred to as the spectrogram. It has a well-established theory. The spectrogram is a positive bilinear distribution of Cohen's class. It is sometimes called the weighted Wigner distribution [149] and it is a typical example of the smoothed Wigner distribution [62, 73 81]. The spectrogram in terms of Wigner distribution is the following [81],

$$|S_f(\tau, u)|^2 = \int_{-\infty}^{\infty} \int_{-\infty}^{\infty} W_f(t, v) W_g(t - \tau, u - v) dt\, dv. \tag{3.59}$$

This smoothed Wigner distribution of the signal has reduced crossterms. Like scalograms, spectrograms make up a subset of Cohen's class of distributions. The number of spectrograms in this class is determined by the number of possible windows. Using a separable smoothing signal in the gaussian window, a continuous pathway exists between Wigner distribution and the spectrogram or scalogram [74].

The window signal, $g(t)$, is centered in time and in frequency at $t = 0$ and $\nu = 0$ respectively, while its generated basis signals, $g_{\tau,u}(t)$, are centered in the time-frequency space at (τ, u). Because $g(t)$ and $g_{\tau,u}(t)$ may be interpreted as impulse responses of a lowpass and a bank of bandpass filters, the short-time Fourier transform is capable of performing both lowpass filtering and bandpass filtering [127, 150, 151, 152] usually of constant bandwidth. This short-time Fourier transform capability permits it to have a dual interpretation in linear filtering. The best results are obtained when the center frequencies of corresponding bandpass filters are much larger than the bandwidth of the lowpass filter. No matter the interpretation of the short-time Fourier transform, once a finite duration window signal is chosen, its duration is usually fixed throughout the short-time Fourier analysis (or synthesis) of a signal. Thus, the choice of the window signal is a fundamental concern because the window critically affects both resolution and concentration in the short-time Fourier transform. Therefore, a window choice should be consistent with the desired time and frequency resolution as well as the signal and its characteristics. The window should be reactive (or even proactive) to changes in signal amplitude and frequency. Nonetheless, irrespective of the window length and time-frequency orientation, there is always an inherent tradeoff between time and frequency resolution

conditioned by the time-frequency uncertainty relation, which put a lower bound on time-frequency resolution. Although good time and frequency resolution demands windows with arbitrarily short length in time and frequency to map the local nonstationarities in the signal, they cannot be used. In general, there is an inverse relationship between time and frequency resolution; improvements in time resolution are achievable only at the expense of degradation in frequency resolution and vice versa. Previously, it was stated that the time-frequency resolution of the wavelet transform is frequency dependent within the constraints of the time-frequency uncertainty relation. In terms of Weyl-Heisenberg uncertainty relation for time-frequency representations, wavelet transform and short-time Fourier transform behave almost alike for an arbitrary signal in the neighborhood of any given time-frequency location because the short-time Fourier transform frequency resolution, Δu, is such that the ratio $u^{-1}\Delta u$ like the fractional bandwidth of the wavelet transform is kept constant.

With appropriately chosen windows, the short-time Fourier transform of a signal is well-resolved and well-concentrated. Ordinarily, the best window signals are the gaussian pulse [38] and the matched filter [117]. Because, generally, there are local changes in the internal characteristics of a signal, windows are needed with time, frequency, and data dependency [51, 59, 72, 152, 153]. These types of windows make the short-time Fourier transform optimally responsive to the signal's behavior. A time and frequency dependent real window signal of the form [59] $g(t, v) = h(a^{-1}tv)$ with parameter $a > 0$ results in the short-time Fourier transform

$$S_f(\tau, u) = \int_{-\infty}^{\infty} f(t) h^*(a^{-1}u(t-\tau)) e^{-2\pi i u t} dt \qquad (3.60)$$

that exhibits the behavior of constant-Q analysis with the cutoff frequency of the window signal relatively small as compared to center frequency of the equivalent basis signals. This modified short-time Fourier transform performs time-frequency analysis in a way that seems natural to the wavelet transform. In addition to optimum (or near optimum) time-frequency resolution, the performance of the short-time Fourier transform may be further optimized by requiring maximal concentration of each signal data in time-frequency space. This can be done by using a time, frequency, and data dependent gaussian pulse as the window signal [72],

$$g(t) = (-2\pi^{-1} Re(\alpha))^{0.25} e^{\alpha t^2}, \quad Re(\alpha) < 0,$$

which generates basis signals of the form

$$g_{\tau,u}(t) = (-2\pi^{-1} Re(\alpha_{\tau,u}))^{0.25} e^{\alpha_{\tau,u}(t-\tau)^2 + 2\pi i u t}$$

with $\alpha_{\tau,u}$ being a time-frequency dependent gaussian parameter. The corresponding short-time Fourier transform automatically adapts to local variation in the signal content with the

continuous selection of the gaussian parameter aimed at maximizing the signal concentration at each time-frequency location.

As with wavelet synthesis of a signal, short-time Fourier synthesis of a signal can be approximated by a short-time Fourier series expansion of the said signal with the expansion coefficients being soundly recoverable sample values of the short-time Fourier transform. This series expansion completely characterizes the inverse short-time Fourier transform. As in the wavelet case, this series is only possible under restricted circumstances. Besides, the short-time Fourier series is quite analogous to the wavelet series [135]. The short-time Fourier series is a restriction of the corresponding short-time Fourier synthesis equation, equation (3.57), onto a discrete lattice of the time-frequency space [47, 49, 114, 154] determined by the discretization of the continuous time-frequency parameters τ and u. To discretize τ and u, positive real constants τ_0 and u_0 are chosen to be the discrete lattice parameters so that for m and n contained in Z, $(\tau, u) = (m\tau_0, nu_0)$. With discrete time-frequency parameters, the basis signals generated from the window signal take the form

$$g_{m,n}(t) = g(t - m\tau_0)e^{2\pi i n u_0 t}.$$

Generally, the discrete set of basis signals, $\{g_{m,n}(t)\}$, preserves both the nonorthogonality and the redundancy properties of the set $\{g_{\tau,u}(t)\}$. Therefore, whenever the short-time Fourier series expansion of a signal is possible, its representation is usually not unique. Nonetheless, the unique expansion of a signal is always guaranteed if $\{g_{m,n}(t)\}$ constitutes a frame or if

somewhat equivalently, the Zak transform of the window signal, g, is nonzero. Frames of $\{g_{m,n}(t)\}$ are always possible for $(T_0, u_0) < 1$ where they are redundant, impossible for $(T_0, u_0) > 1$ where they are an incomplete set, and may be possible for $(T_0, u_0) = 1$ where they are exact [45, 47, 149]. The existence of $\{g_{m,n}(t)\}$ as an exact frame means that it is at least biorthogonal to its dual. If $\{g_{m,n}(t)\}$ is exact and tight, it is an orthogonal set and it is equal to its dual. In spite of the desired properties of biorthogonality [154] in general and orthogonality in particular [127], the existence of a single peaked window signal, g, with good time and frequency localization properties is impossible by Balian-Low theorem.

In the context of frames, the short-time Fourier series is the wavelet series with a structural change in the set of basis signals, $\{g_{m,n}(t)\}$. Hence, equation (3.53) also defines the short-time Fourier series. The coefficients $c_{m,n} = S_f(mT_0, nu_0)$. The remainder, R, approximately equals zero for snug frames and it equals zero for tight frames. In fact, for tight frames the frame bound $A = (T_0 u_0)^{-1} \|g\|^2$ and for tight exact frames $A = \|g\|^2$. If $\|g\|^2 = 1$, $\{g_{m,n}(t)\}$ is an orthonormal basis and the corresponding short-time Fourier series is simply

$$f(t) = \sum_{m=-\infty}^{\infty} \sum_{n=-\infty}^{\infty} S_f(mT_0, nu_0) g_{m,n}(t). \tag{3.61}$$

The short-time Fourier coefficients are recoverable from the series expansion through the means of the following formula,

$$S_f(mT_0, nu_0) = \int_{-\infty}^{\infty} f(t) g^*_{m,n}(t) dt. \qquad (3.62)$$

This short-time Fourier series pair is an efficient, valid, and unique representation of its continuous counterpart.

Efficient and economical implementation of the short-time Fourier transform analysis and synthesis formulas can be executed using the corresponding series expansion pair with the continuous time variable discretized. This implementation is usually accomplished by means of FFT algorithms or filter-banks methods [64, 126, 151, 152]. The definition of the short-time Fourier transform presented in this treatise is more conducive to filter-bank methodologies, but it can be indirectly and efficiently realized using FFT algorithms [126, 152]. A direct realization of the short-time Fourier transform using FFT methods requires its redefinition wherein the signal slides relative to a fixed window.

3.2.3 Weyl-Heisenberg Expansion

Weyl-Heisenberg expansion is a generalization of Gabor's nonorthogonal series expansion [38] of the form

$$f(t) = \sum_{m=-\infty}^{\infty} \sum_{n=-\infty}^{\infty} c_{m,n} g_{m,n}(t), \tag{3.63}$$

where $f(t)$ is any signal, $c_{m,n}$ are expansion (Gabor) coefficients and $g_{m,n}(t) = g(t - mT)e^{2\pi i nSt}$ are nonorthogonal basis signals, with $ST = 1$, generated from the gaussian window signal $g(t) = e^{-\pi t^2}$ through the process of time and frequency translation. Gabor chose the gaussian pulse from the set of Fourier invariant Hermite functions because he found these functions to have the minimum effective time-bandwidth product with the gaussian's product being smallest. The effective time-bandwidth product of the gaussian pulse is the lower bound of Weyl-Heisenberg uncertainty relation. Daubechies [55] established that Hermite functions are eigenfunctions of simultaneous time-frequency localization operators associated with disk-shaped or ellipse-shaped regions of the time-frequency space. She claimed that although these Hermite functions related operators are similar to prolate spheroidal wave functions [5, 39, 41, 42, 158] related operators, but instead of shuffling back and forth between the time and frequency domain and having respectively sharp and negative powers decay properties, they are based in the time-frequency space and have gaussian-like decay properties in the time and frequency directions. Notwithstanding, Klein and Beutter [159] contested Gabor's claim that Hermite functions minimize the Weyl-Heisenberg uncertainty relation for real signals, they argued, instead, that Hermite functions maximize the uncertainty. The time-frequency lattice on whose critical sample points Gabor coefficients are computed is generally referred to as Von Neumann in quantum mechanics [127, 160] and as Gabor lattice in signal

processing. The coefficients are computed by means of the inverse of Gabor's series (Gabor expansion) [161], which is sometimes called Gabor transform. Lerner [1] objected to Gabor's strict reliance on a convenient time-bandwidth product in choosing the window signal, $g(t)$, and in determining, through $g(t)$, the cell structure of the discrete lattice of the time-frequency space. He, instead, emphasized the use of an arbitrary $g(t)$ of finite energy and desirable properties including small time-bandwidth product, capable of generating from its time and frequency translates a complete set of basis signals, $g_{m,n}(t) = g(t - mT)e^{2\pi inSt}$, so that with a sufficiently well-behaved analyzed signal, $f(t)$, equation (3.63) remains valid. While Lerner retained Gabor's critical sampling grid, $ST = 1$, he required that a free choice of the time translate, T, should determine the time-frequency discrete lattice cell structure. In this way, the expansion coefficients, $c_{m,n}$, are mutually dependent on $g(t)$ and T. Despite Lerner's misgivings about time-bandwidth product except for its role in signal expansion coefficients estimation, it can play a pivotal part in the resolution analysis problem of bandlimited (time-limited) and essentially time-limited (bandlimited) signals [162, 163, 164].

The series expansion of equation (3.63) possesses an exact continuous counterpart of which it is only an approximation. This continuous integral expansion is related to Glauber's [57] expression of an arbitrary quantum mechanical state as an integral involving the overcomplete (redundant) set of a harmonic oscillator. Corresponding to Gabor's suggestion of the series and Lerner's generalization of it, is Helstrom's [58] establishment of this series continuous counterpart and Montgomery and Reed's generalization of it. The continuous integral expansion has a unique inverse that exists even for not necessarily square integrable signals if the kernel

signal is square integrable. The general form of the continuous version of Gabor expansion is the synthesis equation of the transform pair

$$f(t) = \int_{-\infty}^{\infty}\int_{-\infty}^{\infty} c(\tau, u)g(t;\tau, u)d\tau\, du \tag{3.64}$$

and

$$c(\tau, u) = \int_{-\infty}^{\infty} f(t)g^{*}(t;\tau, u)dt, \tag{3.65}$$

where the kernel signal generates basis signals

$$g(t;\tau, u) = g(t-\tau)e^{2\pi i u t}e^{-2\pi i(\alpha-0.5)\tau u}, \quad \|g\|^2 = 1.$$

In general, $\|g\|^2 = 1$ is the normalization of $\|g\|^2 < \infty$. Clearly, $c(\tau, u)$ is the generalized cross-ambiguity function, or preferably $c(\tau, u)$ is the short-time Fourier transform of $f(t)$, which is uniquely recoverable from it. It is now obvious that Gabor coefficients $c_{m,n}$ are related to the sample values of the short-time Fourier transform $c(m\tau_0, n u_0)$ defined on a Gabor lattice having τ_0 and u_0 as lattice parameters and are structurally equivalent to the wavelet series coefficients of equation (3.53). The relationship between $c_{m,n}$ and $c(m\tau_0, n u_0)$ was acknowledged by both Gabor and Lerner as is apparent in their application of the series expansion. In spite of the acknowledged and established connection between Gabor expansion and the short-time Fourier transform, it was not until 1980 when Bastiaans [161] published a

solution to the inverse problem corresponding to Gabor expansion that it then became public as how to analyze a signal in terms of its expansion coefficients. In his pursuit to establish a unique analysis form of Gabor expansion which he assumed existed, Bastiaans confirmed some results previously reached by Lerner; namely, any arbitrary well-behaved signal can be expressed in terms of Gabor's signal expansion technique and the kernel signal can be any arbitrary finite energy signal.

A distinguishing feature of Gabor expansion relates to the unit density, $(ST)^{-1} = 1$, of Gabor lattice, which has cell area, $ST = 1$. This density $(ST)^{-1} = 1$ is exactly the Nyquist density, which is the minimum density needed for the full transmission of information. Balian-Low theorem prohibits good time-frequency localization behavior in all directions of any valid single-peak window signal, g, associated with the set basis signals, $\{g_{m,n}(t)\}$, defined on Gabor lattice. This implies that if the usually nonorthonormal set, $\{g_{m,n}(t)\}$, is an orthonormal basis or is a member of a biorthonormal set, good time-frequency localization properties of g are generally impossible. It further follows that the coefficients, $c_{m,n}$, which depend on Gabor lattice parameters, T and S, and, g will have decreased time-frequency resolution and the associated series expansion will be numerically unstable. Nonetheless, stable signal expansion may still be possible via cleverly designed robust algorithms. Despite the efforts of Gabor, Lerner, and Bastiaans, numerically stable Gabor-type series expansion of a signal, $f(t)$, relative to a well-localized g in both time and frequency, is guaranteed only if the set $\{g_{m,n}(t)\}$ is defined on a discrete time-frequency lattice of density greater than Nyquist density. Density less than Nyquist density does not in general lead to meaningful Gabor-type expansion because

the set $\{g_{m,n}(t)\}$ cannot span the entire space of finite energy signals. In general, Gabor-like series expansion is only possible over Gabor-like lattice of density $(ST)^{-1} \geq 1$. This density corresponds to a cell area of $ST \leq 1$ resulting in $\{g_{m,n}(t)\}$ generally remaining a redundant nonorthonormal set of basis signals. Thus, for a freely chosen finite energy g and parameter T (or S), parameter S (or T) must be selected so as to satisfy the time-frequency density conditions for the relevant Gabor-like lattice. In consequence, the conditions for valid Gabor-like series expansion are equivalent to those for perfect reconstruction of a bandlimited signal from its samples.

A Gabor-like series expansion of $f(t)$ effected with the aid of $\{g_{m,n}(t)\}$ defined on a Gabor-like lattice with density $(ST)^{-1} \geq 1$, is called a Weyl-Heisenberg expansion [114] if the Gabor-like series is exactly the short-time Fourier series with expansion coefficients, $b_{m,n}$, being the sample values $S_f(mT, nS)$ of the short-time Fourier transform. The set of basis signals, $\{g_{m,n}(t)\}$, is called a Weyl-Heisenberg system, (g, T, S), with $ST \leq 1$. The relation describing a Weyl-Heisenberg expansion of $f(t)$ over (g, T, S) conditioned on $ST \leq 1$ is the following,

$$f(t) = \sum_{m=-\infty}^{\infty} \sum_{n=-\infty}^{\infty} b_{m,n} g_{m,n}(t), \quad g_{m,n}(t) = g(t - mT) e^{2\pi i n S t}. \tag{3.66}$$

Weyl-Heisenberg expansion is a generalization of Gabor expansion. Although some researchers have stated explicitly and implicitly [1, 38, 154, 161] that Gabor coefficients, $c_{m,n}$, are identical to Weyl-Heisenberg expansion coefficients, $b_{m,n}$, this equality is generally less precise. The equality relationship holds to within a constant factor only when $\{g_{m,n}(t)\}$ constitutes a tight

frame [49]. Under tight frame conditions, $c_{m,n} = (ST)b_{m,n}$, $\|g\|^2 = 1$, because the modulus squared of the Zak transform of g is a nonzero constant, implying that $\{g_{m,n}(t)\}$ "is a complete and orthogonal set." Otherwise, $b_{m,n}$ is the smoothed version of $c_{m,n}$ [49, 167] experienced through the two-dimensional convolution of $c_{m,n}$ with $a_{m,n} = \langle g, g_{m,n} \rangle$, the sampled auto-ambiguity function of the kernel signal. In other words, $b = a * c$. This relationship is quite similar to equation (3.32), where the expected value of the ambiguity surface is the smoothed version of the target scattering function.

Weyl-Heisenberg expansion is resilient to noise contribution $\eta_{m,n}$ added to the coefficients $b_{m,n}$ [47, 170]. The noise reduction experience in the synthesis of a signal $f(t)$ from contaminated coefficients $b_{m,n} + \eta_{m,n}$ is a consequence of time-frequency space localization to permit only a finite number of coefficients and of oversampling.

As previously noted, Weyl-Heisenberg expansion has a dual representation in frequency. In this case, the Weyl-Heisenberg system is $(\hat{g}, S, -T)$. It describes the set of spectral basis signals $\{e^{2\pi i n m S T} \hat{g}_{n,-m}(v)\}$. Moreover, Weyl-Heisenberg-type expansion is also possible with a kernel that generates the basis signals in the time-frequency space. An example of this type of expansion uses Wigner space basis signals [171].

A Weyl-Heisenberg expansion or its related Gabor expansion of a signal is generally difficult to implement efficiently and economically because of the subtlety involved in finding the coefficients, $b_{m,n}$ or $c_{m,n}$. This difficulty arises, in part, from the restrictions of Balian-Low

theorem and minimum permissible time-frequency density placed on the Weyl-Heisenberg system, (g, T, S). In addition, (g, T, S) is a restriction on the set of continuous basis signals, $\{g_{\tau,\nu}(t)\}$. This means that (g, T, S) is usually a redundant and nonorthogonal set of basis signals, $\{g_{m,n}(t)\}$. These characteristics of $\{g_{m,n}(t)\}$ have influenced the adoption of several different methods used to find $b_{m,n}$ or $c_{m,n}$. The first method adopted was an iterative procedure called successive approximations [38]. Some, of the other methods include (1) the imposition of linear independence on $\{g_{m,n}(t)\}$ to permit, by means of correlation matrix $\Phi^{-0.5}$, its orthogonalization to a set of orthonormal basis signals [1], which, with $ST = 1$, leads to $b_{m,n} = c_{m,n}$, (2) the use of concept of biorthonormal basis [160, 161] as it relates to the biorthonormality of $\{g_{m,n}(t)\}$ and another set of basis signals, $\{\tilde{g}_{m,n}(t)\}$, and the recovery of $b_{m,n}$ or $c_{m,n}$ from the signal relative to $\{\tilde{g}_{m,n}(t)\}$, and (3) the use of Zak transform, wherein $b_{m,n}$ or $c_{m,n}$ results from the inversion of a two-dimensional Fourier series [167]. Moreover, when resolution is the central concern, $c_{m,n}$ are preferred to $b_{m,n}$ and may be recovered from it by means of the two-dimensional deconvolution [174]. Henceforth, Gabor expansion will be understood in the context of Weyl-Heisenberg expansion unless it is otherwise stated.

3.2.4 Zak Transform

The Zak transform is the simplest time-frequency representation of a signal. Its simplicity, computational efficiency, and conceptual elucidating capability have caused it to be used as a problem-solving tool in mathematics, quantum mechanics, and signal processing. The Zak transform was used in these disciplines for quite some time before it was proven and acclaimed

to be a valid representation of a function. Often, the Zak transform was only used as an intermediary step in a computational process. This usual secondary role was, perhaps, the single most important reason for the delayed formal acceptance of the Zak transform as a robust and competitive representational instrument. The inconsistency with which the Zak transform was used to validly represent functions has led to separate formal adaptations of it in mathematics and physics [4, 17, 175]. Since its formal introduction into quantum mechanics in 1967 [4], the Zak transform, under the name of *kq*-representation, has become universally and conveniently applicable to a large class of quantum mechanical problems [176]. For example, the Zak transform is recognized as the 'most quantum-mechanical' way to represent coherent states [57]. A Weyl-Heisenberg system is a set of coherent states [55, 133]. It is in this context that the Zak transform has found its formal recognition in the signal processing community [1, 154] where it is used to determine the existence of Weyl-Heisenberg expansions and expedite their processing. Many results obtained from the application of Zak transform to Weyl-Heisenberg expansions have parallels in coherent states [127, 134]. The power of Zak transform lies in its ability to render some otherwise unwieldy linear system problems [177] mathematically tractable and conceptually clear while providing the domain for viewing them. In other words, the Zak transform is an efficient and convenient mathematical tool with clear display capability.

The Zak transform is an adaptive form of classical Fourier analysis. It has included both the discrete-time and continuous-time Fourier analysis. The discrete part is sampled at the Nyquist rate. In the degenerative case, the Zak transform becomes either the signal or its Fourier representation. More precisely, this suggests that the Zak transform is a mixture of Fourier

analysis and Fourier synthesis. In fact, it resides at a crossroad of analysis and synthesis in classical Fourier theory. Moreover, the Zak transform is inherent in the structure of the Cooley-Tukey algorithm and can be derived from it. Like the Fourier transform, the Zak transform is an intertwining unitary operator and is an isometry between signal spaces [178]. The deep relationship between the theories of Fourier and Zak analyses is a well-established concept in Heisenberg group theory. The Zak transform may be defined as a Fourier transform or Fourier series of a time-varying discrete signal. However, in this discourse, the Zak transform will be defined as a Fourier series. This definition is consistent with the formalism of certain expected results experienced from the application of Zak transform to a Weyl-Heisenberg system.

In formal language, the Zak transform Z linearly maps signals f defined on $\mathbb{R}$ onto two-variable signals Z_f of the form:

$$Z_f(\tau, \theta) = \sum_{k=-\infty}^{\infty} f((\tau + k)T)e^{2\pi i k\theta}, \quad \forall \tau, \theta \in \mathbb{R}, \tag{3.67}$$

with sampling time T. The time and frequency variables τ and θ respectively are normalized. The frequency variable θ is normalized on the sampling rate $S = T^{-1}$. The Zak transform is periodic in frequency and quasi-periodic in time, with a period one in each case. That is

$$Z_f(\tau, \theta + 1) = Z_f(\tau, \theta) \quad \text{and} \quad Z_f(\tau + 1, \theta) = e^{-2\pi i\theta} Z_f(\tau, \theta), \quad \forall \tau, \theta \in \mathbb{R}. \tag{3.68}$$

Thus, Z_f is completely determinable on the unit square ($\mathbb{I}$). This is a result from the fact that Z maps $L_2(\mathbb{R})$ injectively and isometrically onto the Hilbert space $L_2(\mathbb{I})$. Consequentially, Z is

norm-preserving: $T\|Z_f\|^2 = \|f\|^2$. Additionally, the signal $f(t)$ is completely recoverable from $Z_f(\tau, \theta)$ by means of

$$f(t) = \int_0^1 Z_f(St, \theta)\,d\theta, \quad \forall t \in \mathbb{R}. \tag{3.69}$$

Naturally, $f(t)$ is also completely recoverable from $Z_f(\tau, \theta)$ by the inversion process:

$$f((\tau + k)T) = \int_0^1 Z_f(\tau, \theta)e^{-2\pi ik\theta}\,d\theta, \quad \tau \in [0, 1). \tag{3.70}$$

More generally, Z maps $L_p(\mathbb{R})$ injectively into $L_p(\mathbb{I})$ for $1 \le p \le 2$, with Z not lower bounded for $1 \le p < 2$; Z is not defined for $p > 2$; and $\|Z_f\|_p \le \|f\|_{p'}$, $T = 1$.

A compelling and distinguishing characteristic of Z_f relates to the fundamental result of the zero theorem that states that a finite energy signal f with a continuous Z_f must have at least one zero somewhere in the unit square. This peculiar property, which is imposed by the uncertainty principle, has many important consequences [125, 134]. Although the zero theorem does not show the exact location of the zeros, they have been determined for signals that are real, even, odd, and real and even under certain conditions. To illustrate, continuous Z_f has zeros at $(\tau, \theta) = (\tau, 0.5)$ for $\tau \in [0, 1]$ when f is real, at $(\tau, \theta) = (0.5, 0.5)$ when f is even, at $\{(\tau, \theta)\} = \{(0, 0), (0, 0.5), (0.5, 0)\}$ when f is odd, and at $(\tau, \theta) = (0.5, 0.5)$ when f is real and even with $f''(t) > 0$, and $f'''(t) < 0$ for positive t.

The Zak transform can be obtained from the short-time Fourier transform with the appropriate choice of a window signal, and from a modulated signal and a Weyl-Heisenberg system by means of Poisson summation formula. To show these relationships, first, the window signal, $g(t)$ of the short-time Fourier transform of equation (3.56) is recalled and set to the impulse train, $\sum \delta(t - kT)$, such that $g(t - \tau) = \sum \delta(t - (\tau + kT))$ and the short-time Fourier transform, $S_f(\tau, \nu)$, becomes

$$S_f(\tau, -\theta) = e^{2\pi i\tau\theta} Z_f(\tau, \theta), \quad \forall \tau, \theta \in \mathbb{R}. \tag{3.71}$$

Secondly, since $(R_\nu f)(t)$ and $(T_\nu \hat{f})(\nu)$, applying Poisson summation formula to $(R_\nu f)(t)$ yields

$$Z_f(\tau, \theta) = e^{-2\pi i\tau\theta} S Z_f(-\theta, \tau), \tag{3.72}$$

where

$$Z_f(-\theta, \tau) = \sum_{m=-\infty}^{\infty} \hat{f}((-\theta + m)S) e^{2\pi i m\tau}, \quad \forall \tau, \theta \in \mathbb{R}.$$

So the Zak transform has a dual representation in frequency, which can be shown to be periodic in time and quasi-periodic in frequency with period one. An implication of equation (3.71) is that the Fourier spectrum can be recovered from the Zak transform via

$$\hat{f}(\nu) = T \int_0^1 Z_f(\tau, -\nu T) e^{-2\pi i \nu T \tau} d\tau, \quad \forall \nu \in \mathbb{R}, \ \nu T = \theta. \tag{3.73}$$

An observation of equations (3.70) and (3.71) clearly shows that the short-time Fourier transform, with normalized time and frequency variables, is equivalent to the Zak transform of the spectrum. That is,

$$S_f(\tau, -\theta) = SZ_f(-\theta, \tau). \tag{3.74}$$

Lastly, the application of Poisson summation formula to a Weyl-Heisenberg system results in a version of the Zak transform that corresponds to equation (3.71), except for a time shift. Because a Weyl-Heisenberg system is a set of signals $\{g_{x,u}(t)\}$ generated from time and frequency shifts of a single signal $g(t)$ and $g_{x,u}(t)$ has Fourier transform $e^{2\pi i u x}\hat{g}_{u,x}(v)$, the Zak transform relationship that results when Poisson summation is applied to $g_{x,u}(t)$ is

$$Z_g(\tau - a, \theta) = e^{2\pi i \tau\theta} SZ_g(-\theta, \tau - a). \tag{3.75}$$

This relationship gives a reason why the Zak transform is a natural tool for studying Weyl-Heisenberg expansions and suggests the possible existence of a generalized Zak transform that is defined on a time-frequency space of finite area $ST \neq 1$.

The representational capabilities of the Zak transform seem to exceed that of any other time-frequency technique. It can be used to confirm many renowned themes in Fourier analysis like Shannon sampling theorem, Parseval's theorem, convolution, and modulation as well as a framework to study other time-frequency techniques such as bilinear distributions, affine wavelet systems, and Weyl-Heisenberg expansions. Apart from the aforementioned properties, some additional properties that gives Zak transform these appealing capabilities are the

relationship between the inner product of finite energy functions, Z_f and Z_g, restricted to the unit square and the inner product of their corresponding finite energy signals, f and g,

$$T\int_0^1\int_0^1 Z_f(\tau,\theta)Z^*_g(\tau,\theta)d\theta\,d\tau = \langle f,g\rangle, \tag{3.76}$$

and time-limitedness of a signal $f(t)$ on an interval [0, 1) corresponds to time-limitedness of its Zak transform, Z_f,

$$Z_f(St,\theta) = f(t), \quad |t| < 0.5, \quad \forall\theta\in\mathbb{R}, \tag{3.77}$$

while bandlimitedness of a signal $f(t)$ on an interval [0, 1) corresponds to bandlimitedness of its Zak transform, Z_f,

$$Z_f(\tau,\nu T) = e^{2\pi i\tau\nu T}S\hat{f}(-\nu), \quad |\nu| < 0.5, \quad \forall\tau\in\mathbb{R}. \tag{3.78}$$

An immediate consequence of equation (3.78) is Shannon sampling theorem [50]. Each integral of the double integral of equation (3.76) leads to a type of Parseval's theorem. For example,

$$\int_0^1 Z_f(\tau,\theta)Z^*_g(\tau,\theta)d\theta = \sum_{k=-\infty}^{\infty} f((\tau+k)T)g^*((\tau+k)T). \tag{3.79}$$

There are other implications of equation (3.76). They include expressions for convolutions, modulations, Weyl-Heisenberg expansions, and bilinear distributions. Because $Z_{f^*}(\tau,\theta) = Z^*_f(\tau,-\theta)$, $Z_{T_a f}(\tau,\theta) = Z_f(\tau - aS,\theta)$, for all $a,\tau,\theta\in\mathbb{R}$ and $S = T^{-1}$, and $Z_{R_b f}(\tau,\theta) = e^{2\pi i b T\tau}Z_f(\tau,\theta+bT)$, for all $b,\tau,\theta\in\mathbb{R}$, the Zak transforms of the

convolution of two signals and the product of two signals can be obtained with the aid of equation (3.76) provided $g = g_{mT,nS}$, $S = T^{-1}$. They are

$$Z_{(f*g)}(\tau, \theta) = T\int_0^1 Z_f(\mu, \theta) Z_g(\tau - \mu, \theta)\, d\mu, \quad \forall \tau, \theta \in \mathbb{R}, \tag{3.80}$$

and

$$Z_{(fg)}(\tau, \theta) = \int_0^1 Z_f(\tau, \phi) Z_g(\tau, \theta - \phi)\, d\phi, \quad \forall \tau, \theta \in \mathbb{R}, \tag{3.81}$$

respectively. Of course, these two statements of a time and frequency convolution in Zak transform framework are obtainable through straightforward application of Zak transform to time convolution and modulation.

It was previously stated that the short-time Fourier transform is the asymmetrical ambiguity function and that its appropriately chosen sample values are Weyl-Heisenberg coefficients. To recall,

$$S_f(\tau, u) = A_{f,g}(\tau, u) = \langle f, g_{\tau,u} \rangle$$

and

$$b_{m,n} = S_f(mT, nS) = A_{f,g}(mT, nS) = \langle f, g_{mT,nS} \rangle = \langle f, g_{m,n} \rangle, \quad ST \leq 1.$$

Instead of using frames, the Zak transform can be used to decide the existence and completeness of Weyl-Heisenberg expansions over coefficients $b_{m,n}$ [125, 134, 179]. The number and type of Zak transform zeros play a crucial role in this endeavor. Additionally, recall that the asymmetrical and the symmetrical ambiguity functions, $A_{f,g}$ and $B_{f,g}$, differ by a phase factor, $e^{\pi i \nu \tau}$, $A_{f,g}$ is the two-dimensional Fourier transform of Rihaczek distribution, $R_{f,g}$, and $B_{f,g}$ is the two-dimensional Fourier transform of Wigner distribution, $W_{f,g}$. Moreover, Cohen's class of bilinear distributions is expressible in terms of $B_{f,g}$ as well as in terms of any bilinear distribution[40]. In the context of $B_{f,g}$, Cohen's class of bilinear distributions is defined as follows,

$$C_{f,g}(t,\nu) = \int_{-\infty}^{\infty}\int_{-\infty}^{\infty} K(\tau,u) B_{f,g}(\tau,u) e^{-2\pi i(ut - \nu\tau)} d\tau\, du, \quad \forall t, \nu \in \mathbb{R}, \tag{3.82}$$

where $B_{f,g}(\tau, u) = e^{\pi i u \tau} A_{f,g}(\tau, u)$ and the arbitrary kernel function K determines the particular distribution. If $ST = 1$, it follows that

$$\langle f, g_{m,n} \rangle = T \langle Z_f, Z_{g_{m,n}} \rangle, \text{ and } \quad Z_{g_{m,n}}(\tau, \theta) = e^{2\pi i(n\theta - m\tau)} Z_g(\tau, \theta).$$

Thus equation (3.76) becomes

$$\langle f, g_{m,n} \rangle = T \int_0^1 \int_0^1 Z_f(\tau, \theta) Z^*_g(\tau, \theta) e^{-2\pi i(n\theta - m\tau)} d\theta\, d\tau, \quad \forall m, n \in Z, \tag{3.83}$$

---

[40] The Wigner distribution is customarily used.

the coefficients of a Fourier series expression. The corresponding Fourier series, which is inverse of equation (3.83) is

$$Z_f(\tau,\theta)Z^*_g(\tau,\theta) = S\sum_{m=-\infty}^{\infty}\sum_{n=-\infty}^{\infty}\langle f, g_{m,n}\rangle e^{2\pi i(m\theta - n\tau)}, \quad \forall \tau,\theta \in \mathbb{R}. \tag{3.84}$$

As a direct consequence of this Fourier series,

$$Z_f(\tau,\theta)Z^*_g(\tau,\theta) = S\sum_{m=-\infty}^{\infty}\sum_{n=-\infty}^{\infty} R_{f,g}((\tau+n)T,(-\theta+m)S), \tag{3.85}$$

where $\forall \tau,\theta \in \mathbb{R}$. Noting that

$$\langle f, g_{m,n}\rangle = (-1)^{mn}B_{f,g}(mT,nS), \quad m,n \in Z,$$

equation (3.85) implies that Cohen's bilinear distributions, $C_{f,g}$, can similarly be expressed in the framework of Zak transform.

While the Zak transform can be used to generalize Walter's [180] extension of Shannon sampling theorem for wavelet subspaces [181], it can be redesigned into a multiplicative Zak transform [182] specifically tailored to study the properties of finite bandwidth affine wavelet systems of the type considered in [128]. Moreover, the Zak transform can be used to determine nontrivial examples of finite energy signals f and g [183] with the property that $fg = 0$ implying that $\hat{f}\hat{g} = 0$. These nontrivial pairs of signals are such that for each pair of unequal signals, the

modulus of the signals are equal and the modulus of their spectrum are equal. Similar results hold when instead of the signals' spectrum, their symmetrical ambiguity functions or their Wigner distributions are considered.

The Zak transform may also be used to explore the conceptual subtleties and computational efficiency of Weyl-Heisenberg expansions. The Weyl-Heisenberg expansion of a signal $f(t)$ may be rewritten as

$$f(t) = \sum_{m=-\infty}^{\infty} \sum_{n=-\infty}^{\infty} c_{m,n} g_{m,n}(t). \tag{3.86}$$

Its Zak transform is

$$Z_f(\tau, \theta) = Z_g(\tau, \theta) \sum_{m=-\infty}^{\infty} \sum_{n=-\infty}^{\infty} c_{m,n} e^{2\pi i (m\theta - n\tau)}, \quad \forall \tau, \theta \in \mathbb{R}, \tag{3.87}$$

and, in principle, the Weyl-Heisenberg coefficients recovered from it have the form,

$$c_{m,n} = \int_0^1 \int_0^1 P(\tau, \theta) e^{-2\pi i (m\theta - n\tau)}, \quad P(\tau, \theta) = \frac{Z_f(\tau, \theta)}{Z_g(\tau, \theta)}, \quad m, n \in Z. \tag{3.88}$$

This formula suggests that the Weyl-Heisenberg coefficients are actually Fourier series coefficients. These coefficients are only valid if the zeros of Z_g correspond to the zeros of Z_f or if Z_g has no zero. The Zak transform can be used to resolve the issue of the zero problem so that the recovery of $c_{m,n}$ is usually possible [49, 179, 184]. In this process, the zero pattern of

g is adapted to suit the zero pattern of f in Zak space. However, the recovery of $c_{m,n}$ do not guarantee their uniqueness except for the case of bounded P. Additionally, choosing window signals g that are nonzero in Zak space is desirable. The coefficients of Weyl-Heisenberg expansion may also be obtained using equation (3.84), which is derived from equation (3.87) by multipling by Z^*_g. This formula states that

$$Z_f(\tau,\theta)Z^*_g(\tau,\theta) = |Z_g(\tau,\theta)|^2 \sum_{m=-\infty}^{\infty} \sum_{n=-\infty}^{\infty} c_{m,n} e^{2\pi i(m\theta - n\tau)}, \quad \forall \tau,\theta \in \mathbb{R}. \tag{3.89}$$

Comparing this equation with equation (3.84), it is observed that

$$b_{m,n} = T|Z_g(\tau,\theta)|^2 c_{m,n}, \quad m,n \in Z, \quad \tau,\theta \in \mathbb{R}. \tag{3.90}$$

Thus, it is shown that the Weyl-Heisenberg coefficients of these two equations are only equal if

$$T|Z_g(\tau,\theta)|^2 = 1.$$

This statement suggests that the set $\{g_{mT,nS}(t)\}$ forms an orthonormal basis, which means that $\{g_{mT,nS}(t)\}$ is linearly independent, a condition corresponding to $ST = 1$ which is the Nyquist density of Zak space. However, if $|Z_g(\tau,\theta)|^2$ is a Fourier series with coefficients $a_{m,n}$, it follows that $b_{m,n}$ are convoluted $c_{m,n}$. This is possible if $ST \leq 1$, which implies that the density of Zak space is exceeded for $ST < 1$.

3.3 Mathematics of Time-Frequency Methods

The Zak transform, Weyl-Heisenberg expansion, and short-time Fourier transform are Heisenberg group concepts [11, 13, 15, 17, 104, 132, 148, 186, 187] while the wavelet transform is an affine group concept [11, 137, 186, 187, 188]. For example, the Zak transform is an instance of an intertwining operator for irreducible representations of Heisenberg Group over locally compact abelian groups. As previously stated, the narrow-band and wide-band ambiguity functions correspond identically and respectively to the short-time Fourier transform and the wavelet transform except for interpretations. Because the Heisenberg group H is a contraction of the group $G \times \mathbb{R}$, where G is the affine group [11], the narrow-band ambiguity function is a limiting case of the wide-band ambiguity function and analogously the short-time Fourier transform is a limiting case of the wavelet transform. The classes of bilinear distributions are linear rank-1 transformations [3] and as such they are Weyl correspondences rather than generalized transforms of a signal into a new space. They are related to linear time and frequency shifts of transforms such as the short-time Fourier transform and the wavelet transform.

3.4 Applications of Time-Frequency Methods

The decision to use bilinear or linear time-frequency apparatus to study a signal is largely influenced by the suitability of the apparatus, the signal's characteristics, the investigator's knowledge of the signal, and the available time-frequency tools. Oftentimes, an investigator who is quite knowledgeable about bilinear distributions may have only limited knowledge about linear time-frequency methods. The converse statement is also true. Moreover, an investigator

may be versed in a subset of bilinear or linear time-frequency representations, or in a set of time-frequency methods, constituted from some subsets of both bilinear and linear representations. The members of this set of bilinear and linear time-frequency methods may not be equally applicable to a given signal, in a concerned set of signals, in revealing its relevant characteristics. While a time-frequency method may yield optimum results in one application, it may not in another. Partly because of the limitations on an investigator's knowledge and the urgency of comparative study to determine the best suited time-frequency method for a given application, both bilinear and linear time-frequency methodologies are used in many of the same applications.

Although the wide-band and the conventional ambiguity functions were originally viewed in this treatise as bilinear distributions, it was later pointed out that they were also linear representations under the respective interpretations of the wavelet transform and the short-time Fourier transform. It can be concluded, therefore, that the class of ambiguity functions sits at the interface of bilinear and linear time-frequency methods. They are both bilinear and linear functional representations. In the bilinear context, the ambiguity function's usual areas of applications include sonar and radar [69, 106], radio astronomy and communications [69], and medical imaging [189]. A presentation of an inexhaustive list of references exemplifying some of the applications of bilinear and linear time-frequency representations in signal processing will shortly follow. Most of these areas of application are identical. For example, time-frequency representations were heralded into signal processing under the names of Weyl-Heisenberg

(Gabor) expansion and the spectrogram, for the sole purpose of studying acoustical signals [38, 60, 61] with emphasis on speech.

Bilinear time-frequency distributions have found use in areas such as detection and classification [190, 191, 192, 193], communications [194], speech [195, 196], biomedicine [92, 197, 198, 199, 200, 201], noise suppression [69], and imaging [202]. In the case of linear time-frequency methods, the wavelet transform and the short-time Fourier transform have been applied to such areas as imaging [203, 204], noise suppression [205, 206, 207, 208], detection and classification [209, 210, 211], speech [212, 213, 214], compression [208, 215, 216, 217], and biomedicine [218, 219, 220, 221], and the Weyl-Heisenberg expansion and the Zak transform have found application in areas that include noise suppression [170], communication [177, 222] detection [222, 223, 224, 225], imaging [226, 227, 228, 229], and biomedicine [228, 230].

Chapter 4

Discrete Zak Transform with Weyl-Heisenberg Expansions

Chapter 3 emphasized continuous time-frequency techniques for finite energy signals wherein the phase (or time-frequency) space was assumed to be of infinite extent. The relationships of these techniques to the classical Fourier transform, the interrelationship among the nonlinear and linear types, and the intra-relationship between the members of either of the nonlinear or linear ones were demonstrated. It was shown that an extension of the classical Fourier transform, the short-time Fourier transform, shares an intimacy with Zak transform and Weyl-Heisenberg expansion. It was further revealed that the infinite sample values of the short-time Fourier transform defined on a sublattice of phase space are merely the Weyl-Heisenberg expansion coefficients, and that the Weyl-Heisenberg system must satisfy certain special constraints to guarantee invertibility of the corresponding Weyl-Heisenberg expansion. One of these constraints relates to the sublattice parameters. The resulting rectangular lattice of phase space must have at least unit density to make possible stable and expeditious computation of the coefficients at the Nyquist rate or higher [231]. In spite of the intimate relatedness of the Zak transform to the short-time Fourier transform, it is otherwise closely tied to the classical Fourier transform via the z-transform [232]. While the Fourier transform is definitively the z-transform evaluated on the unit circle, the Zak transform, which is equivalent to a multirate signal analysis, is equal to the modified z-transform evaluated on the unit circle. It, therefore, follows that like the short-time Fourier transform, the Zak transform is an

extension of the Fourier transform; namely, the Zak transform is an example of the modified Fourier transform, which is analogous to the running Fourier transform (and z-transform) in recursive frequency-domain filtering and to the inverse of one of the functions contained in the generalized sampling expansion [117]. Moreover, equivalent multirate natures and similar sampling grids of Zak transform and Weyl-Heisenberg expansion make the Zak transform the most natural tool for studying Weyl-Heisenberg expansions.

Transforms of the integral and series expansion forms defined in terms of continuous variables over a finite or infinite space serve no meaningful computational purpose in practical applications of digital signal processing. Practical digital signal processing efficiently processes both *inherently discrete sequences and continuous functions (signals or transforms)* that are first converted into discrete sequences. These two types of sequences must assume finite extent--really finite, essentially finite, or periodic--before processing. The discretization of continuous functions can be done in any one of several ways, but under the assumption of time-limitedness or bandlimitedness of the function, the most commonly used method is periodic sampling [233]. The high computational efficiency attained in the digital processing for even continuous functions is due to the continued rapid development in digital computer technology's increasing computing speed and storage capacity at decreasing cost. Still, practical digital signal processing has its physical limitations [234]. Henceforth in this research, all input and output functions will be sequences[41] that may or may not represent continuous functions. The

[41] However, there may be momentary digression to the discrete-time case wherein the spectrum is analog.

representative finite input sequences will experience digital processing. While many of the concepts and results of continuous Zak transform and Weyl-Heisenberg theories carry over to the discrete case, in some instances the concepts differ slightly whereas the corresponding results differ greatly. For example, the infamous zero theorem that plagues the continuous Zak transform, can be shrewdly avoided in the discrete Zak transform.

The previous representations of Zak transform and Weyl-Heisenberg expansion are of much theoretical interest, but of little practical value in digital signal processing because of their dependency on continuous time and frequency variables, which may be defined over the entire phase space. Nonetheless, these representations are models for their discrete counterparts. Physically feasible phase space must contain essentially all the signal energy within a discretized finite area capable of holding at least the number of samples in the signal and window respectively. If the input sequence is representative of a continuous function, the respective discrete Zak transform and discrete Weyl-Heisenberg expansion of the sequence should correspond to its continuous counterpart in order to maintain consistency with the model. There are many avenues to a clear understanding and useful interpretation to discrete Weyl-Heisenberg expansion theory. These avenues lead to ways that feasibly and expeditiously implement Weyl-Heisenberg expansion of a sequence and recover its reconstruction coefficients. Some of these ways include discrete frame theory [235, 236, 237], biorthogonal sequence theory [238, 239, 240, 241, 242, 243], matrix theory [244, 245, 246], digital filter-bank theory [147, 247, 248, 249, 250, 251], and discrete Zak transform theory [252, 253, 254, 255, 256, 257]. While the discrete Zak transform method provides a very suitable venue for efficiently evaluating and

judiciously studying the intricacies of discrete Weyl-Heisenberg expansion and its coefficients, it can be combined in a leading or subordinate role with any or some of the other methods used to facilitate the evaluation of Weyl-Heisenberg expansion (or coefficients) and makes the ensuing investigation more useful [239, 258, 259, 260]. In general, any two or more methods may be concerted to expedite the synthesis of Weyl-Heisenberg expansions and the analysis of its coefficients. For example, matrix factorization may be combined with discrete frames to evaluate and study Weyl-Heisenberg synthesis and analysis [246] in Zak space. In short, each approach has its advantages and they perform more expeditiously in concert.

4.1 Some Other Numerical Methods for the Discrete Weyl-Heisenberg Expansions

A very basic and self-contained apparatus for the study of Weyl-Heisenberg expansion of a sequence and its reconstruction coefficients is Zak transform. There are many other approaches and associated ways to study Weyl-Heisenberg expansion and its coefficients. Some of these are often used well-established or well-known mathematical and engineering concepts. They are fundamental to Weyl-Heisenberg analysis. They include bases, frames, matrices, and filter-banks. They may be employed in the framework of Zak space or each other. For example, in the filter-bank context of discrete Weyl-Heisenberg theory, digital filters that satisfy certain frames or biorthogonal (or biorthogonal-like) basis conditions may be chosen. A more general scenario, may involve the filter-bank method conditioned on the concept of biorthogonal basis or frame in the venue of Zak space where the analysis is performed with matrices. These sundry combinations of means into a method are possible because there is no

unique nor precise method available for Weyl-Heisenberg analysis. Furthermore, different methods and their variations may lead to equivalent results. This is especially true for biorthogonal bases and frames [239, 261]. Here, the minimum energy biorthogonal sequence, which is responsible for a Weyl-Heisenberg expansion with minimum energy coefficients, is actually the sequence that generates the dual frame over which the expansion is made.

In equation (3.66), the continuous Weyl-Heisenberg expansion was defined as

$$f(t) = \sum_{m=-\infty}^{\infty} \sum_{n=-\infty}^{\infty} c_{m,n} g(t - mT) e^{2\pi i n S t},$$

with $ST \leq 1$ wherein the validity of the coefficients is guaranteed, except for some Weyl-Heisenberg wavelet system (g, T, S) at $ST = 1$, allowing for their stable recovery. Valid Weyl-Heisenberg coefficients for $ST > 1$ are generally not guaranteed because (g, T, S) is incomplete. Nonetheless, the validity of expansions corresponding to an incomplete Weyl-Heisenberg system may be possible [47] for some signals. Because the discrete lattice associated with the phase space of a Weyl-Heisenberg system has infinite extent, it is impractical for implementable discrete Weyl-Heisenberg expansions regardless of the signal length. This, therefore, suggests that practical phase space must be finite. Finitization of phase space can be done in several ways [55]. Typically, finite discrete phase space is a rectangular lattice. This lattice is adequate for Weyl-Heisenberg signal representation within acceptable error, so long as the pair of lengths of the mutually orthogonal sides of the rectangle sufficiently support the signal and its spectrum respectively.

With a finite discrete lattice, equation (3.66) can be discretized and finitized in several ways [259, 243] into a finite discrete Weyl-Heisenberg expansion that is quite proper for numerical implementation. Alternatively, a finite Weyl-Heisenberg expansion of any sequence $f(k)$ defined over the discrete Weyl-Heisenberg system (g, N, N) is

$$f(k) = \sum_{m=0}^{N-1} \sum_{n=0}^{N-1} c_{m,n} g(k - m) e^{2\pi i k n / N}, \quad k \in Z, \tag{4.1}$$

with the pair (N, N) being the lattice parameters. The number of Weyl-Heisenberg coefficients, $c_{m,n}$ may be deemed finite or periodic in both integer variables such that $0 \le m, n < N$. In either case, there are always more $c_{m,n}$ available than are required to sufficiently represent f, which will admit several Weyl-Heisenberg expansions because the set of all wavelet systems,

$$\{g_{m,n}: \quad 0 \le m, n < N\},$$

is linearly dependent. The discrete Weyl-Heisenberg expansion of $f(k)$ is definable over the less dense Weyl-Heisenberg system (g, M', L) with a form [156, 237, 239, 242, 243, 245, 246, 251, 254, 257] equivalent to

$$f(k) = \sum_{m=0}^{L'-1} \sum_{n=0}^{M-1} c_{mM',nL} g(k - mM') e^{2\pi i n k / M}, \quad k \in Z/N. \tag{4.2}$$

This representation of $f \in l_2(Z/N)$ may be unique for a fixed factorization of N. It is defined on the lattice $M'Z/N \times LZ/N$, a decimated subset of the discrete lattice $Z/N \times Z/N$

[32, 122] on which equation (4.1) is defined. The coefficients $c_{mM',nL}$ are a subset of decimated values of coefficients $c_{m,n}$. The sequence $f(k)$ and the window sequence $g(k)$ may or may not have the same length [242, 257]. When $f(k)$ and $g(k)$ are of different lengths, the range of m is different from L'. In this treatise, all sequences belong to the space of finite energy (square summable) sequences and the sequences $f(k)$ and $g(k)$ will assume the same length. In practice, equation (4.2) is preferred to equation (4.1) because it requires fewer coefficients to synthesize $f(k)$. To stably recover the coefficients, $c_{mM',nL}$, from equation (4.2), several methods are available. The most noteworthy and commonly used are Zak transform, biorthogonal bases, and frames. Less commonly used are matrix algebra and filters. While matrices are often used as an intermediary step in computing the biorthogonal sequence [241, 242, 243] and the discrete dual frame [235, 236, 237], they are sometimes used in a dominant role [244, 245, 246]. Digital filter-bank formulation of Weyl-Heisenberg expansion of $f(k)$ relating $f(k)$ with $c_{mM',nL}$ has a long history [64, 152]. In [152], the condition for recovering $f(k)$ from $c_{mM',nL}$ of the inverse series expansion was established as

$$\sum_{r=-\infty}^{\infty} g(n - rL)h(rL - n + kM) = \delta(k), \quad \forall n,$$

which is a biorthogonal condition where $g(n)$ is the synthesis filter associated with the series expansion and $h(n)$ is the analysis filter associated with the inverse. When the decimation time factor L is equal to the number of frequency samples M, no redundancy occurs. In recent years there has been a resurgence of activities in the filter-bank interpretation of Weyl-Heisenberg synthesis and analysis [238, 250, 251]. This updated filter-bank interpretation brings into

account the concept of frames in establishing the equivalence between Weyl-Heisenberg expansions and filter-banks. In fact, this updated idea establishes that tight Weyl-Heisenberg frames are equivalent to modulated filter-banks [250, 251] and that critically sampled modulated finite impulse response filter-banks do not have good frequency selectivity while permitting perfect reconstruction, a restriction tantamount to Balian-Low theorem.

4.1.1 Frames

The general theory of frames was reviewed in section (2.5.7). The theory of Weyl-Heisenberg frames is expounded in [12, 47, 56, 114, 128] where many important results critical to Weyl-Heisenberg expansion were proven. The essential features of continuous Weyl-Heisenberg frames carry over to the discrete case. Discrete Weyl-Heisenberg frames, which are generally nonorthogonal and redundant, are commonly used as bases sequences in a nonorthogonal series expansion of a signal sequence having generally nonunique coefficients. In special cases of exactness or exactness and tightness, these frames respectively become either biorthogonal or orthogonal bases, but they generally differ from either type of bases. Since frames are mostly inexact and non-tight, the associated signal representation nonunique.

If a window sequence $g(k)$, $k \in Z$, generates a set of sequences $\{g_{m,n}(k)\}$, $m \in Z$ and $n \in Z/M$, that constitutes a Weyl-Heisenberg frame for Weyl-Heisenberg expansion of a signal sequence $f(k)$, then

$$A\|f\|^2 \le \sum_{m=-\infty}^{\infty} \sum_{n=0}^{M-1} |\langle f, g_{m,n} \rangle|^2 \le B\|f\|^2, \quad 0 < A \le B < \infty, \tag{4.3}$$

with frame bounds A and B and

$$g_{m,n}(k) = g(k - mM')e^{2\pi ink/M}, \quad M \ge M'.$$

This condition implies that a dual Weyl-Heisenberg frame $\{h_{m,n}(k)\}$ exists with lower and upper frame bounds B^{-1} and A^{-1} respectively. The generator of the set $\{h_{m,n}(k)\}$ is $h(k) = (S^{-1}g)(k)$. S^{-1} is the unique inverse of the bounded, self-adjoint, linear frame operator S that maps $l_2(Z)$ onto $l_2(Z)$. S is defined as

$$(Sf)(k) = \sum_{m=-\infty}^{\infty} \sum_{n=0}^{M-1} \langle f, g_{m,n} \rangle g_{m,n}(k)$$

and any signal sequence $f(k)$ is expressible as

$$f(k) = \sum_{m=-\infty}^{\infty} \sum_{n=0}^{M-1} \langle f, h_{m,n} \rangle g_{m,n}(k) \tag{4.4}$$

or alternatively as

$$f(k) = \sum_{m=-\infty}^{\infty} \sum_{n=0}^{M-1} \langle f, g_{m,n} \rangle h_{m,n}(k). \tag{4.5}$$

Equation (4.4) is a discrete Weyl-Heisenberg expansion of any sequence $f(k)$ with expansion coefficients $c_{m,n} = \langle f, h_{m,n} \rangle$.

The most computationally useful Weyl-Heisenberg frames are tight (or snug), exact, or tight and exact. Tight Weyl-Heisenberg frames, $\{g_{m,n}(k)\}$, whose dual is generated by $h(k) = A^{-1}g(k)$, generally give rise to a redundant ($M > M'$) and nonorthogonal orthogonal-like expansion of any signal sequence $f(k)$ that is written as

$$f(k) = A^{-1} \sum_{m=-\infty}^{\infty} \sum_{n=0}^{M-1} \langle f, g_{m,n} \rangle g_{m,n}(k). \tag{4.6}$$

This expansion becomes an orthogonal one when $A = 1$. In this case, the frame $\{g_{m,n}(k)\}$ is actually an orthogonal basis which implies that it is a tight exact frame. Frames that satisfy the orthogonality condition are linearly independent. Moreover, they are critical sampled at $M = M'$ and the number of expansion coefficients, $\langle f, g_{m,n} \rangle$, equals the number of samples in the sequence $f(k)$. Further implications are that the dual frame $h(k) = g(k)$ and the coefficients $c_{m,n} = \langle f, h_{m,n} \rangle$ are unique. In spite of the desirability of frames being orthogonal bases, this desired condition only occurs at critical sampling. Critical sampling can lead to a numerically unstable computation of the expansion coefficients unless M' is carefully chosen [49, 253] to avoid the dilemma posed by Balian-Low theorem or $g(k)$ of $\{g_{m,n}(k)\}$ is bimodal [241].

If the set $\{g_{m,n}(k)\}$ is an exact Weyl-Heisenberg frame, it forms a biorthonormal basis with dual $\{h_{m,n}(k)\}$. That is, $\langle g_{m,n}, h \rangle = \delta(m)\delta(n)$. This condition occurs at critical sampling and oversampling ($M > M^*$) rates. While in the critical case $\{h_{m,n}(k)\}$ can be uniquely determined, it cannot be in the oversampled case.

The Weyl-Heisenberg wavelet system $\{g_{m,n}(k)\}$ is not a frame when it is undersampled ($M < M^*$). In this case of the Weyl-Heisenberg expansion of $f(k)$, recovering the coefficients $c_{m,n} = \langle f, g_{m,n} \rangle$ is a numerically delicate issue. These $c_{m,n}$ are even insufficient to determine $f(k)$ without error. Nonetheless, reasonably good $\tilde{c}_{m,n}$ can be found to allow the Weyl-Heisenberg expansion of $\tilde{f}(k)$ to be the best estimate of $f(k)$ [245].

4.1.2 Biorthogonal

The biorthogonal method is among the most common methods used in Weyl-Heisenberg expansion coefficients recovery. Its renowned application dates back to Bastiaans [154, 161]. Although the biorthogonal method has a longer history than the frame method, it is a special case of the frame method. As previously stated, if a Weyl-Heisenberg system is an exact frame, its dual and it are biorthogonal. Furthermore, the generator of the dual frame is the minimum energy biorthogonal sequence [257]. The biorthogonal method in discrete Weyl-Heisenberg signal analysis is commonly executed wholly or partially in Zak space [240, 257, 258,259, 260]. Other frameworks for finding the Weyl-Heisenberg biorthogonal sequence can be found in [241, 242, 243]. The biorthogonal method hinges on the biorthogonality condition which establishes

through an inner product that the synthesis and analysis Weyl-Heisenberg systems constitute a biorthogonal basis.

Reverting to equation (4.2) with Weyl-Heisenberg system (g, M', L), written as

$$g_{mM',nL}(k) = g(k - mM')e^{2\pi ikn/M}, \quad k \in Z/N.$$

The finite energy of $g(k)$ is normalized such that $\|g\|^2 = 1$. The validity of

$$f(k) = \sum_{m=0}^{L'-1} \sum_{n=0}^{M-1} c_{mM',nL} g_{mM',nL}(k), \quad k \in Z/N,$$

is grounded in the existence of the biorthogonal sequence $h(k)$ that allows for the coefficients $c_{mM',nL}$ to be recovered via

$$c_{mM',nL} = \sum_{k=0}^{N-1} f(k)h(k - mM')e^{2\pi ikn/M}, \quad m \in Z/L' \text{ and } n \in Z/M \tag{4.7}$$

under the biorthogonality of $g(k)$ and $h(k)$. In the adherence of Wexler and Raz nomenclature [243], if

$$\langle g_{-mM,-nL'}, h^* \rangle = (N/ML')\delta(mM)\delta(nL') \text{ for } m \in Z/L \text{ and } n \in Z/M',$$

the biorthogonality condition is satisfied. This condition is equivalent to saying that the Weyl-Heisenberg series expansion is complete. With proper selection of the respective discrete time and discrete frequency coarse sampling intervals M' and L of discrete phase space, the state $ML' = N$ corresponds to critically sampled Weyl-Heisenberg systems. Here, both the biorthogonal sequence and the coefficients are unique for a given system. $ML' > N$ corresponds to oversampled Weyl-Heisenberg systems. In this case, coefficients and the biorthogonal sequence are generally not unique for any particular Weyl-Heisenberg system. However, the nonuniqueness of the biorthogonal sequence can be exploited to put desirable properties on the representation and coefficients [242, 243, 257]. Some of these properties include orthogonal-likeness of series expansion and minimum energy coefficients.

The biorthogonal sequence is usually unknown for arbitrary Weyl-Heisenberg systems. Even when it is known, it may be very difficult to find. When $h(k)$ is found, its coarse sampling pattern over discrete phase space must be carefully chosen to avoid a numerically unstable representation. Discrete phase space has axes of length N with respective composite lengths $M'L'$ and ML in time and frequency.

4.2 Discrete Zak Transform

The discrete Zak transform has its root in pure mathematics [31]. In [31], Good wrote the statement of the discrete Zak transform in the expression of the generalized discrete Poisson summation formula in a multidimensional space. This Poisson summation formula has embedded

in it the relationship that defines the Zak transform of a time sequence with respect to the Zak transform of its Fourier sequence. This relationship is written in section 2.5.6 as

$$\sum_{m=0}^{M-1} a_{n-mL} e^{2\pi i n k/M} = L^{-1} \sum_{l=0}^{L-1} \hat{a}_{-k-lM} e^{-2\pi i l k - lMn/N}, \qquad (4.8)$$

$$n, k \in Z/N \quad \text{and} \quad ML = N.$$

It was long known that this relationship had applications outside of pure mathematics. At the turn of the last decade, Auslander *et al* [49, 122, 167] introduced the discrete Zak transform into digital signal processing. They introduced it as a viable substitute for the discrete Fourier transform (DFT) in dealing with nonstationary signals. They wanted a time-frequency tool that shared the many desirable properties of the DFT including the computational efficiency of FFT. They found it in the discrete Zak transform. It is a modified DFT. The discrete Zak space is not only most appropriate to study nonstationary signals in a mixed time-frequency space, but it is also very suitable to investigate and to better utilize other time-frequency (linear and nonlinear) and time-scale representations and is an ideal place for multirate digital filtering and polyphase implementation [49, 147, 167, 247, 249, 250, 252, 254, 255, 262, 263, 264]. Besides the discrete Zak space is amenable to a multiresolution signal analysis [143, 144, 147] because it possesses multiresolutional properties [264]. Since the zero theorem is a property of continuous Zak space, the discrete Zak space generally does not have this property which is a consequence of the uncertainty principle. However, if the continuous Zak space is numerically related to the discrete one, the zero theorem property can carry over and must, therefore, be avoided.

Like in the continuous case, there are many variant definitions of the discrete Zak transform. The definition adopted here is consistent with the continuous version. It is contained in the expression of equation (4.8). It is defined for a finite discrete sequence, f, of length N, but f may also be considered as defined over Z with periodicity constraints limiting each period to N. A sequence f is called N-periodic if for $f(n)$, $n \in Z$, the condition

$$f(n + N) = f(n), \quad n \in Z,$$

is satisfied. Thus, no more distinction will be made between a finite sequence of length N and a periodic one with period N. N is assumed to be composite. It may contain many different sets of factors. The finite discrete Zak transform, $Z_f(b, a)$, $a, b \in Z$, of a sequence $f \in l_2(Z/N)$ is defined as

$$Z_f(b, a) = \sum_{r=0}^{L-1} f(a + rM) e^{2\pi i r b / L}, \quad N = LM. \tag{4.9}$$

Clearly, the finite Zak transform can be interpreted as the L-point Fourier series expansion of a decimated sequence $f(rM)$ shifted by an integer parameter a. $l_2(Z/N)$ denotes the Hilbert space of all N-periodic sequences with inner product

$$\langle f, g \rangle = \sum_{k=0}^{N-1} f(k) g^*(k), \quad f, g \in l_2(Z/N).$$

The discrete Zak transform has another useful and very important interpretation in the z-plane. It is the type-1 polyphase transform [147, 254] evaluated on the unit circle [250, 254]. This interpretation is especially useful when adapting the finite Zak transform to multirate digital filtering. In the extreme cases of the existence of the finite Zak transform, $Z_f(b, a)$, $a, b \in Z$, it loses its time-frequency capability as it respectively degenerates into the signal at $b = 0$ for $L = 1$ $(Z_f(0, a) = f(a))$ and its finite spectrum (N-point Fourier series) at $a = 0$ at $M = 1$ $(Z_f(b, 0) = \hat{f}(r))$.

Like the DFT, the above discrete Zak transform is defined for any sequence, f, defined on the group Z/N but if f represents a continuous signal for discrete processing, the above discrete Zak transform, again like the DFT, can be derived from its continuous counterpart through the process of periodization and sampling [49, 58]. While the properties of the discrete Zak transform can be derived directly from the properties of the continuous version, they are independently formulated in the discrete framework using procedures analogous to those used in the continuous case. Many properties of the discrete Zak transform are found in [252] and supplemented in [254], where some proofs are also provided.

The discrete Zak transform, Z_f, is respectively periodic in frequency and time integer variables b and a with period N. That is

$$Z_f(b + N, a + N) = Z_f(b, a), \quad N = ML \text{ and } a, b \in Z.$$

Moreover, Z_f is periodic in frequency b with period L and quasi-periodic in time a with quasi-period M, as indicated symbolically in

$$Z_f(b + L, a + M) = e^{-2\pi ib/L} Z_f(b, a), \quad N = ML, \quad a, b \in Z,$$

with the implication that it is completely determined by its values

$$Z_f(b, a), \quad 0 \le b < L, \quad 0 \le a < M.$$

Therefore, the second dual periodicity condition completely describes the space of L-point Zak transforms where Z_f is computed using M L-point inverse DFTs in the sense that for each $0 \le a < M$, the L-point inverse DFT is performed on $f(r, a) = f(a + rM)$ for $0 \le r < L$, to get L values of $Z_f(b, a)$, $0 \le b < L$.

The periodicity in frequency with period L and quasi-periodicity in time with period M property of the Zak transform is of fundamental importance in Zak transform operations. This property, which affects the limits of time and frequency translations in Zak space, is intimately related to the time and frequency translations of a signal sequence. To illustrate, for $m, n \in Z/N$ and $f \in Z/N$, $f_{m,n} = R_n T_m f$, where

$$(R_n T_m f)(k) = f(k - m) e^{2\pi ikn/N}, \quad k \in Z/N,$$

and in Zak space

$$Z_{f_{m,n}}(b, a) = e^{2\pi i na/N} Z_f(b + n, a - m) \quad N = ML, \quad a, b \in Z. \tag{4.10}$$

In particular, if, instead, m and n are chosen on the subset $(mM, nL) \subset Z/N \times Z/N$ such that $0 \le m < L$ and $0 \le n < M$, equation (4.10) becomes by decimation and the second periodicity condition

$$Z_{f_{mM,nL}}(b, a) = e^{2\pi i(mb/L - na/M)} Z_f(b, a), \quad a, b \in Z, \quad N = ML. \tag{4.11}$$

This relationship is pivotal with regards to Weyl-Heisenberg expansion in Zak space because it leads nicely into a 2-dimensional inverse discrete Fourier transform on $M \times L$ points.

In a similar manner, dilation of signal sequence and its effect on its spectrum is reflected in Zak space. For example

$$Z_{D_\lambda f}(b, a) = \sqrt{\lambda} Z_f(\lambda^{-1} b, \lambda a), \quad \lambda, a, b \in Z, \tag{4.12}$$

with the special meaning

$$Z_{D_{2^n} f}(b, a) = \sqrt{2^n} Z_f(2^{-n} b, 2^n a), \quad \lambda = 2^n, \quad n, a, b \in Z.$$

The finite discrete Zak transform, Z_f is both invertible and norm-preserving (equivalently, inner product-preserving). Z is an intertwining unitary operator that is a linear isometry from

$l_2(Z/N)$ onto $l_2(Z/M, Z/L)$. $l_2(Z/M, Z/L)$ denotes the Hilbert space of all sequences $F(b, a)$, $a, b \in Z$, with inner product

$$\langle F, G \rangle = \sum_{a=0}^{M-1} \sum_{b=0}^{L-1} F(b, a) G^{*}(b, a)$$

provided the condition

$$F(b + L, a + M) = e^{-2\pi i b/L} F(b, a), \quad M, L > 0 \text{ and } a, b \in Z$$

is satisfied. This condition implies that $f \in l_2(Z/N)$, $N = ML$,

$$f(a) = L^{-1} \sum_{b=0}^{L-1} F(b, a), \quad a \in Z,$$

and

$$F(b, a) = Z_f(b, a), \quad a, b \in Z,$$

if $f \in l_2(Z/N)$ is similarly recoverable from $Z_f \in l_2(Z/M, Z/L)$. f is certainly recoverable from Z_f. By summing both sides of equation (4.9) with respect to $b \in [0, L)$ and solving, f is recovered:

$$f(a) = L^{-1}\sum_{b=0}^{L-1} Z_f(b, a) \quad 0 \le a < N. \tag{4.13}$$

This is only one of two ways to recover the signal sequence from the discrete Zak transform, Z_f. The signal sequence can be recovered in a customary way using Fourier inversion. In this case, f depends solely on the values of Z_f described on the Hilbert space $l_2(M, L)$. In other words,

$$f(a + rM) = L^{-1}\sum_{b=0}^{L-1} Z_f(b, a)e^{-2\pi irb/L} \quad 0 \le b < L, \quad 0 \le a < M. \tag{4.14}$$

Henceforth, Z_f and F are used synonymously with restriction to the space $l_2(M, L)$.

The finite discrete Zak transform is the main building block of the Cooley-Tukey FFT algorithm [265]. The main part of the FFT algorithm is contained in equation (4.8) which when restated in terms of the signal sequence $f \in l_2(Z/N)$ and its the N-point DFT spectrum $\hat{f}$ becomes for $0 \le b < L$ and $0 \le a < M$,

$$Z_f(b, a) = e^{-2\pi iab/N} M^{-1} Z_f(a, -b), \quad N = ML, \tag{4.15}$$

or alternatively

$$Z_f(-b, a) = e^{2\pi iab/N} M^{-1} Z_f(a, b), \quad N = ML. \tag{4.16}$$

Either alternative statement is critical to understanding the role of the discrete Zak transform in digital signal processing as it relates to the DFT. In fact, it can be said that rotating the Zak transform Z_f 90° produces, up to the factor $M^{-1}e^{2\pi iab/N}$, the Zak transform $Z_{\hat{f}}$ and vice versa. Moreover, this duality of the Zak transform makes it possible to similarly recover the Fourier spectrum from discrete Zak transform and to categorically prove Parseval's theorem for the discrete Zak transform and the DFT. Consequentially, energy conservation is established between Zak space and signal space, between Zak space and Fourier space, and between Fourier space and signal space.

In terms of the spectrum $\hat{f} \in Z/N$, the Zak transform is defined as

$$Z_f(a,b) = \sum_{s=0}^{M-1} \hat{f}(b+sL)e^{2\pi isa/M}, \quad 0 \le a < M, \quad 0 \le b < L, \quad N = mL. \qquad (4.17)$$

It can be easily shown that Z_f is periodic in time variable a with period M and quasi-periodic in frequency variable b with quasi-period L. In other words,

$$Z_f(a+M, b+L) = e^{-2\pi ia/M} Z_f(a,b), \quad 0 \le a < M, \quad 0 \le b < L.$$

By extending Zak space beyond its minimal fundamental limits described over the space $l_2(M, L)$, it can be found that Z_f is N-periodic in each variable.

The most natural inverse of Z_f over the fundamental Zak space utilizes the concept of Fourier inversion with Zak transform duality property to produce

$$\hat{f}(b + sL) = \sum_{a=0}^{M-1} Z_f(-b, a) e^{-2\pi i(b - sL)a/N}, \quad N = ML, \tag{4.18}$$

where $0 \leq b < L$ and $0 \leq a < M$. Without bringing to bear Fourier inversion techniques, summing equation (4.17) with respect to a and substituting for Z_f from Zak transform duality property produces, through simplification,

$$\hat{f}(b) = \sum_{a=0}^{M-1} Z_f(-b, a) e^{-2\pi iab/N}, \quad 0 \leq b < N. \tag{4.19}$$

In this inversion procedure and the previous analogous one for f, the sequence is recovered on a strip of Zak space over which the Zak transform is periodic in both variables.

There are two Parseval's relations for Zak space. Starting with two sequences $f \in Z/N$ and $g \in Z/N$ with DFTs $\hat{f}$ and $\hat{g}$ respectively, two Parseval-like relations are obtained. One with respect to the sequences,

$$\sum_{b=0}^{L-1} Z_f(b, a) Z^*_g(b, a) = L \sum_{r=0}^{L-1} f(a + rM) g^*(a + rM), \quad 0 \leq a < M, \tag{4.20}$$

and the other with respect to their DFTs,

$$\sum_{a=0}^{M-1} Z_f(b,a)Z^*_g(b,a) = M^{-1}\sum_{s=0}^{M-1} \hat{f}(-b+sL)\hat{g}^*(-b+sL), \quad 0 \le b < L. \tag{4.21}$$

By summing equations (4.20) and (4.21) over a and b respectively, the two Parseval's relations are determined:

$$\sum_{a=0}^{M-1}\sum_{b=0}^{L-1} Z_f(b,a)Z^*_g(b,a) = L\sum_{a=0}^{N-1} f(a)g^*(a), \quad N = ML, \tag{4.22}$$

and alternatively

$$\sum_{a=0}^{M-1}\sum_{b=0}^{L-1} Z_f(b,a)Z^*_g(b,a) = M^{-1}\sum_{b=0}^{N-1} \hat{f}(b)\hat{g}^*(b), \quad N = ML. \tag{4.23}$$

An immediate consequence of equations (4.22) and (4.23) is Parseval's relation in Fourier space:

$$\sum_{a=0}^{N-1} f(a)g^*(a) = N^{-1}\sum_{b=0}^{N-1} \hat{f}(b)\hat{g}^*(b). \tag{4.24}$$

In particular, when $f = g$, energy is conserved between spaces:

$$\| Z_f \|^2 = L \| f \|^2 = M^{-1} \| \hat{f} \|^2.$$

The Zak transform of a conjugated signal sequence f^* is a frequency reversed conjugated Zak transform Z^*_f; namely

$$Z_{f^*}(b,a) = Z^*_f(-b,a), \quad 0 \le b < L, \quad 0 \le a < M.$$

In addition, a time and frequency reversed Zak transform Z_f results from a time reversed signal sequence f_-:

$$Z_{f_-}(b,a) = Z_f(-b,-a), \quad 0 \le b < L \quad 0 \le a < M.$$

Convolution and modulation are two very important properties in Fourier representations. They can be quite useful in the framework of Zak space where convolution,

$$Z_{(f*g)}(b,a) = \sum_{c=0}^{M-1} Z_f(b,c)Z_g(b,a-c), \quad 0 \le b < L, \quad 0 \le a < M, \qquad (4.25)$$

occurs with respect to the time variable and modulation,

$$Z_{(f\cdot g)}(b,a) = L^{-1}\sum_{d=0}^{L-1} Z_f(d,a)Z_g(b-d,a), \quad 0 \le b < L, \quad 0 \le a < M, \qquad (4.26)$$

occurs with respect to the frequency variable.

While the discrete Zak transform is a natural and well-adapted tool for the computational analysis of discrete Weyl-Heisenberg representations (or ambiguity functions) especially at critical and integer oversampling and it maintains a crucial role in undersampling and fractional oversampling of such representations, the Zak transform is equally important in the numerical analysis of discrete Weyl-Heisenberg systems in the context of biorthogonals and frames. Beyond Weyl-Heisenberg systems and representations, the Zak transform maintains a conceptual, numerical, and computational advantage in the study and implementation of polyphase representations of digital multirate filters. In this context, the Zak transform a multiresolution analysis feature is brought to bear in imaging and in the windowed Zak transform formulation [263] to perform decimated discrete time-frequency distributions that tradeoff bandwidth for computational speed at a given frequency resolution and lower implementation cost. Additionally, The Zak transform has proven to be very efficient in the "filtering and reconstruction of periodic signals"at undersampling and critical sampling. Zak space is a convenient place to maximally implement certain fast wavelet transform filter-bank realization [264]. Once in Zak space, the actual procedures in the computational analysis may be carried out using matrix computation, overlap-add method of block convolution or some other appropriate mathematical procedure.

The classical Zak transform is limited to a critical sampling formulation. This limitation makes the discrete Zak transform operation in Weyl-Heisenberg representations more challenging at other than computational critical sampling and integer oversampling. A desirable solution to this inherent sampling problem may entail broadening the definition of the Zak transform. This may

be done by specifying a frequency sampling constant that is different from the reciprocal of the time sampling constant wherein undersampling, critical sampling, and oversampling are natural consequences. In this new formulation, the discrete Zak transform would behave like the DFT with regard to sampling.

4.3 Discrete Weyl-Heisenberg Expansions in Zak Space

Some of the approaches to discrete Weyl-Heisenberg representations in Zak space include the concepts of frames [237, 253, 254], least-squares norm criterion [256], and DFT [156, 252, 255, 257, 258, 259,262]. The aforementioned references contain many algorithms designed to efficiently compute the Weyl-Heisenberg expansion and its inverse. Undoubtedly, the most computationally efficient algorithms among these have speed and efficiency that rival those of the FFT algorithms.

The discrete Weyl-Heisenberg expansion as an approximation of the exact Weyl-Heisenberg expansion contain some subtleties as well as errors [262, 266]. Moreover, the zero problem presented by the zero theorem in the exact expansion can be avoided in the discrete case provided the number of time samples in Zak space is odd.

In Zak space, a Weyl-Heisenberg system can be conveniently used to establish conditions for the existence and uniqueness of discrete Weyl-Heisenberg expansions for any sequence $f \in l_2(N)$. The Weyl-Heisenberg expansion of equation (4.2),

$$f(k) = \sum_{m=0}^{L'-1} \sum_{n=0}^{M-1} c_{mM',nL} g(k - mM') e^{2\pi i nk/M}, \quad 0 \le k < N, \quad N = ML = M'L',$$

is defined over the Weyl-Heisenberg system (g, M', L), having window sequence g and time-frequency sampling rate (M', L), with corresponding Weyl-Heisenberg coefficients $c_{mM',nL}$. The general Weyl-Heisenberg system (g, M', L) is a set of ML' window sequences

$$\{g_{mM',nL}: \quad 0 \le m < L', \quad 0 \le n < M\}.$$

The sampling rate (M', L) corresponds to the respective coarse sampling intervals of phase space time and frequency axes. The corresponding set of sampling points within (M', L) is (L', M) where L' is the number of time samples and M is the number of frequency samples. Thus, phase space the time axis is $N = M'L'$ while the frequency axis is $N = ML$. Since N is the number of samples in the signal sequence f, it follows from recalled equation (4.2) that when the number frequency sample points M equals the time sampling interval M' $(M = M')$, the number of Weyl-Heisenberg coefficients equals the number of signal samples and the critical sampling condition exists; when $M > M'$, the number of Weyl-Heisenberg coefficients is greater than the number of signal samples and the oversampling condition exists wherein the set of coefficients is redundant; and when $M < M'$, the number of Weyl-Heisenberg coefficients is less than the number of signal samples and the undersampling condition exists. Corresponding joint relationships hold for L and L' because they are constituents in the composites of N. The Weyl-Heisenberg system (g, M', L) may be shifted to other Weyl-Heisenberg systems

$(g, M', L)_{m',n'}$ where $0 \le m' < M'$ and $0 \le n' < L$ are fixed. The system $(g, M', L)_{m',n'}$ is the set of window sequences

$$\{g_{m'-mM',n'-nL}: \quad 0 \le m < L', \quad 0 \le n < M\}.$$

These two types of Weyl-Heisenberg systems are related via

$$g_{m'-mM',n'-nL} = e^{-2\pi i m n'/L'} (g_{m',n'})_{mM',nL}.$$

In Zak space, the same conditions are imposed on (g, M', L) and $(g, M', L)_{m',n'}$ and the same operations are performed on them to yield equivalent algebraic results that differ only by the phase factor $e^{-2\pi i m n'/L'}$. In addition, systems (g, M', L) and $(g, M', L)_{m',n'}$ are concerted in the computation of Weyl-Heisenberg coefficients with sequentially increased resolution [252, 255].

In general, Weyl-Heisenberg coefficients, $c_{mM',nL}$, are not uniquely determined. However, they are uniquely determined in the critically sampled case where the system (g, M', L) forms a basis of $I_2(N)$. Critically sampled (g, M', L) are extensively studied [252, 255]. In the oversampled case, the coefficients $c_{mM',nL}$ are redundant and the Weyl-Heisenberg system (g, M', L) is either integer oversampled ($M/M' \in Z$) or rationally oversampled ($M/M' \notin Z$). In either case of oversampling, algorithms are designed to parameterize the collection of all Weyl-Heisenberg expansions of f over a given (g, M', L) during a computation [156, 267].

Using the critically sampled Weyl-Heisenberg system, (g, M, L), as the benchmark, the application of the discrete Zak transform to discrete Weyl-Heisenberg representations is governed by the nilpotent action on the window signal, $g \in l_2(N)$ [132] to produce simultaneous time-frequency translates. Zak space separates this nilpotency on g by equation (4.11),

$$G_{m,n}(b, a) = e^{2\pi i(mb/L - na/M)} G;$$

where

$$a, b \in Z, \quad 0 \le m < L, \; 0 \le n < M, \quad N = ML, \quad G = Z_g;$$

which is the fundamental formula that relates the Weyl-Heisenberg wavelets of a Weyl-Heisenberg system to the corresponding generator window signal. With this very significant formula, Zak space isometry and Parseval's relation in equation (4.11) aid in bringing about an almost all important result in the analysis of Weyl-Heisenberg expansions of any signal $f \in l_2(N)$ having Zak transform $F \in l_2(M, L)$. This result,

$$F(b, a)G^*(b, a) = M^{-1} \sum_{m=0}^{L-1} \sum_{n=0}^{M-1} \langle f, g_{mM,nL} \rangle e^{2\pi i(mb/L - na/M)}, \qquad (4.27)$$

$$a, b \in Z, \quad N = ML,$$

is a Fourier series expansion in $l_2(M, L)$ with L-periodicity in variable b and M-periodicity in variable a. It can be interpreted as the Fourier series expansion of the nonlinear decimated cross ambiguity function,

$$A_{f,g}(mM, nL) = \langle f, g_{mM,nL} \rangle, \quad 0 \le m < L, \ 0 \le n < M.$$

Equation (4.27) is related to Zak space formulation of Weyl-Heisenberg expansion through the coefficient sets in relation

$$\langle f, g_{mM,nL} \rangle = M |G(b,a)|^2 c_{mM,nL}, \quad a, b \in Z, \quad 0 \le m < L, \ 0 \le n < M,$$

which is actually the double convolution relationship

$$\langle f, g_{mM,nL} \rangle = \sum_{r=0}^{L-1} \sum_{s=0}^{M-1} c_{(m-rM),(n-sL)} \langle f, g_{rM,sL} \rangle, \quad 0 \le m < L, \ 0 \le n < M.$$

The Weyl-Heisenberg expansion of $f \in I_2(N)$,

$$f(k) = \sum_{m=0}^{L-1} \sum_{n=0}^{M-1} c_{mM,nL} g_{mM,nL}(k),$$

$$g_{mM,nL}(k) = g(k - mM) e^{2\pi i nk/M}, \quad 0 \le k < M, \quad N = ML,$$

over the system (g, M, L) can be unraveled in Zak space as the product,

$$F = GP, \tag{4.28}$$

where

$$P(b,a) = \sum_{m=0}^{L-1} \sum_{n=0}^{M-1} c_{mM,nL} e^{2\pi i (mb/L - na/M)} \in I_2(M,L), \quad a, b \in \mathbb{I}(M,L)$$

and

$$\mathbb{I}(M, L) = \{(a, b): \quad 0 \le a < M, \quad 0 \le b < L\}.$$

It is in this formulation that Zak space is most crucial for analysis of Weyl-Heisenberg expansions. It decomposes the inherent nilpotency of Weyl-Heisenberg expansions into two distinct abelian stages. In addition, equation (4.27) is a powerful tool for analyzing Weyl-Heisenberg systems.

The critically sampled Weyl-Heisenberg system

$$(g, M, L) = \{g_{mM,nL}: \quad 0 \le m < L, \quad 0 \le n < M\}$$

is a basis for $l_2(N)$ if and only if G never vanishes. It follows that equation (4.28) defines a linear isomorphism from $l_2(M, L)$ onto $l_2(N)$. The resulting Weyl-Heisenberg coefficients for the expansion of f over (g, M, L) are given by the Fourier transform of $P = FG^{-1}$. More generally, a signal sequence $f \in l_2(N)$ is in the linear span of (g, M, L) if and only if F vanishes on ζ, the zero set of G in $\mathbb{I}(M, L)$. The dimension of the linear span of (g, M, L) is $N - J$, where J is the number of points in ζ. In this case, equation (4.28) defines a linear homomorphism from $l_2(M, L)$ onto the linear span of (g, M, L). If $f \in l_2(N)$ is in the linear span of (g, M, L), a $Q(b, a)$, with $(a, b) \in \mathbb{I}(M, L)$ can be defined such that

$$Q(b,a) = \begin{cases} \text{arbitrary } \alpha(b,a), & (a,b) \in \zeta, \\ F(b,a)G^{-1}(b,a), & (a,b) \notin \zeta, \end{cases}$$

where the space of Q is a J-dimensional subspace of $l_2(M,L)$. When $Q(b,a) = \alpha(b,a)$, the Weyl-Heisenberg coefficients for the expansion of f over (g,M,L) obtained by means of the Fourier transform of Q in Zak space are not uniquely determined.

Oversampled Weyl-Heisenberg systems (g,M',L) are characterized into two classes: integer oversampled with $M = RM'$, $R \in Z$, and rationally oversampled with $M = RM'$, $R \notin Z$; recall $N = ML = M'L'$ with $M > M'$, implying $L < L'$.

The integer oversampled Weyl-Heisenberg system (g,M',L), $M = RM'$, is a disjoint union of critically sampled Weyl-Heisenberg systems. By setting $g' = (g,M',L)$,

$$g' = \bigcup_{r=0}^{R-1} g_r', \quad g_r' = (g_r,M,L), \quad g_r = g_{rM',0}, \quad 0 \le r < R.$$

This statement implies that

$$g_{m'M',nL} = (g_{rM',0})_{mM,nL}, \quad 0 \le m' < L', \quad 0 \le r < R, \quad 0 \le m < L, \quad 0 \le n < L.$$

If $f \in l_2(N)$ is in the linear span of g', F can be written as

$$F(b,a) = \sum_{r=0}^{R-1} G_r(b,a)P_r(b,a), \quad (a,b) = \mathbb{I}(M,L), \quad P_r(b,a) \in l_2(M,L),$$

where $G_r P_r \in I_2(M, L)$ vanishes on ζ_r, $0 \le r < R$. The zero set ζ_r of G_r is contained in

$$\zeta = \bigcap_{r=0}^{J-1} \zeta_r,$$

where J is the order of ζ, the zero set of G. In the slightly more general case where $g^{\cdot}$ is the disjoint union of arbitrary critically sampled Weyl-Heisenberg systems, if $g^{\cdot}$ is the disjoint union of critically sampled Weyl-Heisenberg systems $g_r^{\cdot} = (g_r, M, L)$, $0 \ge r < R$, and ζ is the intersection of the zero sets ζ_r of the collection of functions G_r, $0 \ge r < R$, in $\mathbb{I}(M, L)$, then the dimension of the linear span of $g^{\cdot}$ is $N - J$ and the sequence $f \in I_2(N)$ is in the linear span of $g^{\cdot}$ if and only if F vanishes on ζ.

The linear span of $g^{\cdot}$ is related to the space of Zak transforms, $I_2(M, L)$, more intricately than in the critically sampled case. For example,

$$G(b, a) = [G_0(b, a)\ G_1(b, a)\ \ldots\ G_{R-1}(b, a)]$$

and

$$P(b, a) = [P_0(b, a)\ P_1(b, a)\ \ldots\ P_{R-1}(b, a)],$$

equation (4.28) takes the matrix form $F = GP^t$, P^t is the transpose of P, that defines a linear homomorphism of the RN- dimensional space of R-tupes of functions in $I_2(M, L)$ onto the linear

span of g'. The algorithm to compute a Weyl-Heisenberg expansion of f over g' is found in [156, 267]. The algorithm incorporates the procedure for the critically sampled case with arbitrary values α assigned to the quotient Q_r, $0 \geq r < R$, at points where the functions G_r vanish. In general, distinctly different decompositions of F may lead to distinctly different Weyl-Heisenberg expansions. Moreover, the coefficient set of Weyl-Heisenberg expansions of $f \in l_2(N)$ over g' is parameterized by the collection of decompositions of F and the arbitrarily assigned values α.

In the rationally oversampled Weyl-Heisenberg system $g' = (g, M', L)$ with $M = RM'$, $R \notin Z$, denote $K = \text{lcm}(M, M')$ and define positive integers S and S' such that $K = MS = M'S'$. From $N = ML \equiv M'L'$, it can be deduced that S divides L and S' divides L'. Using arguments similar to the integer oversampled case, it can be said that g' is the disjoint union of the undersampled Weyl-Heisenberg systems. That is,

$$g' = \bigcup_{s=0}^{S'-1} (g_s, K, L),$$

where

$$(g_s, K, L) = \{(g_{sM',0})_{m'K,nL'}, \quad 0 \geq m' < L_1, \quad 0 \leq n < M\}, \quad L_1 = \frac{L}{S}.$$

The undersampled system (g_s, K, L) is contained in the critically sampled system (g_s, M, L). Since $g_s = g_{sM',0'}$ a signal sequence $f \in l_2(N)$ is in the linear span of g' if and only if F is expressible in the form

$$F(b,a) = \sum_{s=0}^{S'-1} G_s(b,a)P_s(b,a), \quad (a,b) = \in \mathbb{I}(M,L), \quad P_s \in L_2(M,L),$$

where P_s is periodic in the frequency variable b with period L_1. This fact is ascertained by

$$P_s(b + L_1, a) = P_s(b,a), \quad 0 \leq s < S', \quad (a,b) \in \mathbb{I}(M,L).$$

When f is in the linear span of g', $P_s(b,a) \in l_2(M, L_1)$, $0 \leq s < S'$, and $F = GP$ is a column vector in Zak space of length S and G is a $S \times S'$ matrix. Furthermore, the collection of Weyl-Heisenberg expansion coefficients is obtainable from the Fourier transform of

$$P_s(b,a), \quad 0 \leq a < M, \quad 0 \leq b < L_1, \quad 0 \leq s < S'.$$

Two available algorithms for computing the Weyl-Heisenberg coefficients of rationally oversampled Weyl-Heisenberg systems are the pseudo-matrix inversion [156] and iterative orthogonal projection [267].

Chapter 5

Orthogonal Projection of Weyl-Heisenberg Expansions in Zak Space and Zak Transform Generalization

This chapter builds upon the previous ones. The previous chapters establish the theoretical foundation for Zak transform and Weyl-Heisenberg expansions as well as the physical realization of Weyl-Heisenberg representations in Zak space. Pursuant to this theoretical basis, the main focus here is the extension of Zak transform theory to include a generalization consistent with discrete Fourier analysis and the orthogonal projection of Weyl-Heisenberg expansions in Zak space from a critically sampled space onto an undersampled subspace. As a precursor to successfully carrying out these respective pursuits, a generalized DFT for arbitrary noncausal signals, without necessarily regarding for periodicity, is developed and the effect of Zak transform numerics on signal analysis and display over different time-frequency subgroups is investigated.

The classical theory for stationary signals includes applications in filtering, system identification, estimation, detection, noise suppression, and digital signal processing algorithms. It is generally desired to have an alternative to this classical theory in phase space for nonstationary signals. As previously mentioned, Zak space is the simplest phase space and it is a convenient place to study other time-frequency representations such as Weyl-Heisenberg expansions, ambiguity functions, distributions, and affine wavelets. In addition, Zak transform shows promise in signal

synthesis; it is effective in filtering noise suppression, and signal restoration using Gerchberg-Papoulis algorithm [156], and it efficiently applies FFT-based digital signal processing algorithms to nonstationary signals.

In the classical theory of signal analysis, the conversion of a continuous function into a discrete one is simple and well-understood. Nyquist-Shannon sampling theorem fully specifies not only the condition but also the minimum number of samples needed for such a conversion. Although the existence of the DFT for stationary signals violates the uncertainty principle by the presupposition that a time-limited signal has a finite spectrum, it is well-known that the DFT yields satisfactory results. However, it is not as simple to convert a continuous nonstationary signal into a discrete one. Nyquist-Shannon sampling theorem generally does not apply. In fact, there is no governing sampling theory for nonstationary signals. Thus, the question arises: What is the best way to sample a nonstationary signal so as to recover its alias-free version from the samples? The signal may have an unknown region of existence or the observational period may seem infinite. Therefore, a certain amount of guessing is required to determine a nonstationary signal sample rate. Moreover, the uncertainty principle plays a crucial role in nonstationary signal analysis as evidenced by its emergence in the zero theorem in Zak space.

5.1 Generalized DFT

It is customary when analyzing a signal using the DFT to assume that the signal is either periodic or causal, aperiodic, and finite [63, 64, 268, 269,]. However, a finite aperiodic signal may be

noncausal and asymmetrical. In fact, a signal may start at any point in time depending on its natural characteristics and mathematical description.

In general [63], a periodic continuous signal has an aperiodic discrete spectrum; an aperiodic discrete signal has a periodic continuous spectrum; and an aperiodic continuous signal has an aperiodic continuous spectrum. The main aim, in this section, is to convert an aperiodic continuous signal into an aperiodic or periodic discrete signal suitable for digital computation. This discrete signal shall retain the central features of its continuous counterpart. Several signals including the zero mean gaussian will be discretized and analyzed with the DFT. However, it is herein contented that the unmodified DFT of an arbitrary unaltered signal can produce results inconsistent to those produced by its continuous counterpart, the continuous Fourier transform (CFT). To remedy this potential defect of the DFT, a generalized DFT is derived on the basis noncausality of the signal. For any arbitrary signal, the generalized DFT emulates the CFT more accurately than the usual DFT. The derivation of the generalized DFT will be done two ways: directly and by means of the Poisson's summation formula [117]. In addition, the aforementioned discretized signals will be analyzed with both DFTs and compared with each other relative to the CFT.

5.1.1 Sampling Theorem

As previously mentioned, if a continuous signal is periodic in the time or frequency domain, then it is discrete and aperiodic in the alternate domain. Adequate knowledge of one period of such a

continuous signal is sufficient to fully describe all the periods. On the contrary, an aperiodic continuous signal is not naturally discrete in the dual domain. Nonetheless, a bandlimited or timelimited aperiodic continuous signal can be accurately represented with discrete samples from which it is recoverable. Moreover, a signal that is neither bandlimited nor time-limited and whose essential energy content falls within a region outside of which the energy is acceptably negligible can be correspondingly made either time-limited or bandlimited. Because a non-bandlimited aperiodic continuous signal can be made into a bandlimited one and time-limited signals are used to represent practical ones (*practical signals are time-limited*), a practical continuous signal can be validly approximated by a bandlimited one having the concerned frequency components with the relevant energy falling within a spectral width of S [12, 270]. In the theoretical sense, a signal can be simultaneously non-time-limited and non-bandlimited but it cannot be simultaneously bandlimited and time-limited [63, 117, 270]. In the reality of digital signal processing, the signals of concern must violate the uncertainty principle in the condition of simultaneous bandlimitedness and time-limitedness because digital signal processing techniques only apply to finite data sets.

5.1.1.1 Bandlimited Signals

In [271], it is stated 'If a function $f(t)$ contains no frequencies higher than W cps it is completely determined by giving its ordinates at a series of points spaced $(1/2W)\,s$ apart.' In other words, if a finite energy aperiodic continuous signal's spectrum exists only over a band of frequencies $S = 2W$, where W is the bandwidth and S is the spectral width, the signal is

recoverable from its uniform time samples taken at intervals $t_s = 1/S$. The sampling interval $t_s = 1/S$ is equivalent to the minimum sampling rate $v_s = S$. This sampling rate is known as the Nyquist rate. A signal sampled at the Nyquist rate is critically sampled. Some critically sampled signals may not be recoverable if the locations of the samples are arbitrarily chosen. For example, a sinusoidal signal critically sampled at its zero crossing is not recoverable. Therefore a sampling rate of $v_s > S$ is a necessary and sufficient condition that absolutely guarantees the full recovery of any bandlimited signal from its samples. A signal sampled at $v_s > S$ is oversampled. Incidentally, a signal sampled at $v_s < S$ is undersampled. An undersampled signal is not completely recoverable from its samples because the energy contained in frequencies outside of v_s are harmonics of frequencies within v_s.

A bandlimited or essentially bandlimited[42] signal $f(t)$ has a Fourier transform that is nonzero within and zero outside of a limited band of frequencies. It is defined as

$$\hat{f}(v) = \int_{-\infty}^{\infty} f(t)e^{-2\pi ivt}dt = 0 \quad \text{for } v \notin [v_a, v_b) \text{ and } 0 < S = v - v_a < \infty$$

with

$$f(t) = \int_{v_a}^{v} \hat{f}(v)e^{2\pi ivt}dv \quad \text{for } t \in \mathbb{R}$$

---

[42] The band limitation of a signal to a maximum frequency W Hz, beyond which the energy content of higher frequencies in the function is negligible, involves setting the energy content of frequencies above W to zero. This bandwidth, depending on the needed accuracy, may be chosen to contain at least 95% of the signal energy.

and in terms of energy

$$E = \int_{-\infty}^{\infty} |f(t)|^2 dt = \int_{v_a}^{v_b} |\hat{f}(v)|^2 dv < \infty \qquad (5.1)$$

A bandlimited signal is transformable into a discrete signal with a periodic spectrum through the process of periodic extension. The spectrum's period $S = v_b - v_a$ is the fundamental period. Therefore, the Fourier transform

$$\hat{f}(v) = \int_{-\infty}^{\infty} f(t) e^{-2\pi i v t} dt, \quad v \in [v_a, v_b) \text{ and } v_a < v_b,$$

is representable as the Fourier series

$$\hat{f}(v) = S^{-1} \sum_{k=-\infty}^{\infty} f(kt_s) e^{-2\pi i v k t_s}, \quad t_s = S^{-1} \text{ and } S = v - v_a, \qquad (5.2)$$

where $(1/S) f(kt_s)$ are the Fourier coefficients.

5.1.1.2 Time-Limited Signals

Time-limited signals are naturally time-limited or essentially time-limited. If a signal $f(t)$ is defined such that

$$f(t) = 0 \quad \forall t \notin [t_a, t_b) \text{ where } T_0 = t_b - t_a,$$

then $f(t)$ is time-limited [63, 117, 270, 272]. A finite duration signal is recoverable from uniform samples of its spectrum taken at the rate $T \geq T_0$ with sample intervals $v_0 = 1/T$. This sampling operation is the dual of the sampling operation discussed for bandlimited signals. Both types of sampling operations share equivalent properties. For example, bandlimited signals are a subset of the class of analytic signals. Correspondingly, the Fourier transforms of time-limited signals are a subset of the class of analytic signals [117, 273].

A time-limited signal $f(t)$ of span T_0 has Fourier transform

$$\hat{f}(v) = \int_{-\infty}^{\infty} f(t) e^{-2\pi i v t} dt = \int_{t_a}^{t_b} f(t) e^{-2\pi i v t} dt, \quad \forall v \in \mathbb{R}. \tag{5.3}$$

Through inverse Fourier transformation, $f(t)$ is be recoverable from $\hat{f}(v)$ by the integral

$$f(t) = \int_{-\infty}^{\infty} \hat{f}(v) e^{2\pi i v t} dt, \quad t \in [t_a, t_b),$$

and alternatively and more importantly by the series

$$f(t) = T^{-1} \sum_{n=-\infty}^{\infty} \hat{f}(n v_0) e^{2\pi i n v_0 t}, \quad v_0 = T^{-1} \text{ and } T \geq T_0, \tag{5.4}$$

because the extension of $f(t)$ gives it a periodic form with fundamental period T. The Fourier coefficients are $T^{-1}\hat{f}(nv_0)$. Therefore, a finite duration $f(t)$ is representable in terms of

scaled samples of $\hat{f}(v)$ taken at intervals $v_0 = 1/T$. To recover $\hat{f}(v)$ from its scaled samples $\hat{f}(nv_0)$, the condition

$$v_0 \equiv T^{-1} \leq T_0$$

must be satisfied. However, error-free recovery of $\hat{f}(v)$ is only absolutely guaranteed for sampling rate $T > T_0$.

5.1.1.3 Relationship Between Resolution and Period

In general, the typical Fourier series representation is not necessarily restricted to naturally periodic signals. It is applicable to any arbitrary signal that satisfies the conditions:

- The signal has finite energy over a finite interval,
- A complete orthogonal set of basis signals can be found to express the signal over the finite interval,
- The Fourier coefficients are calculable from the appropriate inner product expression of the signal and its orthogonal basis signals, and
- Any error introduced from the finitization of the signal must be minimal [274].

Moreover, any arbitrary signal $f(t)$ with compact support or that decays rapidly to zero at infinity, and energy

$$E = \int_{t_a}^{t_b} |f(t)|^2 dt < \infty$$

is describable in terms of the Fourier series

$$f(t) = \sum_{k=-\infty}^{\infty} c_k \Phi_k(t), \quad \Phi_k(t) = e^{2\pi i k v_0 t}. \tag{5.5}$$

$\Phi_k(t)$ is a complete orthogonal set of basis signals. The coefficients

$$c_k = \langle \Phi_k, f \rangle = \int_{t_a}^{t_b} f(t)\Phi_k^*(t)dt \tag{5.6}$$

are the Fourier coefficients.

An aperiodic signal can be efficiently sampled in both time and the frequency through the process of periodization and sampling. Knowing a signal time duration and the spectral duration[43] are sufficient to provide sound information on the minimum number of sample values required to faithfully represent it in the time or frequency domain. Suppose an aperiodic signal has time duration T_0 and spectral duration S and its time period $T \geq T_0$ while its spectral period $v_s \geq S$, the periodization of the time signal (Fourier spectrum) results in a sampled spectrum (signal) at intervals $v_0 = 1/T$ ($t_s = 1/v_s$). The number of samples needed to represent an aperiodic signal $f(t)$ (spectrum $\hat{f}(v)$) is T/t_s (v_s/v_0). If N is defined as the number of samples in $f(t)$ ($\hat{f}(v)$), then

---

[43] In this context, duration means the actual duration or the essential duration. A signal may be conditioned to essential time-limitedness, bandlimitedness, or both.

$$N = \frac{T}{t_s} \Rightarrow N = Tv_s \Rightarrow \frac{v_s}{v_0} = N.$$

These relationships establish that the number of samples required to represent an aperiodic time signal is exactly the same as the number of samples required to represent its spectrum. The minimum number of samples is achieved when $T = T_0$ and $v_s = S$. However, the number of samples used to describe a signal (spectrum) may be chosen with only partial knowledge of its spectrum (signal). Nonetheless, it is imperative in any sampling operation to capture in the signal (spectrum) samples the small but significant details that exist in the variations of the original. Hence the resolution of a recovered signal (spectrum) from its samples is a very important factor. Resolution and aliasing of a sampled signal (spectrum) are related to each other and to the number of samples $N \geq N_0$, $N_0 = T_0S$, in the signal (spectrum). They are closely related to the sample interval and period of a sampled signal (spectrum); equivalently, the resolution of a sampled signal (spectrum) is closely related to the aliasing in its spectrum (signal).

Thorough analysis of a signal sometimes necessitates a dual investigative approach wherein subtle information in it and its spectrum are unraveled. To study an aperiodic continuous signal using digital signal processing techniques, the signal and its spectrum must each be characterized by a finite representative set of samples regardless of the signal's nature. These finite sets of samples are obtained by means of periodization and sampling of the signal in time and frequency. Periodization and sampling of a time signal correspond to sampling and periodization of its spectrum and vice versa. The operations of periodization and sampling on an aperiodic continuous signal in both time and frequency produce a periodic discrete signal in both

time and frequency. A resultant finite discrete signal (spectrum) is extracted from over the fundamental period of its periodic counterpart. This finite discrete signal is a discrete replica of the original aperiodic continuous signal. Since a signal cannot be both time-limited and bandlimited, resolution and aliasing always affect a sampled signal. Aliasing is always inherent to a sampled signal and its sampled spectrum resulting from periodization and sampling of a non-time-limited non-bandlimited signal. In this case, tradeoffs must be made between the desired resolution and allowed aliasing in the signal and its spectrum. Because the number of samples in a sampled signal (spectrum) is directly proportional to its duration (or period) and inversely proportional to its sampling interval, improved resolution in a sampled signal (spectrum) corresponds to reduced aliasing in its spectrum (signal) and ultimately itself.

5.1.2 Fourier Transform Interpretations

For an Abelian group G [27, 275, 276] on which a finite energy function is defined, the definition of the Fourier transform on G has four different interpretations. Each interpretation depends upon the form of G. When $G = \mathbb{R}$, the Fourier transform is the CFT while when $G = Z$, it is the discrete-time Fourier transform (DTFT). The continuous CFT and the DTFT have different and independent interpretations. Nevertheless, they share many of the same properties. Z is a subgroup of $\mathbb{R}$ under addition. Another interpretation of the Fourier transform is the DFT. This occurs when G is the finite group Z/NZ (abbreviated Z/N), a subgroup of Z. N is the positive number of elements in the DFT. Finally, the Fourier transform has an interpretation

when G is the quotient group $\mathbb{R}/Z$. In this formulation, the function f is a member of $L_2(\mathbb{R}/Z)$ and its Fourier transform $\hat{f}$ is a member of $L_2(Z)$.

5.1.2.1 DTFT

The theory of the Fourier transform is well developed for finite energy functions defined on the group $G = \mathbb{R}$. In addition, a reasonably solid Fourier transform theory exists for finite energy functions defined on the group $G = Z$. This is the Fourier Transform of an aperiodic finite energy sequence $f(k)$, $k \in Z$, defined as

$$\hat{f}(v) = \sum_{k=-\infty}^{\infty} f(k) e^{-2\pi i k v}, \quad v \in [-1/2, 1/2), \tag{5.7}$$

and the inverse Fourier transform, which is equal to the original function, is

$$f(k) = \int_{-1/2}^{1/2} \hat{f}(v) e^{2\pi i k v} dv, \quad k \in Z, \tag{5.8}$$

where $\hat{f} \in L_2(G = \mathbb{R}/Z)$ is periodic with period one and the orthogonal set of complex exponential functions $\{e^{2\pi i v s}\}$ is a map of the group Z into the group $\mathbb{R}/Z$. Moreover, the Fourier transform of a sequence can be interpreted as the z-transform

$$\hat{f}(z) = \sum_{-\infty}^{\infty} f(k) z^{-k}, \quad ROC: R_2 < |z| < R_1,$$

evaluated on the unit circle, U, provided U is within the region of convergence of $\hat{f}(z)$. That is, $\hat{f}(v) = \hat{f}(z)|_{z=e^{2\pi iv}}$. Furthermore, the groups $\mathbb{R}/Z$ and U are isomorphic because of the isomorphism of the exponential map $e^{2\pi i}: \mathbb{R}/Z \Rightarrow U$. Equivalently, any 1-periodic function f with finite energy over its period such that $f \in L_2(\mathbb{R}/Z)$ has Fourier transform

$$\hat{f}(n) = \int_{-1/2}^{1/2} f(t) e^{-2\pi int} dt, \quad \hat{f} \in L_2(Z), \tag{5.9}$$

and the inverse Fourier transform, which is equal to the original function, is given by the Fourier series expansion

$$f(t) = \sum_{n=-\infty}^{\infty} \hat{f}(n) e^{2\pi int}, \quad t \in [-1/2, 1/2). \tag{5.10}$$

It is now established that a periodic function in one domain is a sequence in the dual domain.

5.1.2.2 DFT

A finite duration aperiodic continuous function can be approximated by a finite number of uniform samples. Any function that is a finite sequence of numbers is a member $G = Z/NZ$, $N > 0$. This group is the group of integers modulo N. Moreover, $G = Z/NZ$ is a cyclic group because there is at least one group element $a \in G$ that can generate all the elements of G such that these elements have the form ma; m is some positive integer. In addition, Z/NZ

is isomorphic to U_N, the multiplicative group of N-th roots of unity. The isomorphism relating these two groups is the exponential map

$$e^{2\pi i/N} : Z/NZ \rightarrow U_N.$$

For any function $f \in L_2(Z/NZ)$, the Fourier transform is defined as

$$\hat{f}(n) = \sum_{k=0}^{N-1} f(k) e^{-2\pi i k n/N}, \quad \forall n \in Z/NZ, \quad N > 0, \tag{5.11}$$

while analogously, the inverse Fourier transform of any function $\hat{f} \in L_2(Z/NZ)$ is defined as

$$f(m) = N^{-1} \sum_{n=0}^{N-1} \hat{f}(n) e^{2\pi i m n/N}, \quad \forall m \in Z/NZ. \tag{5.12}$$

Equations (5.11) and (5.12) constitute a DFT pair:

$$f(k) \overset{DFT}{\Leftrightarrow} \hat{f}(n),$$

which becomes obvious from substituting equation (5.11) into equation (5.12).

5.1.3 The DFT of any Arbitrary Finite Energy Signal

Given any arbitrary square integrable function with "nice" properties, the DFT may be derived through two different processes: truncation and sampling and periodization and sampling. A function with "nice" properties is any function f satisfying the condition $|f(t)| \leq M_n |t|^{-n}$ as $t \to \infty$, $n \geq 1$, where M_n are constants. Moreover, a signal is defined as any information carrying function. Theoretically, a signal cannot be simultaneously time-limited and bandlimited but practically, a simultaneous time-limited and bandlimited signal yields acceptable results. In truncation and sampling, the signal -- time-limited, bandlimited, or neither -- is assumed to be both time-limited and bandlimited with tolerable truncation error or none. Then the minimum number of samples required to characterize the signal is the time-bandwidth product, which is also called Shannon number. In other words, if a signal has time duration T_0 and spectral duration S, the minimum number of samples needed to adequately represent it is $N_0 = T_0 S$. After, the signal's temporal and spectral durations are established, further improvement in resolution (reduction in aliasing) may be desired. In this case, N is increased from $N = N_0$ to $N > N_0$ accordingly. Therefore, $N \geq N_0$ uniform samples completely characterize an essentially time-limited and bandlimited signal. This sampling approach is rooted in the Fourier definition of a signal on the finite Abelian group Z/NZ, where the Fourier transform is the DFT.

The periodization and sampling process is an indirect approach to the derivation of the DFT. At the end of the process, the DFT is obtained by means of an extraction procedure. Poisson's summation formula is the essence of the periodization and sampling operation. To get the DFT of an arbitrary finite energy signal by means of periodization and sampling, Poisson's summation

formula is applied to the signal and its dual. Poisson's summation formula applied to a signal transform the signal and its dual onto the Abelian groups $\mathbb{R}/T\mathbb{Z}$, $T > 0$, and $\mathbb{Z}$ respectively. Poisson's summation applied to the dual signal yields similar results. Subsequently, the number of uniform samples $N \geq N_0$, in each period of the signal and its dual signal are specified. N_0 is the *minimum number of samples required to minimize aliasing*. Thereafter, the DFT is extracted from over the fundamental period of the Fourier series of the periodized and sampled original signal.

Poisson's summation formula for an arbitrary continuous absolutely integrable function $f(t)$, $-\infty < t < \infty$ with Fourier transform $\hat{f}(\nu)$ is

$$\sum_{k=-\infty}^{\infty} f(t + kT) = T^{-1} \sum_{n=-\infty}^{\infty} \hat{f}(n\nu_0) e^{2\pi i n \nu_0 t}, \quad \nu_0 = T^{-1}. \tag{5.13}$$

5.1.3.1 Truncation and Sampling

Suppose an arbitrary well-behaved signal f with Fourier spectrum $\hat{f}$ is analyzed using digital signal processing techniques, and further suppose that $f(t)$ is definable on the interval $t \in [t_a, t_b)$ such that $t_a < t_b$ for $T_0 = t_b - t_a$ and $\hat{f}(\nu)$ is essentially definable on the interval $\nu \in [\nu_a, \nu_b)$ such that $\nu_a < \nu_b$ for $S = \nu_b - \nu_a$, knowing the effective temporal and spectral supports of f correspondingly give definitive information on the spectral and temporal sample intervals of f. Moreover, the minimum number of samples needed to adequately describe

finite aperiodic f ($\hat{f}$) in terms of a finite sequence is the Shannon number. This number is equal to N_0, $N_0 = T_0 S$. N_0 establishes the upper bounds on the temporal and spectral resolutions of sampled f. Since the signal f has a time support T_0 and spectral support S, its corresponding sample intervals in time and in frequency are $1/S$ and $1/T_0$ respectively. By taking N_0 uniform samples of $f(t)$ and $\hat{f}(v)$ respectively, $f(t)$ and $\hat{f}(v)$ are effectively sampled critical rate. If the sampled version of $f(t)$ is $f(kt_s)$, k takes on only N_0 integer values for $t_s = 1/S$, and the sampled version of $\hat{f}(v)$ is $\hat{f}(nv_0)$, n takes on only N_0 integer values for $v_0 = 1/T_0$, the processing of $f(t)$ ($\hat{f}(v)$) can be accomplished through the processing of $f(kt_s)$ ($\hat{f}(nv_0)$). Because kt_s is equivalent to k and nv_0 is equivalent to n (the constants t_s and v_0 each represents one sample) $f(kt_s)$ and $\hat{f}(nv_0)$ can be rewritten as $f(k)$ and $\hat{f}(n)$ respectively. With $f(t)$ ($\hat{f}(v)$) describable in terms of $f(k)$ ($\hat{f}(n)$), f ($\hat{f}$) has the meaning of a signal defined on the finite Abelian cyclic group Z/NZ of order N. Therefore, f ($\hat{f}$) can be interpreted as a signal defined on Z/NZ with $N = N_0$. Since the sequences $f(k)$ and $\hat{f}(n)$ contain only a finite number of samples, the DFT can be used to establish the Fourier transform relationship between $f(k)$ and $\hat{f}(n)$. The DFT is the Fourier transform of a sequence defined on a finite Abelian group. However, this DFT should retain the essential properties of the signal in a manner similar to the CFT. If it becomes necessary to improve the resolution of either or both of the sequences $f(k)$ and $\hat{f}(n)$ so as to ascertain some subtle details that are known to exist in $f(t)$ and/or $\hat{f}(v)$, then N must be increased to $N > N_0$.

Consider a finite energy Schwartz space[44] signal $f \in S(\mathbb{R})$ with Fourier transform $\hat{f} \in S(\mathbb{R})$ defined as

$$\hat{f}(v) = \int_{-\infty}^{\infty} f(t) e^{-2\pi i v t} dt, \quad v \in \mathbb{R}. \tag{5.14}$$

The inverse Fourier transform of the Fourier transform of $f(t)$ is equal to $f(t)$ almost everywhere. It is given

$$f(t) = \int_{-\infty}^{\infty} \hat{f}(v) e^{2\pi i v t} dt, \quad t \in \mathbb{R}. \tag{5.15}$$

Because $f \in S(\mathbb{R})$ implies $\hat{f} \in S(\mathbb{R})$, the supports of f and $\hat{f}$ can be effectively limited to the respective intervals $t_a \le t \le t_b$ and $v_a \le v \le v_b$ with virtually no loss of energy. Hence $\hat{f}$ and its inverse f can be respectively rewritten as

$$\hat{f}(v) = \int_{t_a}^{t_b} f(t) e^{-2\pi i v t} dt, \quad v \in [v_a, v_b),$$
$$\text{and} \quad f(t) = \int_{v_a}^{v_b} \hat{f}(v) e^{2\pi i v t} dt, \quad t \in [t_a, t_b). \tag{5.16}$$

With this new formulation of $f(t)$ and $\hat{f}(v)$, each signal with negligible loss of information is representable by the Shannon number, N_0, of sample values taken uniformly over their

---

[44] See section 5.1.3.2 for more information on Schwartz space.

respective intervals of support. Since $f(t)$ and $\hat{f}(v)$ are each expressible in terms of a finite duration sequence, the Fourier integral can be replaced by the Fourier series with at least N_0 terms. This means that $f(t)$ is describable in terms of a trigonometric polynomial of order $N \geq N_0$. That is

$$f(t) = \sum_{n \in Z} c_n e^{2\pi i n / T_0 t}, \quad t_a \leq t < t_b \text{ and } T_0 = t_b - t_a, \tag{5.17}$$

where the Fourier coefficients c_n are computable from $\hat{f}(v)$,

$$c_n = v_0 \hat{f}(n v_0) = v_0 \int_{t_a}^{t_b} f(t) e^{-2\pi i n v_0 t} dt, \quad n \in Z, \quad v_0 = T_0^{-1}, \tag{5.18}$$

are scaled sample values of $\hat{f}(v)$. This means that the signal $f(t)$ is expressible in terms of the spectrum samples, $\hat{f}(n v_0)$:

$$f(t) = v_0 \sum_{n \in Z} \hat{f}(n v_0) e^{2\pi i n v_0 t}, \quad t_a \leq t < t_b, \quad v_a \leq n v_0 < v_b, \quad v_0 = T_0^{-1}. \tag{5.19}$$

Because

$$v_a \leq n v_0 < v_b \Rightarrow v_a T_0 \leq n < v_b T_0, \quad n \in Z \text{ and } v_0 = T_0^{-1},$$

$v_a T_0$ and $v_b T_0$ may not be generally contained in Z. Therefore, integer constants n_1 and n_2 must be chosen such that

$$v_a T_0 \le n_1 < n_2 < v_b T_0 \Rightarrow n_1 v_0 < n_2 v_0$$

and $\quad n_2 - n_1 + 1 = N \ge N_0, \quad for \quad n_1 \le n \le n_2.$

As a consequence, $f(t)$ becomes

$$f(t) = v_0 \sum_{n=n_1}^{n_2} \hat{f}(n v_0) e^{2\pi i n v_0 t} \qquad t_a \le t < t_b \quad \text{and} \quad v_0 = T_0^{-1}. \tag{5.20}$$

Since $f(t)$ is restricted to the interval $t_a \le t < t_b$ can be represented by $N \ge N_0$ uniform samples, setting $t = k\Delta t$, $k \in Z$, results in

$$\frac{t_a}{\Delta t} \le k < \frac{t_b}{\Delta t}.$$

Further setting $\Delta t = T_0/N$, the time interval can be rewritten as

$$k_1 \le k \le k_2, \quad k_1, k_2, k \in Z, \quad N_0 \le N = k_2 - k_1 + 1,$$

and $\qquad k_1 \ge N t_a v_0, \quad k_2 < N t_b v_0, \quad v_0 = T_0^{-1}.$

Hence, the Fourier transform relationship between $f(t)$ and $\hat{f}(v)$ finds expression in terms of the sets of samples $\{f(kT_0/N)\}$ and $\{\hat{f}(n/T_0)\}$. Thus,

$$f(kT_0/N) = \frac{1}{T_0} \sum_{n=n_1}^{n_2} \hat{f}(n v_0) e^{2\pi i n k/N}, \quad k_1 \le k \le k_2, \quad v_0 = T_0^{-1}. \tag{5.21}$$

Equation (5.21) can be rewritten as

$$\frac{T_0}{N} f(kT_0/N) = \frac{1}{N} \sum_{n=n_1}^{n_2} \hat{f}(n/T_0) e^{2\pi i n k/N}, \quad \Delta t = \frac{T_0}{N} \quad \text{and} \quad k_1 \le k \le k_2. \tag{5.22}$$

This equation is a form of the statement for the inverse DFT of the sequence $\{\hat{f}(n/T_0)\}$. Because $N \ge N_0$, the sequences $\{T_0/N f(kT_0/N)\}$ and $\{\hat{f}(n/T_0)\}$ may or may not contain the same number of samples on the region of support described for their respective continuous counterparts, $f(t)$ and $\hat{f}(v)$.

Using an approach similar to the one used to obtain the inverse DFT of $\{\hat{f}(n/T_0)\}$, the DFT of the sequence $\{T_0/N f(kT_0/N)\}$ can be derived. Like $f(t)$, $\hat{f}(v)$ is expressible in terms of the trigonometric polynomial

$$\hat{f}(v) = \sum_{k \in Z} d_k e^{-2\pi i v k/S}, \quad v_a \le v < v_b \quad \text{and} \quad S = v_b - v_a, \tag{5.23}$$

of order $N \ge N_0$. The Fourier coefficients d_k obtainable from the inverse Fourier transform of $\hat{f}(v)$ is $(1/S) f(k/S)$, $k \in Z$. With $d_k = (1/S) f(k/S)$, the scaled sample values of $f(t)$, the expresion for $\hat{f}(v)$ becomes

$$\hat{f}(v) = S^{-1} \sum_{k \in Z} f(k/S) e^{-2\pi i v k/S}, \quad v_a \le v < v_b \quad \text{and} \quad t_a \le \frac{k}{S} < t_b. \tag{5.24}$$

If t_s is the interval between the uniform samples $f(k/S)$ of $f(t)$, then t_s is equivalent to S^{-1}. The time support of $f(t)$ with some manipulation becomes $k_1 \le k \le k_2$, $k_1, k_2, k \in Z$ and $k_2 - k_1 + 1 = N \ge N_0$, the support of the sequence $\{S^{-1} f(kt_s)\}$, $t_s = S^{-1}$. If δv is chosen as the frequency separation between spectral samples such that $v = n\delta v$, $n \in Z$ and $\delta = S/N$, the spectral sequence $\{\hat{f}(nS/N)\}$ has support $n_1 \le n \le n_2$, $n_1, n_2, n \in Z$ and $n_2 - n_1 + 1 = N \ge N_0$, corresponding to the support of $\hat{f}(v)$. Therefore, the Fourier transform relationship between $f(t)$ and $\hat{f}(v)$ written in terms of their respective sequences $\{S^{-1} f(kt_s)\}$ and $\{\hat{f}(nS/N)\}$ is given by

$$\hat{f}(nS/N) = t_s \sum_{k=k_1}^{k_2} f(k/S) e^{-2\pi i kn/N}, \quad n_1 \le n \le n_2, \quad t_s = S^{-1}. \tag{5.25}$$

If $S^{-1} = \Delta t$, then

$$t_s = S^{-1} = \Delta t = \frac{T_0}{N} = \frac{1}{Nv_0} \Rightarrow v_0 = \frac{S}{N} = \delta v, \quad v_0 = \frac{1}{T_0}.$$

With this in mind, the DFT of the sequence $\{S^{-1} f(kt_s)\}$ can be rewritten as

$$\hat{f}(n/T_0) = \sum_{k=k_1}^{k_2} \left\{ \frac{T_0}{N} f(kT_0/N) \right\} e^{-2\pi i nk/N}, \tag{5.26}$$

where

$$n_1 \le n \le n_2 \quad \text{and} \quad N = n_2 - n_1 + 1,$$

which is the dual of the inverse DFT of the sequence $\{\hat{f}(n/T_0)\}$ expressed in equation (5.22). Thus, equations (5.22) and (5.26) constitute a DFT pair.

The DFT pair of equations (5.22) and (5.26) are not in the typical form shown in section 5.1.2.2. To formalize the DFT relationships of equations (5.22) and (5.26), the lower limits on the summations must be modified to start at zero. Equation (5.26) is used to show how a DFT with arbitrary lower limit can be formalized to start at zero.

As previously stated, the sequences $\{\hat{f}(n/T_0)\}$ and $\{f(kT_0/N)\}$ are replaceable with the respective sequences $\{\hat{f}(n)\}$ and $\{f(k)\}$ because the indices (n/T_0), $n \in Z$, and (kT_0/N), $k \in Z$, are equivalent to n and k respectively. Accordingly, for $n, k \in Z$, the supporting indexing sets $n_1 \le n \le n_2$ and $k_1 \le k \le k_2$ of the respective sequences can be manipulated such that the indices n and k start at zero. Therefore, it follows that

$$\hat{f}(n) = \hat{f}(n + n_1) \quad \text{and} \quad f(k) = f(k + k_1)$$

and

$$\sum_{\substack{k=k_1 \\ n_1 \le n \le n_2}}^{k_2} \{\Delta t f(k)\} e^{-2\pi i n k/N} = \sum_{k=0}^{N-1} \{\Delta t f(k + k_1)\} e^{-\frac{2\pi i}{N}(n_1 k_1 - n_1 k + n k_1 - n k)}, \tag{5.27}$$

where

$$\Delta t = \frac{T_0}{N} \quad \text{and} \quad 0 \le n < N.$$

As a result the formal definition for the DFT of a time sequence f is expressible as

$$\begin{aligned} &\left\{ e^{2\pi i n_1 k_1 / N} \hat{f}(n + n_1) e^{2\pi i n k_1 / N} \right\} \\ &\quad = \sum_{k=0}^{N-1} \left\{ \Delta t f(k + k_1) e^{-2\pi i n_1 k / N} \right\} e^{-2\pi i n k / N}, \quad 0 \le n < N. \end{aligned} \tag{5.28}$$

The corresponding inverse DFT of the sequence $\hat{f}$ is

$$\begin{aligned} &\left\{ \Delta t f(k + k_1) e^{-2\pi i n_1 k / N} \right\} \\ &\quad = \frac{1}{N} \sum_{n=0}^{N-1} \left\{ e^{2\pi i n_1 k_1 / N} \hat{f}(n + n_1) e^{2\pi i n k_1 / N} \right\} e^{2\pi i n k / N}, \end{aligned} \tag{5.29}$$

where $0 \le k < N$. By setting

$$h(k) = \left\{ \Delta t f(k + k_1) e^{-2\pi i n_1 k / N} \right\}$$

and

$$\hat{h}(n) = \left\{ e^{2\pi i n_1 k_1 / N} \hat{f}(n + n_1) e^{2\pi i n k_1 / N} \right\},$$

the typical form of the DFT is obtained in the following representation,

$$\hat{h}(n) = \sum_{k=0}^{N-1} h(k) e^{-2\pi i n k/N}, \quad 0 \le n < N, \tag{5.30}$$

with the corresponding inverse representation being

$$h(k) = \frac{1}{N} \sum_{n=0}^{N-1} \hat{h}(n) e^{2\pi i n k/N}, \quad 0 \le k < N. \tag{5.31}$$

These two equations constitute a generalized DFT pair, which model very closely the operations perform by the CFT pair. Apart from making a signal finite for the generalized DFT operation, there is no need to further restrict or modify the signal's behavior. In this sense, the generalized DFT behaves and performs more naturally than the regular DFT; it performs at the level of the CFT and requires only straightforward implementation.

5.1.3.2 Periodization and Sampling

In this section, Poisson's summation formula is the instrument used to make continuous signals suitable for digital signal processing analysis. Poisson's formula cannot be arbitrarily applied to all signals. It is only applicable to signals that fulfill the requirements for membership in certain signal spaces. These signal spaces include Schwartz space $S(\mathbb{R})$[277, 278], the intersection of the signal spaces of twice continuously differentiable signals and absolutely integrable signals, $C^2(\mathbb{R}) \cap L_1(\mathbb{R})$, where the signals'decay properties are relatively mild at infinity [278], and the

intersection of the signal spaces of absolutely integrable signals and bounded variation signals, $L_1(\mathbb{R}) \cap BV(\mathbb{R})$, provided Poisson's summation formula for each signal is defined at the discontinuity points and is equal to the average value of the right- and left-hand limits at each of these points [278, 279, 280]. In general, suppose a continuous function f with Fourier transform $\hat{f}$, is absolutely integrable over $\mathbb{R}$; if P_f is a function defined on the quotient group $G = \mathbb{R}/T\mathbb{Z}$, $T > 0$, in terms of f such that

$$P_f(t) = \sum_{k=-\infty}^{\infty} f(t + kT),$$

then $P_f(t)$ converges uniformly on the interval $t_0 \le t < t_0 + T$. It follows that the Fourier coefficients of P_f exist and are expressible in terms of $\hat{f}$. That is

$$c_n = \frac{1}{T} \int_{t_0}^{t_0 + T} P_f(t) e^{-2\pi i n t / T} dt \tag{5.32}$$

and

$$\frac{1}{T} \int_{t_0}^{t_0 + T} \sum_{k=-\infty}^{\infty} f(t + kT) e^{-2\pi i n t / T} dt = \frac{1}{T} \hat{f}\left(\frac{n}{T} \right).$$

Thus the coefficients c_n of P_f are a restriction to the scaled integers values of $\hat{f}$ [277, 278, 281, 282]. Furthermore, if P_f is defined as above, it is summable on the group $\mathbb{R}/T\mathbb{Z}$ and the L_1-norm of P_f is conditioned on the L_1-norm of f [278, 282],

$$\|P_f\|_{L_1(\mathbb{R}/T\mathbb{Z})} = \int_{t_0}^{t_0+T} |P_f(t)|dt \leq \sum_{k\in\mathbb{Z}} \int_{t_0}^{t_0+T} |f(t+kT)|dt = \|f\|_{L_1(\mathbb{R})}. \quad (5.33)$$

Additionally, uniformly convergent P_f over interval T has $|P_f|$ equal or less than some positive constant M. In accordance with Weierstrass M test, if

$$\left|\hat{f}\left(\frac{n}{T}\right)\right| = M \quad \text{and} \quad \sum_{n=-\infty}^{\infty} \left|\hat{f}\left(\frac{n}{T}\right)\right|$$

converges, then P_f is uniformly and absolutely convergent on the interval T because

$$P_f(t) = \sum_{n=-\infty}^{\infty} \{T^{-1}\hat{f}(nv_0)\}e^{2\pi i n v_0 t}, \quad v_0 = T^{-1},$$

and

$$|P_f(t)| = \frac{1}{T}\left|\sum_{n=-\infty}^{\infty} \hat{f}(nv_0)e^{2\pi i n v_0 t}\right| \leq \sum_{n=-\infty}^{\infty} |\hat{f}(nv_0)|, \quad v_0 = \frac{1}{T}. \quad (5.34)$$

Therefore, if P_f is defined on a space where it is an uniformly and absolutely convergent series, then

$$P_f(t) = \sum_{k=-\infty}^{\infty} f(t+kT) = \frac{1}{T}\sum_{n=-\infty}^{\infty} \hat{f}(nv_0)e^{2\pi i n v_0 t}, \quad v_0 = \frac{1}{T} \text{ and } |t| < \infty, \quad (5.35)$$

is a valid definition of Poisson's summation formula. However, if the two series of equation (5.34) are only absolutely convergent on a function space, the validity of Poisson's summation formula cannot be guaranteed on that space because the functions will exist with both series converging to different numbers [277, 282].

Prior to using Poisson's summation formula to derive the DFT of a finite energy signal, Poisson's summation formula is derived for Schwartz space, $S(\mathbb{R})$, functions. $S(\mathbb{R})$ is a linear space of all infinitely differentiable functions, $C^{\infty}(\mathbb{R})$, of rapid decrease satisfying the condition

$$\sup_{0 \le i \le m} \sup_{t \in \mathbb{R}} (1 + |t|^2)^m |f^{(i)}(t)| < \infty, \quad m \ge 0.$$

It is a subspace of $L_1(\mathbb{R}) \cap L_2(\mathbb{R}) \cap A(\mathbb{R})$. $A(\mathbb{R})$ is the space of Fourier transforms of all functions $f \in L_1(\mathbb{R})$. In addition, $S(\mathbb{R})$is closed under Fourier transformation, translation, modulation, addition, multiplication, multiplication by polynomials, and convolution. Moreover, $S(\mathbb{R})$ is dense in $L_1(\mathbb{R})$ as well as in $L_2(\mathbb{R})$. Because $S(\mathbb{R})$ is a dense subspace of $L_2(\mathbb{R})$, Plancherel's theorem and Parseval's formula for L_2-functions hold for every function $f \in S(\mathbb{R})$ [283] and the unique linear functional operator $\mathcal{F}$ is such that $\mathcal{F}f = \hat{f}$ is an isomorphism of order 4 on S. This implies that each $f \in S(\mathbb{R})$ is also a $f \in L_2(\mathbb{R})$. It further suggests that under uniform convergence, L_2-functions are extensions of S-functions and can therefore be approximated by them. When Poisson's summation formula is applied to a function $f \in S(\mathbb{R})$ with Fourier transform $\hat{f} \in S(\mathbb{R})$, a function $P_f(t)$, $t \in \mathbb{R}$, is produced. $P_f(t)$ satisfies the condition

$$P_f(t+T) = P_f(t), \quad T > 0, \quad t \in \mathbb{R}.$$

Therefore, it uniformly and absolutely converges to a periodic C^∞-function.

5.1.3.2.1 Poisson's Summation Formula

Since a function $f \in L_2(\mathbb{R})$ can be approximated by any of the sequence of functions f_i, $i \in Z^+$, contained in $S(\mathbb{R})$ that converges to f in the mean square sense, Poisson's summation formula is derivable in terms of any function $f_i \in S(\mathbb{R})$. This formula is applicable to functions $f \in L_2(\mathbb{R})$. Suppose a function $f_i \in S(\mathbb{R})$, with Fourier transform $\hat{f}_i \in S(\mathbb{R})$, is convolved with the impulse train

$$\sum_{n=-\infty}^{\infty} \delta(t \pm nT) = \frac{1}{T} \sum_{m=-\infty}^{\infty} e^{2\pi i m v_0 t}, \quad v_0 = \frac{1}{T},$$

the following equation is obtained:

$$f_i(t) * \sum_{m=-\infty}^{\infty} \delta(t \pm mT) = f_i(t) * \frac{1}{T} \sum_{n=-\infty}^{\infty} e^{2\pi i n v_0 t}, \quad v_0 = \frac{1}{T}, \quad T > 0, \quad t \in \mathbb{R}. \quad (5.36)$$

The consequence of this convolution is the statement of Poisson's summation formula,

$$\sum_{m=-\infty}^{\infty} f_i(t \pm mT) = \frac{1}{T} \sum_{n=-\infty}^{\infty} \hat{f}_i(nv_0) e^{2\pi i n v_0 t}, \quad v_0 = \frac{1}{T}, \quad (5.37)$$

of any time function f_i. Similarly, Poisson's summation formula is derivable for any function $\hat{f}_i \in S(\mathbb{R})$ with inverse Fourier transform $\mathcal{F}^{-1}\hat{f}_i = f_i$ contained in S. The convolution of $\hat{f}_i$ with the Fourier spectrum of the impulse train,

$$\sum_{l=-\infty}^{\infty} \delta(t \pm lv_s) = \frac{1}{v_s}\sum_{k=-\infty}^{\infty} e^{-2\pi i v k t_s}, \quad t_s = \frac{1}{v_s},$$

yields the spectral description Poisson's summation formula

$$\sum_{l=-\infty}^{\infty} \hat{f}_i(v \pm lv_s) = t_s \sum_{k=-\infty}^{\infty} f_i(kt_s) e^{-2\pi i v k t_s}, \quad t_s = \frac{1}{v_s}. \tag{5.38}$$

The coefficients, $f(kt_s)$, of the series expansion of

$$P_{\hat{f}_i}(v) = \sum_{l=-\infty}^{\infty} \hat{f}_i(v \pm lv_s)$$

are a restriction to integer values of $f_i(t)$. The periodicity condition of $P_{\hat{f}_i}(v)$ is satisfied with the relationship

$$P_{\hat{f}_i}(v + v_s) = P_{\hat{f}_i}(v), \quad v_s > 0,$$

where v_s is the spectral period.

5.1.3.2.2 Poisson's Summation Formula and the DFT

In accordance with the arguments presented in the previous section, suppose a signal $f \in L_2(\mathbb{R})$ and its Fourier transform $\hat{f} \in L_2(\mathbb{R})$ have periodized versions of the forms of Fourier series expansions in equations (5.37) and (5.38), where the coefficient sets $\{v_0 \hat{f}(nv_0)\}$ and $\{t_s f(kt_s)\}$ are uniform samples of $\hat{f}(v)$ and $f(t)$ respectively, the Fourier series expansion of $P_{\hat{f}}(v)$ may also be viewed as the DTFT of the sequence, $\{t_s f(kt_s)\}$. Since on the unit circle the Fourier transform of a sequence is equal to its z-transform whenever $z = e^{2\pi i v t_s}$, the series expansion of $P_{\hat{f}}(v)$ can be further viewed as the z-transform of $\{t_s f(kt_s)\}$ on the unit circle:

$$P_{\hat{f}}(z)_{z=e^{2\pi i v t_s}} = \sum_{k=-\infty}^{\infty} \{t_s f(kt_s)\} z^{-k}.$$

Since the sequences $f(kt_s)$ and $\hat{f}(nv_0)$ are the sample values of $f(t)$ and $\hat{f}(v)$ respectively, $t = kt_s$, $k \in Z$ and $v = nv_0$, $n \in Z$. Therefore, $P_f(t)$ and $P_{\hat{f}}(v)$ are expressible in terms of their discrete sample values:

$$P_f(kt_s) = \frac{1}{Nt_s} \sum_{n=-\infty}^{\infty} \hat{f}(nv_0) e^{2\pi i n k/N}, \quad v_0^{-1} = T = Nt_s, \quad N > 0, \tag{5.39}$$

and

$$P_{\hat{f}}(nv_0) = t_s \sum_{k=-\infty}^{\infty} f(kt_s) e^{-2\pi i n k/N}, \quad t_s^{-1} = v_s = Nv_0, \quad N > 0. \tag{5.40}$$

The positive integer constant N is the Shannon number determinable from the time bandwidth product of periods T and v_s. If the product Tv_s is not an integer, N is the greatest integer equal or less than Tv_s. Moreover, $P_f(kt_s)$ and $P_{\hat{f}}(nv_0)$ are periodic with period N. Hence,

$$P_f((k+N)t_s) = P_f(kt_s) \quad \text{and} \quad P_{\hat{f}}((n+N)v_0) = P_{\hat{f}}(nv_0), \quad n,k \in Z, \tag{5.41}$$

are expressions of these periodicities. Since periodic sequences $P_f(kt_s)$ and $P_{\hat{f}}(nv_0)$ are both of period N, their fundamental ranges may exist on the closed intervals $k_i \le k \le k_i+N-1$ and $n_i \le n \le n_i+N-1$, respectively. The integer constants k_i and n_i are the initial values of the respective fundamental periods of $P_f(kt_s)$ and $P_{\hat{f}}(nv_0)$.

Since

$$P_f(kt_s) = \sum_{m=-\infty}^{\infty} f((k \pm mN)t_s) \quad \text{and} \quad P_{\hat{f}}(nv_0) = \sum_{l=-\infty}^{\infty} \hat{f}((n \pm lN)v_0)$$

and the complex exponentials in the expansions are periodic in integer variables k and n with period N, the Fourier series expansions of $P_f(kt_s)$ and $P_{\hat{f}}(nv_0)$ can be respectively rewritten as

$$t_s \sum_{m=-\infty}^{\infty} f((k \pm mN)t_s) = \frac{1}{N} \sum_{n=n_i}^{n_i+N-1} \left\{ \sum_{r=-\infty}^{\infty} \hat{f}((n \pm rN)v_0) \right\} e^{2\pi i n k/N} \qquad k_i \le k \le k_i+N-1 \tag{5.42}$$

and

$$\sum_{l=-\infty}^{\infty} \hat{f}((n \pm lN)v_0) = \sum_{k=k_i}^{k_i+N-1} \left\{ t_s \sum_{s=-\infty}^{\infty} f((k \pm sN)t_s) \right\} e^{-2\pi i n k/N} \qquad (5.43)$$

$$n_i \le n \le n_i + N - 1.$$

Since $l, m, r, s \in Z$, these periodic sequences constitute a DFT pair:

$$\left\{ t_s \sum_{m \in Z} f((k \pm mN)t_s) \right\} \overset{DFT}{\Leftrightarrow} \left\{ \sum_{l \in Z} \hat{f}((n \pm lN)v_0) \right\}, \quad k, n \in Z/N. \qquad (5.44)$$

To show this relationship, utilize the general solution to a geometric series and exploit the orthogonality condition of the set of complex exponentials.

The synthesis and analysis equations of the DFT pair are not written in the usual manner. To conform with practice, the lower indices of the summations of the inverse DFT and the DFT must start at zero. With the procedure used in the previous section to initialize the DFT of a sequence to zero, it can be easily shown that the synthesis and analysis equations of the DFT pair rewritten in their accustomed form are

$$\left\{ t_s \sum_{m=-\infty}^{\infty} f((k + k_i \pm mN)t_s) e^{-2\pi i n k_i/N} \right\}$$

$$= \frac{1}{N} \sum_{n=0}^{N-1} \left\{ e^{2\pi i n k_i/N} \sum_{l=-\infty}^{\infty} \hat{f}((n + n_i \pm lN)v_0) e^{2\pi i n k_i/N} \right\} e^{2\pi i n k/N} \qquad (5.45)$$

$$0 \le k \le N - 1$$

and

$$\left\{e^{2\pi i n f_i/N}\sum_{l=-\infty}^{\infty}\hat{f}((n+n_i\pm lN)v_0)e^{2\pi i n k_i/N}\right\}$$
$$=\sum_{n=0}^{N-1}\left\{t_s\sum_{m=-\infty}^{\infty}f((k+k_i\pm mN)t_s)e^{-2\pi i n f_i/N}\right\}e^{-2\pi i n k/N} \qquad (5.46)$$
$$0\le n\le N-1.$$

By setting

$$h(k)=\left\{t_s\sum_{m=-\infty}^{\infty}f((k+k_i\pm mN)t_s)e^{-2\pi i n f_i k/N}\right\}$$

and

$$\hat{h}(n)=\left\{e^{2\pi i n f_i/N}\sum_{l=-\infty}^{\infty}\hat{f}((n+n_i\pm lN)v_0)e^{2\pi i n k_i/N}\right\},$$

the typical form of the synthesis and analysis equations of the DFT pair is respectively obtained in

$$h(k)=\frac{1}{N}\sum_{n=0}^{N-1}\hat{h}(n)e^{2\pi i n k/N},\quad 0\le k\le N-1, \qquad (5.47)$$

and

$$\hat{h}(n)=\sum_{k=0}^{N-1}h(k)e^{-2\pi i n k/N},\quad 0\le n\le N-1. \qquad (5.48)$$

From an application point of view, this DFT pair is equivalent to the one consisting of equations (5.30) and (5.31). These DFT pairs consist of generalized equations that efficiently and acceptably duplicate the operations performed by the CFT pair. In addition, the periodicity inherent in the synthesis and analysis equations of the DFT pairs give insight into the generalized discrete Zak transform.

5.1.4 Discussion of Results

In comparing the processing capability and efficiency of the generalized DFT with the regular DFT relative to continuous signals, several signals were studied. Whereas the regular DFT assumes the signal is causal, the generalized DFT does not. An investigator using the regular DFT to analyze a noncausal aperiodic signal would be required to modify this signal into a related causal one that could be easily periodically extended to make it suitable for DFT operation. The investigator would have to be cognizant about signal's causality [284], periodicity, and region of existence in order to properly analyze it using the regular DFT. Therefore, the regular DFT cannot be arbitrarily applied to a sampled continuous signal because the results obtained may lead to erroneous interpretation.

Of the signals that were investigated, the ones presented here are demonstrative examples. They include $\sin(\pi t)/\sinh(2\pi t)$, $sinc^2(t)$, hyperbolic secant, $sech(\pi t)$, and members of the Hermite family with $\alpha = 4\pi$. The Hermite family is describable by recursion relations in the signal domain and in the spectral domain:

$$h_n(t) = \alpha t h_{n-1}(t) - (n-1)\alpha h_{n-2}, \quad n \geq 2, \quad t \in \mathbb{R},$$

and where

$$h_0(t) = e^{-0.25\alpha t^2} \quad \text{while} \quad h_1(t) = \alpha t h_0(t);$$

in terms of the Fourier transform,

$$\hat{h}_n(v) = 4\pi i v \hat{h}_{n-1}(v) + (n-1)\alpha \hat{h}_{n-2}(v), \quad n \geq 2, \quad v \in \mathbb{R},$$

and where

$$\hat{h}_0(v) = \sqrt{4\pi\alpha^{-1}}\, e^{-(4\pi^2\alpha^{-1})v^2} \quad \text{while} \quad \hat{h}_1 = (4\pi i v)\hat{h}_0(t).$$

Each signal studied was defined on a time span $t \in [-4, 4)$. Each signal's sampled version contained $N = 64$ uniform samples. The first five members of the Hermite family of signals that were studied are shown in figures 5.1a-b through figures 5.5a-b; in each case a is the general DFT and its inverse and b is the regular DFT and its inverse. Figures 5.6a-b through figures 6.8 a-b show the DFT and its inverse of the hyperbolic secant, $\sin(\pi t)/\sinh(2\pi t)$, and the square sinc respectively. Provided the regular DFT is carefully manipulated to account for periodicity, causality and the signal's region of existence, its performance is essentially the same as the general DFT. Because the signals for analysis may not be periodic and may be noncausal,

the regular DFT can result in erroneous analysis. For example, figures 5.1a-b and figures 5.6a-b show the Fourier transformation invariant gaussian $e^{-\pi t^2}$ and hyperbolic secant $sech(\pi t)$ which are similar in many respects. Having only the regular DFT of one of these signals, an investigator could conceivably confuse the gaussian for the hyperbolic secant and vice versa. Moreover, there are many other signals that share similar properties including their spectrums being symmetrical about zero. For this reason one would normally prefer a DFT that accurately and unadulteratedly computes the spectrum of a signal regardless of where it exists.

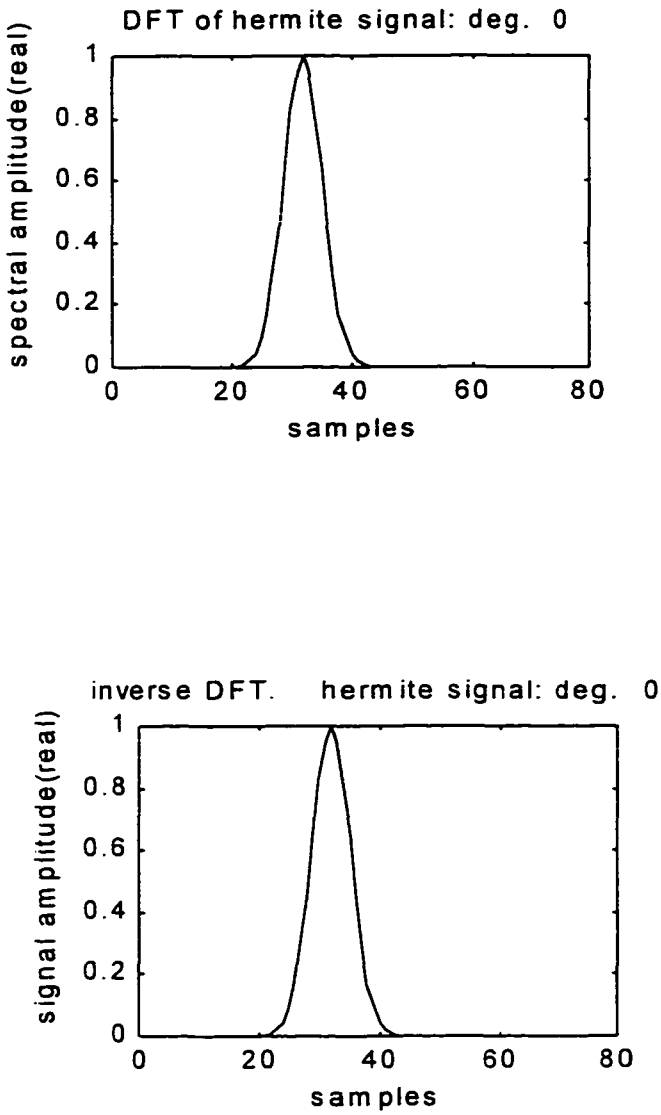

Figure 5.1a. Generalized DFT of the zeroth degree Hermite signal and its inverse; the zeroth degree Hermite is the gaussian signal.

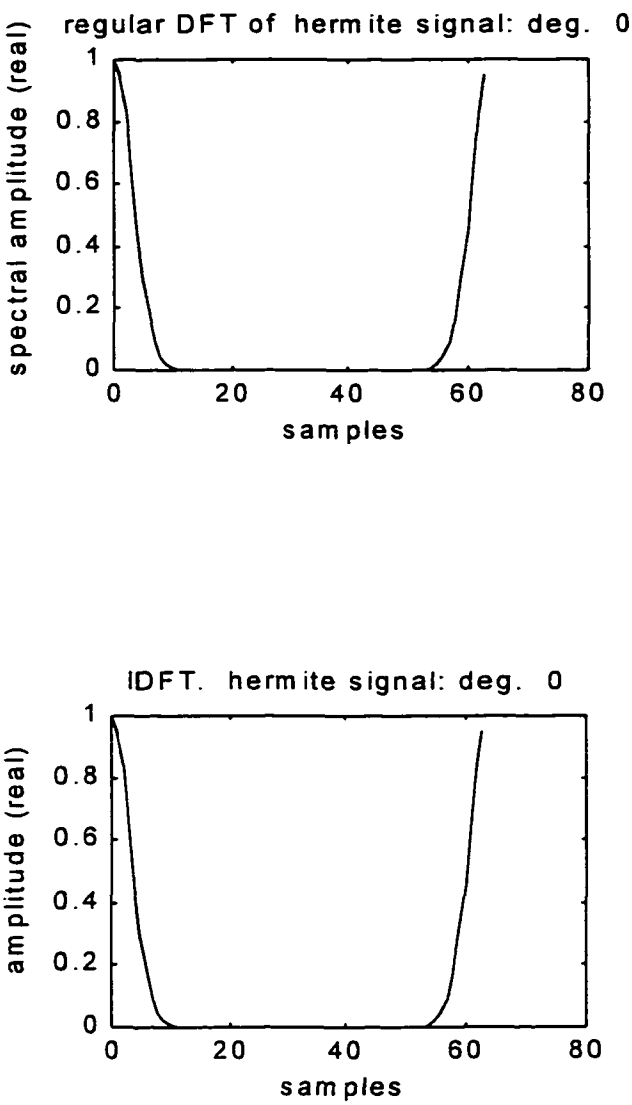

Figure 5.1b. Regular DFT of the periodic extension of the zeroth degree Hermite signal and its inverse.

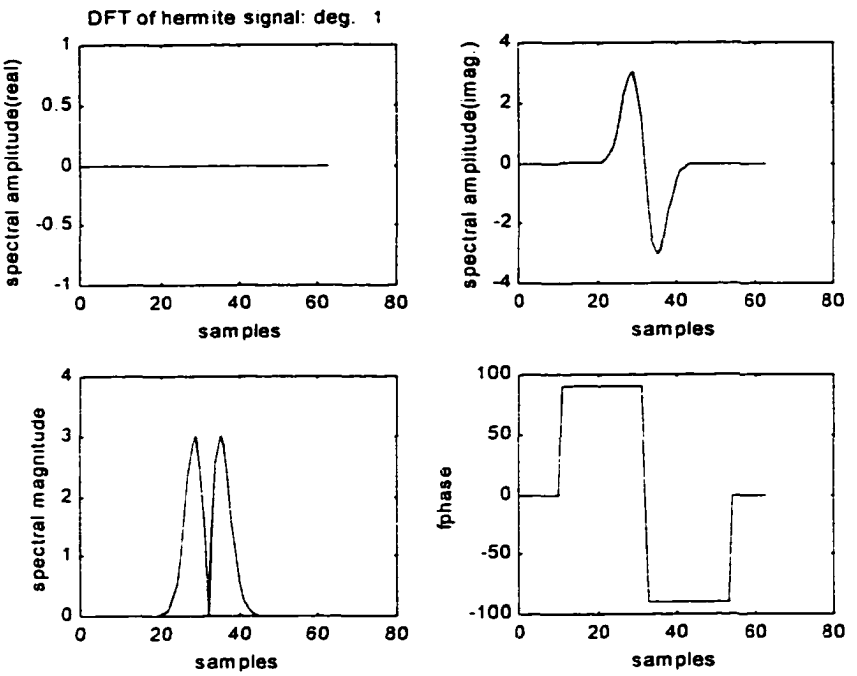

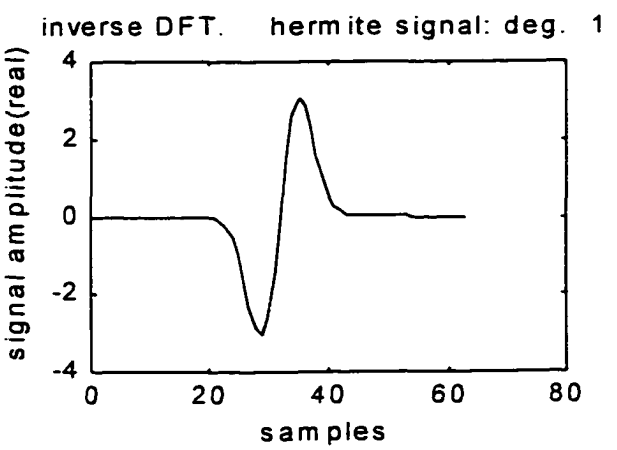

Figure 5.2a. Generalized DFTof the first degree Hermite signal and its inverse.

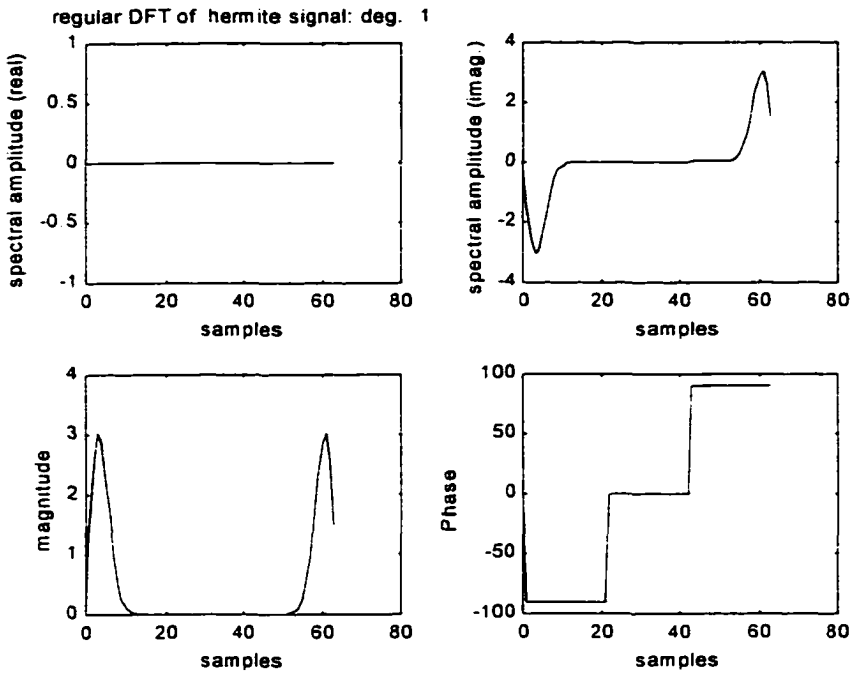

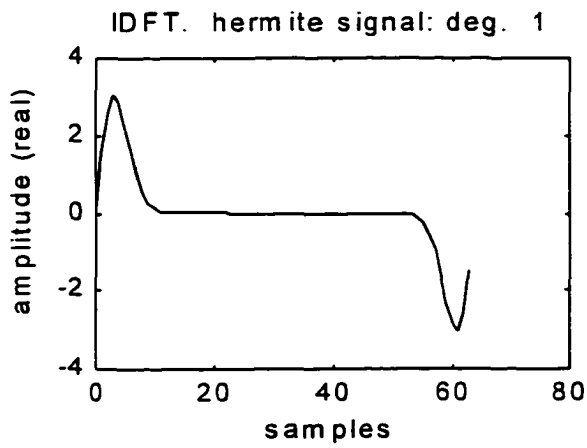

Figure 5.2b. Regular DFT of the periodic extension of the first degree Hermite signal and its inverse.

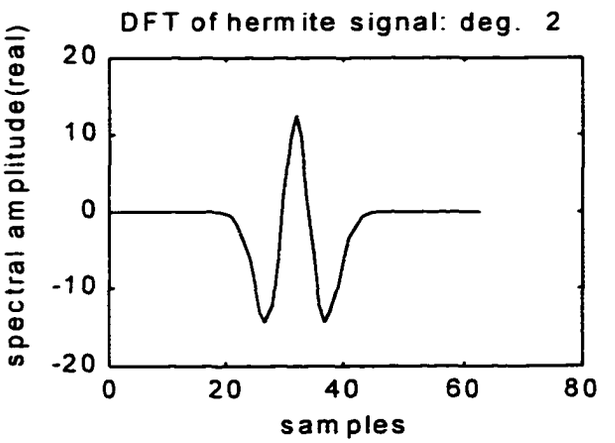

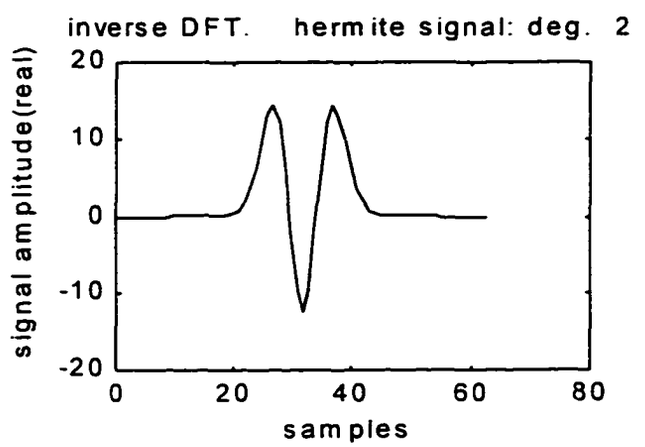

Figure 5.3a. Generalized DFT of the second degree Hermite signal and its inverse.

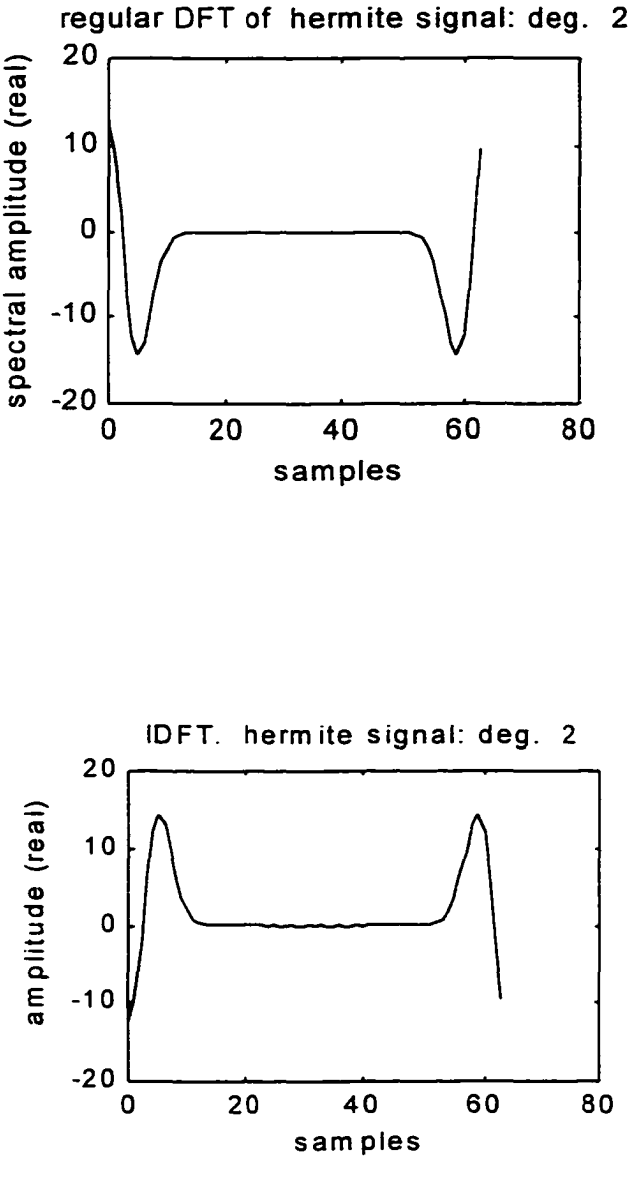

Figure 5.3b. Regular DFT of the periodic extension of the second degree Hermite signal and its inverse.

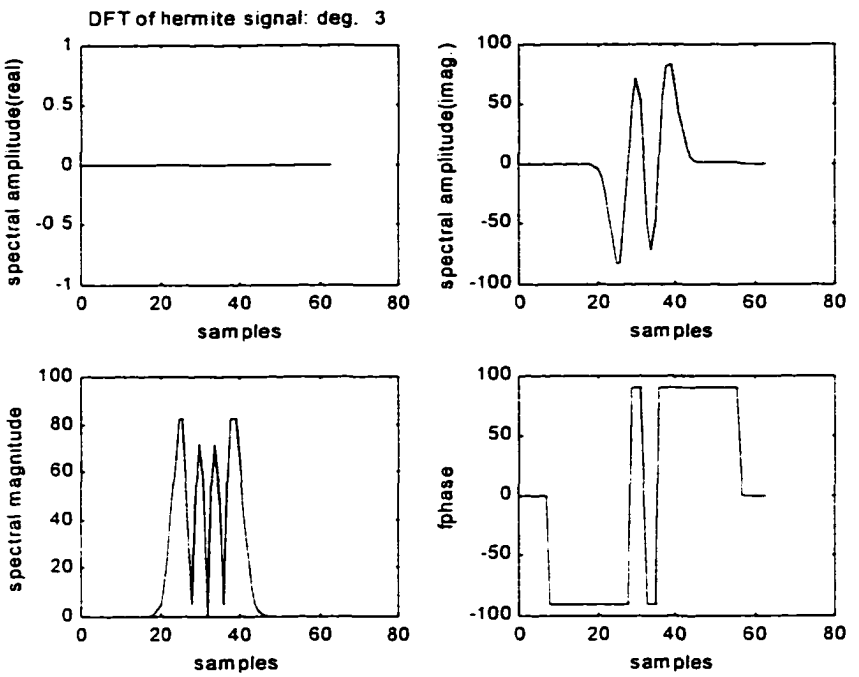

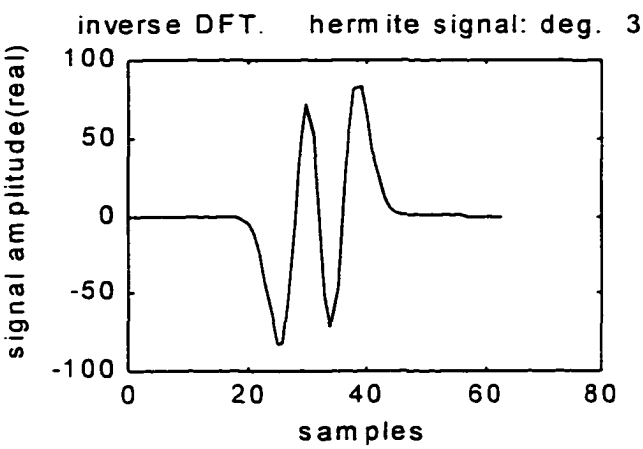

Figure 5.4a. Generalized DFT of the third degree Hermite signal and its inverse.

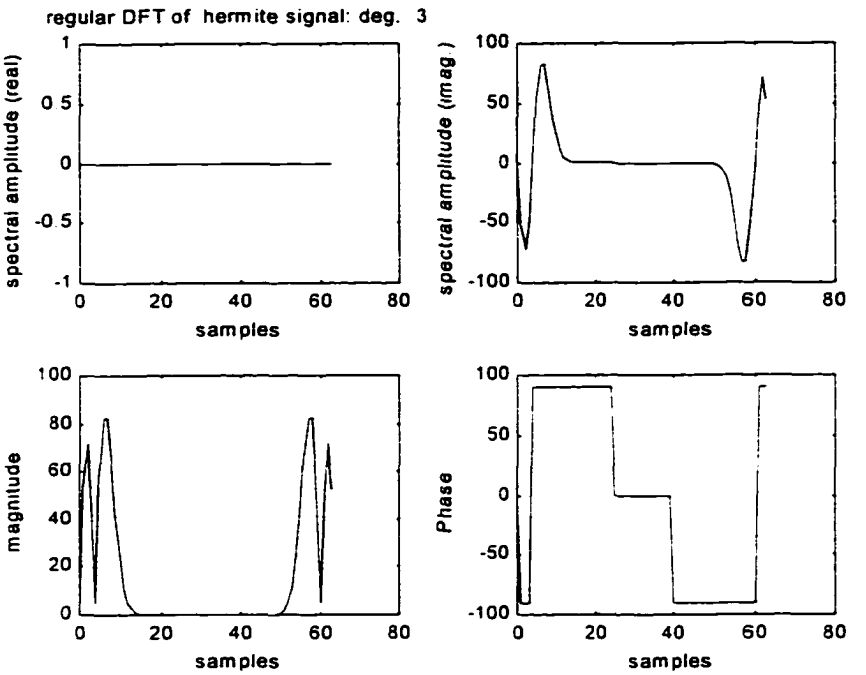

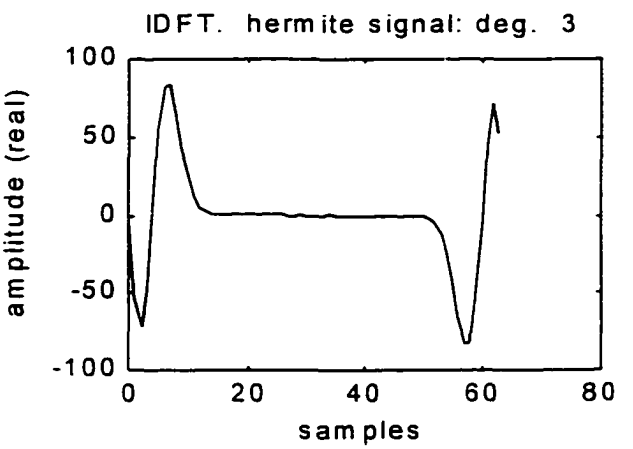

Figure 5.4b. Regular DFT of the periodic extension of the third degree Hermite signal and its inverse.

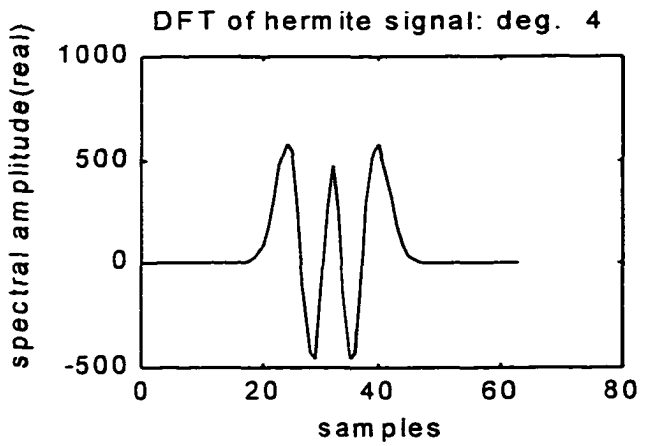

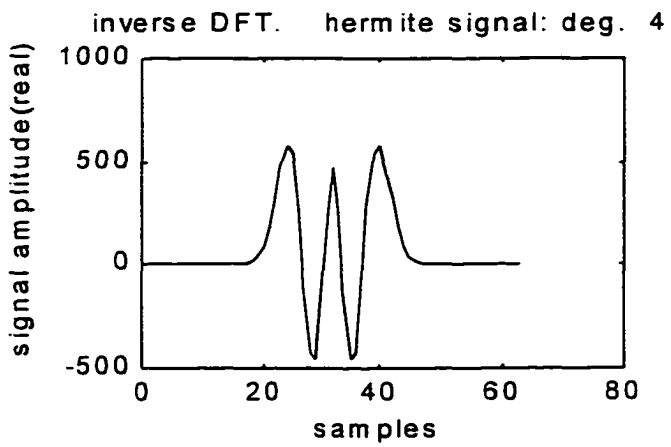

Figure 5.5a. Generalized DFT of the fourth degree Hermite signal and its inverse.

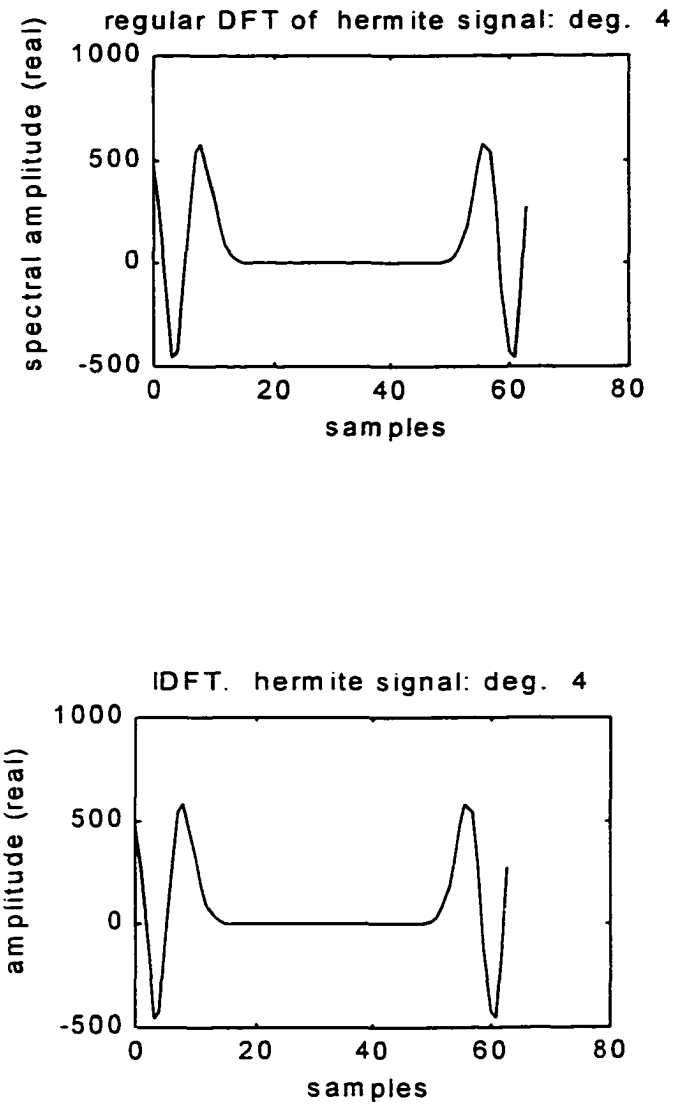

Figure 5.5b. Regular DFT of the periodic extension of the fourth degree Hermite signal and its inverse.

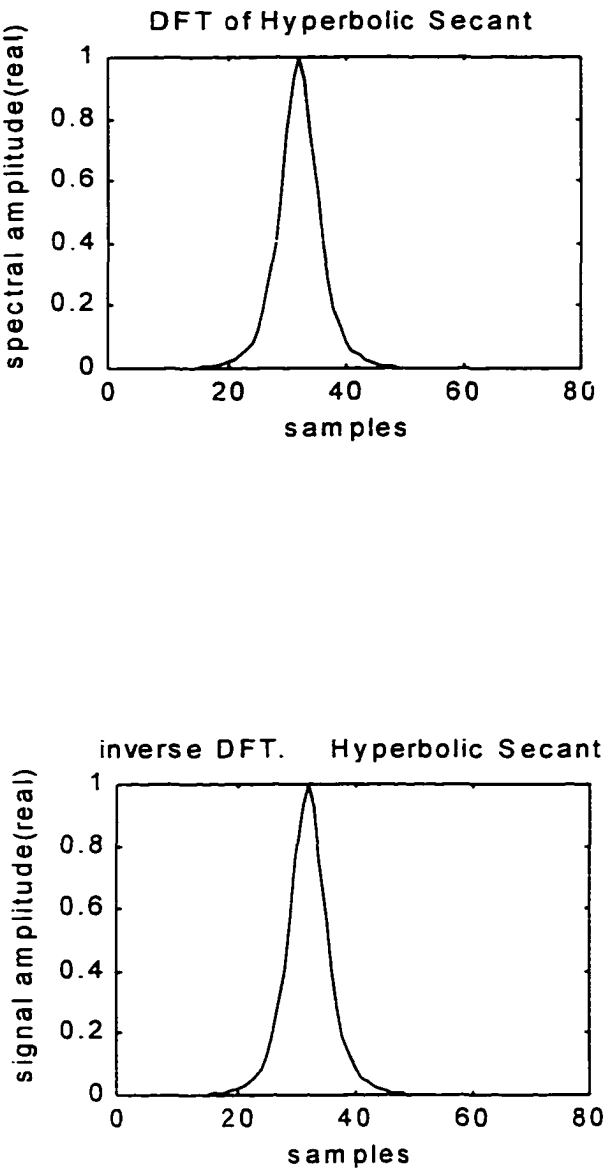

Figure 5.6a. Generalized DFT of hyperbolic secant and its inverse; the argument of the hyperbolic secant is πt.

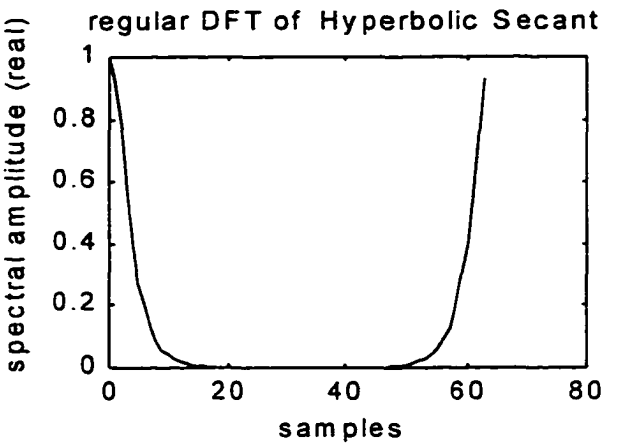

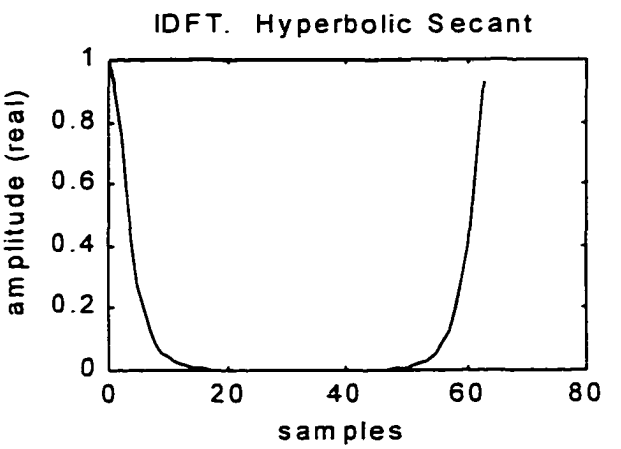

Figure 5.6b. Regular DFT of the periodic extension of hyperbolic secant at argument πt and its inverse.

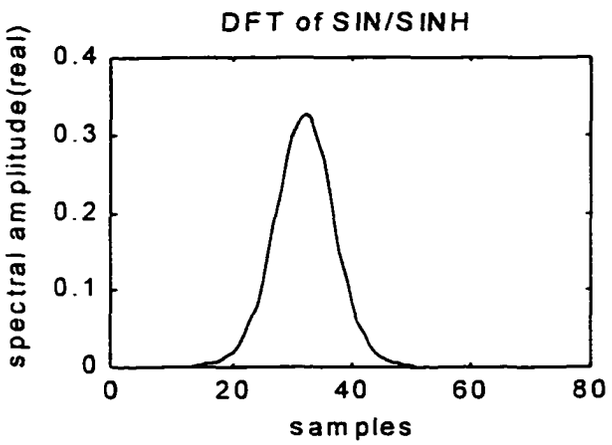

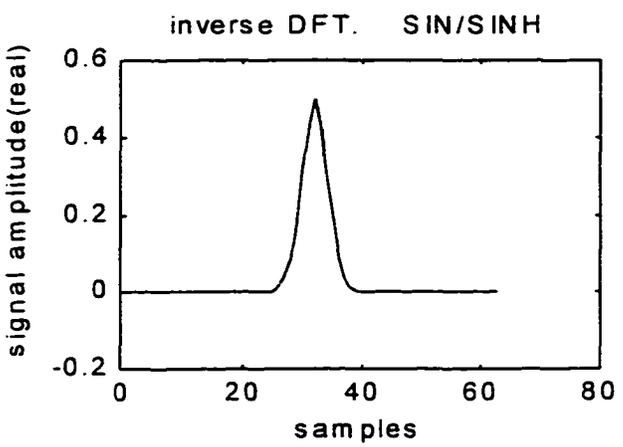

Figure 5.7a. Generalized DFT of $\sin(\pi t)/\sinh(2\pi t)$ and its inverse.

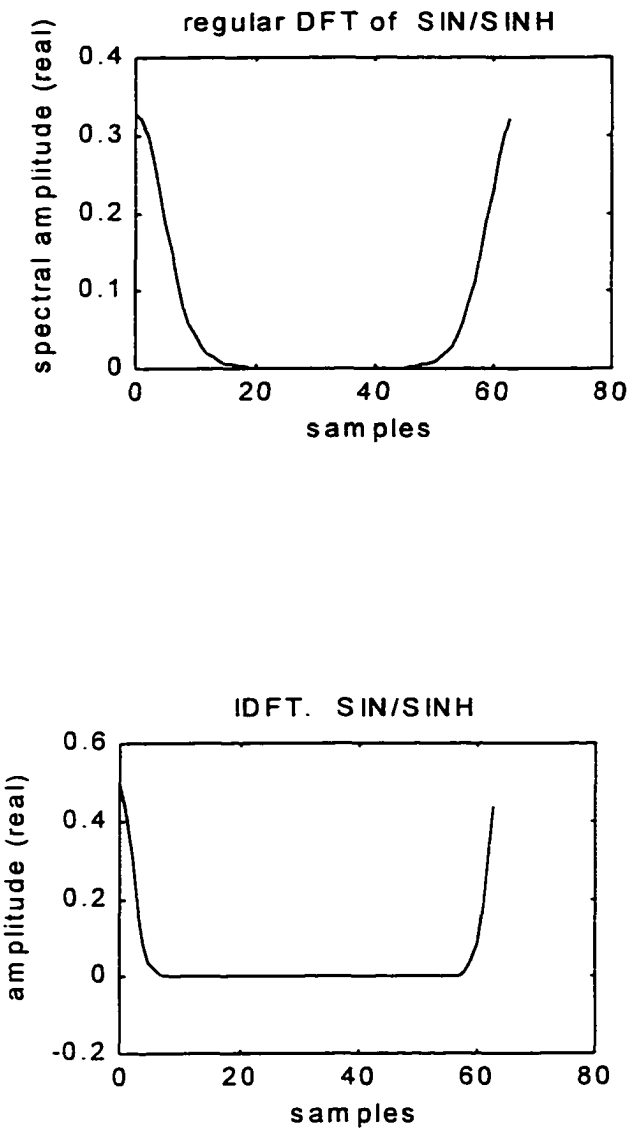

Figure 5.7b. Regular DFT of the periodic extension of the signal in (5.7a) and its inverse.

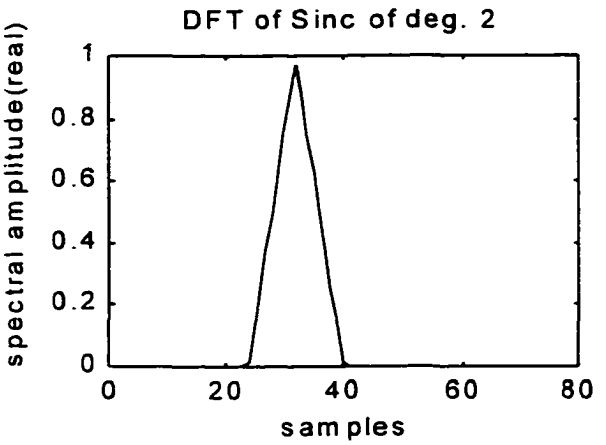

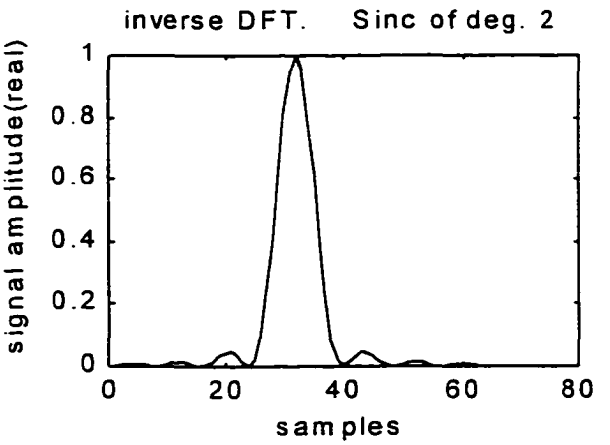

Figure 5.8a. Generalized DFT of $sinc^2 t$ and its inverse.

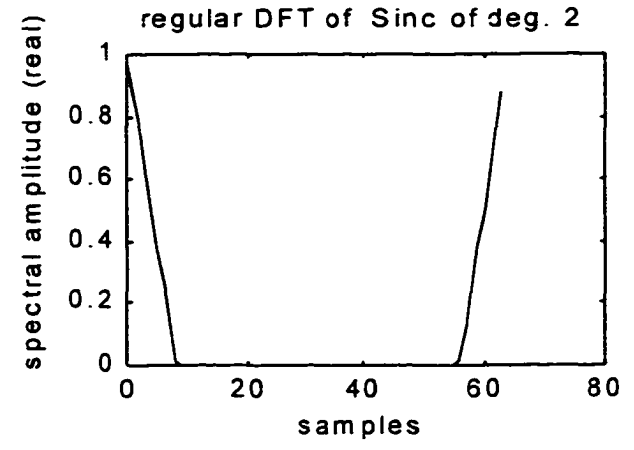

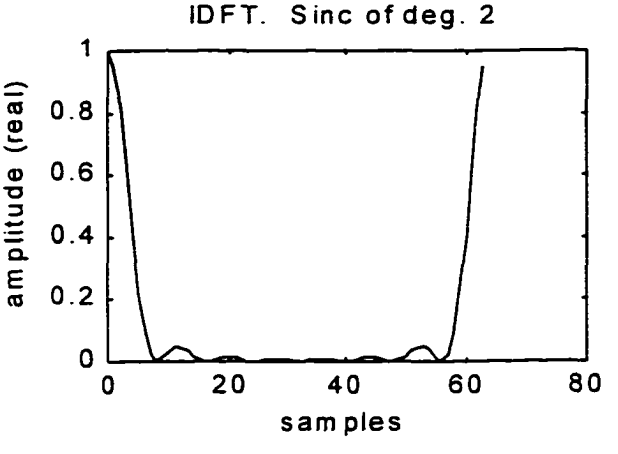

Figure 5.8b. Regular DFT of the periodic extension of $sinc^2 t$ and its inverse.

5.2 Zak Transform Time-Frequency Numerics

In this section the numerics of Zak transform phase space is explored with respect to signal analysis and visualization. The signals involved may be combined in several ways: superposition, modulation, and convolution. The Zak transform maps a time (or frequency) signal into a time-frequency signal in Zak space. Zak space is a subspace of the signal's phase space. It is determined by the subgroup definition of the Zak transform. Each subgroup definition of the Zak transform leads to a corresponding set of time-frequency numerics for the signal representation in Zak space. The nature of each of these representations depends on its time-frequency numerics set. Therefore, a time-frequency signal representation of any time signal can vary greatly in Zak space. The choice of the numerics set on Zak analysis impacts both signal visualization and interpretation. However, the numerics set may be chosen to suit the desired application. Moreover, Zak space has two degenerative states: the signal space and Fourier space.

5.2.1 Signals in Zak Space

The signals that were investigated in Zak space included the gaussian, triangle, 2-sided exponential, rectangle, and the 2^{nd} degree Hermite. From the time-frequency representations of these signals in Zak space over different numerics sets, it can be inferred that the Zak transform of a signal cannot be arbitrarily taken if optimum or near-optimum resolution for its magnitude is desired in both time and frequency. A time-frequency representation in Zak space has optimum

resolution if the signal's temporal and spectral (Fourier) descriptions are clearly visible and fully described along the time and frequency axes respectively. This type of representation facilitates time-frequency signal analysis and visualization.

In the experiments performed, the gaussian, triangular pulse, rectangular pulse, and the 2nd degree Hermite showed their maximum simultaneous time and frequency information in Zak space when the time sample number (number representing the time samples) in the numerics set was equaled to the reciprocal of the fine sample interval of these signals, which is related to their spectral durations. The excepted 2-sided exponential signal showed its maximum simultaneous time and frequency information at a time sample number that was equaled to twice the reciprocal of the fine sample interval. This optimum visual representation of a signal's time and frequency information in Zak space is also influenced by the signal's parameters. For example, the optimum cone-like visual representation of the gaussian signal's magnitude in Zak space is valid for the above time sample number only when the variance is $(2\pi)^{-1}$. Since for a given signal the optimum orientation of the time-frequency display occurs at a specific time sample number in the numerics set, a signal's visual representation consists of mainly its temporal or its Fourier spectral components at other time sample numbers. The time-frequency display orientation is influenced by the greater of the time and the frequency sample numbers in the numeric set. When the time sample number is greater than the frequency sample number, the signal's visual representation is oriented along the time axis of Zak space as shown in figure 5.9b to figure 5.13b; when the time sample number is less than the frequency sample number, the signal's visual representation is oriented along the frequency axis (figures 5.9c-d through

5.13c-d). Additionally, as a signal evolves through Zak space, it starts and ends in a degenerative state of the Zak transform; namely, the Zak transform is equal to the signal and its Fourier spectrum respectively as shown in figure 5.9a to 5.13a. Intermediate between these two extreme cases is the time-frequency Zak transform representation of the signal, which shows the signal representation and the degree to which its orientation is influenced by the time and the frequency sample numbers in the numerics set (figures 5.9b-d through 5.13 b-d).

In the experiments, the gaussian, triangle, rectangle, and 2nd degree Hermite were defined on a time span $t \in [-4, 4)$ while the 2-sided exponential was defined on $t \in [-8, 8)$. Specifically these signals were the gaussian,

$$f(t) = e^{-\pi t^2},$$

triangle,

$$f(t) = \begin{cases} 1 - |t|, & |t| < 1 \\ 0, & 1 < |t| < 4, \end{cases}$$

2-sided exponential,

$$f(t) = e^{-|t|},$$

rectangle,

$$f(t) = \begin{cases} 1, & |t| < 0.5 \\ 0, & 0.5 < |t| < 4, \end{cases}$$

and the 2nd degree Hermite,

$$f_2(t) = 4\pi(4\pi - 1)e^{-\pi t^2}.$$

Each signal was uniformly sampled for N = 64 samples. N has factors M and L; M is the time sample number and L is the frequency sample number in the numerics set. In the evolution of the signal through Zak space (figures 5.9a-d through figures 5.13a-d), L was varied from 1 to 64 in steps of 2^n, $0 < n < 6$, and M was computed from N/L. Zak space was totally described by $ML = 64$ discrete sample points, the number of samples in the signal.

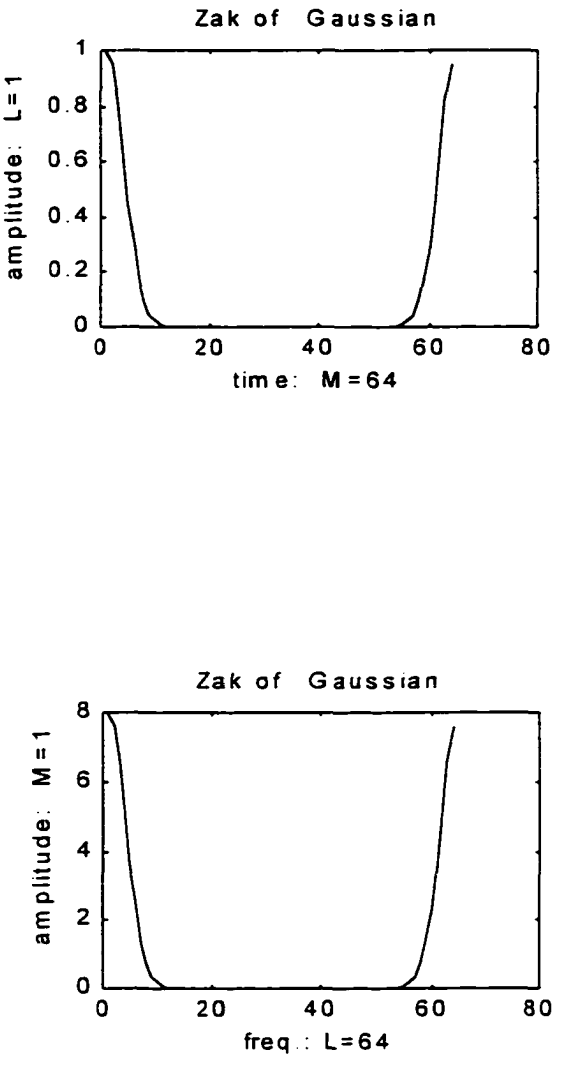

Figure 5.9a. Zak transform of the gaussian at $L = 1$ and $M = 1$ respectively; it degenerates into the signal and its spectrum.

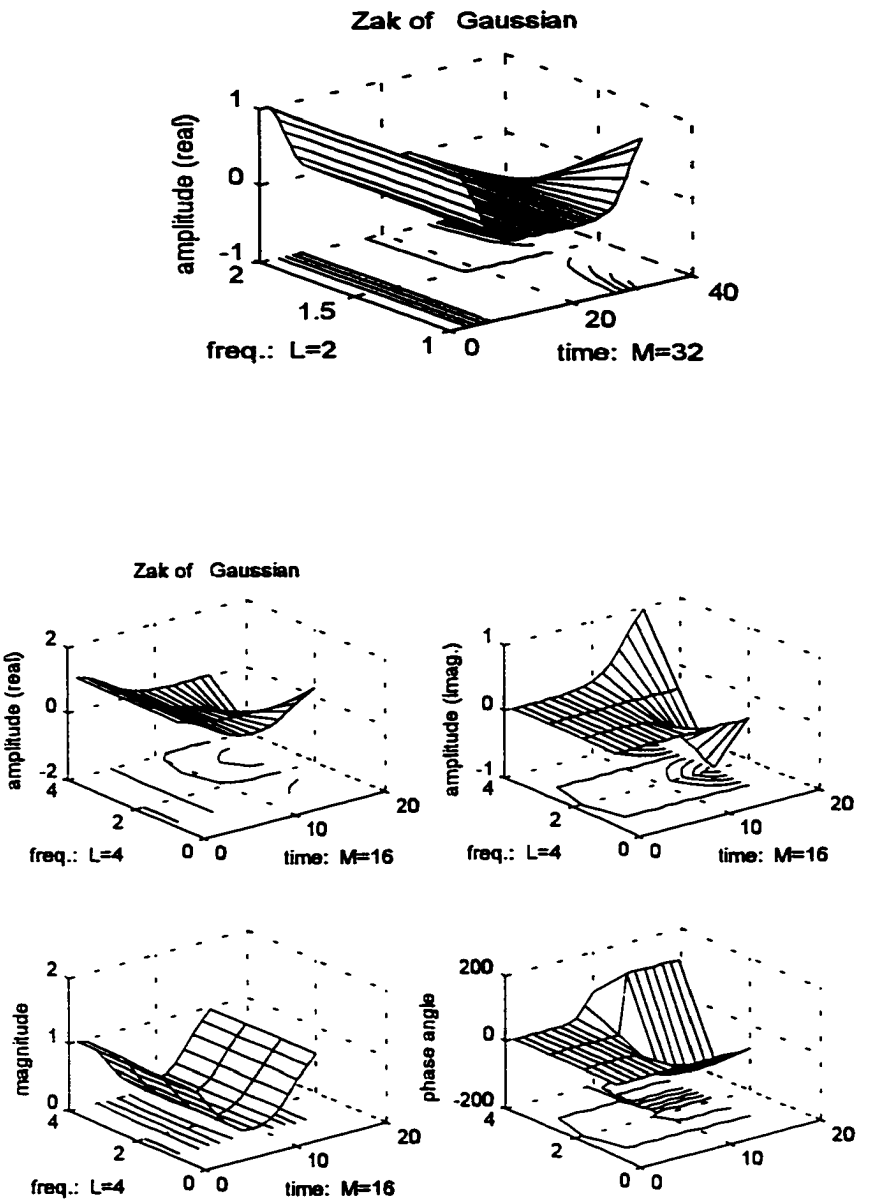

Figure 5.9b. In the evolution of the Zak transform through the time-frequency space, the Zak transform of the gaussian at $L = 2$ and $L = 4$ respectively.

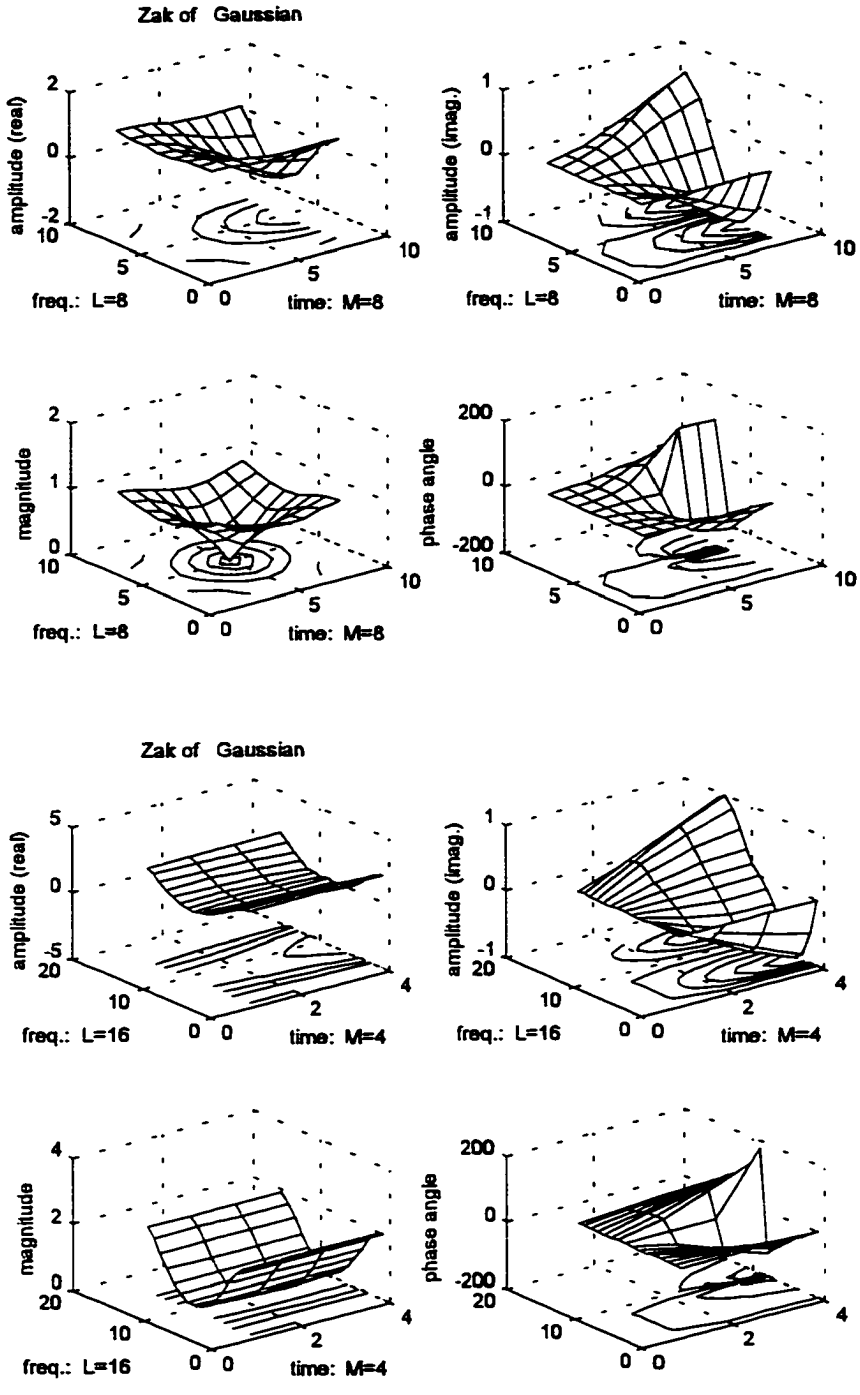

Figure 5.9c. In the evolution of Zak transform through the time-frequency space, the Zak transform of the gaussian at $L = 8$ and $L = 16$ respectively.

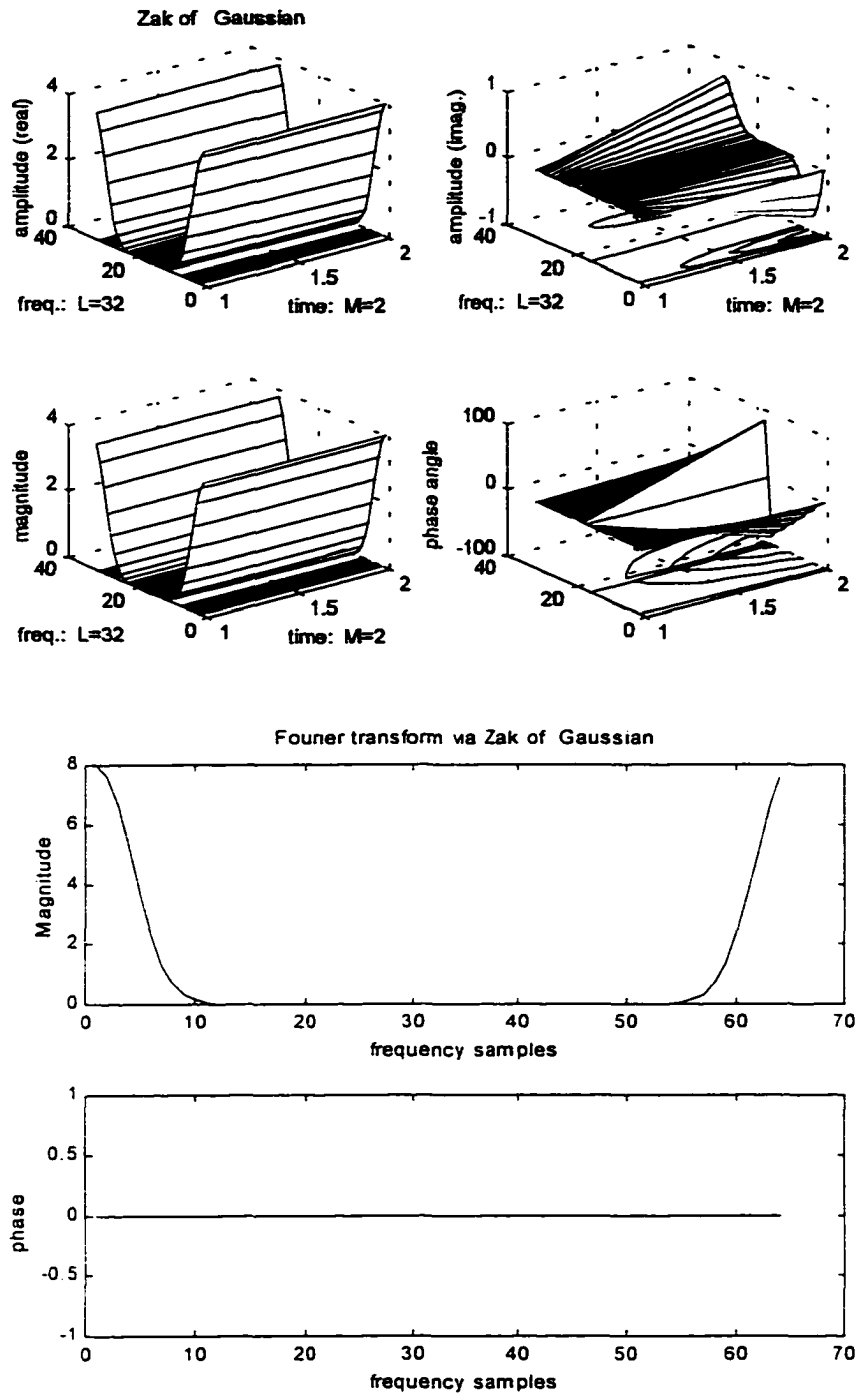

Figure 5.9d. In the evolution of Zak transform through the time-frequency space, the Zak transform of the gaussian at $L = 32$ and the spectrum of the gaussian via Zak transform.

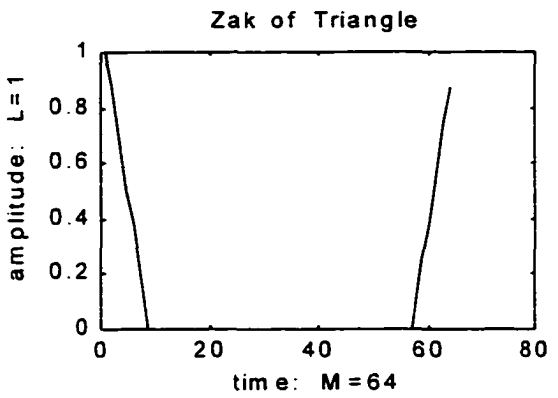

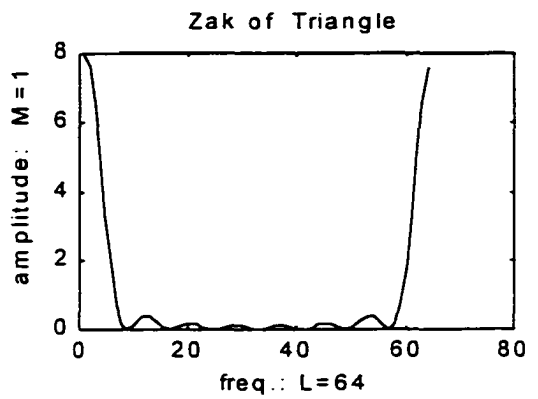

Figure 5.10a. Zak transform of triangle at $L = 1$ and $M = 1$ respectively; it degenerates into the signal and its spectrum.

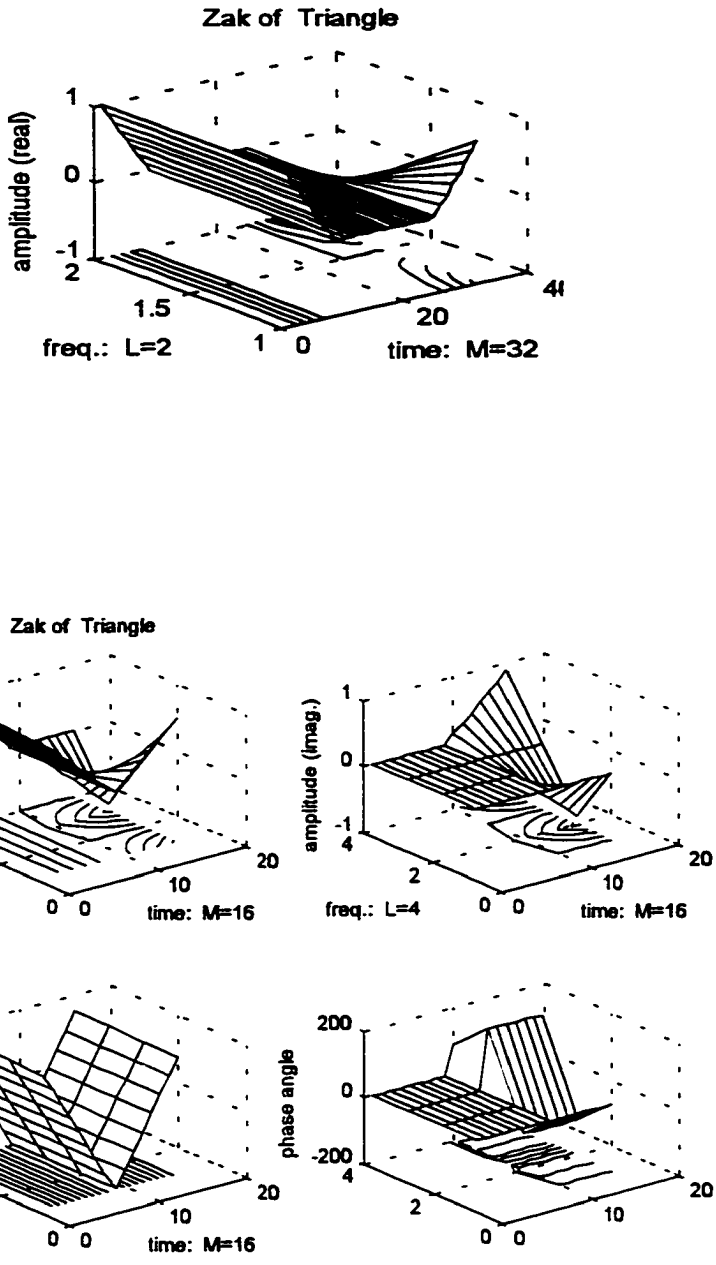

Figure 5.10b. In the evolution of Zak transform through the time-frequency space, the Zak transform of the triangle at $L = 2$ and $L = 4$ respectively.

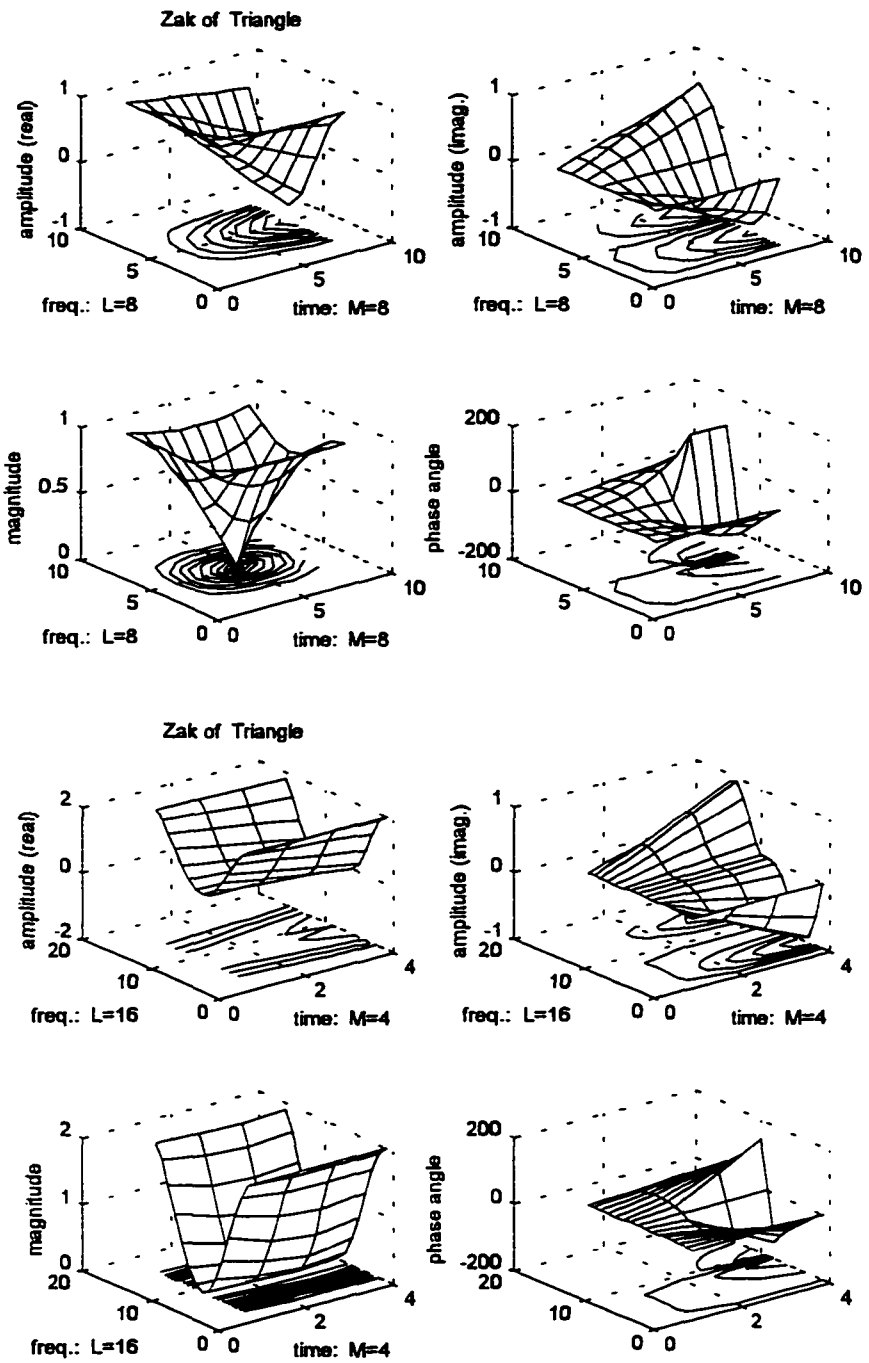

Figure 5.10c. In the evolution of Zak transform through the time-frequency space, the Zak transform of the triangle at $L = 8$ and $L = 16$ respectively.

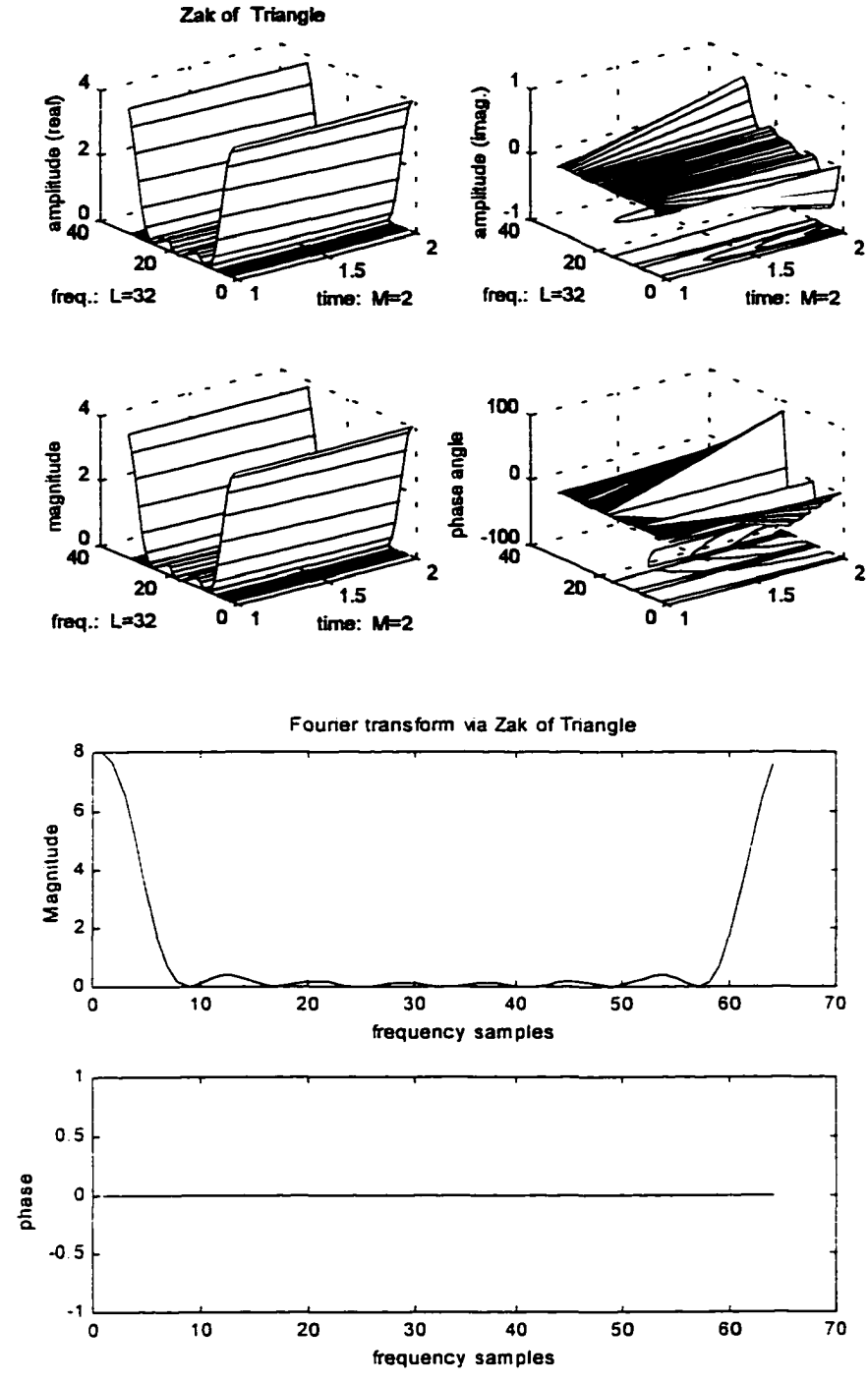

Figure 5.10d. In the evolution of Zak transform through the time-frequency space, the Zak transform of the triangle at $L = 32$ and the spectrum of the triangle via Zak transform.

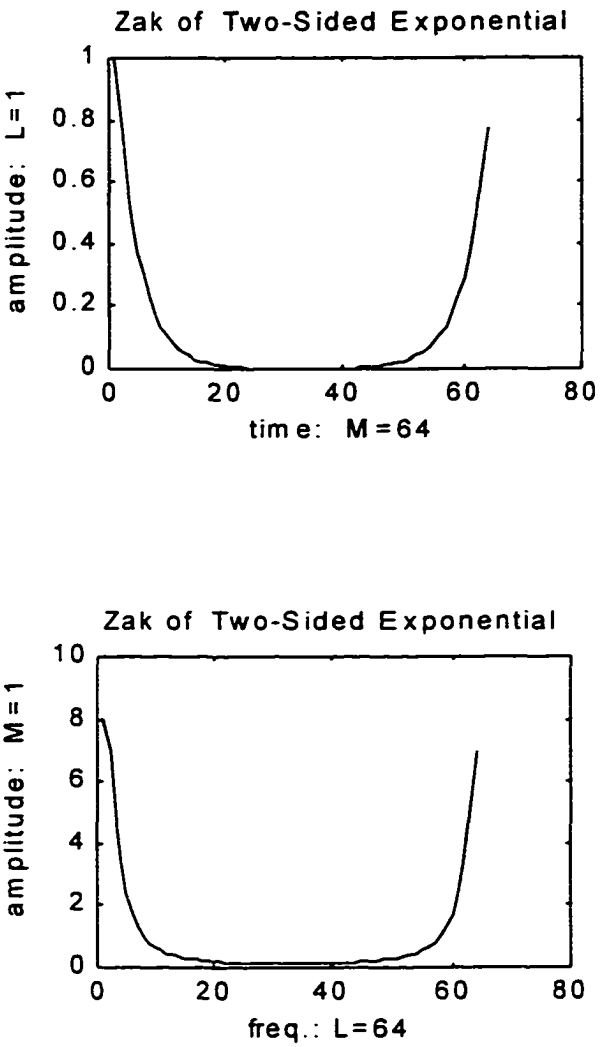

Figure 5.11a. Zak transform of the 2-sided exponential at $L = 1$ and $M = 1$ respectively; it degenerates into the signal and its spectrum.

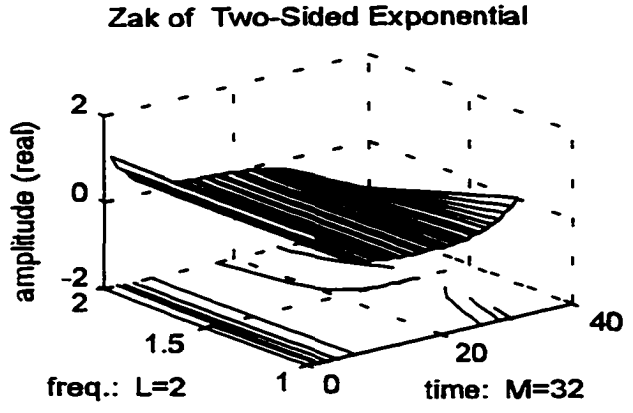

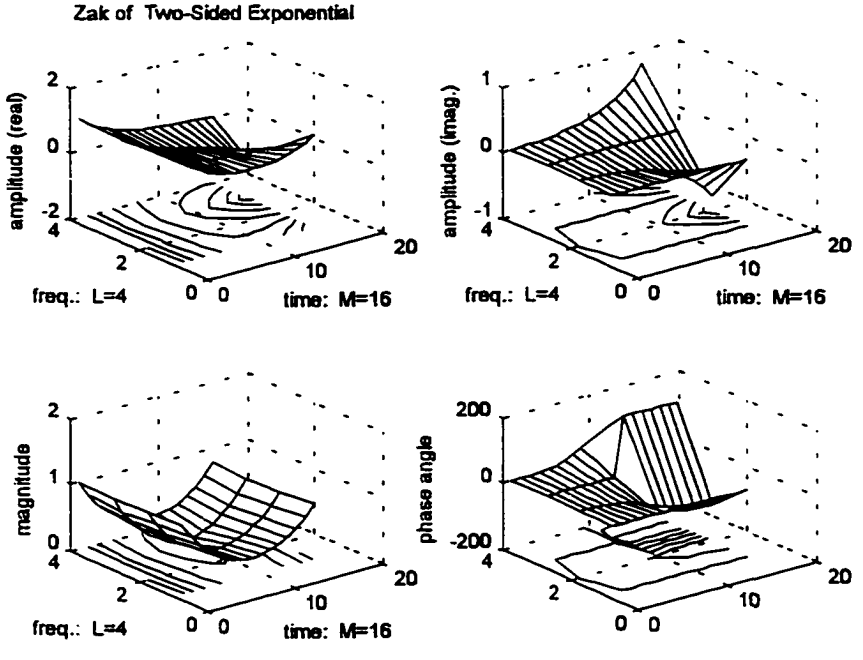

Figure 5.11b. In the evolution of the Zak transform through the time-frequency space, the Zak transform of the 2-sided exponential at $L = 2$ and $L = 4$ respectively.

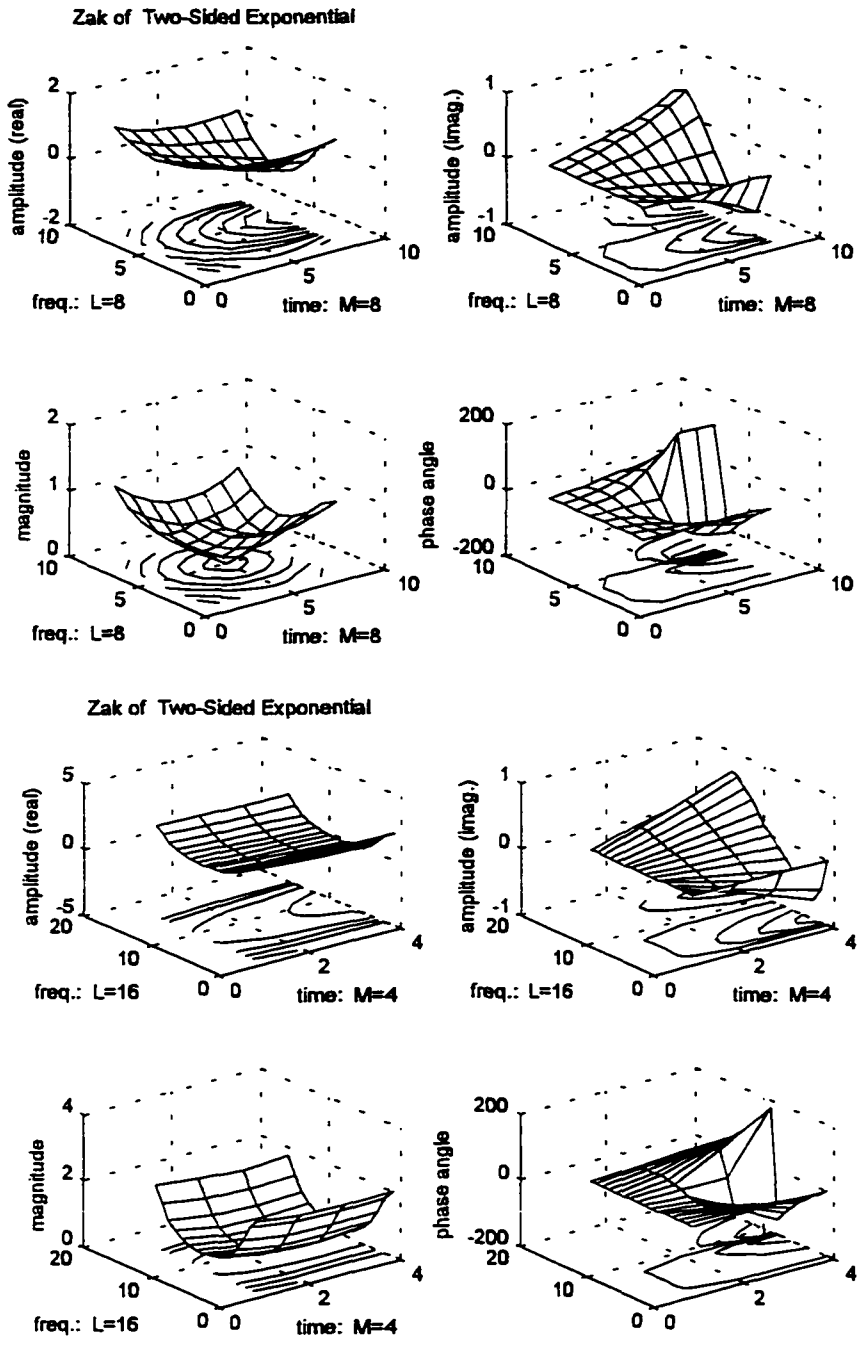

Figure 5.11c. In the evolution of the Zak transform through the time-frequency space, the Zak transform of the 2-sided exponential at $L = 8$ and $L = 16$ respectively.

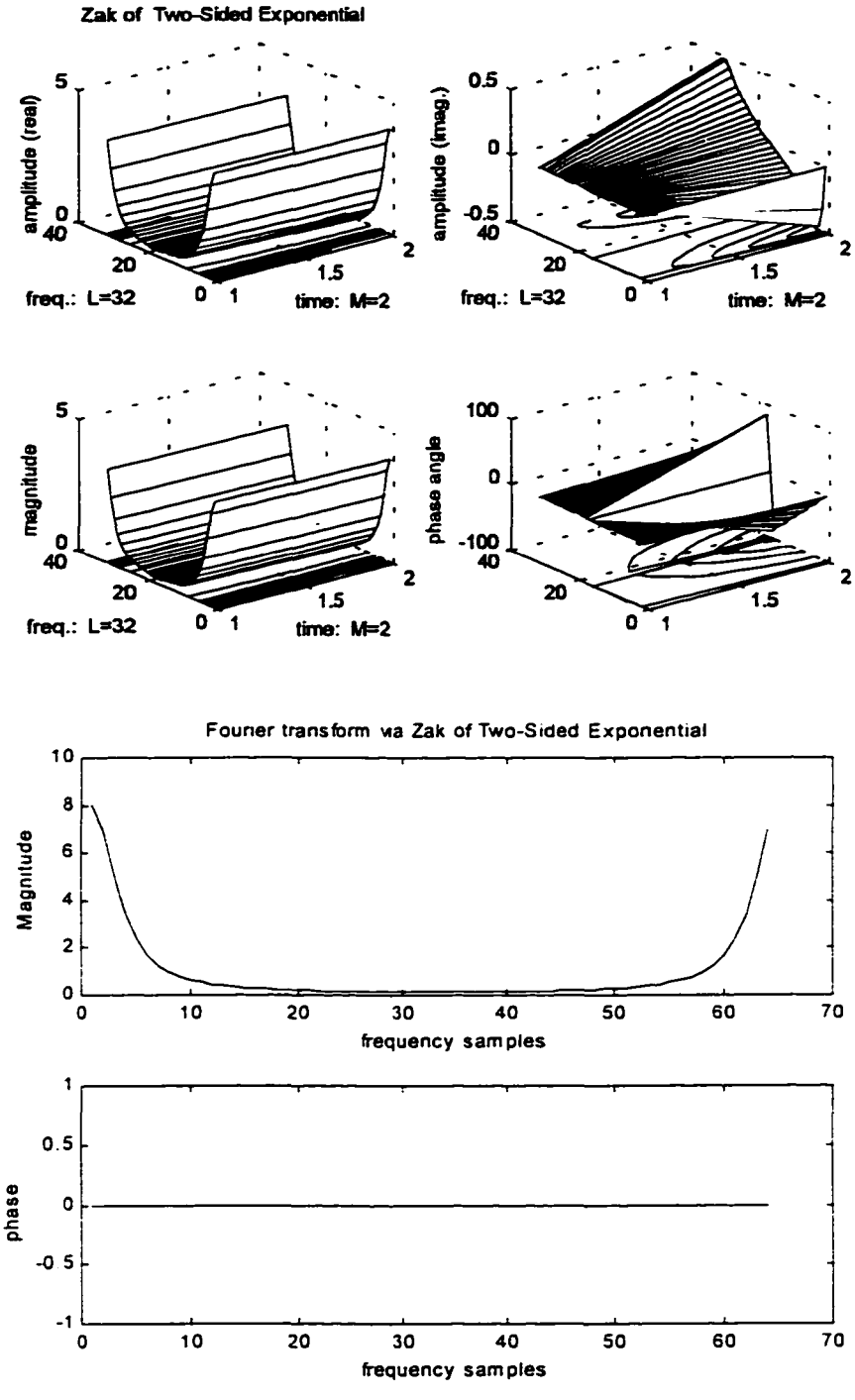

Figure 5.11d. In the evolution of the Zak transform through the time-frequency space, the Zak transform of the 2-sided exponential at $L = 32$ and the spectrum of the 2-sided exponential via Zak transform.

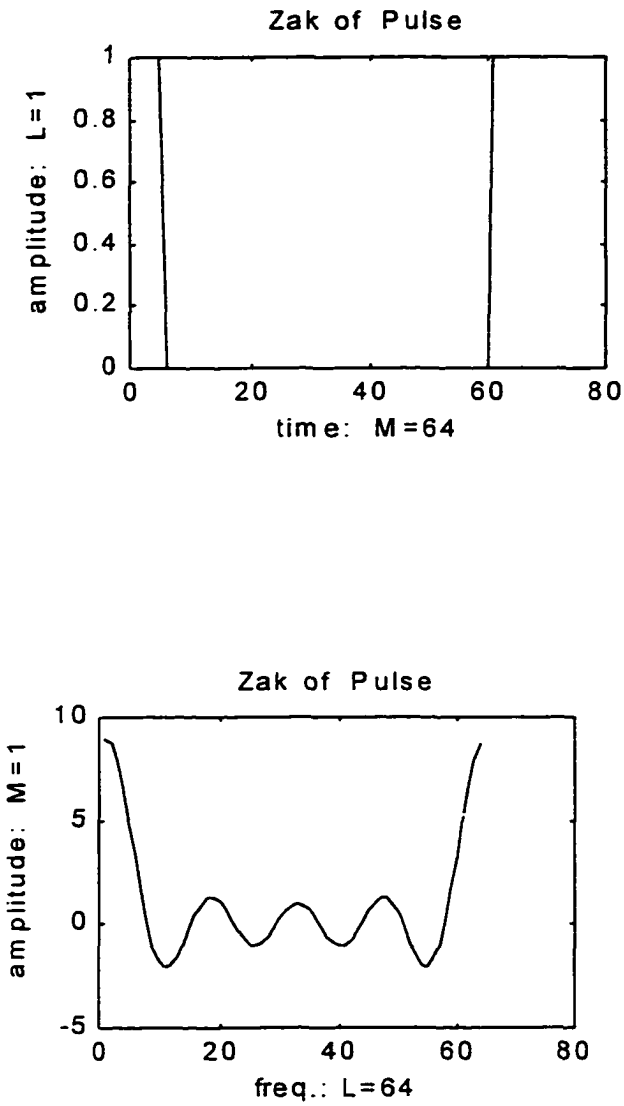

Figure 5.12a. Zak transform of the rectangular pulse at $L = 1$ and $M = 1$ respectively; it degenerates into the signal and its spectrum.

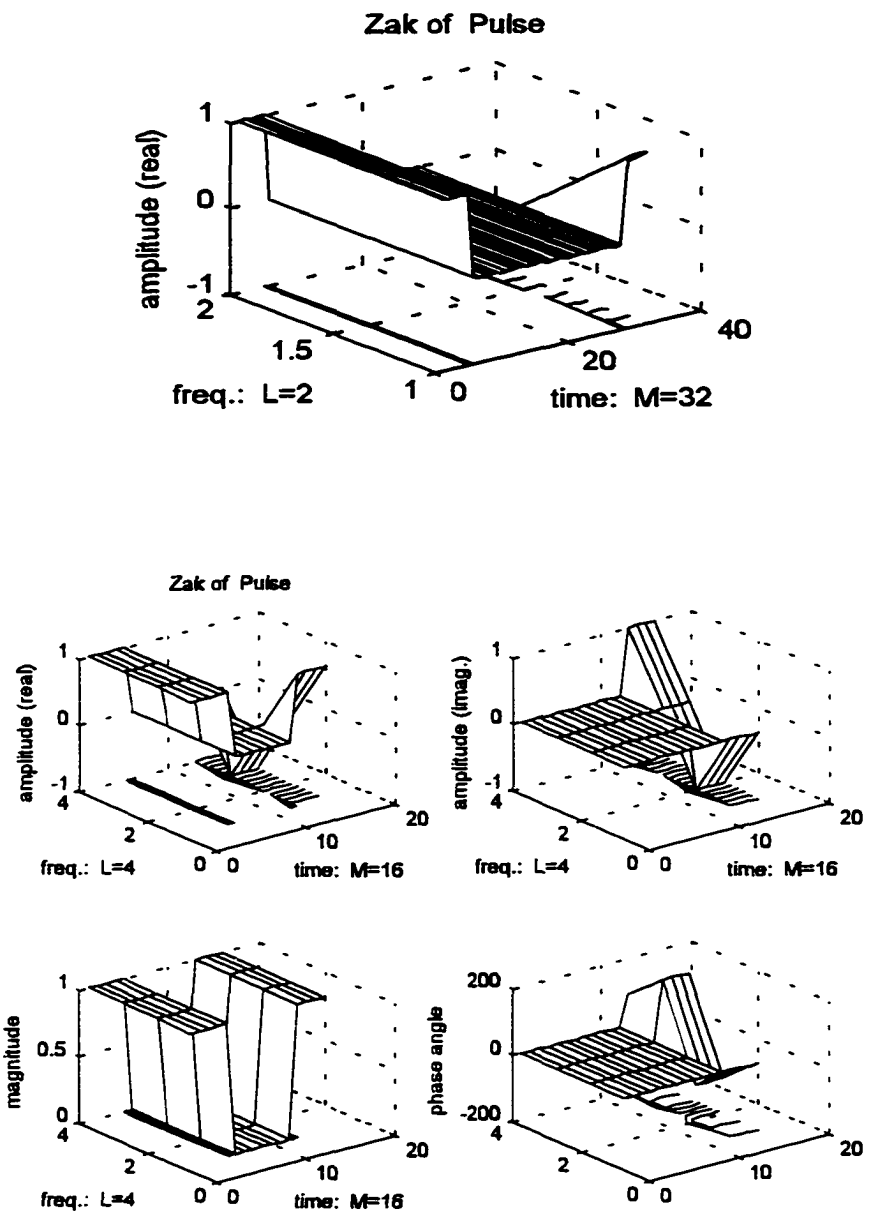

Figure 5.12b. In the evolution of the Zak transform through the time-frequency space, the Zak transform of the rectangular pulse at $L = 2$ and $L = 4$ respectively.

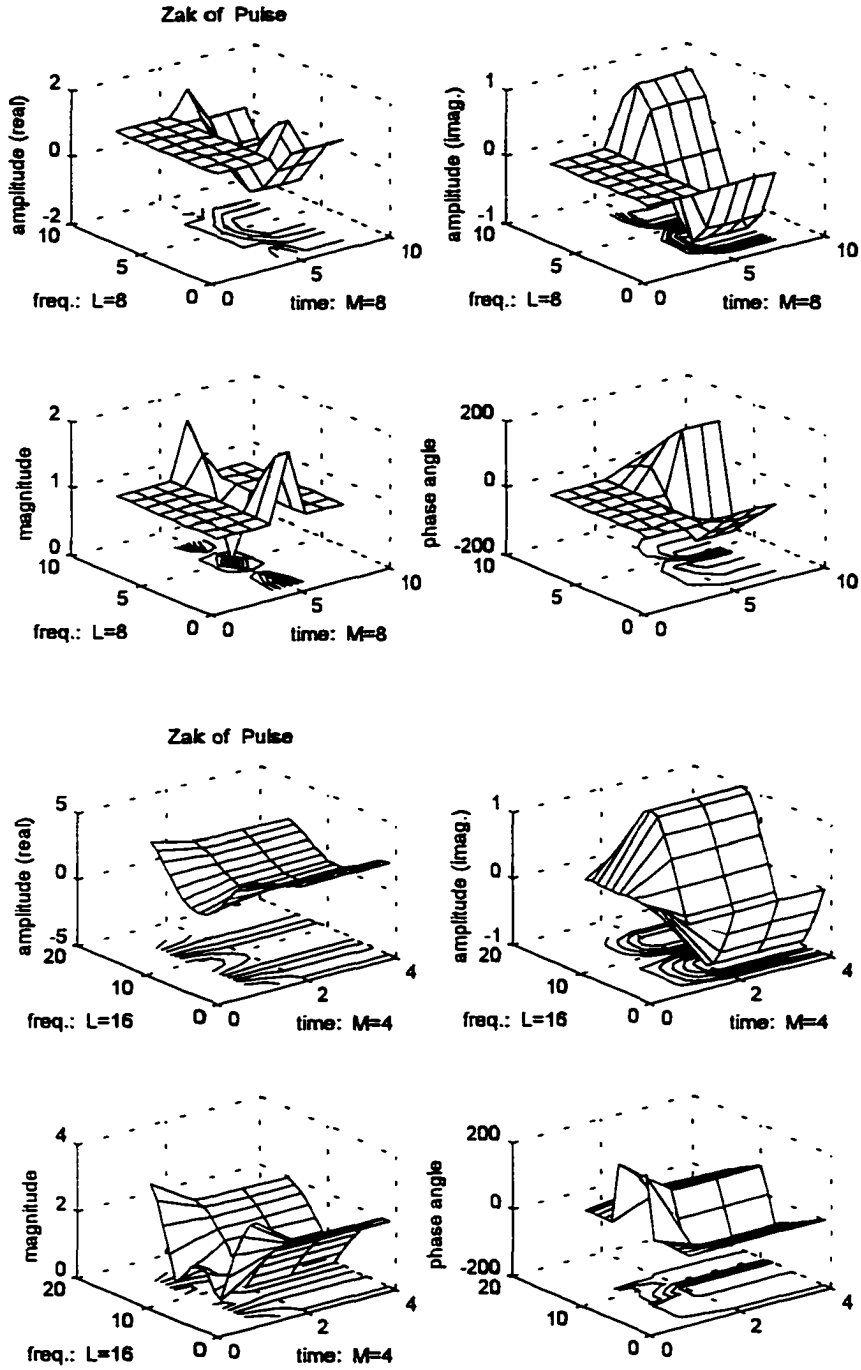

Figure 5.12c. In the evolution of the Zak transform through the time-frequency space, the Zak transform of the rectangular pulse at $L = 8$ and $L = 16$ respectively.

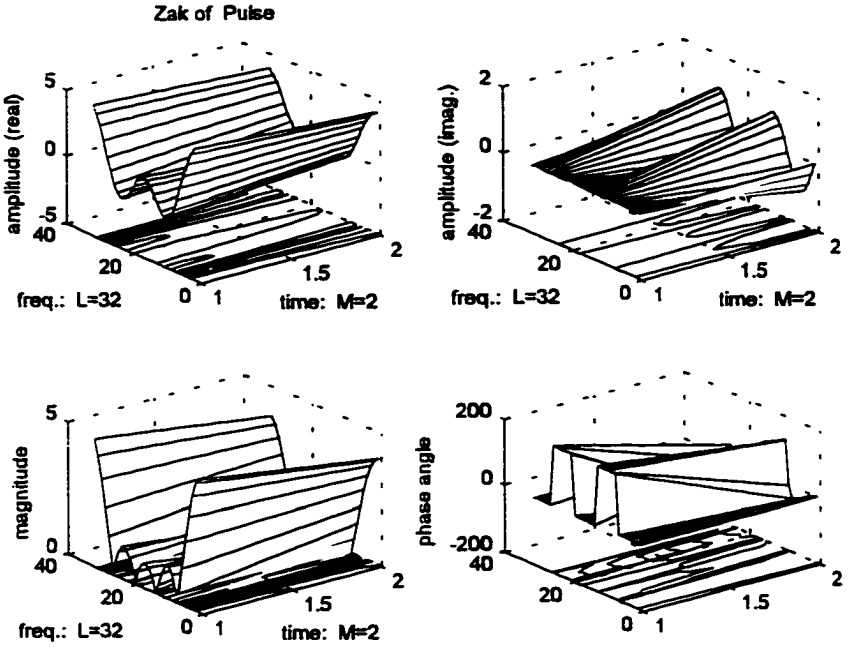

Figure 5.12d. In the evolution of Zak transform through the time-frequency space, the Zak transform of the rectangular pulse at $L = 32$.

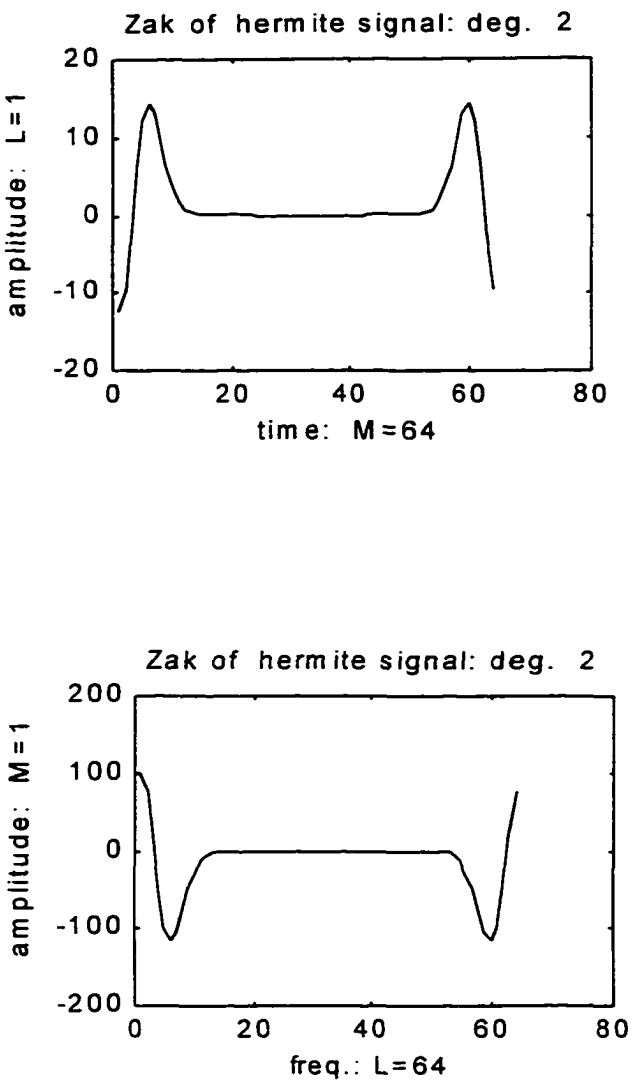

Figure 5.13a. Zak transform of the 2nd degree Hermite at $L = 1$ and $M = 1$ respectively; it degenerates into the signal and its spectrum.

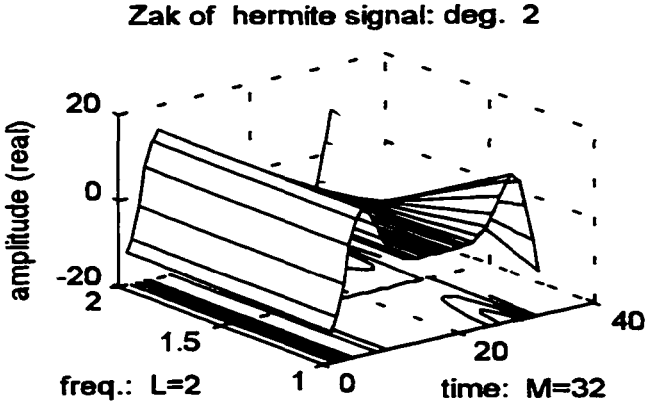

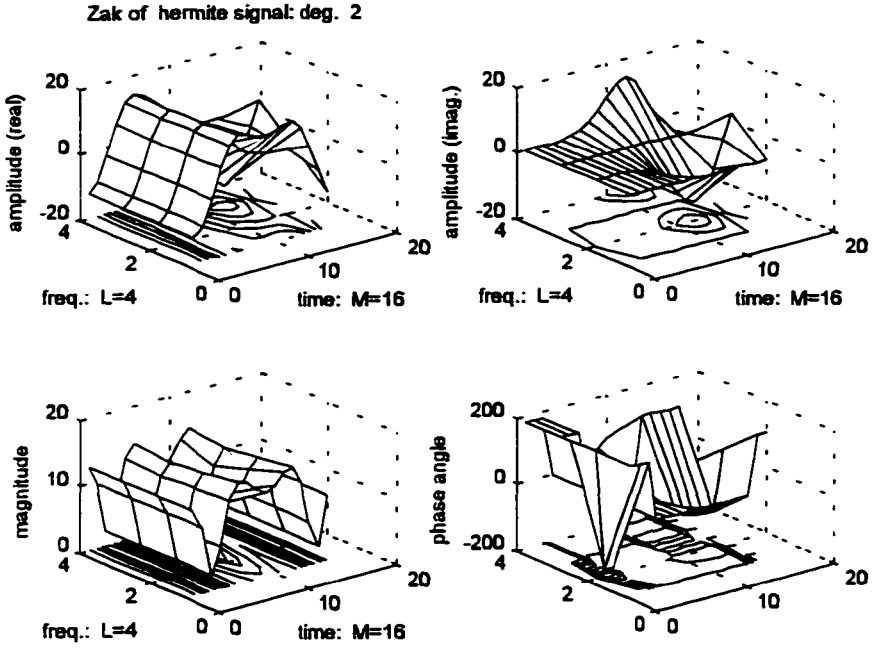

Figure 5.13b. In the evolution of Zak transform through the time-frequency space, the Zak transform of the 2nd degree Hermite at $L = 2$ and $L = 4$ respectively.

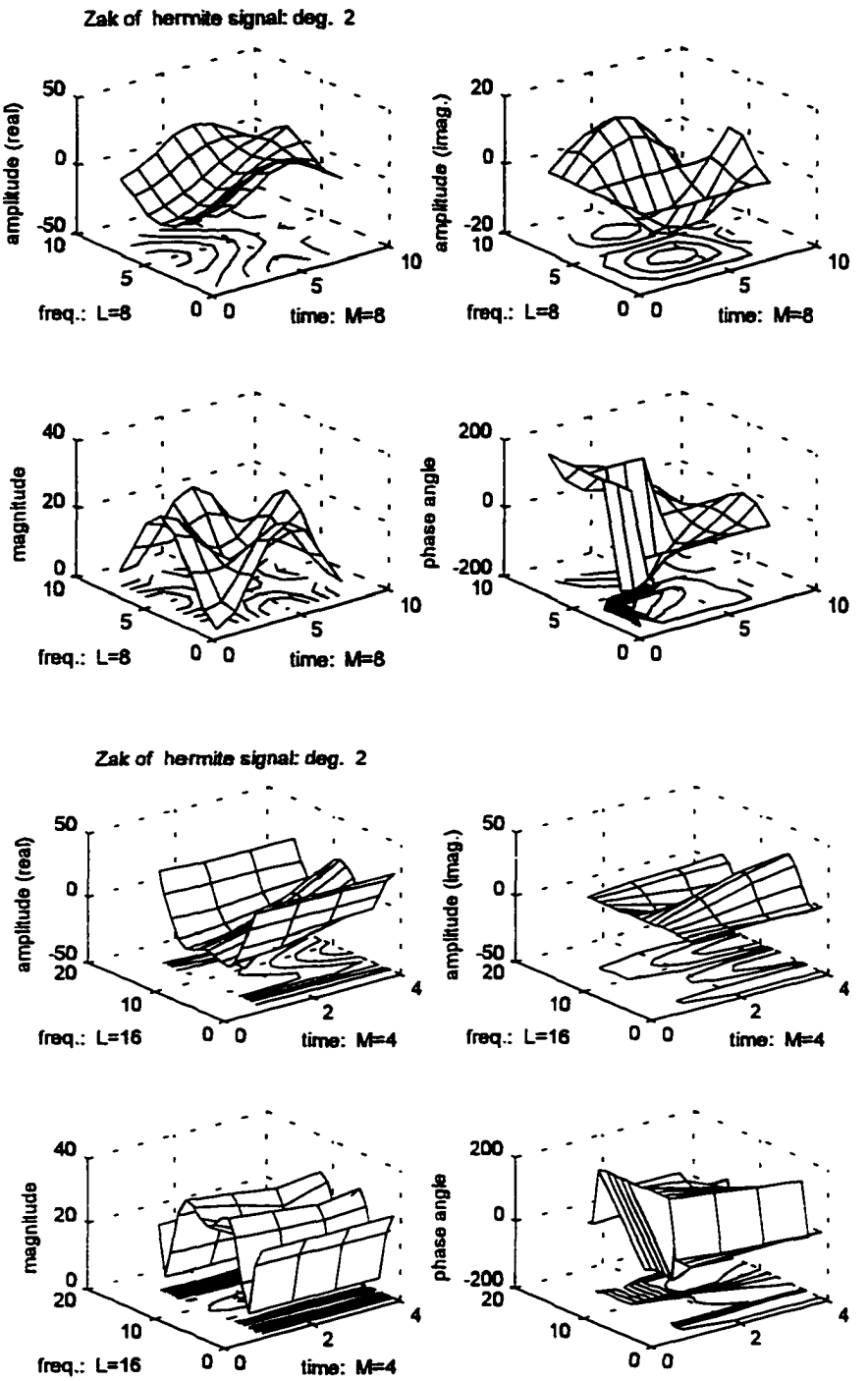

Figure 5.13c. In the evolution of Zak transform through the time-frequency space, the Zak transform of the 2nd degree Hermite at $L = 8$ and $L = 16$ respectively.

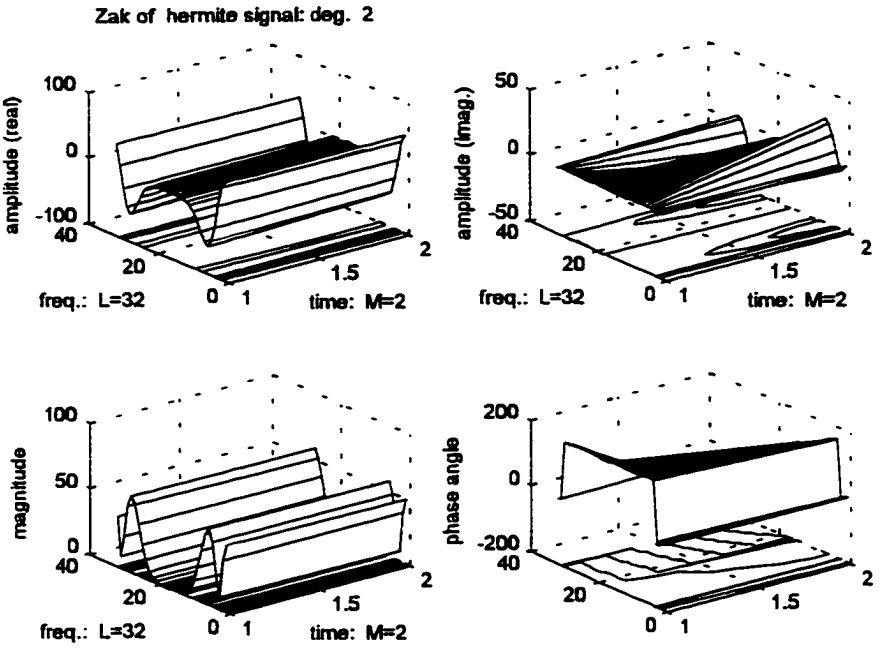

Figure 5.13d. In the evolution of Zak transform through the time-frequency space, the Zak transform of the 2nd degree Hermite at $L = 32$.

5.3 Orthogonal Projection in Zak Space

A very crucial issue in any digital signal processing application is the size of the data set. The raw data set of many applications is too large for any meaningful digital processing operation, transmission, or storage. In these cases, the data set must be reduced to a manageable size before it can be adequately processed, transmitted, or stored. However, reducing the information content of a continuous signal (or an image) in a digital framework below the Shannon number is not a straightforward operation [291]. When Gabor [38] introduced the Weyl-Heisenberg expansion of a signal in 1946, he proposed an economical and cost-effective application in compression of speech and musical information bearing signals for the purpose of transmission or storage. According to the Nyquist-Shannon sampling theorem, the samples of an information bearing signal can never be transmitted at higher than the Nyquist rate for the channel [163].

Over the past few decades, rapid growth in biomedicine, telecommunications, and computer technology has continually demanded and received advanced data compression techniques for flexible digital signal processing operations, efficient data transmission, and mass storage. Data compression effectively aids in the development of fast and efficient digital signal processing algorithms for operation on manageable data sets; it necessitates a minimized channel bandwidth for the transmitted data in real time; and it demands minimal memory storage. One way to achieve data compression is through orthogonal multiresolution decomposition [141, 143, 147, 229].

Closely related to the data compression issue is the quality of the raw data and the compressed transmitted digital information at the receiver. A signal's raw data may be distorted with measurement related noise and its compressed transmitted data set may be distorted by "variations or uncertainties" in the analog transmission medium's properties. In either case, some type data equalization [177] or signal enhancement [292] is needed. Signal enhancement is a slight modification of the signal's data to achieve the desired properties of the known signal.

Orthogonal multiresolution analysis is an integral part of Zak transform properties [264]. Visual systems information [228, 229] and transient signal detection lend them to efficient Weyl-Heisenberg representation and analysis [224, 293, 294, 295]. Weyl-Heisenberg expansions are adaptable to the multiresolutional decomposition inherent in visual image processing. A critical step in many signal detection processes is data compression through linear transformation [293, 296].

Subsequently, an orthogonal projection algorithm will be presented in a group theoretic setting. This algorithm orthogonally projects a signal expressed in terms of Weyl-Heisenberg expansion, which usually consists of nonorthogonal basis signals, from a critically sampled subspace of Weyl-Heisenberg systems into an undersampled subspace. The entire projection process is executed using periodization and decimation in Zak space. The projection signal on the undersampled subspace of the critically sampled subspace of the signal is synthesized with a subset of the signal's Weyl-Heisenberg coefficient set. The values of these coefficients are actually different from those in the equivalent subset of the signal's Weyl-Heisenberg coefficient

set. This change in values is a consequence of the orthogonality condition in the projection. If the values of the projection signal's Weyl-Heisenberg coefficient set were merely a subset of the values in the signal's coefficient set, the projection would have been nonorthogonal. There are other methods available to obtain a Weyl-Heisenberg expansion of an undersampled signal [297, 298, 299]. In [297], Qui developed an algorithm in the context of frames and a pseudo-inverse matrix to compute the Weyl-Heisenberg coefficients of the best approximation of a signal on an undersampled subspace of Weyl-Heisenberg systems. In addition, he showed that the best approximation of a signal is its orthogonal projection. In [298], Polyak and Pearlman used the concept circular stationarity of vector sequences in the Weyl-Heisenberg representational setting to obtain the Weyl-Heisenberg coefficients on the undersampled subspace.

The orthogonal projection algorithm presented herein has potential application in data compression with perhaps the added feature of signal enhancement. It can be employed to perform data compression by means of multiresolution decomposition. The multiresolutional attribute of this algorithm is exploited when it is applied recursively or iteratively.

5.3.1. Review of Essential Theory

In the context of abelian group theory, a signal $f \in L(Z/N)$ with Fourier transform $\hat{f} \in L(Z/N)$ has a possible Weyl-Heisenberg expansion of the form,

$$f(a) = \sum_{m=0}^{N-1} \sum_{n=0}^{N-1} c_{m,n} g(a - m) e^{2\pi i n a / N}, \tag{5.49}$$

where $a \in Z/N$, $c \in L(Z/N \times Z/N)$, and $g \in L(Z/N)$ is the window signal. The signal space $L(Z/N)$ is the inner product space with the inner product

$$\langle f, g \rangle = \sum_{m=0}^{N-1} f(m) g^{*}(m)$$

over Z/N. It is often denoted by $L_2(Z/N)$. When the set of basis signals generated by g is defined on the subgroup $MZ/N \times LZ/N$ of $Z/N \times Z/N$, ML does not necessarily equal N, the expansion of f for $a \in Z/N$ and $c \in L(MZ/N \times LZ/N)$ becomes

$$f(a) = \sum_{m=0}^{L-1} \sum_{n=0}^{M-1} c_{mM,nL} g(a - mM) e^{2\pi i n L a / N}, \tag{5.50}$$

over the Weyl-Heisenberg system

$$(g, M, L) = \{g_{mM,nL} : m \in Z/L, n \in Z/M\}.$$

The space of a Weyl-Heisenberg system is its linear span. Any signal f contained in it can have several valid Weyl-Heisenberg expansions. In addition, the space of a Weyl-Heisenberg system and the space of its orthogonal complement are each a subspace of $L(Z/N)$. Their orthogonal

direct sum is equal to the signal space $L(Z/N)$. They are invariant under the set of Weyl-Heisenberg operators,

$$\{W_{mM,nL} = R_{nL}T_{mM} : m \in Z/L,\ n \in Z/M\},$$

of $L(Z/N)$ where $g_{mM,nL} = W_{mM,nL}g$ are the time-frequency translates of g over $MZ/N \times LZ/N$. These Weyl-Heisenberg operators are related through the Zak transform to those Weyl-Heisenberg operators defined on $L(Z/N \times Z/N)$. For a subgroup MZ/N of Z/N, $N = ML$, the collection of Weyl-Heisenberg operators over $MZ/N \times LZ/N$ is commutative. However, Weyl-Heisenberg operators do not generally commute because of the noncommutativity of translation and modulation operators, T and R. This noncommutativity is an interpretation of the Heisenberg uncertainty principle.

Although Poisson's summation formula simply describes the behavior of the Fourier transform under periodization in the sense that its description of the Fourier expansion of a signal f over some subgroup MZ/N of Z/N, $N = ML$, evaluates an orthogonal projection of f on the subspace spanned by the dual subgroup LZ/N in the signal space $L(Z/N)$, Poisson's summation of the Weyl-Heisenberg expansion of f is more difficult to analyze. In fact, the periodization of the Weyl-Heisenberg expansion of f over some critically sampled Weyl-Heisenberg system, (g, M, L), $ML = N$, is generally coupled; that is, the application of Poisson's summation formula to equation (5.50) over a subgroup $M_1Z/N \subset MZ/N$ contained in Z/N when

$$ML = N = M_1 L_1,$$

yields the result,

$$\sum_{s=0}^{L_1-1} f(a + sM_1) = \sum_{m=0}^{L-1} \sum_{n=0}^{M-1} c_{mM,nL} \sum_{s=0}^{L_1-1} g((a + sM_1) - mM) e^{2\pi i(a - sM_1)n/M}, \qquad (5.51)$$

where $a \in Z/N$. Nonetheless, it is possible to uncouple the periodized Weyl-Heisenberg expansion of f to some extent if the periodization process is done in Zak space.

The Zak transform $F \in L(Z/N \times Z/N)$ of a signal $f \in Z/N$ is defined over a subgroup MZ/N of Z/N as

$$F(b, a) = \sum_{r=0}^{L-1} f(a + rM) e^{2\pi i r b/L}, \quad a, b \in Z/N, \quad N = ML. \qquad (5.52)$$

It maps $L(Z/N)$ onto Zak space. The application of the Zak transform to the Weyl-Heisenberg expansion of f,

$$f(a) = \sum_{m=0}^{L-1} \sum_{n=0}^{M-1} c_{mM,nL} g(a - mM) e^{2\pi i n a/M}, \quad a \in Z/N, \quad N = ML,$$

yields in Zak space the product of the window signal G and a 2-dimensional trigonometric polynomial P with its coefficients being the Weyl-Heisenberg coefficients $c_{mM,nL}$:

$$F(b,a) = G(b,a)P(b,a), \quad a,b \in Z/N, \tag{5.53}$$

where the trigonometric polynomial P has the form,

$$P(b,a) = \sum_{m=0}^{L-1} \sum_{n=0}^{M-1} c_{mM,nL} e^{2\pi i(an/M - bm/L)}, \quad a,b \in Z/N, \quad N = ML.$$

This trigonometric polynomial is tied to other trigonometric polynomials under Zak space formalism. In fact, these other trigonometric polynomials are related to the cross-ambiguity function of $f,g \in L(Z/N)$ expressed as

$$A_{f,g}(mM,nL) = \langle f, g_{mM,nL} \rangle, \quad m \in LZ/N, \quad n \in MZ/N, \quad N = ML,$$

and when $f = g$, the auto-ambiguity function is obtained:

$$A_g(mM,nL) = \langle g, g_{mM,nL} \rangle.$$

Since Zak space is isometrically isomorphic to the signal space $L(Z/N)$, inner products on $L(Z/N)$ are equivalent to inner products on Zak space; that is,

$$\langle f, g_{mM,nL} \rangle = L^{-1} \langle F, G_{mM,nL} \rangle, \quad m \in MZ/N, \quad n \in LZ/N, \quad N = ML.$$

Thus, linear Zak space is a venue to perform nonlinear operations such as those relating to the ambiguity function.

In radar theory, the expected value of the cross-ambiguity surface is the smoothed version of the scattering function. Analogously, the inner product form of the cross-ambiguity function, which is a more general set of Weyl-Heisenberg coefficients, is a smoothed version of the Weyl-Heisenberg coefficients $c_{mM,nL}$.

The inner products of $F \in L(Z/N \times Z/N)$ on Zak space is describable in terms of a 2-dimensional inverse Fourier series with $N = ML$:

$$\langle F, G_{mM,nL} \rangle = \sum_{a=0}^{M-1} \sum_{b=0}^{L-1} F(b,a) G^{*}(b,a) e^{-2\pi i(an/M + bm/L)}, \tag{5.54}$$

where $m \in MZ/N$ and $n \in LZ/N$. By Fourier inversion this equation has a related trigonometric polynomial of the form,

$$F(b,a) G^{*}(b,a) = M^{-1} \sum_{m=0}^{L-1} \sum_{n=0}^{M-1} \langle f, g_{mM,nL} \rangle e^{2\pi i(an/M + bm/L)}, \tag{5.55}$$

with $a, b \in Z/N$ and the coefficients $\langle f, g_{mM,nL} \rangle$ contained in the critical sampling subspace $L(MZ/N \times LZ/N)$. When $f = g$, this trigonometric polynomial becomes

$$|G(b,a)|^2 = M^{-1}\sum_{m=0}^{L-1}\sum_{n=0}^{M-1}\langle g, g_{mM,nL}\rangle e^{2\pi i(an/M + bm/L)}, \quad a,b \in Z/N. \tag{5.56}$$

From $F = GP$, it is clear that multiplication by G^* yields

$$F(b,a)G^*(b,a) = |G(b,a)|^2 P(b,a), \quad a,b \in Z/N. \tag{5.57}$$

Since $\langle f, g_{mM,nL}\rangle$ equals $L^{-1}\langle F, G_{mM,nL}\rangle$, the relationship between $\langle f, g_{mM,nL}\rangle$ of f over (g, M, L) and $c_{mM,nL}$ over $MZ/N \times LZ/N$ is established by expressing $\langle f, g_{mM,nL}\rangle$ in terms of

$$|G(b,a)|^2 P(b,a), \quad a,b \in Z/N,$$

and then solving to obtain the convolution of $c_{mM,nL}$ and $\langle g, g_{mM,nL}\rangle$:

$$\langle f, g_{mM,nL}\rangle = \sum_{r=0}^{L-1}\sum_{s=0}^{M-1} c_{rM,sL}\langle g, g_{(m-rM),(n-sL)}\rangle, \tag{5.58}$$

where $m \in MZ/N$ and $n \in LZ/N$. Thus $\langle f, g_{mM,nL}\rangle$ is a smoothed form of $c_{mM,nL}$. The set of inner products $\langle f, g_{mM,nL}\rangle$, which is the cross-ambiguity function $A_{f,g}(mM, nL)$, is the Weyl-Heisenberg coefficient set of the product function $FG^* \in L(Z/N \times Z/N)$. This product function can be restated as

$$F(b,a)G^{*}(b,a)$$
$$= M^{-1}\sum_{m=0}^{L-1}\sum_{n=0}^{M-1}\left\{\sum_{r=0}^{L-1}\sum_{s=0}^{M-1} c_{rM,sL}\langle g, g_{(m-rM,(n-sL)}\rangle\right\} e^{2\pi i(mn/M - bm/L)} \quad (5.59)$$

for $a, b \in Z/N$; that is, the coefficient set of the Fourier series expansion FG^{*} is the smoothed coefficient set $c_{mM,nL}$.

5.3.2 Projection Algorithm

Suppose $MZ/N \times L_1 Z/N$ is a subgroup of $Z/N \times Z/N$, $MZ/N \times LZ/N$ is the critical sampling subgroup, and $g \in L(Z/N)$ is the window signal, the relationship between a signal f over the Weyl-Heisenberg system (g, M, L_1) and its related set of Weyl-Heisenberg coefficients is more complex than the relationship between f and its Fourier coefficients. Because the main goal is to process signals in terms of their Weyl-Heisenberg coefficients, standard operations on signals must be interpreted as operations on Weyl-Heisenberg coefficients.

5.3.2.1 Sampling Subgroups

The implementation of the orthogonal projection algorithm requires periodization over different sampling subgroups. The sampling subgroup used depends on whether the periodization is done in time, in frequency, or in both time and frequency. If the periodization is done in frequency over the group Z/N and

$$N = ML = M_1 L_1$$

with M divides M_1 such that

$$\frac{M_1}{M} = \frac{L}{L_1} = R \in Z,$$

the integer oversampling subgroup is $MZ/N \times L_1 Z/N$, a subgroup of Z/N. The order of the integer oversampling subgroup is LM_1, which is greater than the order of Z/N by R. Contained in $MZ/N \times L_1 Z/N$ is the critical sampling subgroup

$$MZ/N \times LZ/N, \quad M_1 Z/N \subset MZ/N.$$

Any critical sampling subgroup has order N, the number of elements in Z/N. Corresponding to the integer oversampling subgroup is the integer undersampling subgroup $M_1 Z/N \times LZ/N$. It is contained in the critical sampling subgroup

$$M_1 Z/N \times L_1 Z/N, \quad LZ/N \subset L_1 Z/N,$$

and it has order $L_1 M$, which is less than the order of Z/N by R^{-1}.

If the periodization is done in both time and frequency over the group $Z/N \times Z/N$ and

$$N = ML = M_1 L_1 = M_2 L_2$$

with M divides M_1 and M_1 divides M_2 which implies that M divides M_2 such that $M_1 = RM$ and $M_2 = RSM$ where R and S are integer constants, the integer oversampling subgroup may be chosen as

$$MZ/N \times L_2 Z/N, \quad M_2 Z/N \subset M_1 Z/N \subset MZ/N.$$

The order of this sampling subgroup is RSN. It contains critical sampling subgroups $M_2 Z/N \times L_2 Z/N$, $M_1 Z/N \times L_1 Z/N$, and $MZ/N \times LZ/N$. The corresponding integer undersampling subgroup is

$$M_2 Z/N \times LZ/N, \quad LZ/N \subset L_1 Z/N \subset L_2 Z/N.$$

It contains $(RS)^{-1}N$ elements and is contained in the critical sampling subgroup $M_2 Z/N \times L_2 Z/N$.

5.3.2.2 Procedural Rationale

Suppose the order of the group over which the signal is defined is composed of many different sets of factors,

$$N = ML = M_1 L_1 = M_2 L_2$$

where M divides M_1, M_1 divides M_2, and M divides M_2 such that $M_1 = RM$ and $M_2 = RSM$, and R and S are constants in Z; and there exist subgroups of $Z/N \times Z/N$ satisfying the condition

$$M_2 Z/N \times LZ/N \subset M_1 Z/N \times L_1 Z/N \subset MZ/N \times L_2 Z/N,$$

where $M_2 Z/N \times LZ/N$ is the integer undersampling subgroup, $M_1 Z/N \times L_1 Z/N$ is the critical sampling subgroup, and $MZ/N \times L_2 Z/N$ is the integer oversampling subgroup; the signal $f_1 \in L(g, M_2, L)$ is the orthogonal projection of a signal $f \in L(g, M_1, L_1)$ into the undersampled subspace $L(g, M_2, L)$. The orthogonal projection processes are derived and carried out in Zak space under the operations of periodization and decimation.

The signal $f_1 \in L(g, M_2, L)$ has a Weyl-Heisenberg expansion

$$f_1(a) = \sum_{m=0}^{L_2 - 1} \sum_{n=0}^{M-1} d_{mM_2, nL} g(a - mM_2) e^{2\pi i n a / M}, \tag{5.60}$$

where $a \in Z/N$, $M_2 = RSM$, and $L = RSL_2$. By Zak transformation of this series expansion over the critical sampling subgroup $M_1 Z/N \times L_1 Z/N$, the expression

$$F_1(b, a) = G(b, a) P_1(b, a), \quad a, b \in Z/N, \tag{5.61}$$

is obtained where the trigonometric polynomial

$$P_1(b,a) = \sum_{m=0}^{L_2-1} \sum_{n=0}^{M-1} d_{mM_2,nL} e^{2\pi i(an/M - bm/L_2)}, \quad M_2 = RSM, \quad L = RSL_2,$$

that is defined over the integer undersampling subgroup $M_2Z/N \times LZ/N$ is periodic over its dual, $MZ/N \times L_2Z/N$. If equation (5.61) is multiplied by G^* and is then periodized over $MZ/N \times L_2Z/N$,

$$F_1(b,a)G^*(b,a) = |G(b,a)|^2 P_1(b,a), \quad a,b \in Z/N, \tag{5.62}$$

while for $M_2 = RSM$, $L = RSL_2$, and $a,b \in Z/N$

$$\begin{aligned} &\sum_{r=0}^{L-1} \sum_{s=0}^{M_2-1} F_1(b + sL_2, a + rM)G^*(b + sL_2, a + rM) \\ &\qquad = \sum_{r=0}^{L-1} \sum_{s=0}^{M_2-1} |G(b + sL_2, a + rM)|^2 P_1(b,a). \end{aligned} \tag{5.63}$$

However, if the periodization is only over L_2Z/N of $MZ/N \times L_2Z/N$, the product function F_1G^* becomes

$$\sum_{s=0}^{M_2-1} F_1(b + sL_2, a)G^*(b + sL_2, a) = \sum_{s=0}^{M_2-1} |G(b + sL_2, a)|^2 P_1(b,a), \tag{5.64}$$

which is periodized with respect to the frequency variable.

Recall that the Weyl-Heisenberg expansion of a signal $f \in L(g, M_1, L_1)$ is

$$f(a) = \sum_{m=0}^{L_1-1} \sum_{n=0}^{M_1-1} c_{mM_1,nL_1} g(a - mM_1) e^{2\pi i an/M_1}, \quad a \in Z/N,$$

over the critically sampled Weyl-Heisenberg system (g, M_1, L_1). Its Zak space formulation is

$$F(b,a) = G(b,a)P(b,a), \quad a,b \in Z/N,$$

over $M_1 Z/N$ of the critical sampling subgroup $M_1 Z/N \times L_1 Z/N$ with the trigonometric polynomial,

$$P(b,a) = \sum_{m=0}^{L_1-1} \sum_{n=0}^{M_1-1} c_{mM_1,nL_1} e^{2\pi i(an/M_1 - bm/L_1)},$$

periodic over $M_1 Z/N \times L_1 Z/N$. Suppose $F = GP$ is multipied by G^* and then periodized over the integer oversampling subgroup $MZ/N \times L_2 Z/N$,

$$F(b,a)G^*(b,a) = |G(b,a)|^2 P(b,a), \quad a,b \in Z/N,$$

while for $M_2 = RSM$, $L = RSL_2$, and $a,b \in Z/N$

$$\sum_{r=0}^{L-1} \sum_{s=0}^{M_2-1} F(b + sL_2, a + rM)G^*(b + sL_2, a + rM) \tag{5.65}$$
$$= \sum_{r=0}^{L-1} \sum_{s=0}^{M_2-1} |G(b + sL_2, a + rM)|^2 P(b + sL_2, a + rM);$$

but for $a,b \in Z/N$,

$$F(b,a)G^*(b,a) = \frac{1}{M_1}\sum_{m=0}^{L_1-1}\sum_{n=0}^{M_1-1}\langle f, g_{mM_1,nL_1}\rangle e^{2\pi i(an/M_1 - bm/L_1)}$$

with

$$|G(b,a)|^2 = \frac{1}{M_1}\sum_{m=0}^{L_1-1}\sum_{n=0}^{M_1-1}\langle g, g_{mM_1,nL_1}\rangle e^{2\pi i(an/M_1 - bm/L_1)}$$

when $f = g$; and

$$\langle f, g_{mM_1,nL_1}\rangle = \sum_{k=0}^{L_1-1}\sum_{l=0}^{M_1-1} c_{kM_1,lL_1}\langle g, g_{(m-kM_1,(n-lL_1}\rangle,$$

where $m \in M_1Z/N$ and $n \in L_1Z/N$. Since $FG^* = |G|^2P$ and $FG^* = |G|^2$ for $f = g$, the periodization of FG^* in both time and frequency over the sampling subgroup $MZ/N \times L_2Z/N$ has consequences in the associated periodizations of $|G|^2P$ and $|G|^2$ with regard to the interrelationship between their coefficient sets. The periodized version of FG^* rewritten in terms of inner products $\langle f, g_{mM_1,nL_1}\rangle$ expressed as the convolution of the Weyl-Heisenberg coefficients c_{mM_1,nL_1} and inner products $\langle g, g_{mM_1,nL_1}\rangle$ has the form

$$\sum_{r=0}^{L-1}\sum_{s=0}^{M_2-1}|G(b+sL_2, a+rM)|^2P(b+sL_2, a+rM)$$
$$= SL\sum_{m=0}^{L_2-1}\sum_{n=0}^{M-1}\left\{\sum_{k=0}^{L_1-1}\sum_{l=0}^{M_1-1} c_{kM_1,lL_1}\langle g, g_{(mS-kM_1,(nR-lL_1}\rangle\right\}e^{2\pi i(an/M - bm/L_2)} \tag{5.66}$$

with $M = RSM$, $L = RSL_2$, and $a, b \in Z/N$. However, the periodized FG^* expressed in terms of the coefficients of inner products $\langle f, g_{mM_1,nL_1}\rangle$ is

$$\sum_{r=0}^{L-1}\sum_{s=0}^{M_2-1} F(b+sL_2, a+rM)G^*(b+sL_2, a+rM) \tag{5.67}$$
$$= SL\sum_{m=0}^{L_2-1}\sum_{n=0}^{M-1} \langle f, g_{mM_2,nL}\rangle e^{2\pi i(an/M - bm/L_2)}, \quad a,b \in Z/N.$$

Consequentially,

$$\sum_{r=0}^{L-1}\sum_{s=0}^{M_2-1} |G(b+sL_2, a+rM)|^2 \tag{5.68}$$
$$= SL\sum_{m=0}^{L_2-1}\sum_{n=0}^{M-1} \langle g, g_{mM_2,nL}\rangle e^{2\pi i(an/M - bm/L_2)}$$

for $f = g$ and $a,b \in Z/N$. Therefore, it is clear that the simultaneous time and frequency periodization over integer oversampling subgroup $MZ/N \times L_2Z/N$ results in the simultaneous frequency and time decimation over the undersampling subgroup $M_2Z/N \times LZ/N$.

Suppose the trigonometric polynomial $P_1 \in L(Z/N \times Z/N)$ is periodic over the subgroup $MZ/N \times L_2Z/N$, the product function of P_1 and periodized $|G|^2$ is

$$\sum_{r=0}^{L-1}\sum_{s=0}^{M_2-1} |G(b+sL_2, a+rM)|^2 P_1(b,a) \tag{5.69}$$
$$= SL\sum_{m=0}^{L_2-1}\sum_{n=0}^{M-1}\left\{\sum_{k=0}^{L_2-1}\sum_{l=0}^{M-1} d_{kM_2,lL}\langle g, g_{(m-kM_2,(n-lL}\rangle\right\} e^{2\pi i(an/M - bm/L_2)}$$

with $a,b \in Z/N$.

5.3.2.3 Algorithmic Processes

If $H, K \in L(Z/N \times Z/N)$ are periodic signals in Zak space defined over the integer oversampling subgroup $MZ/N \times L_2 Z/N$ such that

$$K(b,a) = \sum_{r=0}^{L-1} \sum_{s=0}^{M_2-1} |G(b + sL_2, a + rM)|^2 P(b + sL_2, a + rM) \tag{5.70}$$

and

$$H(b,a) = \sum_{r=0}^{L-1} \sum_{s=0}^{M_2-1} |G(b + sL_2, a + rM)|^2, \quad a,b \in Z/N, \tag{5.71}$$

the zero set of H is contained in the zero set of K. Therefore, a trigonometric polynomial $P_1 \in L(Z/N \times Z/N)$ exists that is periodic over $MZ/N \times L_2 Z/N$ and that satisfies the condition

$$K(b,a) = H(b,a)P_1(b,a), \quad a,b \in Z/N. \tag{5.72}$$

Since this statement equates equation (5.66) with equation (5.69),

$$\begin{aligned} &\sum_{k=0}^{L_1-1} \sum_{l=0}^{M_1-1} c_{kM_1, lL_1} \langle g, g_{(mS-kM_1, nR-lL_1)} \rangle \\ &\quad = \sum_{k=0}^{L_2-1} \sum_{l=0}^{M-1} d_{kM_2, lL} \langle g, g_{(m-kM_2, n-lL)} \rangle \end{aligned} \tag{5.73}$$

for $m \in M_2 Z/N$, $n \in LZ/N$, $M_2 = SM_1$, and $L = RL_1$. Moreover, a signal $F_1 \in L(Z/N \times Z/N)$ defined by the formula

$$F_1(b,a) = G(b,a)P_1(b,a), \quad a,b \in Z/N,$$

is a Zak space signal. Additionally, a signal $F - F_1 \in L(Z/N \times Z/N)$ is orthogonal to every Zak space signal of the form GQ, where Q is periodic over $MZ/N \times L_2Z/N$. This means that the inner product of $F - F_1 = G(P - P_1)$ and GQ is zero.

Because Zak space signal F_1 is invertible, its related time signal $f_1 \in L(g, M_2, L)$ is obtainable from it via inverse Zak transformation with respect to the subgroup M_1Z/N of Z/N:

$$f_1(a + rM_1) = \frac{1}{L_1}\sum_{b=0}^{L_1-1} F_1(b,a)e^{-2\pi iab/L_1}, \quad r \in M_1Z/N, \quad a \in Z/N. \tag{5.74}$$

As a consequence of the isometry between Zak space and the signal space, this derivation of f_1 is an orthogonal projection of $f \in L(g, M_1, L_1)$ onto the space $L(g, M_2, L)$.

To apply the orthogonal projection algorithm, start with a signal $f \in L(g, M_1, L_1)$, then

- Compute F and G, the Zak transforms of f and g over the subgroup M_1Z/N of Z/N;
- Compute $P \in L(Z/N \times Z/N)$, a periodic signal over $M_1Z/N \times L_1Z/N$ satisfying the condition $F = GP$;
- Compute the periodizations over $MZ/N \times L_2Z/N$, H and K with

$$H(b,a) = \sum_{r=0}^{L-1}\sum_{s=0}^{M_2-1} |G(b + sL_2, a + rM)|^2$$

and

$$K(b,a) = \sum_{r=0}^{L-1} \sum_{s=0}^{M_2-1} |G(b + sL_2, a + rM)|^2 P(b + sL_2, a + rM)$$

respectively;

- compute $P_1 \in L(Z/N \times Z/N)$, a periodic signal over $MZ/N \times L_2Z/N$ satisfying the condition $K = HP_1$; and
- Compute $F_1 = GP_1$.

The inverse Zak transform of F_1 over M_1Z/N is the orthogonal projection f_1 of f onto the undersampled subspace $L(g, M_2, L)$, contained in the critically sampled subspace $L(g, M_1, L_1)$.

The orthogonal projection algorithm applied recursively produces a multiresolution approximations of the signal f. These approximations are orthogonal projections of f onto progressively smaller undersampled subspaces.

5.3.3 Applications

In this section the efficacy of the orthogonal projection algorithm is demonstrated. It is shown that this projection algorithm is an effective data compression tool with potential signal enhancement capability. The orthogonal projection of a Weyl-Heisenberg coefficient set from the critically sampled subspace onto an undersampled subspace results in a subset of the coefficient set that contains values dissimilar to those on the corresponding subset of the

critically sampled subspace. Additionally, it is shown that merely decimating a Weyl-Heisenberg coefficient set does not lead to an orthogonal projection of the signal as is the case in Fourier analysis. This is a consequence of the orthogonality condition of the set of basis signals. The set of basis signals for the Weyl-Heisenberg expansion of a signal is generally nonorthogonal while the set of basis signals for the Fourier series expansion is orthogonal. Therefore, the usual Fourier analysis techniques of periodization and decimation do not apply in Weyl-Heisenberg signal expansion.

The following two sets of experiments are designed to show that the orthogonal projection algorithm for Weyl-Heisenberg expanded signals is efficient. Because the orthogonal projection signal on the undersampled subspace retains many of the key properties of the original signal appropriately conditioned with the proper window signal, the change experienced in the decimated coefficient subset values caused by the projection algorithm can be viewed as a form of signal enhancement of the compressed signal. The signals investigated in the experiments are well-known and belong to a well-documented class of sophisticated signals commonly used in time-frequency signal analysis. They include the class of transients [224, 225, 296] and the chirp modulated with a gaussian envelope [51]. The three window signals used to create the required sets of basis signals for the Weyl-Heisenberg expansion of each of the studied signals are the one-sided exponential, gaussian, and triangular pulse. Each of these windows constitutes a single-window signal as opposed to a multiwindow signal, which could have been used in some of the cases. Multiwindow signals are especially useful for Weyl-Heisenberg representations of multicomponent signals. An implication of these data compression

experiments relates to the transmission of information on sufficiently noisy channels. In these situations, data compression at the receiver can be performed on the received information that is extracted from the least noisy acceptable decimated subset.

In the experiments performed, H and K of the orthogonal projection algorithm are periodized only in frequency instead of in both time and frequency. Therefore, the corresponding Weyl-Heisenberg coefficient set is decimated in time implying that the orthogonal projection signal is made up of time decimated Weyl-Heisenberg coefficients.

5.3.3.1 Experiments

In the experiments, the general form of the class of transients [224] was

$$f(t) = \sum_{i=0}^{2} a_i e^{-b_i(t-\tau_i)} \sin[2\pi v_i(t-\tau_i) + \phi_i] u(t-\tau_i), \quad t \in [0, 16),$$

where the amplitudes $a = \{0.5, 0.6, 0.9\}$, damping coefficients $b = 0.5$, arrival times $\tau = \{1, 5, 11\}$, frequencies $v = \{0, 1, 7\}$, and phases $\phi = \{\pi/2, 0, 0\}$.

The formula for the chirp modulated with a gaussian envelope was

$$f(t) = e^{-\pi t^2 \cdot i\pi t^2 \cdot 24i\pi t}, \quad t \in [-8, 8),$$

where the average frequency for a given time is 12 and the instantaneous frequency is $\pi t + 12$. These two types of signals were compressed by a factor of four using the orthogonal projection algorithm.

The window signals used to condition the set of transients and the modulated chirp were each defined on the time interval $t \in [-8, 8)$. They are the 1-sided exponential,

$$g(t) = e^{-0.5t}u(t),$$

gaussian,

$$g(t) = e^{\pi t^2},$$

and the triangular pulse,

$$g(t) = \begin{cases} 1 - |t|, & |t| < 1 \\ 0, & 1 < |t| < 8. \end{cases}$$

Each signal and each window was discretely represented with $N = 240$ uniform samples.

In each experiment, the number of time samples, M, in the Zak transform was chosen to be an odd number, 15, to avoid the occurrence of zeros in the Zak transform of the windows. The number of frequency samples L was chosen to be 16. As previously mentioned, to compress the

signal by means of the orthogonal projection algorithm in Zak space, the projection was done only in frequency. Also, a nonorthogonal projection was performed wherein the Weyl-Heisenberg coefficient set on the critically sampled subspace was appropriately inserted with zeros corresponding to the zero set produced by the projection algorithm in the decimated coefficient set on the undersampled subspace. In either type of projection, the Weyl-Heisenberg coefficient set of 240 values on the critically sampled subspace was decimated in time by four to produce a coefficient set of 60 values on the relevant undersampled subspace. The frequency parameter L was reduced from $L = 16$ to $L = 4$. In figures 5.14a-f, figures 5.15a-e, and figures 5.16a-e, the signal of transients is shown with the respective previously specified window signals: 1-sided exponential, gaussian, and triangular pulse. In each case, the nonorthogonal projection produced a compressed projection signal of negligible magnitude; the corresponding error signals are essentially equal to the signal of transients. The orthogonal projection algorithm applied to the signal of transients with the gaussian and the triangle window signals produced compressed orthogonal projection signal that are essentially the same as shown in figure 5.15d and figure 5.16b; they are dissimilar to the projected signal of transients. However, with the -sided exponential window signal, the produced orthogonal projection signal bears a strong resemblance to the projected signal; but as shown in figure 5.14c, it appeared to have shifted to the left with its magnitude reduced by about a half. Moreover, the Weyl-Heisenberg coefficient sets corresponding to the signal of transients and its orthogonal projections are found in figure 5.14e for the 1-sided exponential window, whereas they are found in figure 5.15d and figure 5.16d for the gaussian and triangle windows respectively. These figures reflect and confirm the degree of similarity between the signal of transients under different windowing conditions and

its orthogonal projections. For the case of the 1-sided exponential window, the signal of transients' Weyl-Heisenberg coefficient set closely resembles its orthogonal projection signal's sub-critical Weyl-Heisenberg coefficient set.

In the experiment with the modulated chirp, the 1-sided exponential, gaussian, and triangle window signals were again used. These window signals had the same parameters as in the case of the signal of transients and were used in the same sequence. Thus, they were not repeated in the supporting set of figures: figures 5.17a-e (1-sided exponential), figures 5.18a-d (gaussian), and figures 5.19a-d. Figure 5.17a shows the chirp signal modulated with a gaussian envelope and its Zak transform. For each window used, the nonorthogonal projection signal's magnitude is negligibly small, of the order of 10^{-3}, while each corresponding nonorthogonal projection error essentially equals the modulated chirp in magnitude but not in phase. Using the orthogonal projection algorithm and relative to the gaussian amplitude modulated chirp (figure 5.17a), the orthogonal projection signal (figure 5.17b) obtained from the orthogonal projection of the modulated chirp with the 1-sided exponential window does not bear a strong resemblance to the modulated chirp compared to the orthogonal projection signals (figure 5.18a and figure 5.19a) obtained from the modulated chirp with the gaussian and triangle windows respectively. These two latter projection signals are quite similar, especially in their coefficient sets shown in figure 5.18c and figure 5.19c. However, the projection signal (figure 5.18a) obtained from the modulated chirp with a gaussian window more strongly resembles the modulated chirp in magnitude and phase.

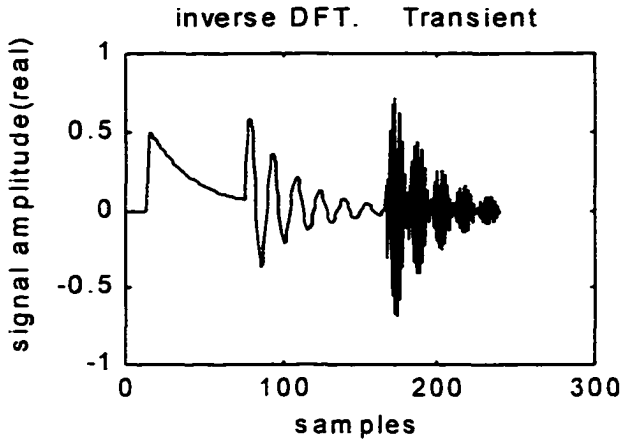

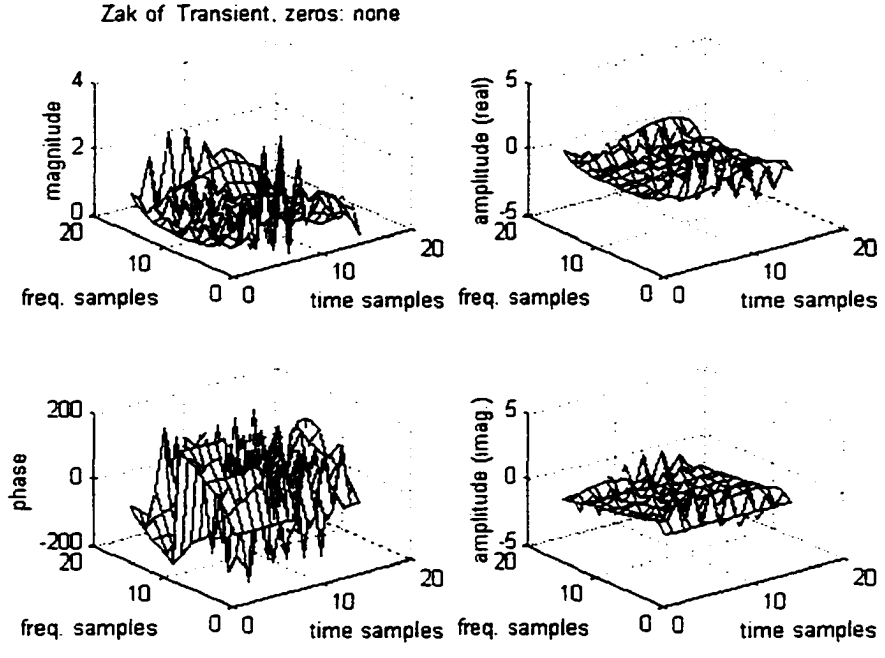

Figure 5.14a. Signal of three transients and its Zak transform.

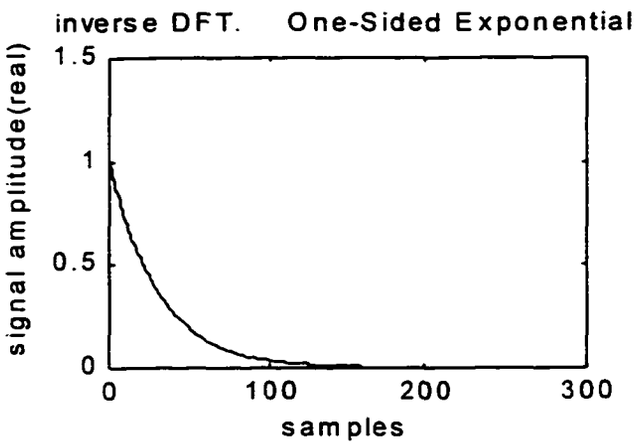

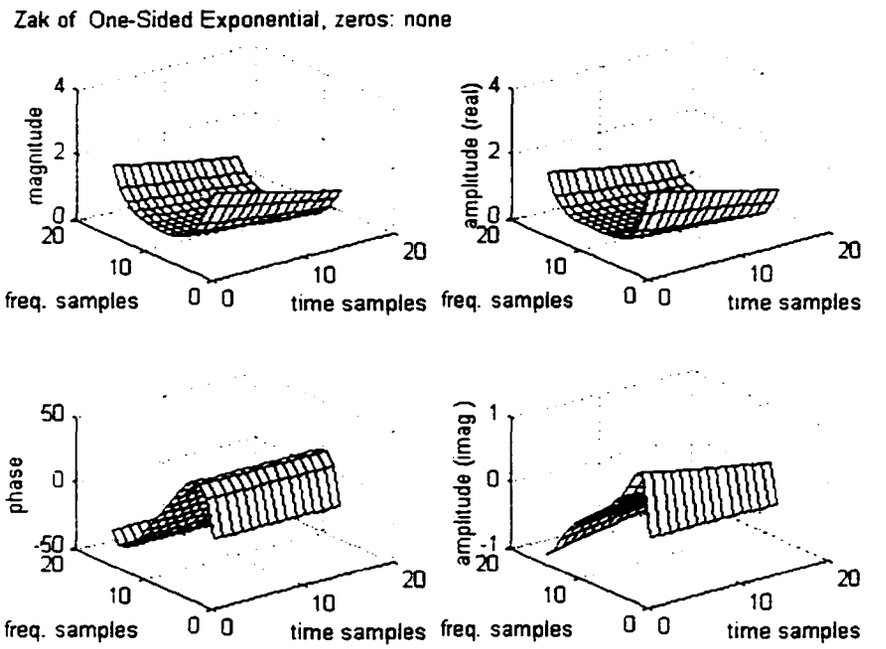

Figure 5.14b. 1-sided exponential window signal and its Zak transform.

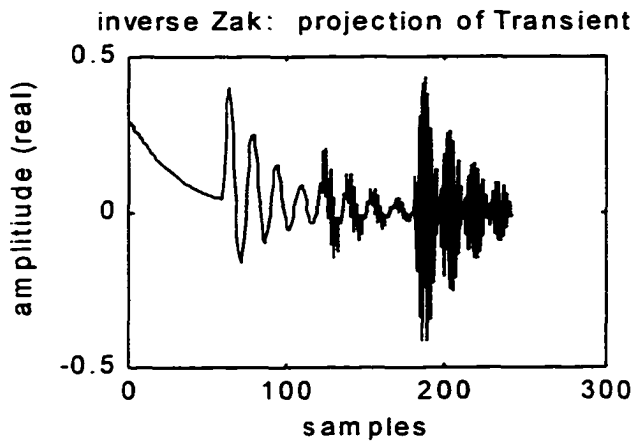

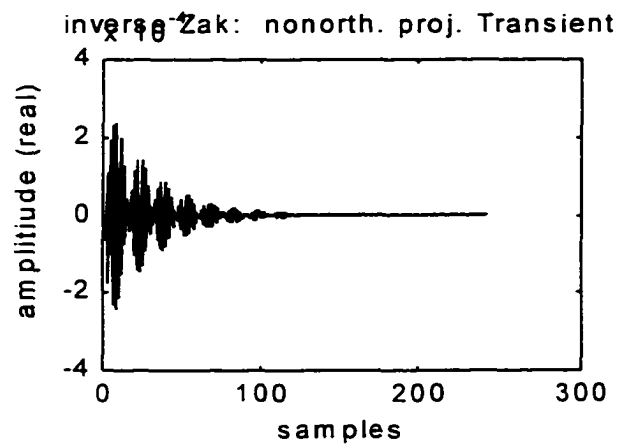

Figure 5.14c. Orthogonal and nonorthogonal projections of transient set.

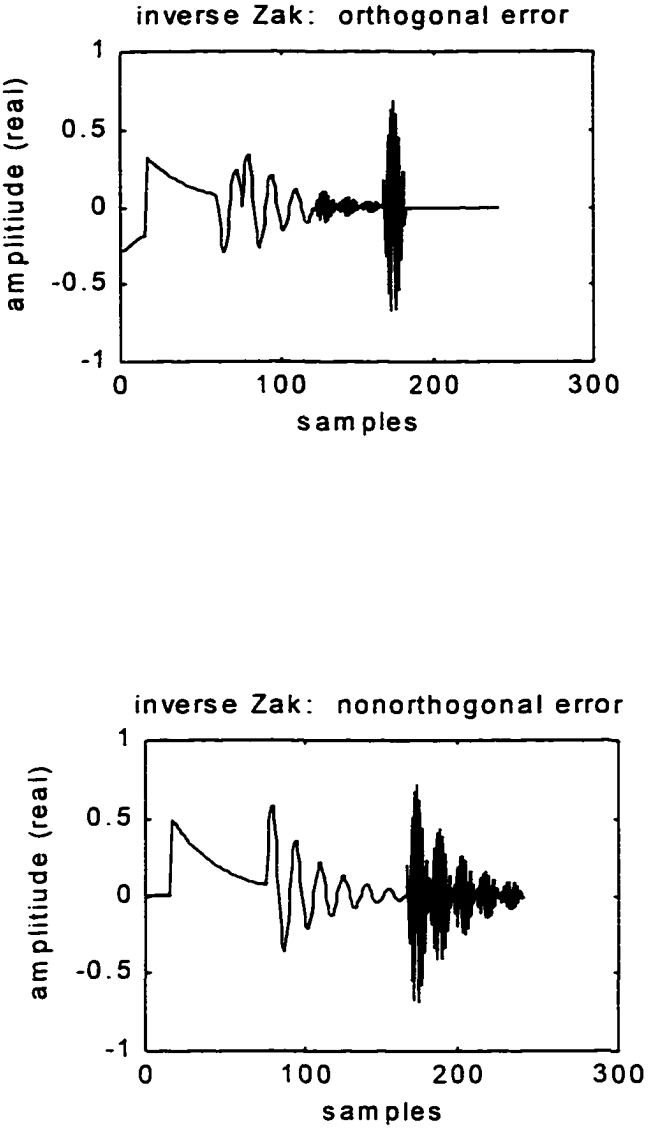

Figure 5.14d. Errors resulting from the projections in (5.14c).

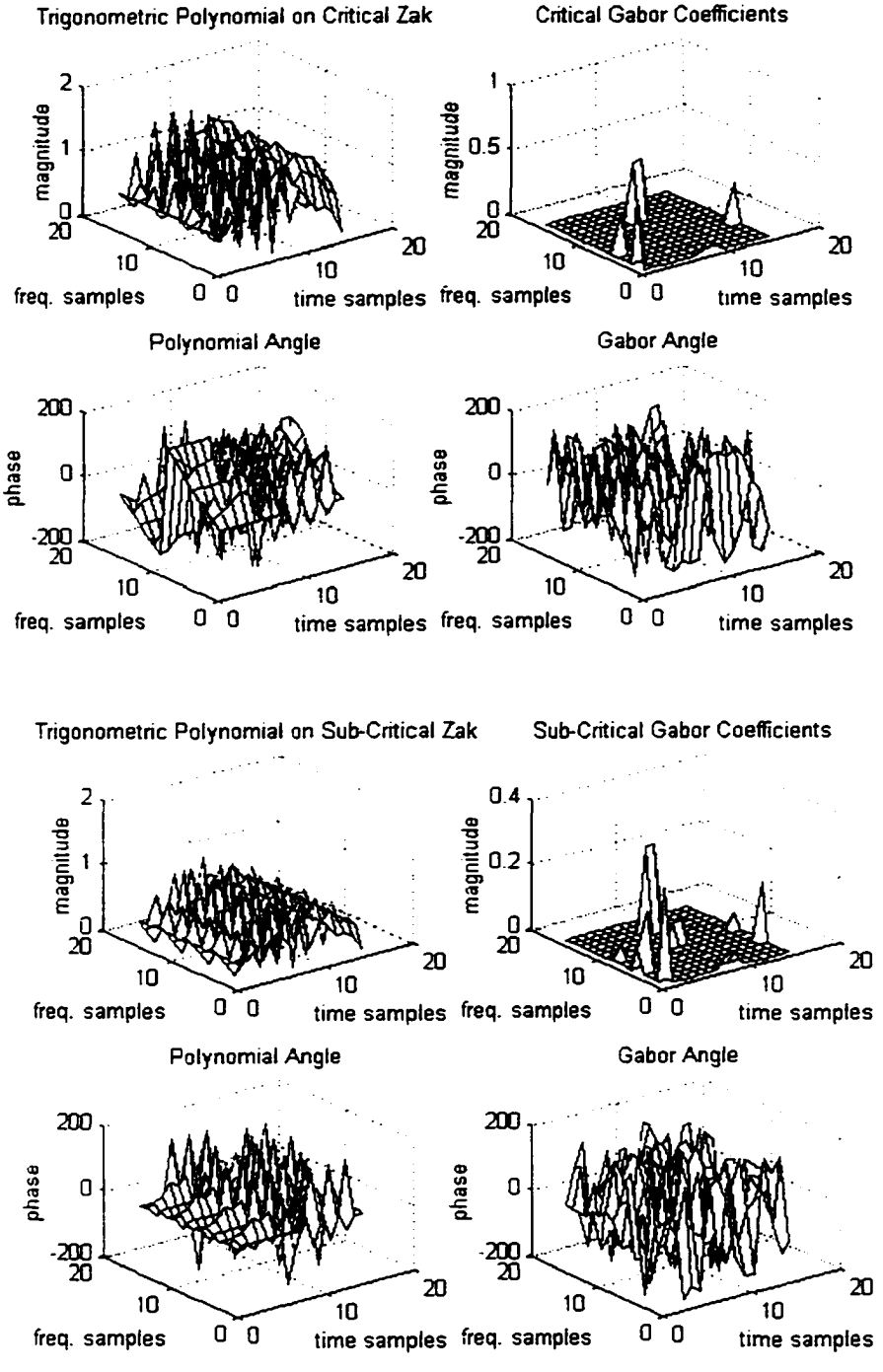

Figure 5.14e. Weyl-Heisenberg coefficient sets of the signal of transients and its orthogonal projection respectively, and their related trigonometric polynomials.

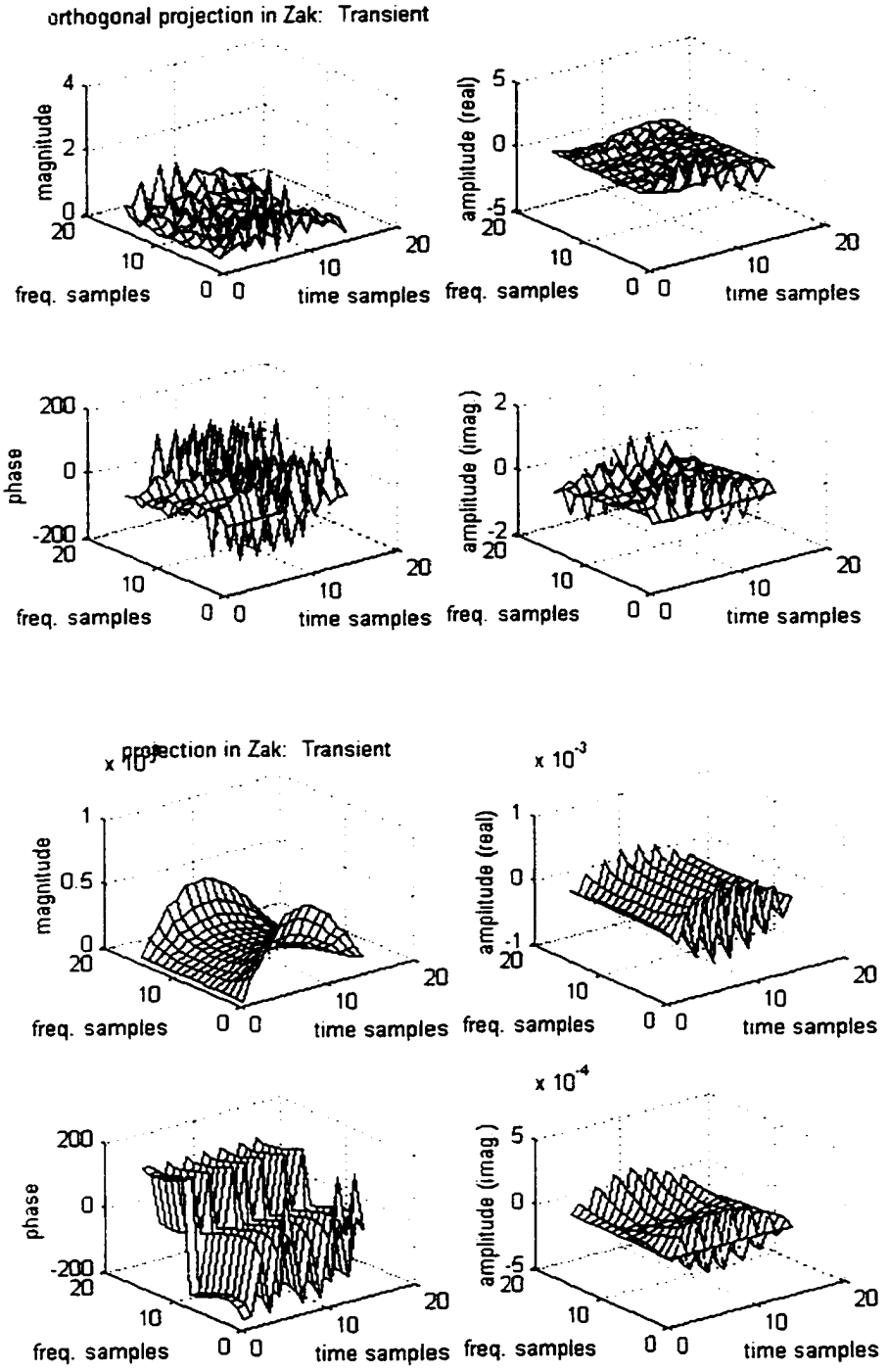

Figure 5.14f. Orthogonal and nonorthogonal projections of transient set in Zak space.

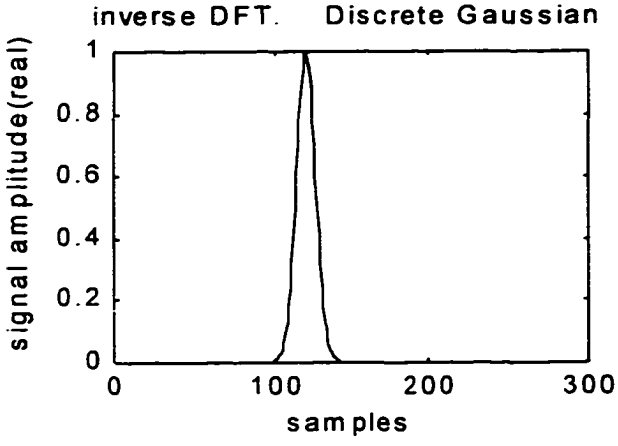

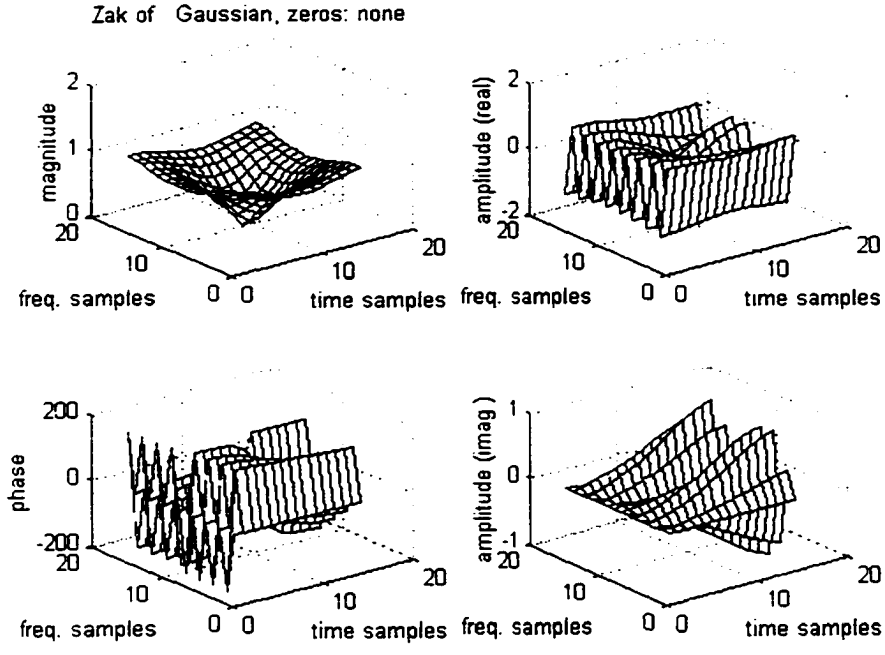

Figure 5.15a. Gaussian window signal and its Zak transform.

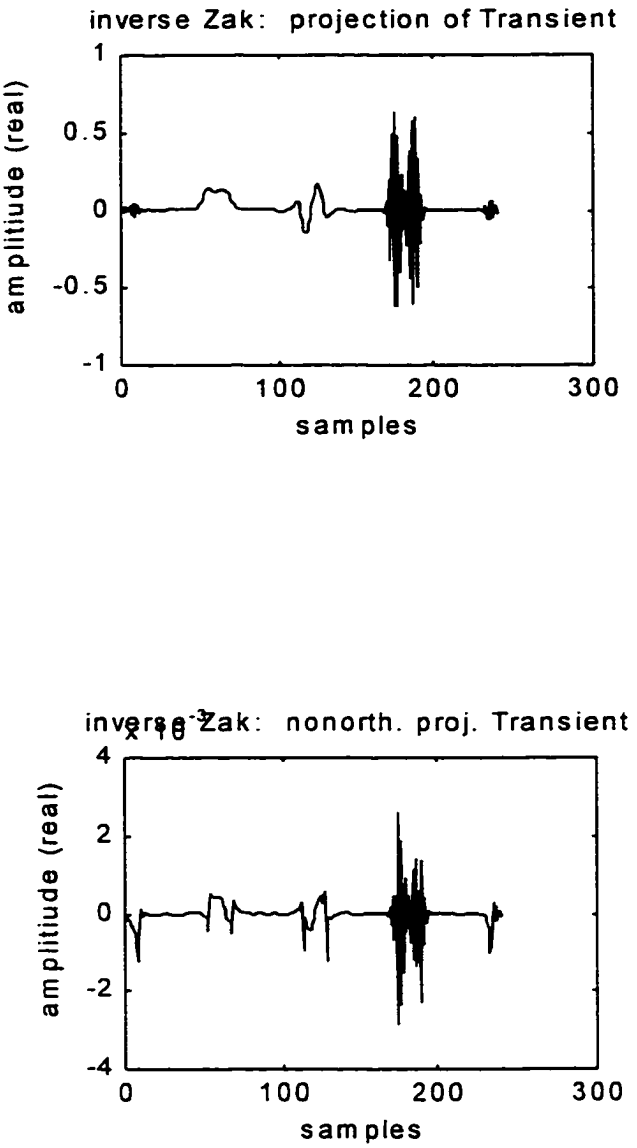

Figure 5.15b. Orthogonal and nonorthogonal projections of transient set conditioned with the gaussian window.

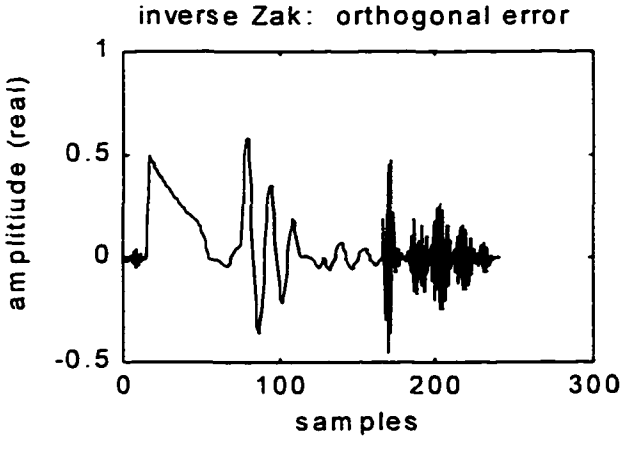

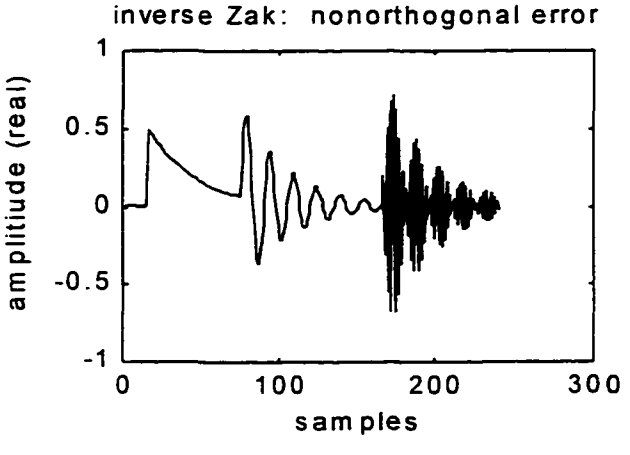

Figure 5.15c. Errors resulting from projections in (5.15b).

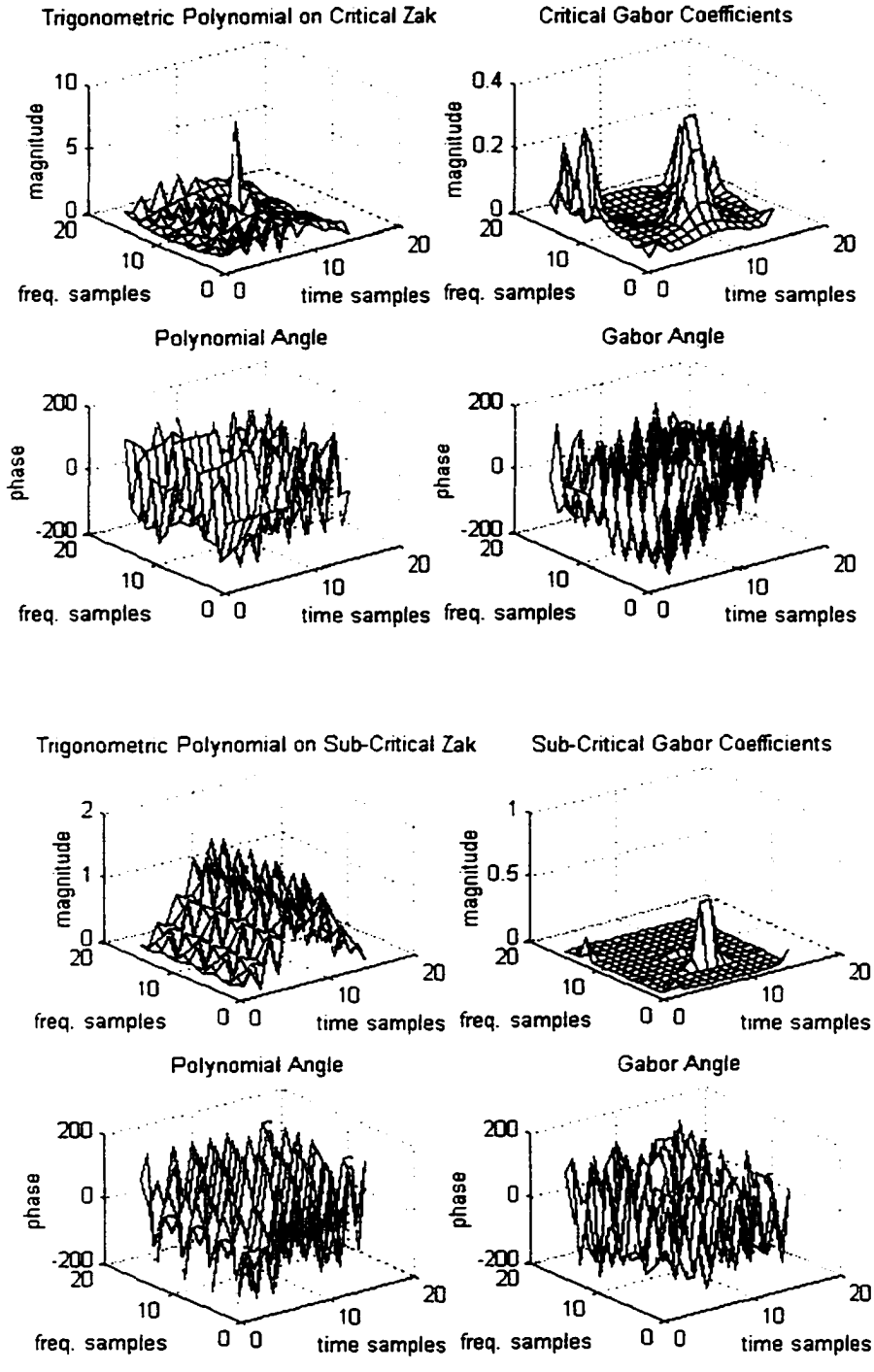

Figure 5.15d. Weyl-Heisenberg coefficient sets of the transient signal set and its orthogonal projection, and their related trigonometric polynomials.

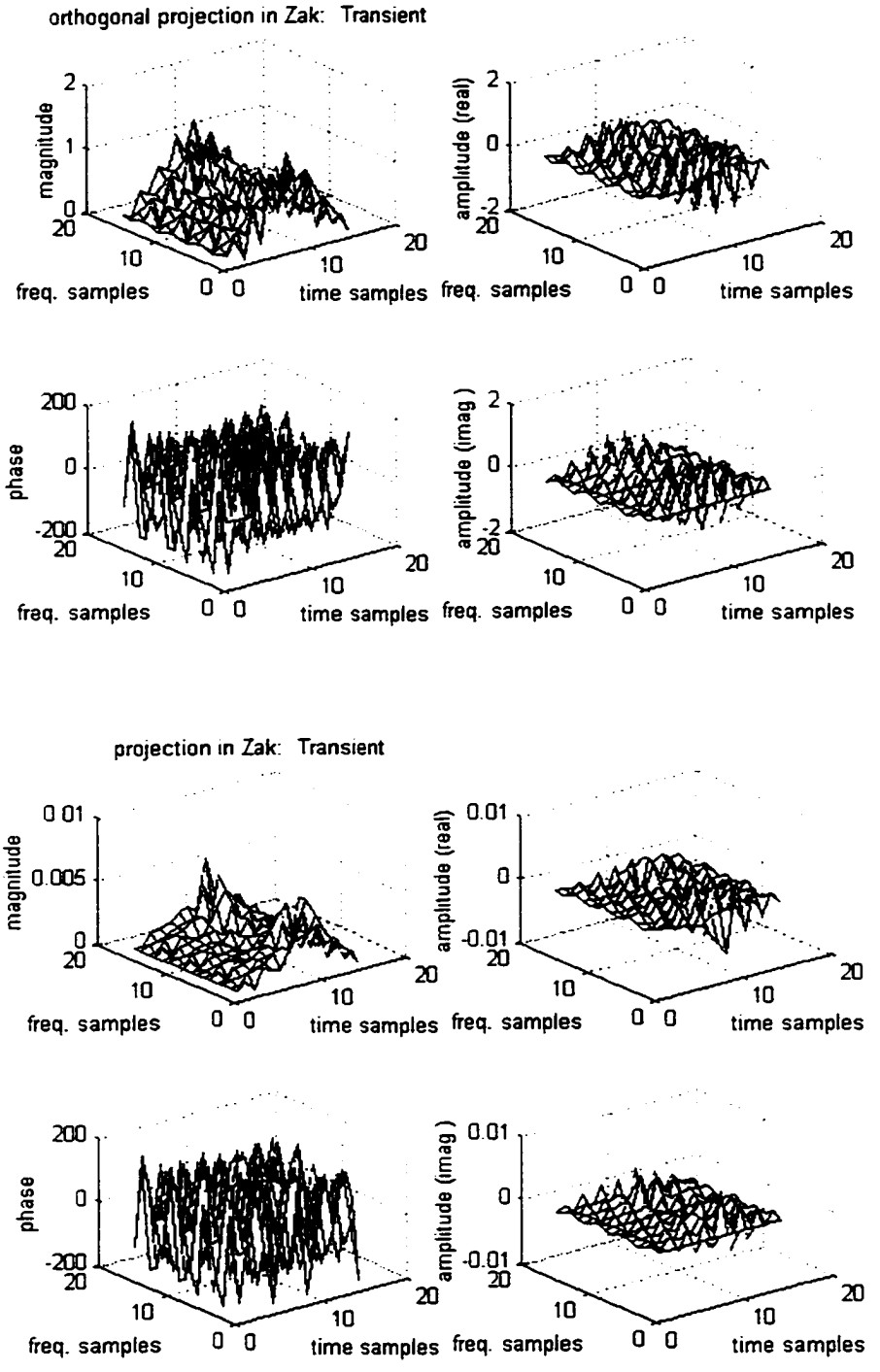

Figure 5.15e. Zak transforms of the respective projection signals in (5.15b).

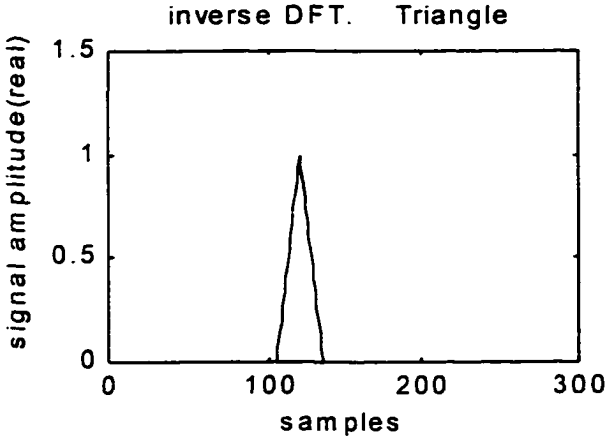

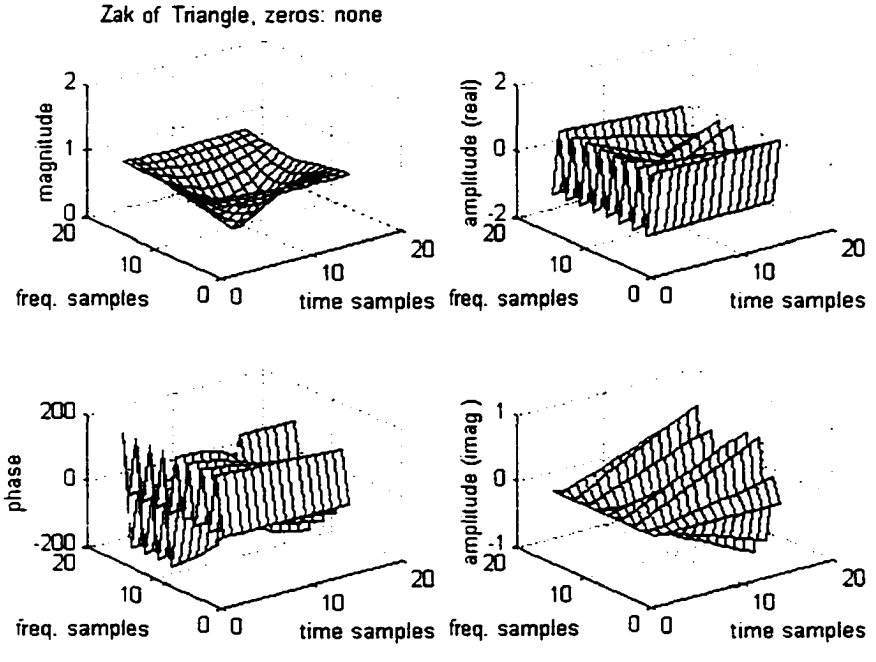

Figure 5.16a. Triangular window signal of unit height and area and its Zak transform.

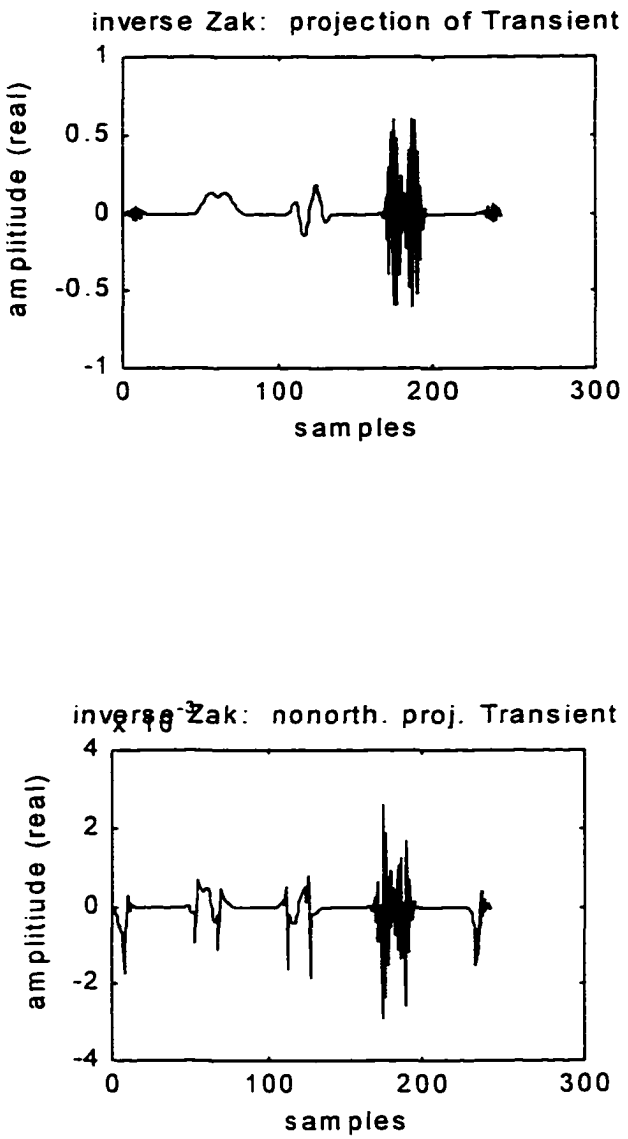

Figure 5.16b. Orthogonal and nonorthogonal projections of transient signal set conditioned with the triangular window.

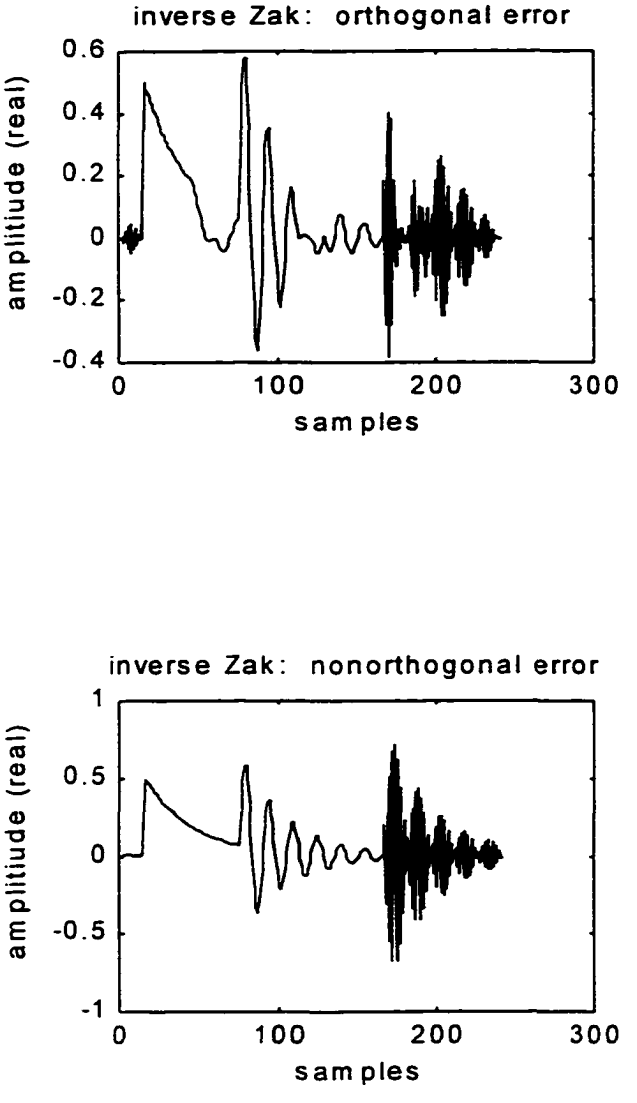

Figure 5.16c. Errors resulting from the respective projection signals in (5.16b).

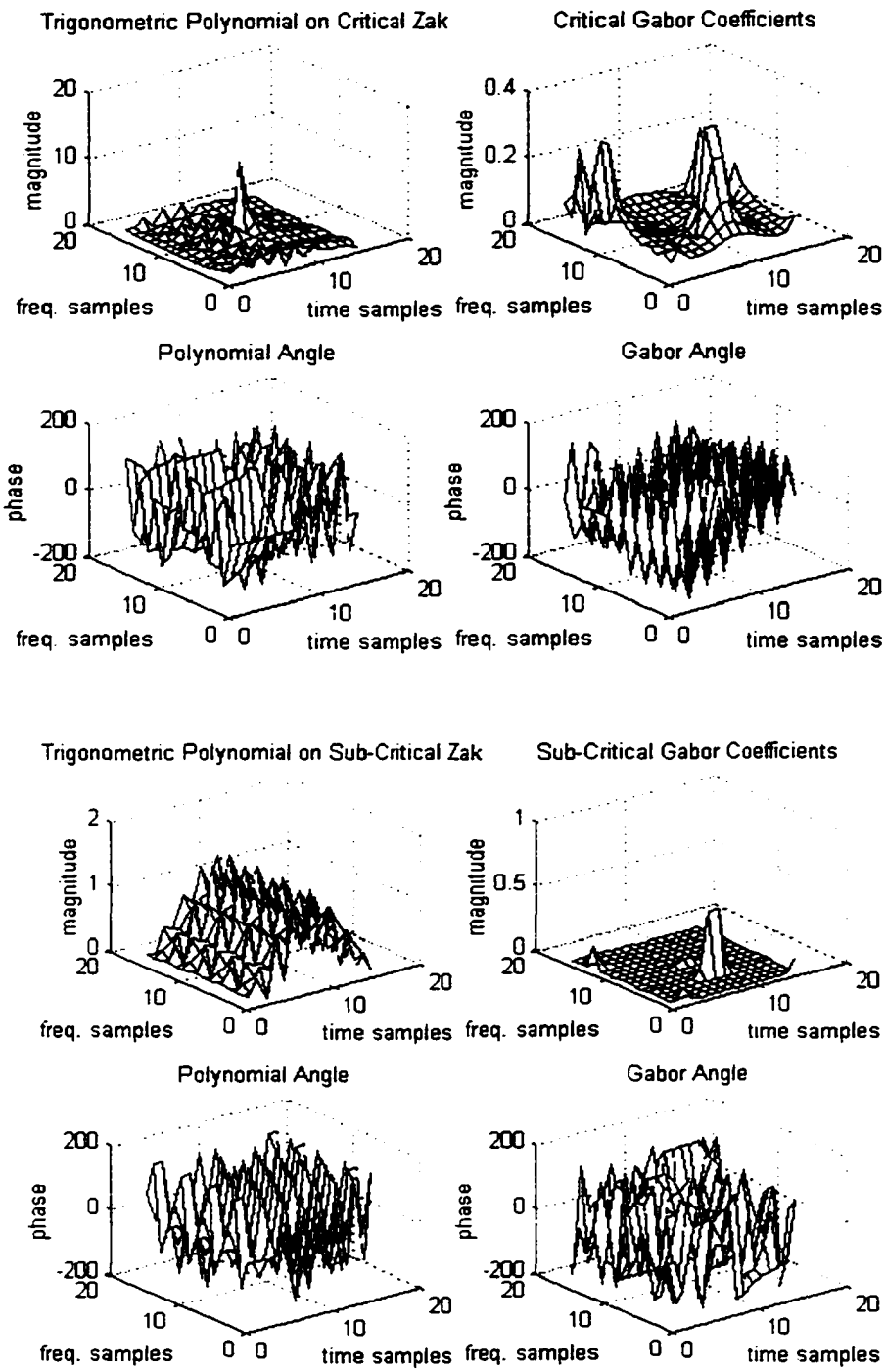

Figure 5.16d. Respective Weyl-Heisenberg coefficient sets for the transient signal set and its orthogonal projection, their related trigonometric polynomials.

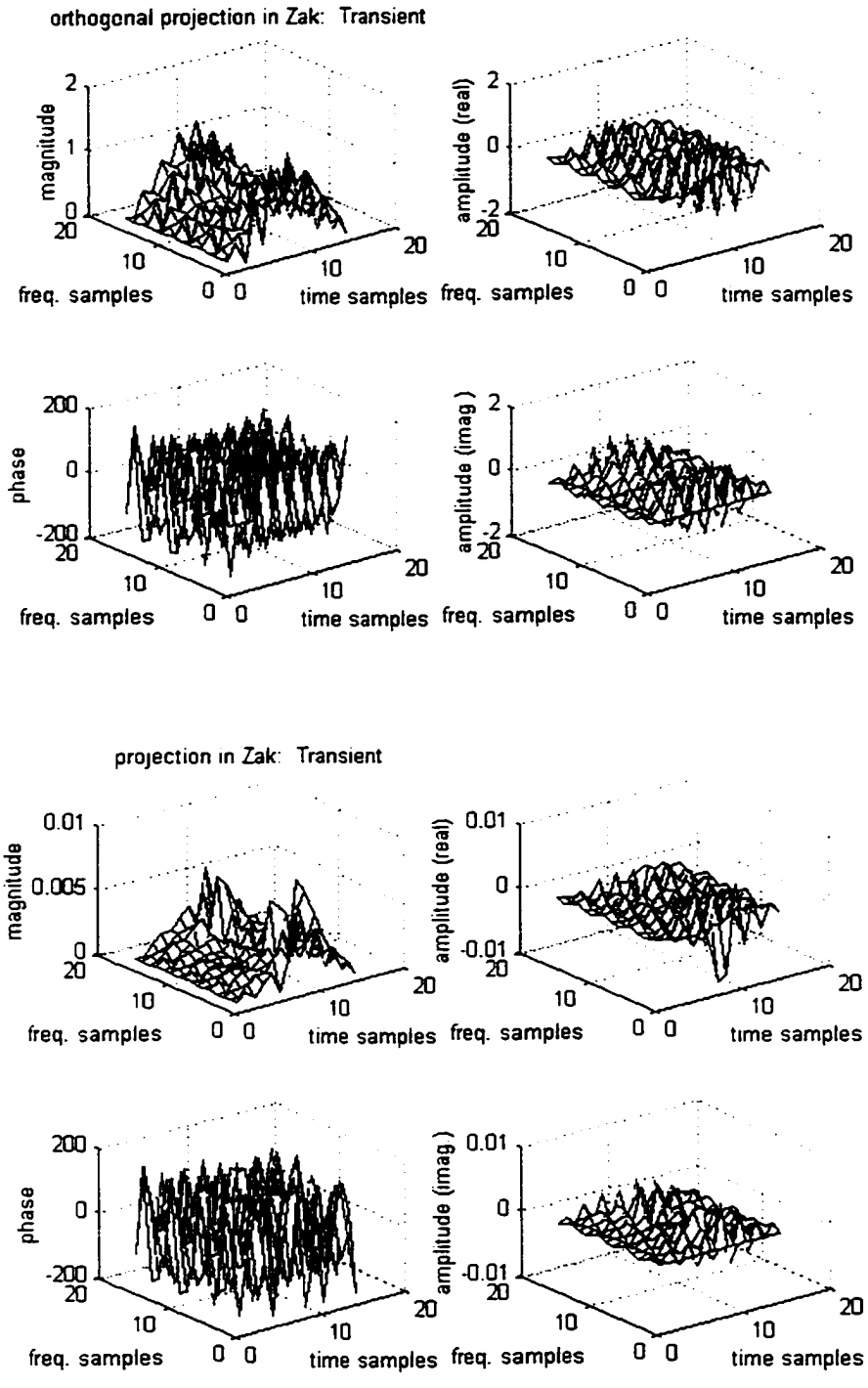

Figure 5.16e. Respective Zak transforms of the projection signals in (5.16b).

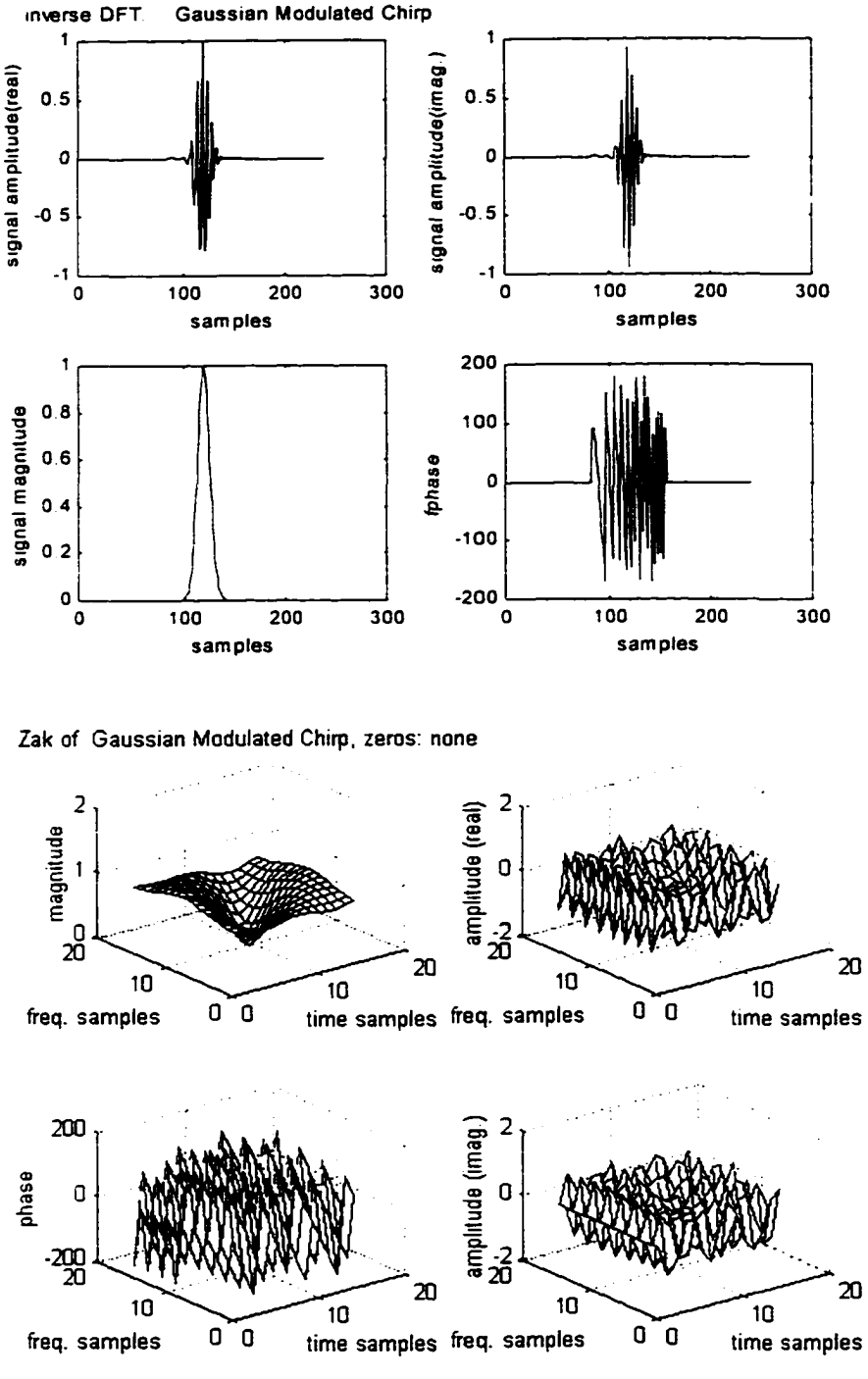

Figure 5.17a. Chirp signal with gaussian envelope and its Zak transform.

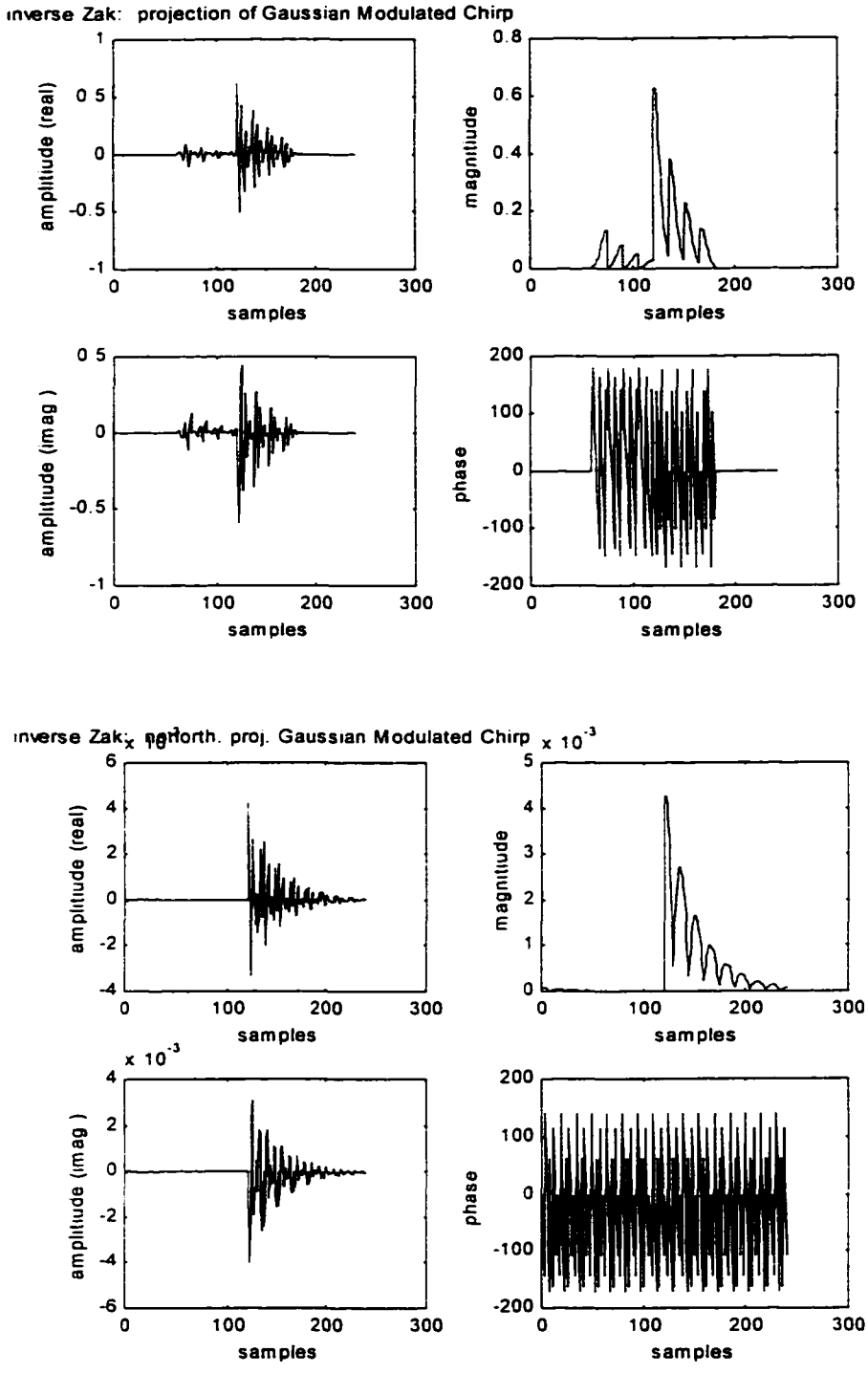

Figure 5.17b. Orthogonal and nonorthogonal projections of the modulated chirp conditioned with the 1-sided exponential of (5.14b).

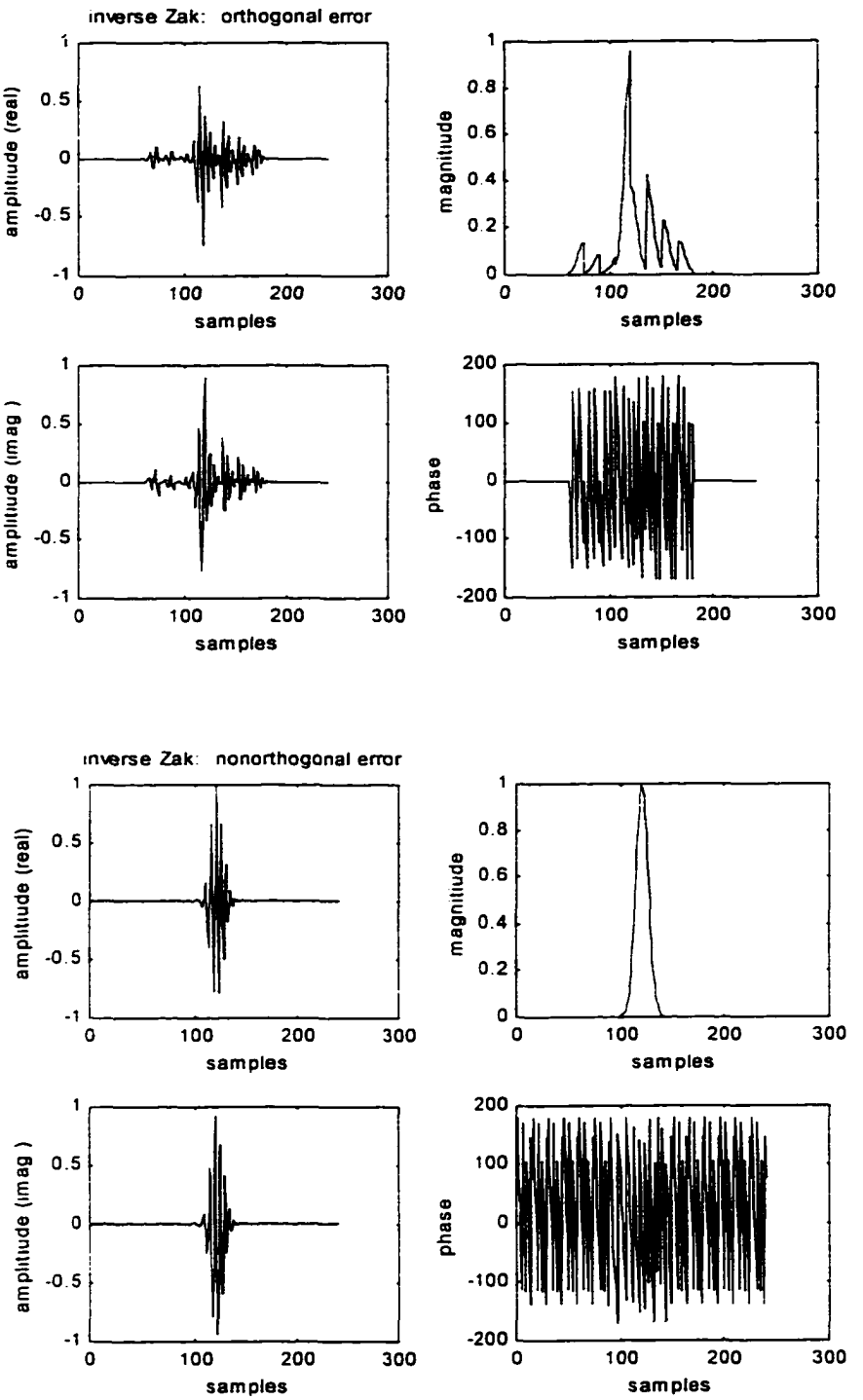

Figure 5.17c. Respective errors resulting from the projections in (5.17b).

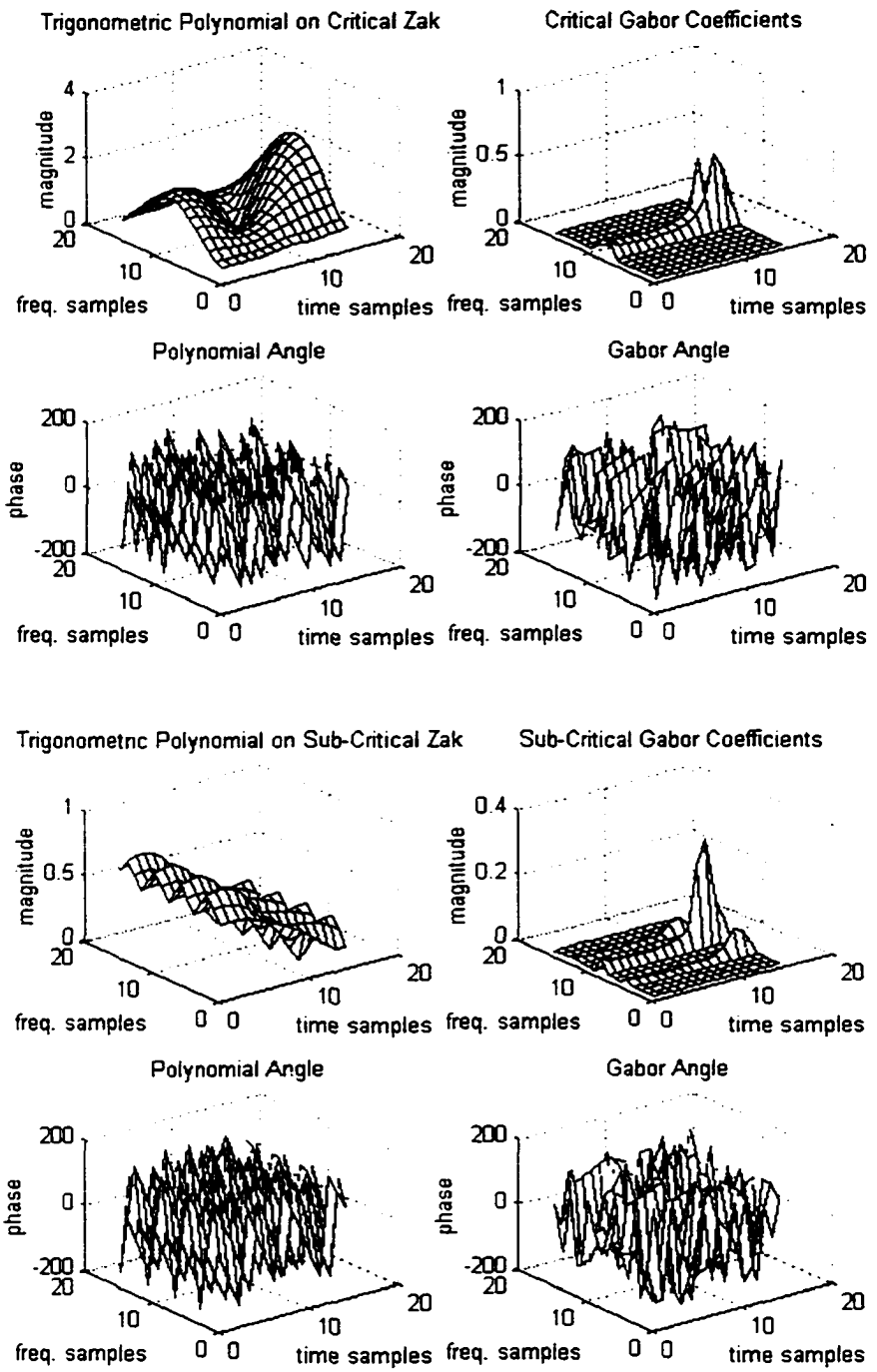

Figure 5.17d. Respective Weyl-Heisenberg coefficient sets of the modulated chirp and its orthogonal projection as well as their related trigonometric polynomials.

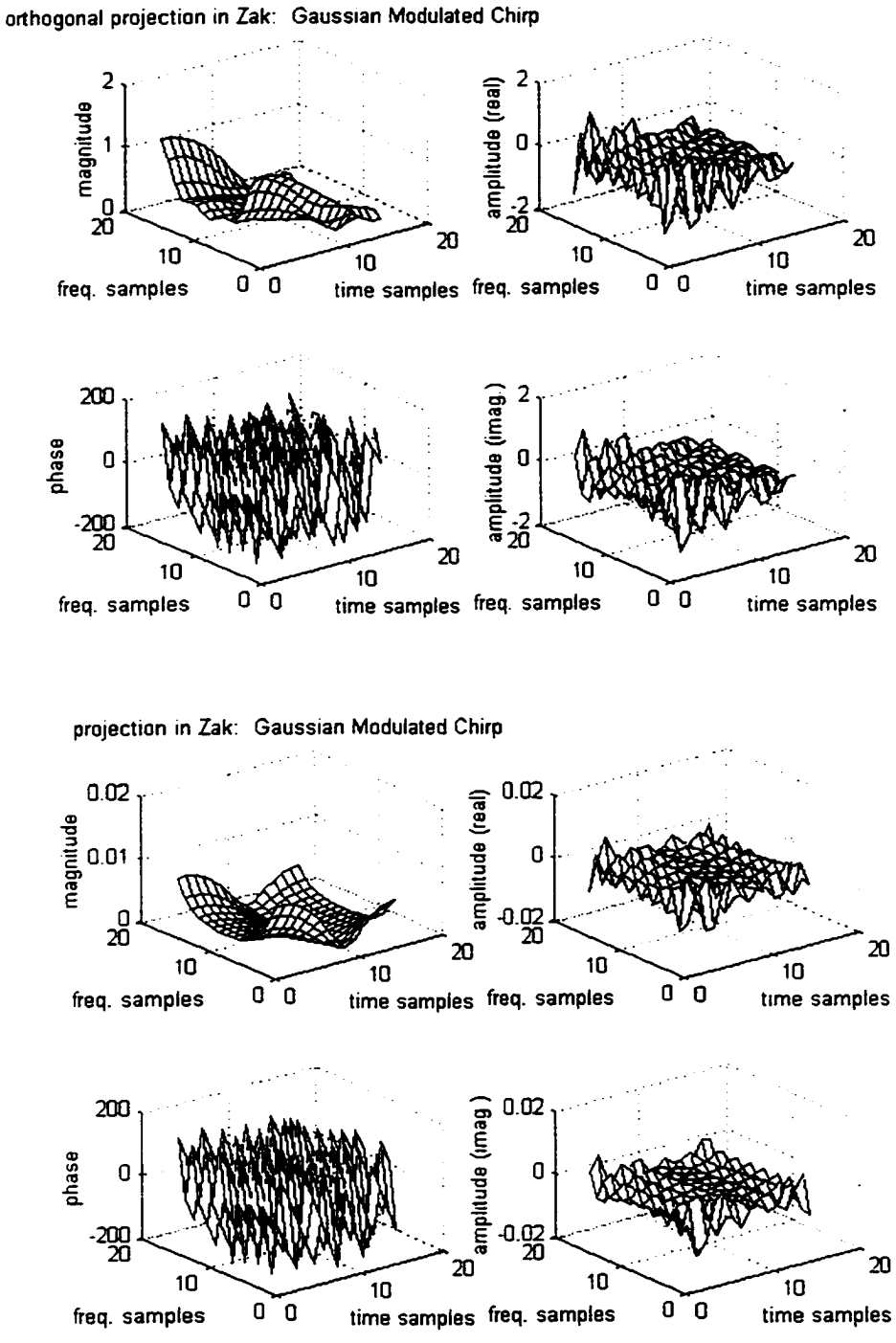

Figure 5.17e. Zak transforms of the respective projection signals in (5.17b).

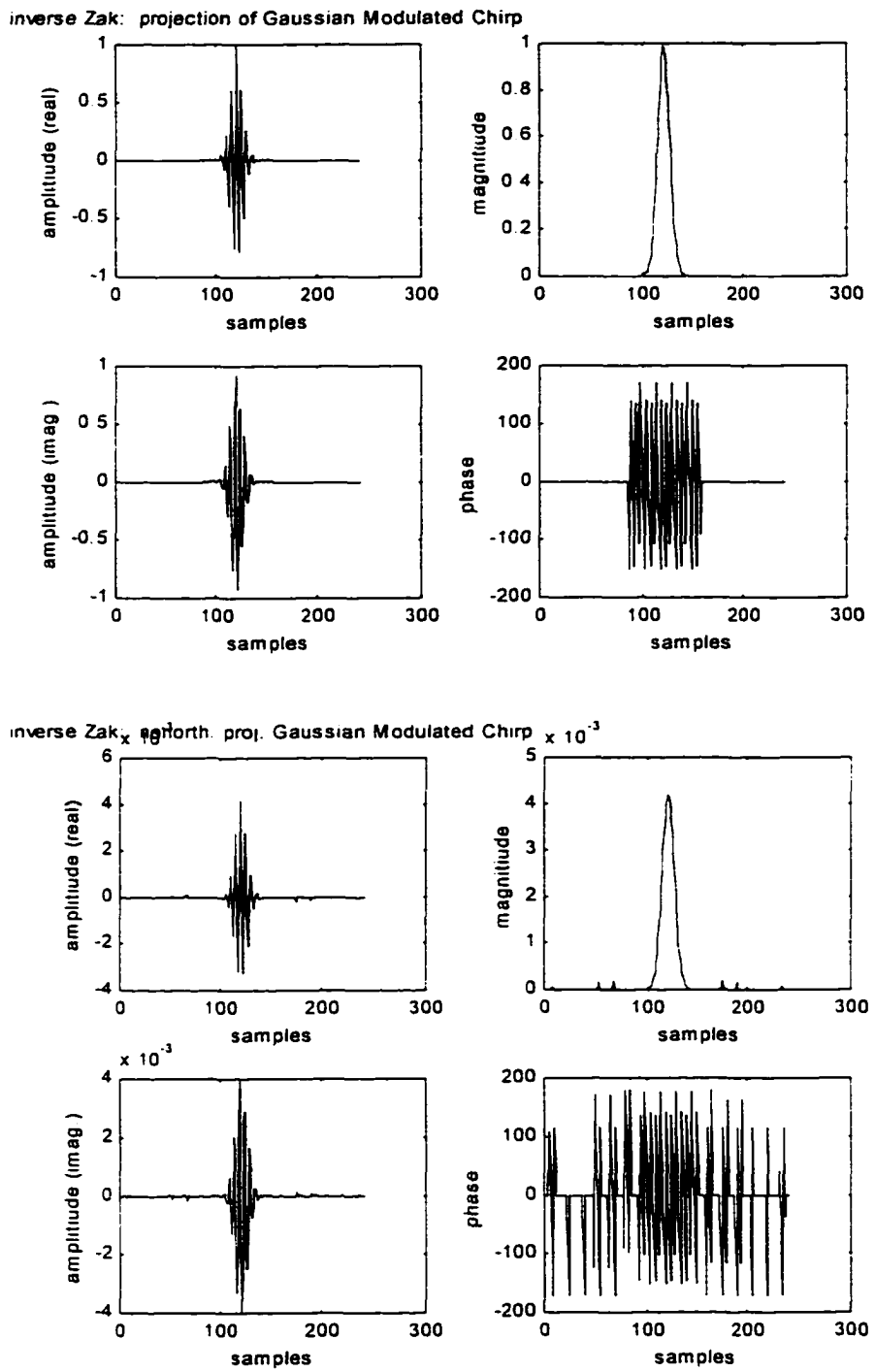

Figure 5.18a. Orthogonal and nonorthogonal projections of the modulated chirp conditioned with the gaussian window of (5.15a).

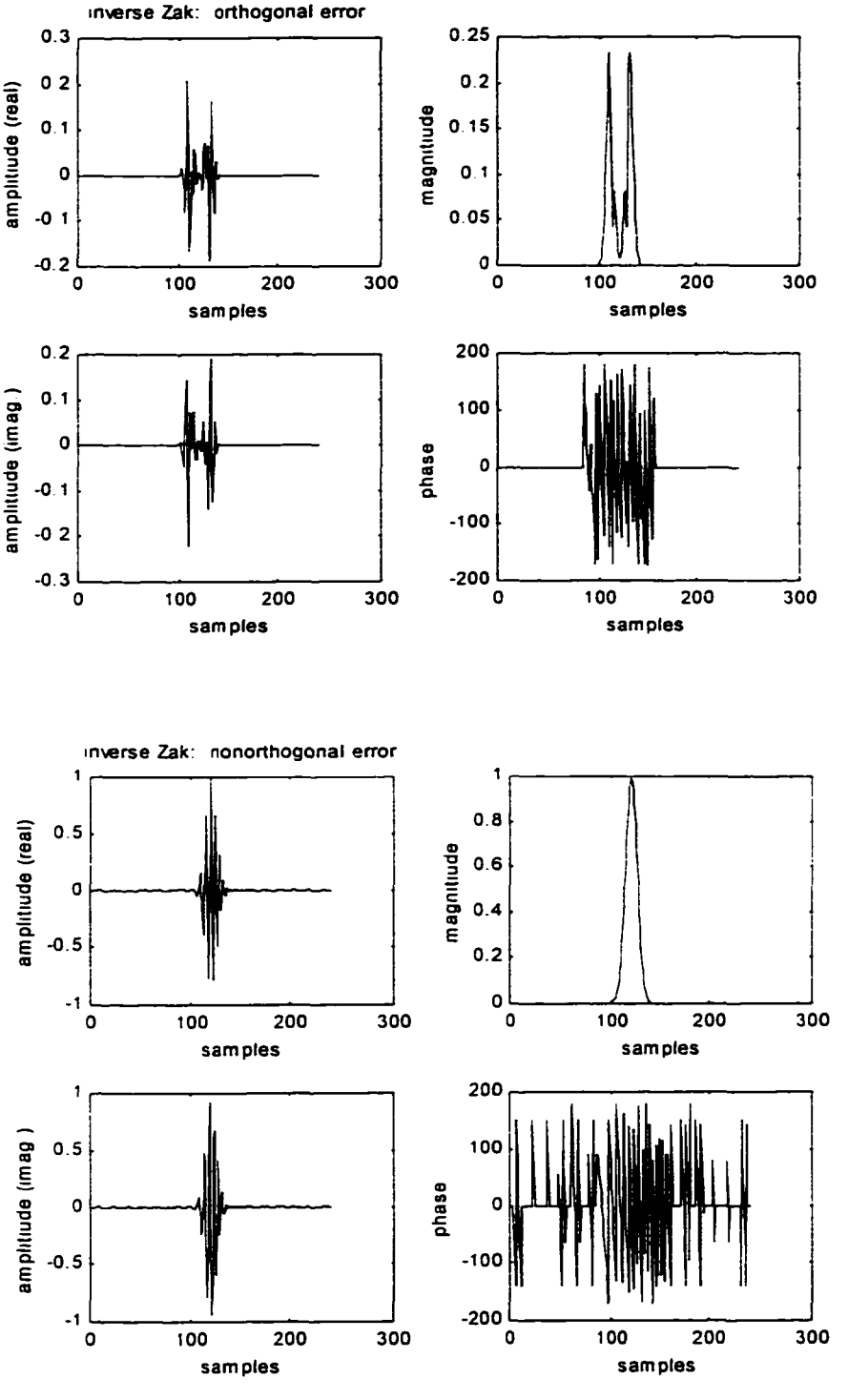

Figure 5.18b. Errors resulting from the respective projections in (5.18a).

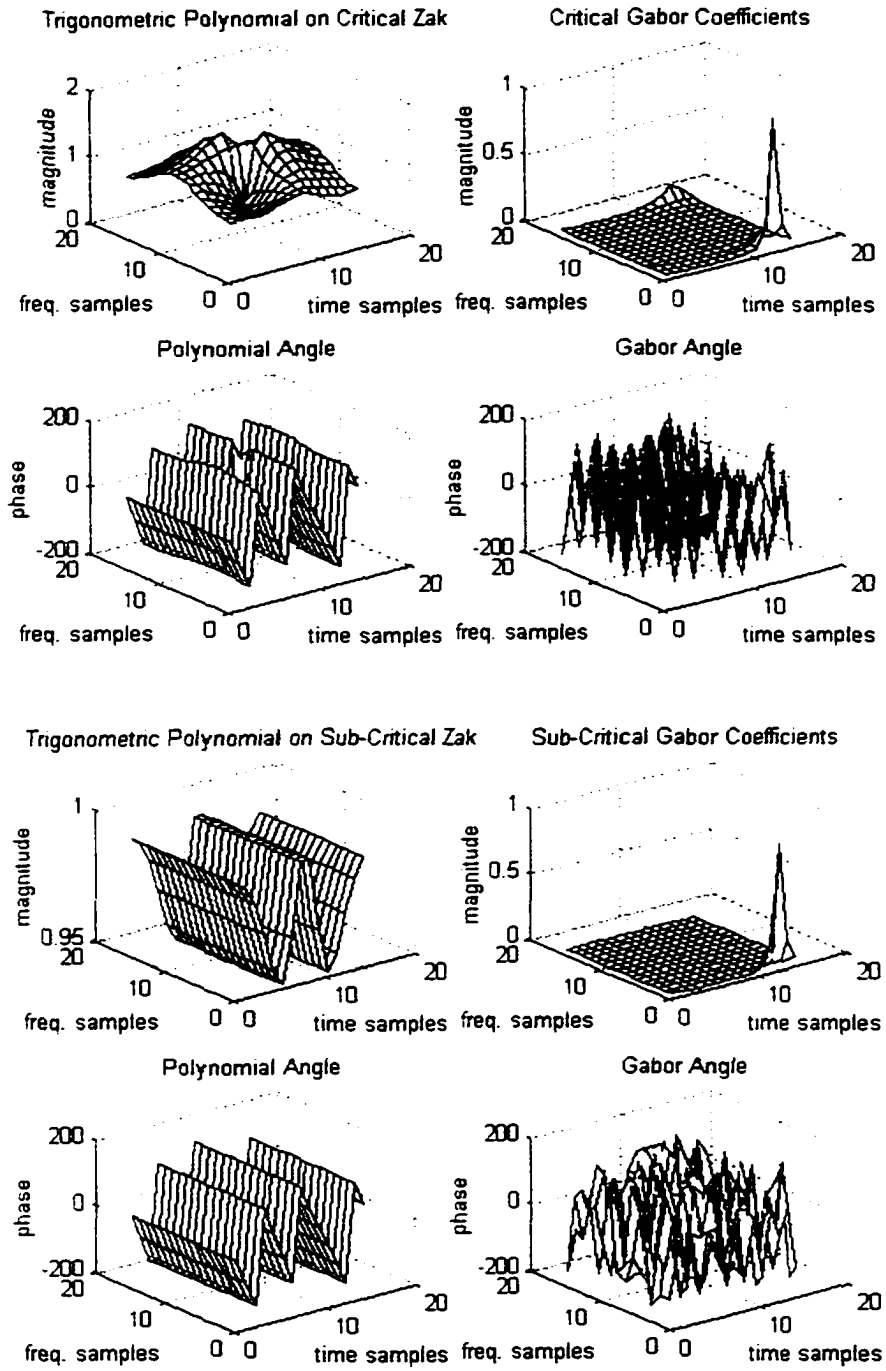

Figure 5.18c. Weyl-Heisenberg coefficient sets of the respective modulated chirp and its orthogonal projection, and their related trigonometric polynomials.

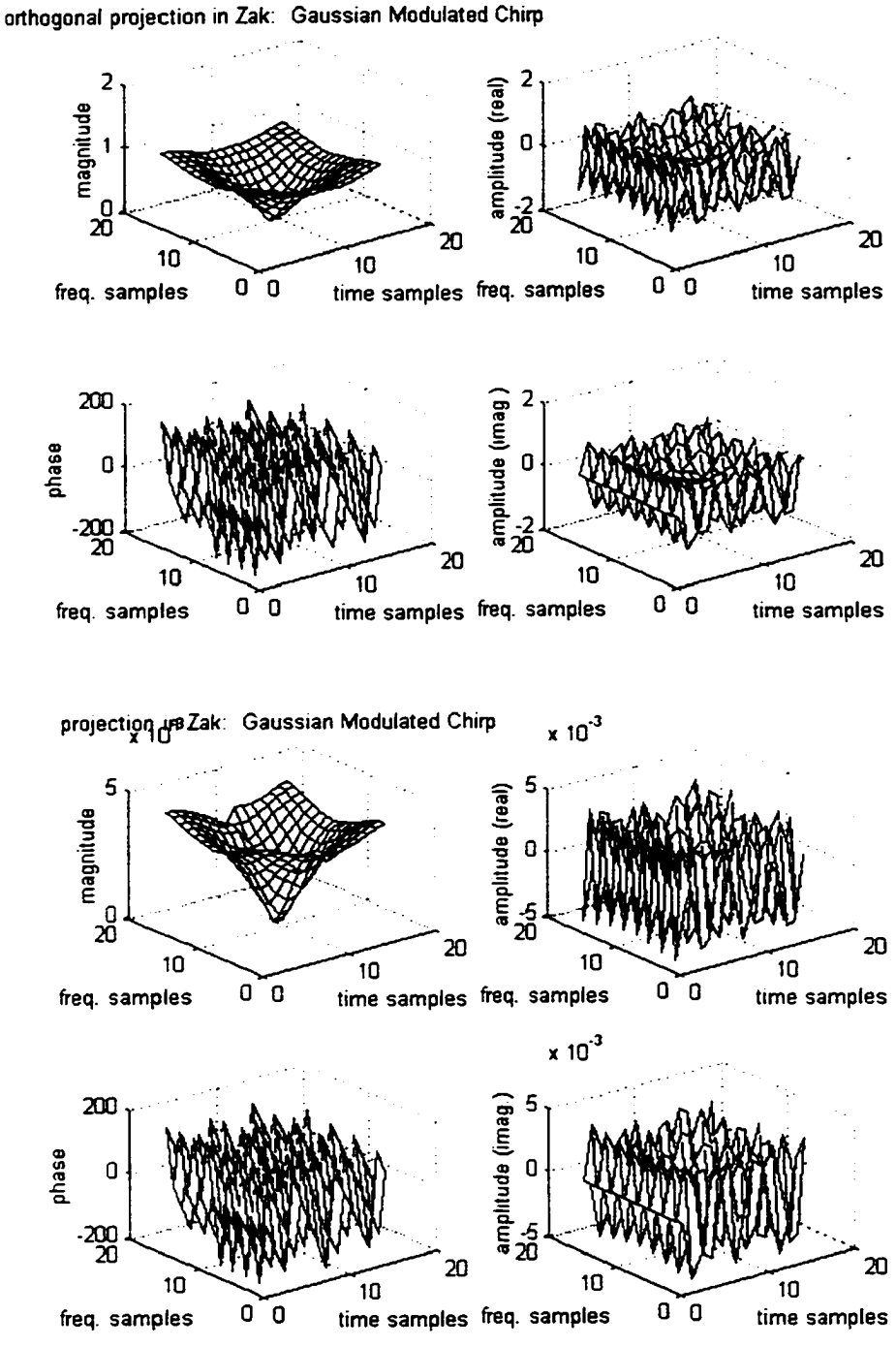

Figure 5.18d. Zak transforms of the projection signals in (5.18a).

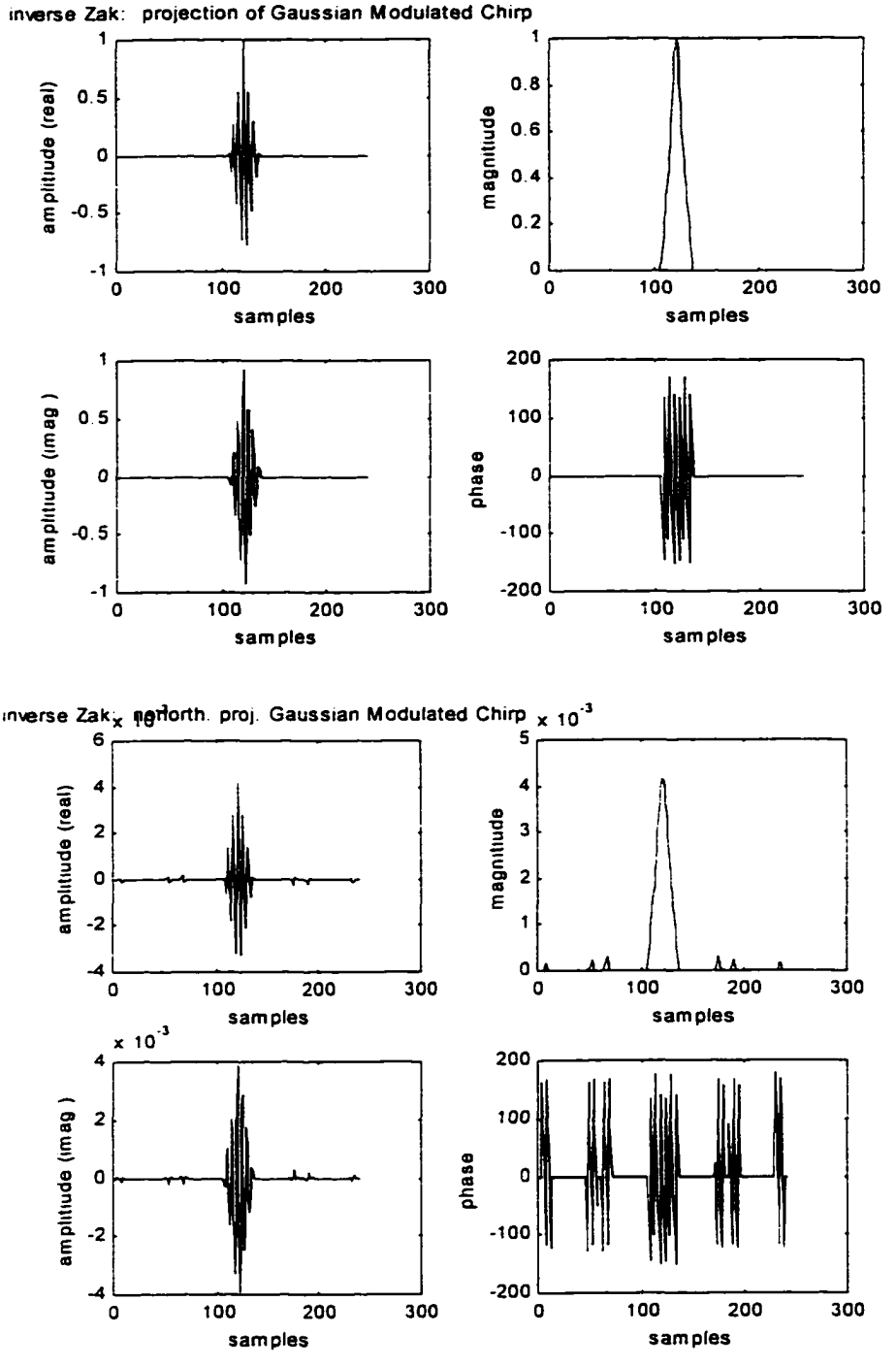

Figure 5.19a. Orthogonal and nonorthogonal projections of the modulated chirp conditioned with the triangular window of (5.16a).

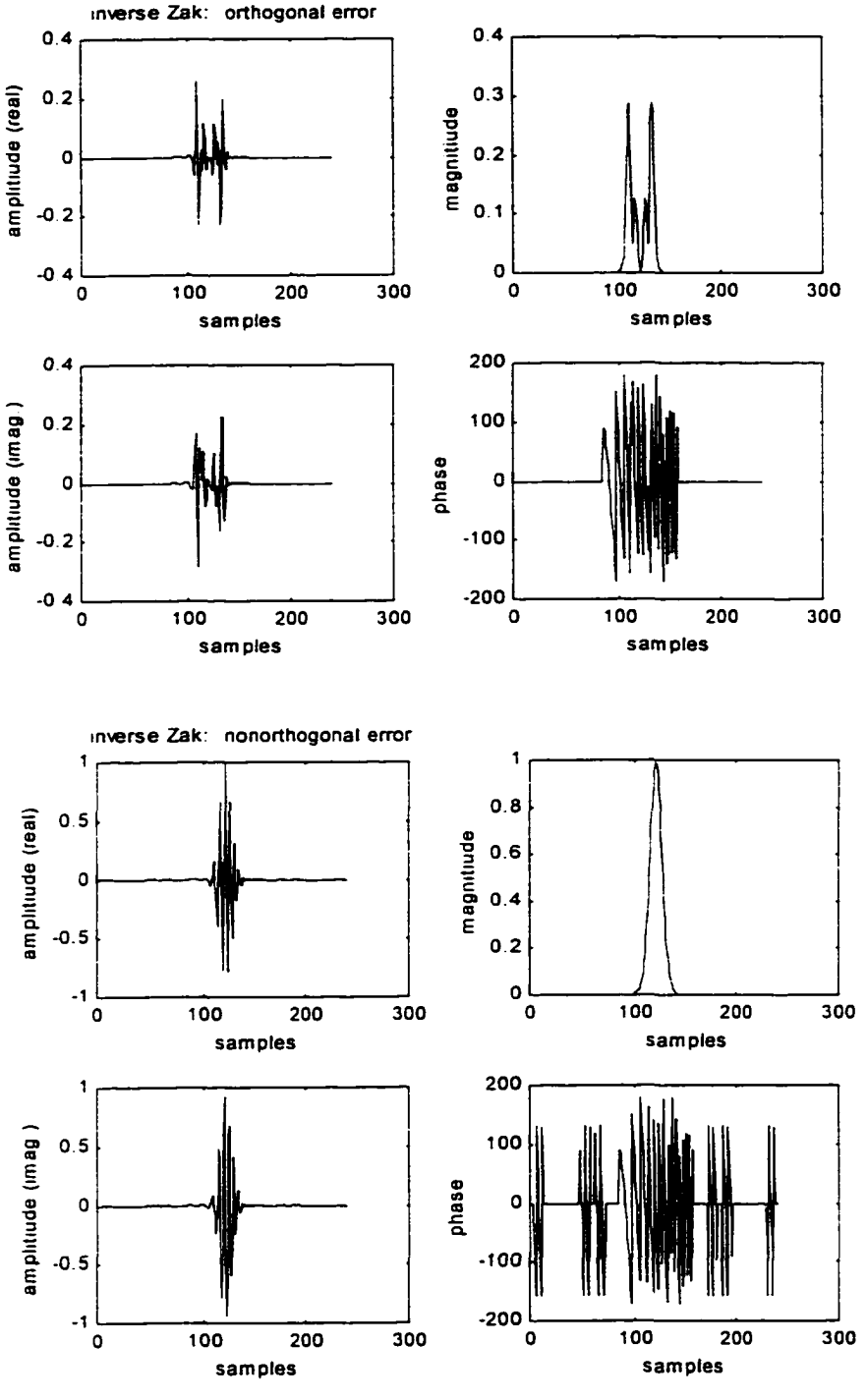

Figure 5.19b. Errors resulting from the respective projections in (5.19a).

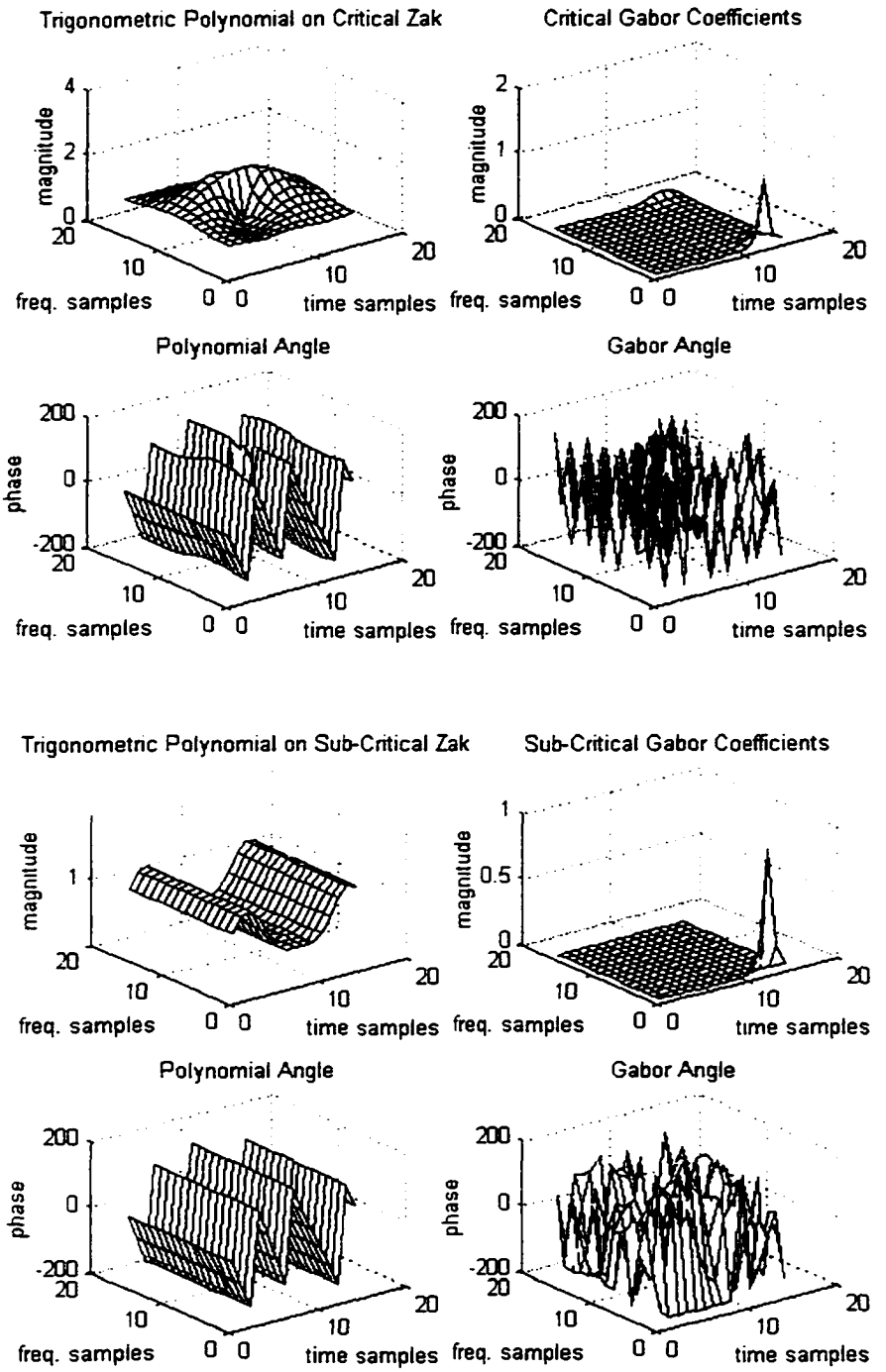

Figure 5.19c. Weyl-Heisenberg coefficient sets of the respective modulated chirp and its orthogonal projection, and their related trigonometric polynomials.

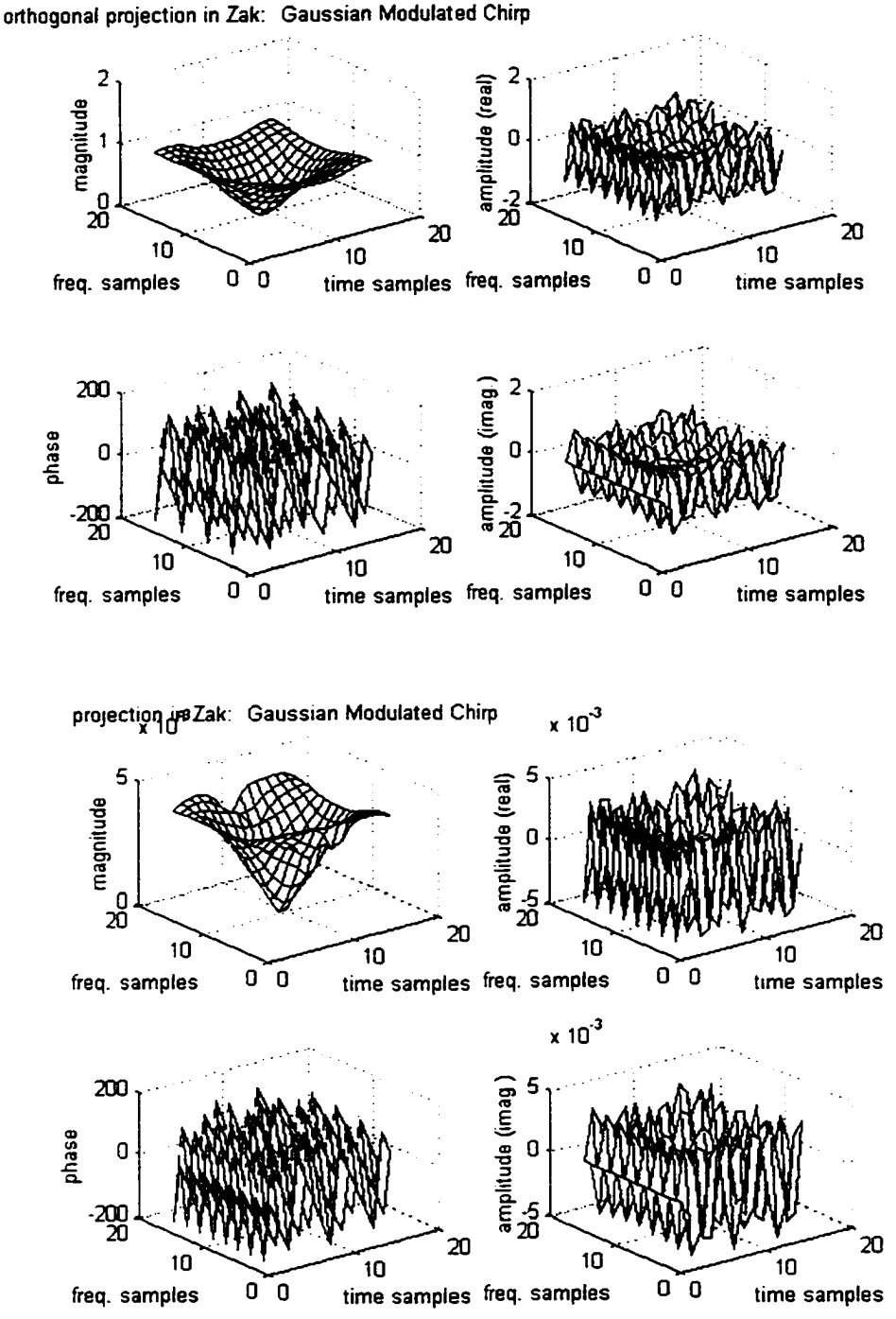

Figure 5.19d. Zak transforms of the projection signals in (5.19a).

5.4 Generalized Zak Transform

The Zak transform is completely definable on a critically sampled subspace of phase space [4, 49, 50]. It is commonly used to perform computation, analysis, and/or display of a signal or signal transform on a critically sampled time-frequency space. Nonetheless, the Zak transform is computationally, analytically, and visually usable for integer oversampling of a signal or signal transform because an integer oversampling subspace is made up of critically sampling subspaces; but it is not readily amenable to fractional oversampling. In [263], O'Hair and Suter broadened the definition of the Zak transform to include the windowed Zak transform, which is fashioned from the short-time Fourier transform, en route to produce the decimated generalized discrete time-frequency distribution from the Zak spectrogram. Sampling the windowed Zak transform may not be as easy as sampling the standard Zak transform if the signal and the window require different sampling rates. In addition, the definition of windowed Zak transform is maintained on the critically sampled time-frequency subspace.

In many computational analyses, while the standard Zak transform may be useful, it is simply inadequate. The standard Zak transform is the best computational and analytic tool for Weyl-Heisenberg expansions over critically sampled Weyl-Heisenberg systems, but its appropriateness deteriorates for such expansions over other types of Weyl-Heisenberg systems. One usually desires a Zak transform that shares the important characteristics of the DFT. This would at least enable the processing of nonstationary signals in ways similar to the processing of stationary signals in Fourier analysis.

In this section, a new Zak transform is proposed. This upgraded Zak transform is denoted as the generalized Zak transform. It maintains the properties of the standard Zak transform while adding some new properties. It is capable of performing analysis on a signal at the undersampling, critical sampling, and oversampling rates. At the critical sampling rate, its operation is identical to the standard Zak transform. A change in sampling rate is effected by the sampling control parameter. The generalized Zak transform is suitable for Weyl-Heisenberg expansions over any Weyl-Heisenberg system; its application is equally simple at any sampling rate.

5.4.1 Definition and Properties

For a signal $f \in L_2(\mathbb{R})$ with Fourier transform $\hat{f} \in L_2(\mathbb{R})$ defined by

$$\hat{f}(a^{-1}v) = \int_{-\infty}^{\infty} f(t) e^{-2\pi i a^{-1} v t}, \quad v \in \mathbb{R}, \quad a \in \mathbb{R}^{+},$$

the generalized Zak transform is defined as

$$(Zf)(v,t) = \sum_{n=-\infty}^{\infty} f(t + nT) e^{2\pi i n v S}, \quad t, v \in \mathbb{R}, \tag{5.75}$$

with S and T being positive nonzero constants. This Zak transform satisfies the functional relationships in

$$(Zf)(v + S^{-1}, t + T) = e^{-2\pi i v S}(Zf)(v, t), \tag{5.76}$$

which pertains to the periodicity conditions. This equation states that the Zak transform is quasi-periodic in the time variable t with quasi-period T and periodic in the frequency variable v with period S^{-1}. T and S^{-1} can be viewed as coarse sample intervals of an otherwise continuous Zak transform. Because of equation (5.76), (Zf) is completely determinable by its values on the arbitrary set

$$\{(t, v) : t_0 \le t < t_0 + T,\ v_0 \le v < v_0 + S^{-1}\}.$$

Consequently, the signal f is recoverable from (Zf) on the time-frequency space of area $S^{-1}T$:

$$f(t + nT) = S \int_{v_0}^{v_0 + S^{-1}} (Zf)(v, t) e^{-2\pi i n v S} dv, \quad n \in \mathbb{Z}, \quad t_0 \le t < t_0 + T. \tag{5.77}$$

In addition, the Fourier transform $\hat{f}$ is recoverable from (Zf) because

$$(Zf)(v, t) = e^{-2\pi i a^{-1} v t} \frac{1}{T} (Z\hat{f})(t, -v), \tag{578}$$

where for $m \in \mathbb{Z}$ and $v_0 \le v < v_0 + S^{-1}$,

$$\hat{f}(a^{-1}(v + mS^{-1})) = \int_{t_0}^{t_0 + T} (Zf)(v, t) e^{-2\pi i a^{-1}(v + mS^{-1})t} dt. \tag{5.79}$$

Contrary to the periodicity conditions of (Zf), $(Z\hat{f})$ is periodic in the time variable and quasi-periodic in the frequency variable. The scaling factor a^{-1} is defined by $\alpha^{-1} = T^{-1}S$. It will be subsequently called the sampling control parameter.

5.4.2 Discrete-Time Discrete-Frequency Zak Transform

Sampling a nonstationary signal can be problematic because information on the signal's region of existence may be unavailable or partially available. Moreover, the region of existence of the signal may be known but no specific information is available on the reasonable limits within which most of the signal's energy lies. In general, some amount of guessing is required to determine the sampling rate for any nonstationary signal. This implies that it may be difficult to generate an alias-free time-frequency analysis of nonstationary signals. In developing a sampling theory for nonstationary signals, it is reasonable to assume that most of the energy in the signals are compacted in a small unknown region somewhere within a much larger region. It may be alternatively assumed that the precise location of most of these signals' energy is known but the duration of the signals are unknown. In either case, a signal's time-width should be sufficiently long so that it captures the essential information of the signal thereby providing an acceptable sampling interval for spectrum; but this is not always possible. Sometimes, the signal is long relative to the transform and it must be aliased for transformation to take place. This suggests that it may not always be possible to recover a signal uniquely from the Zak transform. Instead, a member of a general class of signals may be recovered.

Suppose it is reasonable to assume that a signal's energy essentially exists within a band of frequencies $T^{-1}M$, M is a positive integer constant; then the derived discrete-time Zak transform can be written as

$$(Zf)(v, t_0 + k\frac{T}{M}) = \sum_{n=-\infty}^{\infty} f(t_0 + k\frac{T}{M} + nT)e^{2\pi invS}, \qquad (5.80)$$

where $0 \le k < M$ and $v_0 \le v < v_0 + 1/S$. Correspondingly, the recovered infinite signal sequence from the discrete-time Zak transform is

$$f(t_0 + k\frac{T}{M} + nT) = S\int_{v_0}^{v_0 + S^{-1}} (Zf)(v, t_0 + k\frac{T}{M})e^{-2\pi invS}dv, \qquad (5.81)$$

where $n \in Z$ and $0 \le k < M$. These two equations constitute a Zak transform pair.

By continuing the sampling in frequency, the discrete-time discrete-frequency Zak transform can be obtained from equation (5.80). For $0 \le k < M$ and $0 \le l < L$,

$$(Zf)\left(v_0 + \frac{l}{LS}, t_0 + k\frac{T}{M}\right) = \sum_{n=-\infty}^{\infty} \left(f(t_0 + k\frac{T}{M} + nT)e^{2\pi inv_0 S}\right) e^{2\pi inl/L} \qquad (5.82)$$

under the condition that the signal f is being observed for a duration of length LS. Alternatively, f can be expressed in terms of (Zf) samples by approximating equation (5.81). Replacing integration with summation and noting that $dv \approx (LS)^{-1}$, for $0 \le k < M$ and $n \in Z$,

$$f(t_0 + k\frac{T}{M} + nT) = e^{-2\pi i n v_0 S}\frac{1}{L}\sum_{l=0}^{L-1}(Zf)\left(v_0 + \frac{1}{LS}, t_0 + k\frac{T}{M}\right)e^{-2\pi i n l/L}. \quad (5.83)$$

Since $LS = a^{-1}LT$, if S and T are chosen so that a^{-1} is a rational number satisfying the condition $LS = KT$ and L divides K, equation (5.82) can be rewritten as

$$\begin{aligned}&(Zf)\left(v_0 + \frac{l}{LS}, t_0 + k\frac{T}{M}\right)\\ &= \sum_{n=0}^{K-1}\sum_{m=-\infty}^{\infty}\left(f(t_0 + k\frac{T}{M} + (n + mK)T)e^{2\pi i n v_0 S}\right)e^{2\pi i n l/L}.\end{aligned} \quad (5.84)$$

If, instead, L does not divide K but $L \geq K$, this equation can be conveniently formulated as

$$\begin{aligned}&(Zf)\left(v_0 + \frac{l}{LS}, t_0 + k\frac{T}{M}\right)\\ &= \sum_{n=0}^{L-1}\sum_{m=-\infty}^{\infty}\left(f(t_0 + k\frac{T}{M} + (n + mL)T)e^{2\pi i n v_0 S}\right)e^{2\pi i n l/L}\end{aligned} \quad (5.85)$$

because f will be appropriately appended with zero values. It is possible to directly recover

$$\sum_{m=-\infty}^{\infty}\left(f(t_0 + k\frac{T}{M} + (n + mL)T)e^{2\pi i n v_0 S}\right)$$

from the discrete-time discrete-frequency (Zf), but to recover

$$\sum_{m=-\infty}^{\infty}\left(f(t_0 + k\frac{T}{M} + (n + mK)T)e^{2\pi i n v_0 S}\right)$$

from it requires that n be further written as

$$n = n_1 + sL, \quad 0 \le n_1 < L, \quad 0 \le s < R, \quad K = RL,$$

since the number of samples, MK, in a period of f is greater than the number of samples, ML, in (Zf). With this Euclid's division lemma formulation of n,

$$\sum_{n=0}^{K-1} \sum_{m=-\infty}^{\infty} \left(f(t_0 + k\frac{T}{M} + (n + mK)T) e^{2\pi i n v_0 S} \right)$$

$$= \sum_{n=0}^{L-1} \left(\sum_{s=0}^{R-1} \sum_{m=-\infty}^{\infty} \left(f(t_0 + k\frac{T}{M} + ((n + sL) + mRL)T) e^{2\pi i n v_0 S} \right) \right)$$

implies that

$$\sum_{s=0}^{R-1} \left(\sum_{m=-\infty}^{\infty} \left(f(t_0 + k\frac{T}{M} + ((n + sL) + mRL)T) e^{2\pi i n v_0 S} \right) \right)$$

can be recovered from (Zf). When L divides K, $a^{-1} = R$ because $K = a^{-1}L$; a^{-1} is the sampling control parameter; $a^{-1} = 1$ is equivalent to the critical sampling case where the number of samples in a period of f equals the number of samples in (Zf); and $a^{-1} < 1$ is equivalent to the oversampling case where the number of samples in a period of f is less than the number of samples in (Zf).

5.4.3 Discrete Zak Transform

If $l_0 = \lfloor L v_0 S \rfloor$, the smallest integer less than or equal to $L v_0 S$, the exponential factor

$$e^{2\pi i n v_0 S} \simeq e^{2\pi i n l_0 / L}.$$

In addition, if

$$F(l,k) = (Zf)\left(v_0 + \frac{l}{LS}, t_0 + k\frac{T}{M} \right), \quad T = M\frac{T}{M},$$

and

$$\sum_{s=0}^{R-1} f(k+(n+sL)M) = \sum_{s=0}^{R-1} f(t_0 + k\frac{T}{M} + ((n+sL)M)\frac{T}{M}),$$

the discrete Zak transform of f over a single observational period, KM, is

$$F(l,k) = \sum_{n=0}^{L-1} \left(\sum_{s=0}^{R-1} f(k+(n+sL)M) e^{2\pi i n l_0 / L} \right) e^{2\pi i n l / L}, \tag{5.86}$$

where $0 \le k < M$ and $0 \le l < L$. This transform is invertible. For $0 \le k < M$ and $0 \le l < L$,

$$\sum_{s=0}^{R-1} f(k+(n+sL)M) e^{2\pi i n l_0 / L} = \frac{1}{L} \sum_{l=0}^{L-1} F(l,k) e^{-2\pi i n l / L}. \tag{5.87}$$

The recovered f is only unique if $s = 0$ in which case $K \le L$.

Setting

$$\tilde{f}(k + nM) = \sum_{s=0}^{R-1} f(k + (n + sL)M)e^{2\pi i n l_0 / L},$$

the periodic relations of the discrete Zak transform can be readily established:

$$F(l + L, k + M) = e^{-2\pi i l/L} F(l, k), \tag{5.88}$$

thereby affirming the Zak transform's periodicity in the frequency variable and quasi-periodicity in the time variable.

5.4.4 Zak Transform with Weyl-Heisenberg Expansions

Suppose the signals $f, g \in L(\mathrm{Z}/N_1)$ with $N_1 = KM$ and g is the window signal, then f has a Weyl-Heisenberg expansion of the form

$$f(a) = \sum_{m=0}^{N_1 - 1} \sum_{n=0}^{N-1} c_{m,n} g_{m,n}(a), \quad a \in \mathrm{Z}/N_1,$$

where

$$g(a) = g(a - m)e^{2\pi i n a / N}, \quad N = ML.$$

By replacing m and n with mM and nL respectively in their ranges,

$$f(a) = \sum_{m=0}^{K-1} \sum_{n=0}^{M-1} c_{mM,nL} g_{mM,nL}(a), \quad a \in Z/N_1,$$

where

$$g(a) = g(a - mM)e^{2\pi ina/M}, \quad 0 \le m < K, \quad 0 \le n < M.$$

In terms of Zak transform, assuming $l_0 = 0$

$$F(l,k) = \tilde{G}(l,k)\tilde{P}(l,k), \quad 0 \le k < M, \quad 0 \le l < L, \tag{5.89}$$

where

$$\tilde{P}(l,k) = \sum_{m=0}^{L-1} \sum_{n=0}^{M-1} \tilde{c}_{mM,nL} e^{2\pi i(ml/L - nk/M)}.$$

This is a 2-dimensional Fourier series. The Weyl-Heisenberg coefficients $\tilde{c}_{mM,nL}$ are aliased for $K > L$. That is,

$$\tilde{c}_{mM,nL} = \sum_{r=0}^{R-1} c_{(m+rL)M,nL}, \quad K > L.$$

Otherwise $\tilde{c}_{mM,nL} = c_{mM,nL}$.

5.4.5 Examples

The generalized Zak transform was used to analyze the gaussian and the hyperbolic secant signals over critical sampling and rational oversampling and undersampling time-frequency subspaces. For the gaussian, $g(t) = e^{-\pi t^2}$, and the hyperbolic secant, $g(t) = sech(\pi t)$, defined on the interval $t \in [4, 4)$, there were $N = 256$ uniform time samples used to represent each of them. These two signals are invariant to Fourier transformation. Choosing $N = ML$, where M is the number of time samples and L is the number of frequency samples for time-frequency Zak space, the number of time samples was set to $M = 32$ in each of the critical and rational non-critical sampling situations. The choice of M was influenced by the desire to have the signals' magnitudes optimally displayed in both time and frequency. The values for L were chosen to permit the description of the gaussian as well as hyperbolic secant on a Zak space for the cases where it was critically sampled, integer oversampled, fractionally oversampled, fractionally undersampled, and integer undersampled. Corresponding to these sampling situations, the respective values of L were 8, 16, 12, 6, and 4. For each sampling situation, the signals used were recovered (figures 5.20a-e through figures 5.21a-e). In the case of integer undersampling shown in figure 5.20a and figure 5.21e, the recovered gaussian and hyperbolic secant were both aliased. In the other cases, the gaussian and the hyperbolic secant were completely recovered as shown is in figures 5.20a-d and figures 5.21a-d respectively. In each sampling situation, the Zak transform zero was located at the equivalent of (0.5, 0.5).

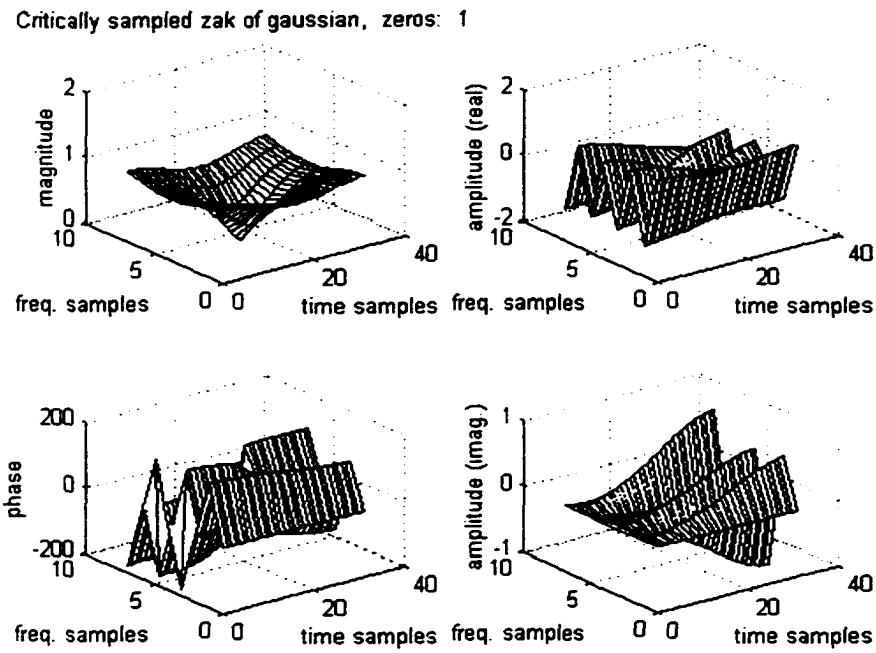

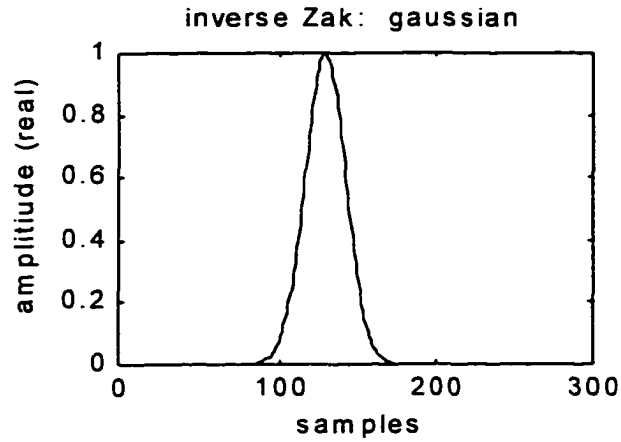

Figure 5.20a. Zak transform of the gaussian on a critically sampled time-frequency subspace and its inverse.

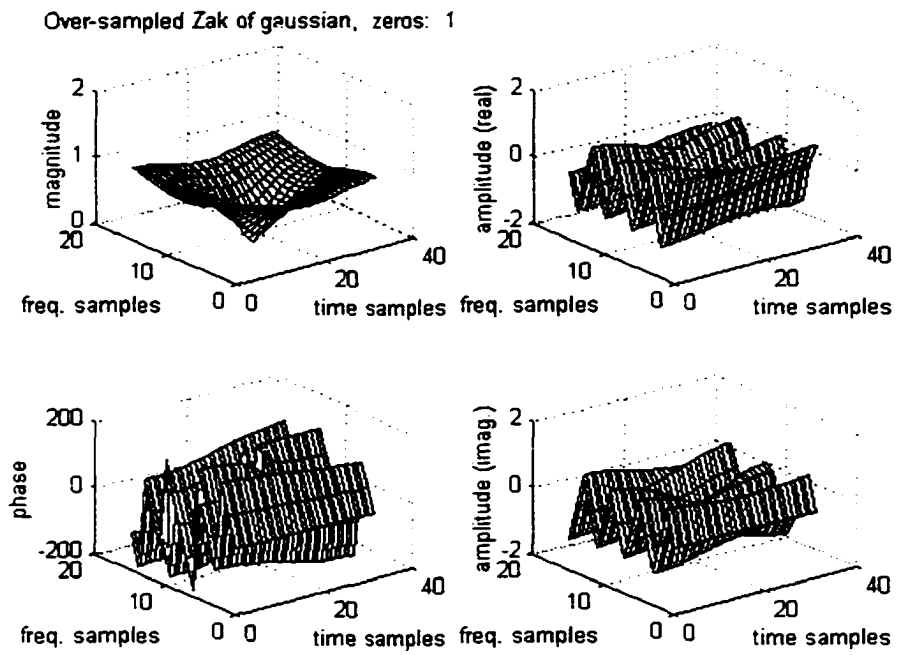

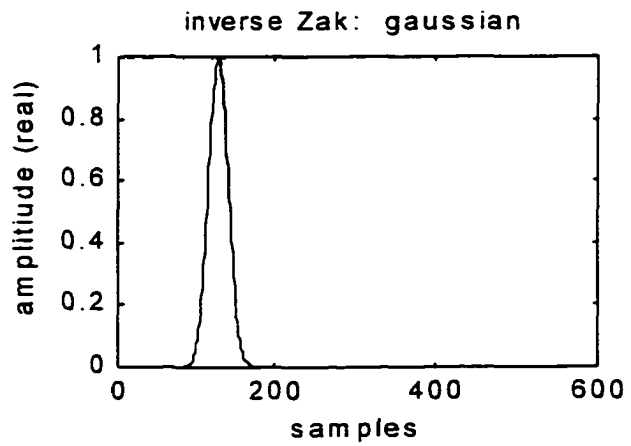

Figure 5.20b. Zak transform of the gaussian on an integer oversampled (by a factor of 2) time-frequency subspace and its inverase.

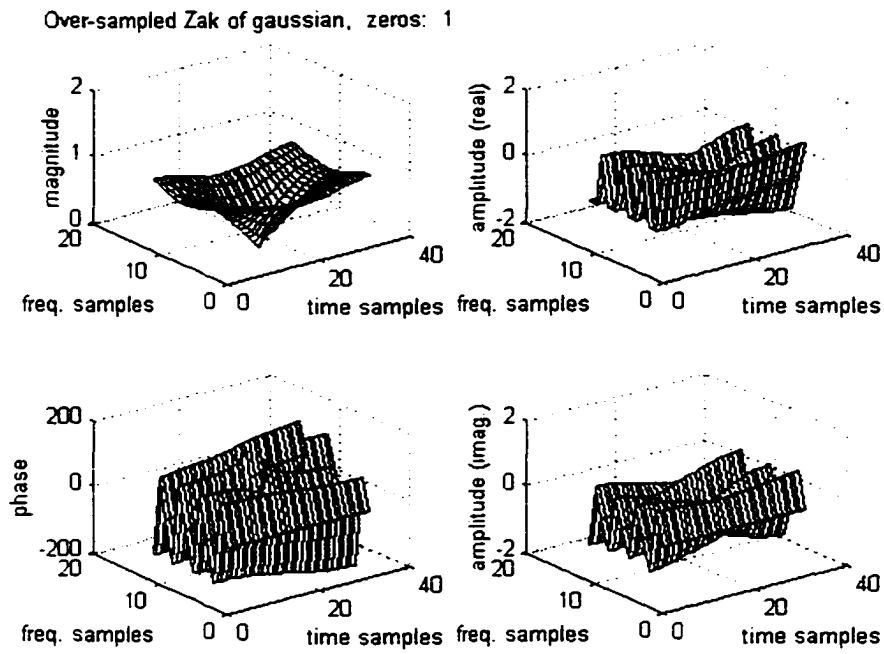

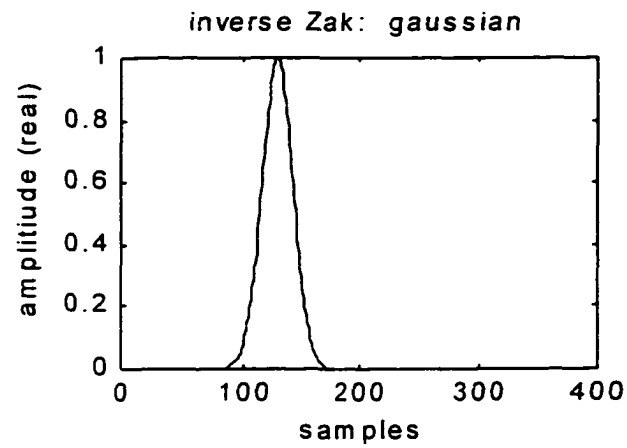

Figure 5.20c. Zak transform of the gaussian on a fractionally over-sampled (by a factor of 1.5) time-frequency subspace and its inverse.

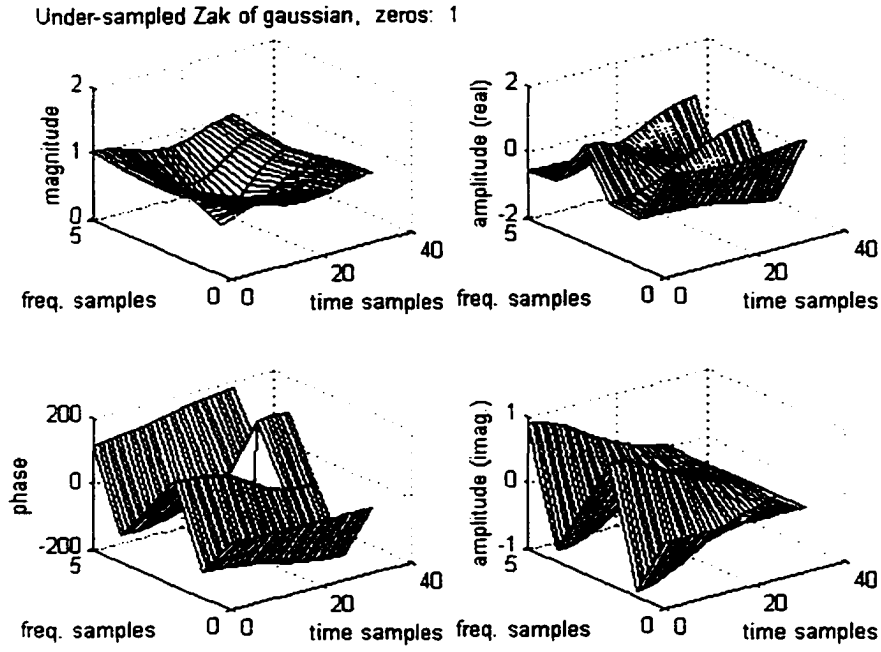

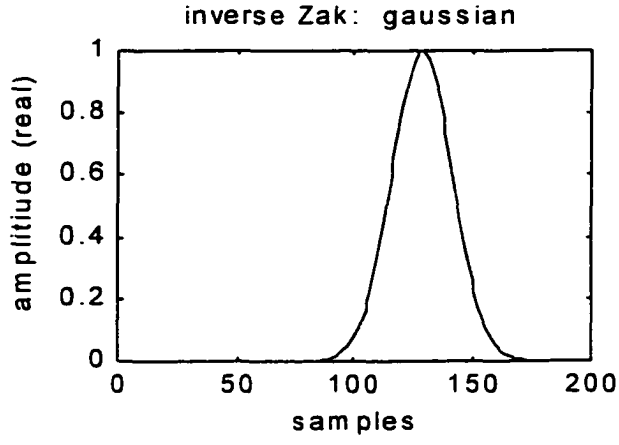

Figure 5.20d. Zak transform of the gaussian on a fractionally under-sampled (by a factor of 0.75) time-frequency subspace and its inverse.

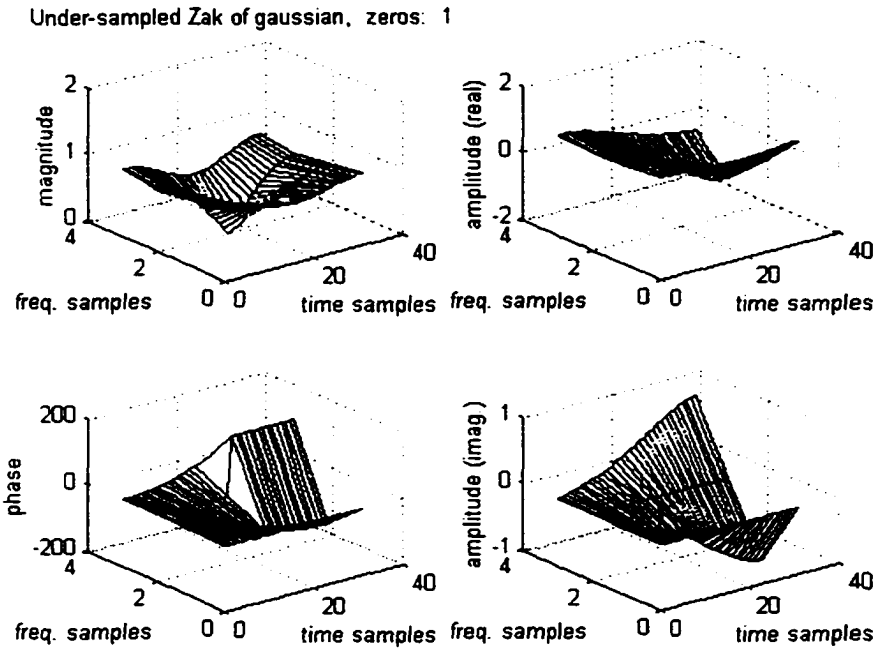

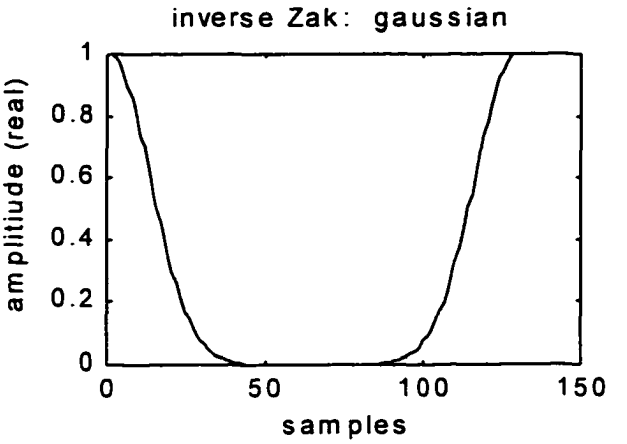

Figure 5.20e. Zak transform of the gaussian on an integer under-sampled (by a factor of 0.5) time-frequency subspace and its inverse.

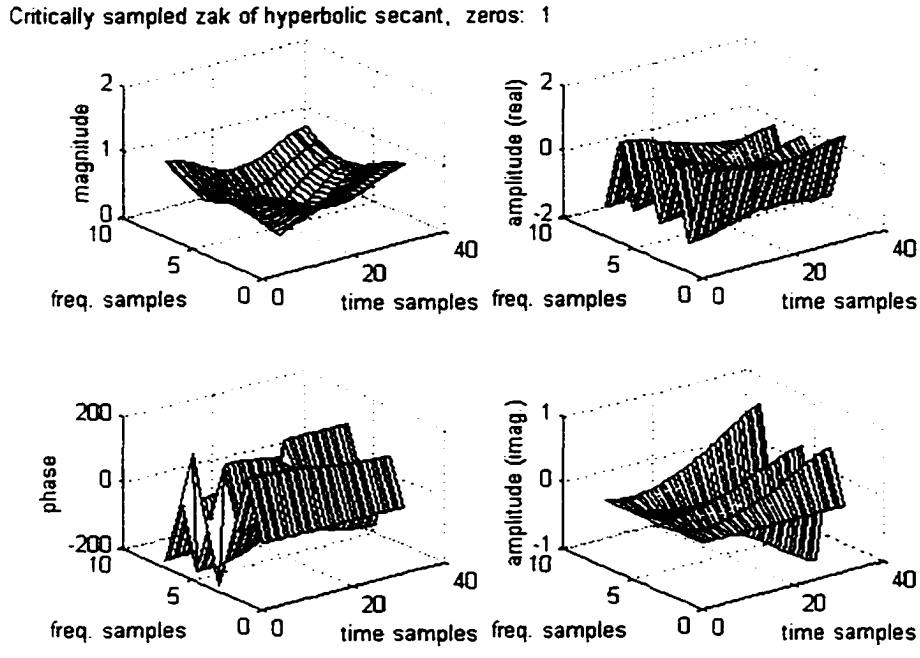

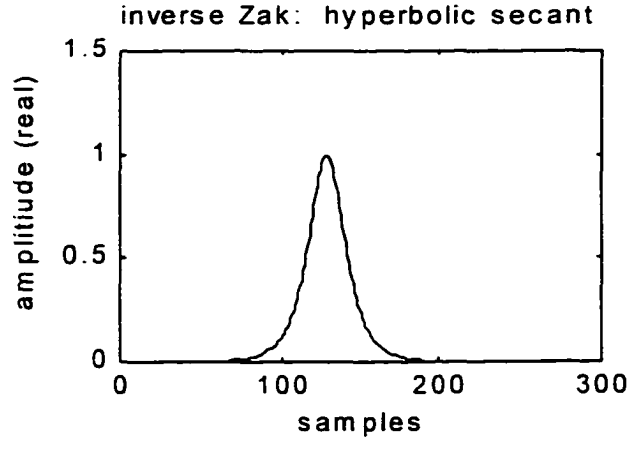

Figure 5.21a. Zak transform of the hyperbolic secant on a *critically sampled time-frequency subspace and its inverse.*

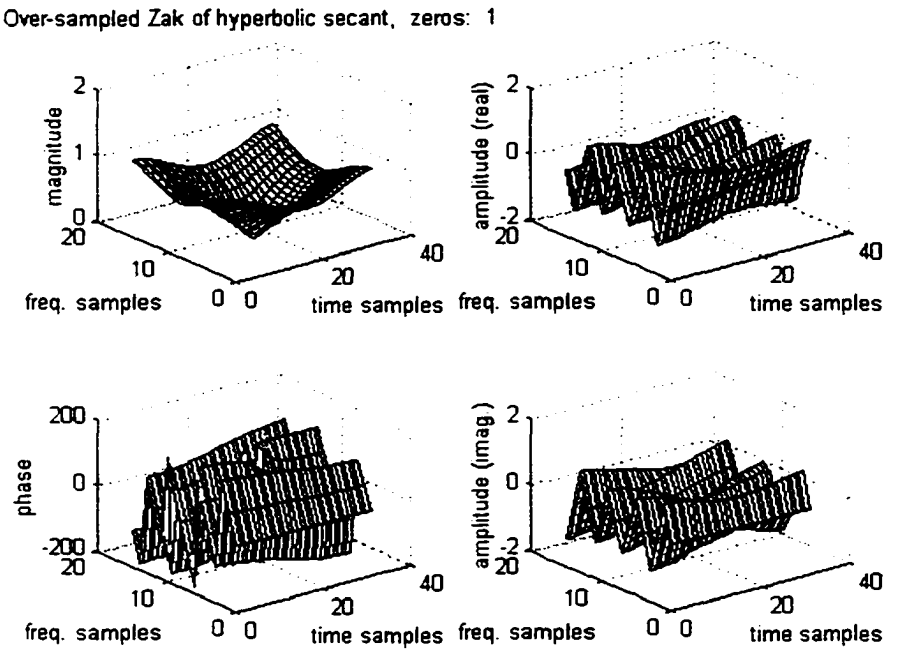

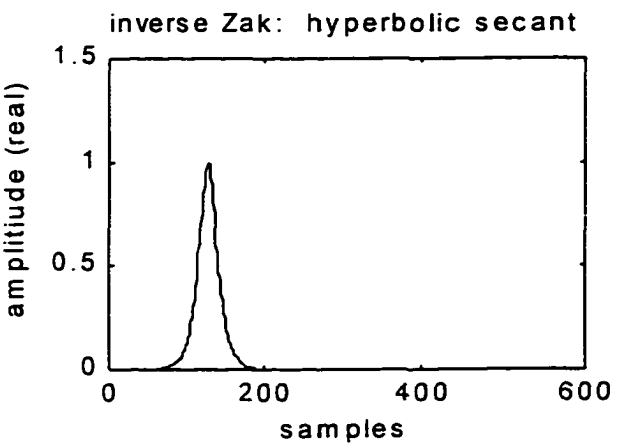

Figure 5.21b. Zak transform of the hyperbolic secant on an integer oversampled (by a factor of 2) time-frequency subspace and its inverse.

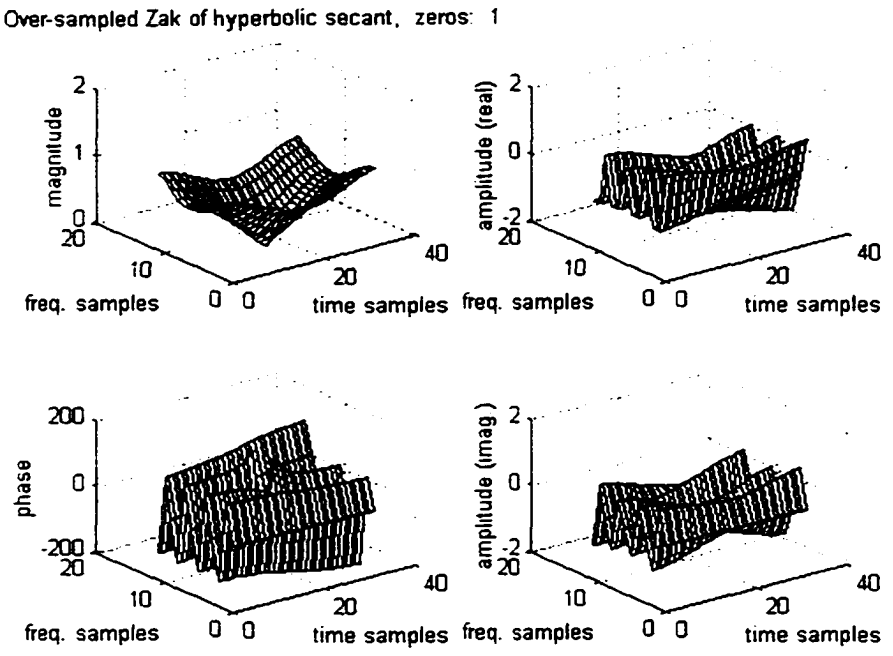

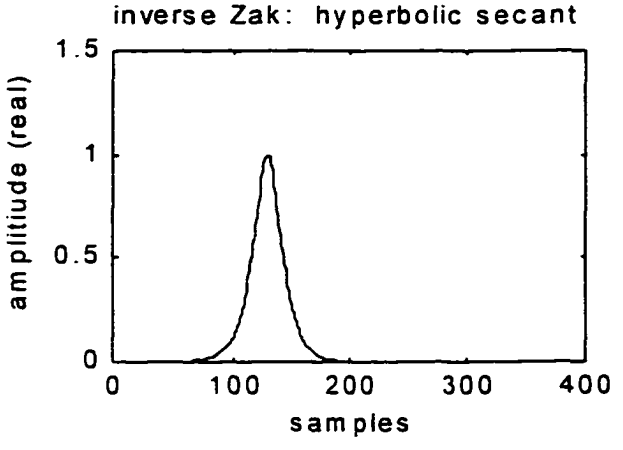

Figure 5.21c. Zak transform of the hyperbolic secant on a fractionally oversampled (by a factor of 1.5) time-frequency subspace and its inverse.

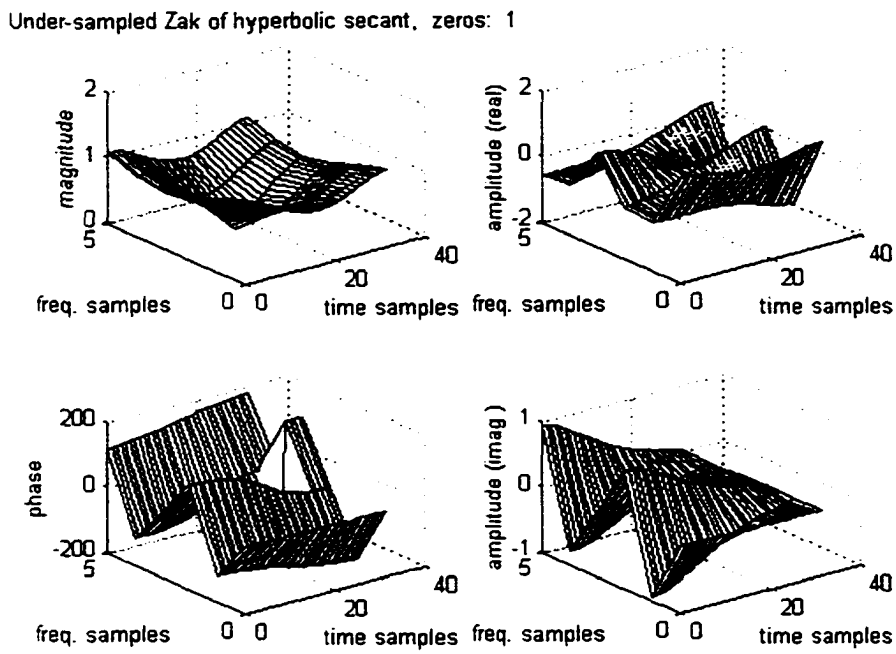

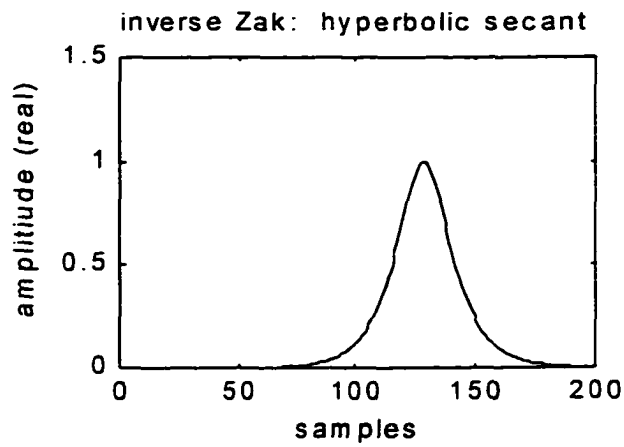

Figure 5.21d. Zak transform of the hyperbolic secant on a fractionally undersampled (by a factor of 0.75) time-frequency subspace and its inverse.

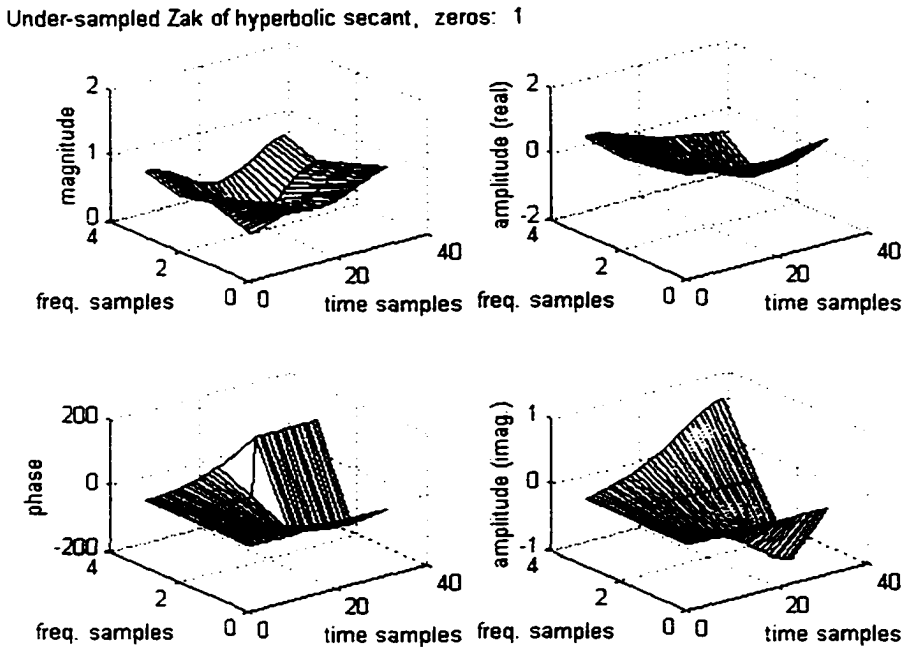

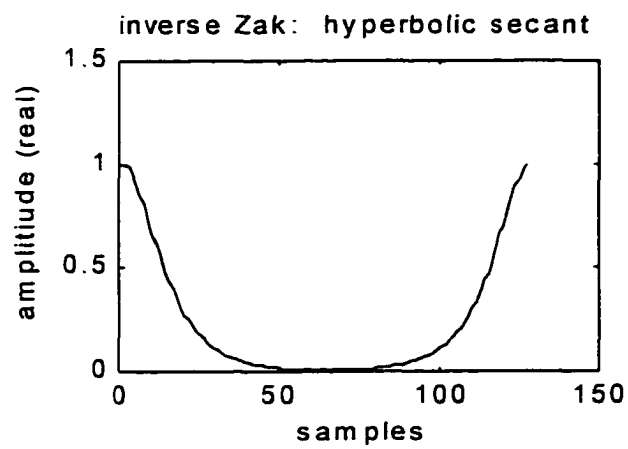

Figure 5.21e. Zak transform of the hyperbolic secant on an integer undersampled (by a factor of 0.5) time-frequency subspace and its inverse.

Chapter 6

Conclusion

It was demonstrated that the Zak transform is a powerful time-frequency analysis tool. It is a modified DFT. By finding ways to bring much of the operations of Fourier analysis into time-frequency analysis through the Zak transform, it will become easy to perform time-frequency analysis of nonstationary signals. With procedures like the orthogonal projection algorithm nonorthogonal nonstationary signals' decomposition can be brought under manageable control. Furthermore, the general Zak transform will allow simpler operations under any sampling condition.

While it is questionable that any particular time-frequency tool will maintain superior status over the others, bringing other time-frequency methods into the framework of Zak transform certainly holds much promise. The application of the orthogonal projection algorithm to the compression of real data is a valuable research exercise which will be investigated at a future date. In addition, the many properties of the standard Zak transform needs to be further studied for adoption by the generalized Zak transform.

Bibliography

[1] R. M. Lerner, "Representation of Signals," in *Communication System Theory*, E. J. Bahgdady, ed., Mc Graw-Hill, New York, 1961, pp. 203-242.

[2] L. Cohen, "Introduction: A Primer on Time-Frequency Analysis," in *Time-Frequency Signal Analysis*, B. Boashash, ed., Longman Cheshire, Melbourne, 1992, pp. 3-42.

[3] R. G. Shenoy and T. W. Parks, *The Weyl Correspondence and Time-Frequency Analysis*, IEEE Trans. Signal Processing, Vol. 42, No. 2, Feb. 1994, pp. 318-331.

[4] J. Zak, *Finite Translation in Solid-State Physics*, Phys. Rev. Lett., Vol. 19, No. 24, Dec. 1967, pp. 1385-1387.

[5] D. Slepian, *On Bandwidth*, Proc. IEEE, Vol. 64, No.3, March 1976, pp. 292-300.

[6] K. Devlin, *The Joy of Sets, Fundamentals of Contemporary Set Theory*, 2nd ed., Springer-Verlag, New York, 1992.

[7] G. E. Andrews, *Number Theory*, Dover Publications, New York, 1994.

[8] W. R. Scott. *Group Theory*, Dover Publications, New York, 1987.

[9] R. E. Blahut, *Theory and Practice of Error Control Codes*, Addison-Wesley, Reading, 1984.

[10] J. B. Fraleigh, *A First Course in Abstract Algebra*, 4 th ed., Addison-Wesley, New York, 1989.

[11] E. G. Kalnins and W. Miller, Jr., "A Note on Group Contractions and Radar Ambiguity Functions," in *Radar and Sonar, Part* II, Vol. 39, IMA Volumes in Mathematics and its Applications, F. A. Grünbaum, M. Bernfeld, and R. E. Blahut, eds., Springer-Verlag, New York, 1992, pp. 71-82.

[12] I. Daubechies, *Ten Lectures on Wavelets*, Society of Industrial and Applied Mathematics, Philadelphia, 1992.

[13] W. Schempp, *Radar Ambiguity Functions, the Heisenberg Group, and Holomorphic Theta Series*, Proc. Amer. Math. Soc., Vol. 92, No. 1, Sept. 1984, pp. 103-110.

[14] R. Howe, *On the Role of the Heisenberg Group in Harmonic Analysis*, Bull. Amer. Math. Soc., Vol. 3, No. 2, Sept. 1980, pp. 821-843.

[15] R. Tolimieri, *Heisenberg Manifolds and Theta Functions*, Trans. Amer. Math. Soc., Vol. 239, May 1978, pp. 293-319.

[16] R. Tolimieri, *Analysis on the Heisenberg Manifold*, Trans. Amer. Math. Soc., Vol. 228, 1977, pp. 329-343.

[17] J. Brezin, *Harmonic Analysis on Nilmanifolds*, Trans. Amer. Math. Soc.,Vol. 150, August 1970, pp. 611-618.

[18] L. Auslander, and J. Brezin, *Translation-Invariant Subspaces in* L_2 *of the Compact Nilmanifold. I*, Invent. Math. 20, 1973, pp. 1-14.

[19] E. B. Vinberg, *Linear Representations of Groups*, Birkhauser Verlag, Boston, 1989.

[20] S. Warner, *Modern Algebra*, Dover Publications, New York, 1990.

[21] A. N. Michel and C. J. Herget, *Applied Algebra and Functional Analysis*, Dover Publications, New York, 1993.

[22] K. Hoffman and R. Kunze, *Linear Algebra*, 2nd ed., Prenctice Hall, Englewood Cliffs, 1971.

[23] N. B. Haaser and J. A. Sullivan, *Real Analysis*, Dover Publications, New York, 1991.

[24] A. Friedman, *Foundations of Modern Analysis*, Dover Publications, New York, 1982.

[25] G. E. Shilov and B. L. Gurevich, *Integral, Mearsure and Derivative: A Unified Approach*, Translated and Edited by R. A. Silverman, Dover Publications, New York, 1977.

[26] N. I. Akhiezer and I. M. Glazman, *Theory of Linear Operators in Hilbert Space*, Two Volumes, Translated by M. Nestell, Dover Publications, New York, 1993.

[27] W. Ruden, *Fourier Analysis on Groups*, John Wiley & Sons, New York, 1990.

[28] M. C. Gemignani, *Elementary Topology*, 2nd ed., Dover Publications, New York, 1990.

[29] E. M. Stein and G. Weiss, *Introduction to Fourier Analysis on Euclidean Spaces*, 6th ed., Princeton University Press, Princeton, 1990.

[30] M. Benedicks, *On Fourier Transforms of Functions Supported on Sets of Finite Lesbesgue Measure*, J. Math. Anal. Appl., Vol. 106, 1985, pp. 180-183.

[31] J. Good, *Analogues of Poisson's Summation Formula*, Amer. Math. Monthly, Vol. 69, 1962, pp. 259-266.

[32] R. Tolimieri, M. An, and C. Lu, *Algorithms for Discrete Fourier Transform and Convolution*, Springer-Verlag, New York, 1989.

[33] R. Tolimieri, M. An, and C. Lu, *Mathematics of Multidimensional Fourier Transform*

Algorithms, 2nd ed., Springer-Verlag, New York, 1997.

[34] D. L. Donoho and P. B. Stark, *Uncertainty Principles and Signal Recovery*, SIAM J. Appl. Math., Vol. 49, No. 3, June 1989, pp. 906-931.

[35] G. Cowling and J. F. Price, *Bandwidth versus Time Concentration: The Heisenberg-Pauli-Weyl Inequality*, SIAM J. Math Anal., Vol. 15, No. 1, Jan. 1984, pp. 151-165.

[36] C. L. Fefferman, *The Uncertainty Princple*, Bull. Amer. Math. Soc., Vol. 9, No. 2, Sept. 1983, pp 129-206.

[37] R. M. Lerner, *Means for Counting 'Effective' Numbers of Objects or Duration of Signals*, Proc. IRE, Vol. 47, Sept. 1959, pp. 1653.

[38] D. Gabor, *Theory of Communication*, J. Inst. Elect. Engrs., Vol. 93, No. 3, Nov. 1946, pp. 429-457.

[39] H. J. Landau and H. O. Pollak, *Prolate Spheroidal Wave Functions, Fourier Analysis and Uncertainty (2)*, Bell Syst. Tech. J., Vol. 40, Jan. 1961, pp. 65-84.

[40] N. G. Bruijn, "Uncertainty in Fourier Analysis," in *Inequalities*, O. Shisa, ed., Academic Press, New York, 1967, pp. 57-71.

[41] D. Slepian, *Some Comments on Fourier Analysis, Uncertainty, and Modeling*, SIAM Review, Vol. 25, No. 3, July 1983, pp. 379-393.

[42] D. Slepian and H. O. Pollak, *Prolate Spheroidal Wave Functions, Fourier Analysis and Uncertainty (1)*, Bell Syst. Tech. J., Vol. 40, Jan. 1961, pp.43-63.

[43] R. M. Young, *An Introduction to Nonharmonic Fourier Series*, Academic Press, New York, 1980.

[44] C. Heil, *Generalized Harmonic Analysis in Higher Dimensions; Weyl-Heisenberg Frames, and Zak Transform*, Ph. D. Thesis, University of Maryland, College Park, Maryland, 1990.

[45] R. J. Duffin and A. C. Schaeffer, *A Class of Nonharmonic Fourier Series*, Trans. Am. Math. Soc., Vol. 72, No. 3, May 1952, pp. 341-366.

[46] J. J. Benedetto, "Irregular Sampling and Frames," in *Wavelets: A Tutorial in Theory and Applications*, C. K. Chui, ed., Academic Press, Boston, 1992, pp. 445-507.

[47] I. Daubechies, *The Wavelet Transform, Time-Frequency Localization, and Signal Analysis*, IEEE Trans. Information Theory, Vol. 36, No. 5, Sept. 1990, pp. 961-1005.

[48] A. Cohen, I. Daubechies, and J. C. Feauveau, *Biorthogonal Basis*, Commun. Pure Applied Math., Vol. XLV, 1992, pp. 485-560.

[49] L. Auslander, I. C. Gertner, and R. Tolimieri, *The Discrete Zak Transform Application to Time-Frequency Analysis and Synthesis of Nonstationary Signals*, IEEE Trans. Signal Processing, Vol. 39, No. 4, April 1991, pp. 825-835.

[50] A. J. E. M. Janssen, *The Zak Transform: A Signal Transform for Sampled Time-Continuous Signals*, Phillips J. Res., Vol. 43, No. 1, 1988, pp. 23-69.

[51] L. Cohen, *Time-Frequency Analysis*, Prentice Hall, Englewood Cliffs, 1995.

[52] L. Stanković, *Highly Concentrated Time-Frequency Distributions: Pseudo Quantum Signal Representation*, IEEE Trans. Signal Processing, Vol. 45, No. 3, March 1997, pp. 543-551.

[53] P. Z. Peebles, Jr. *Probability, Random Variables, and Random Signal Principles*, McGraw-Hill, New York, 1980.

[54] A. Papoulis, *Probability, Random Variables, and Stochastic Processes*, 3rd ed., McGraw-Hill, New York, 1991.

[55] I. Daubechies, *Time-Frequency Localization Operators: A Geometric Phase Space Approach*, IEEE Trans. Information Theory, Vol. 34, No. 4, July 1988, pp. 605-612.

[56] C. E. Heil and D. F. Walnut, *Continuous and Discrete Wavelet Transforms*, SIAM Review, Vol. 31, No. 4, Dec. 1989, pp. 628-666.

[57] R. J. Glauber, *Coherent and Incoherent States of the Radiation Field*, Phys. Rev., Vol. 131, No. 6, Sept. 1963, pp. 2766-2788.

[58] C. W. Helstrom, *An Expansion of a Signal in Gaussian Elementary Signals*, IEEE Trans. Information Theory, IT-12, Jan. 1966, pp. 81-82.

[59] P. Flandrin, "Some Aspects of Non-Stationary Signal Processing with Emphasis on Time-Frequency and Time-Scale Methods," in *Wavelets, Time-Frequency Methods, and Phase-Space*, Springer-Verlag, New York, 1989, pp. 68-98.

[60] R.K. Potter, G. Kopp, and H. C. Green, *Visible Speech*, D. Van Nostrand Co, New York, 1947.

[61] W. Koenig, H. K. Dunn, and L. Y. Lacy, *The Sound Spectrograph*, J. Acoust. Soc. Am., Vol. 18, No. 1, 1946, pp. 19-49.

[62] L. Cohen, *Time-Frequency Distributions: A Review*, Proc. IEEE, Vol. 77, No. 7, July 1989.

[63] J. G. Proakis, and D. G. Manolakis, *Introduction to Digital Signal Processing*, Macmillan Publishing, New York, 1988.

[64] A. V. Oppenheim and R. W. Schafer, *Discrete-time Signal Processing*, Prentice Hall, New Jersey, 1989.

[65] J. Ville, "Theorie et Applications de la Notion de Signal Analytique," in *Cabes et Transmissions*, Vol. 2A, 1948, pp. 61-74.

[66] E. Wigner, *On the Quantum Correction for Thermodynamic Equilibrium*, Phys. Rev., Vol. 40, 1932, pp. 749-759.

[67] T. A. C. M. Claasen and W. F. G. Mecklenbräuker, *The Wigner Distribution - A tool for Time-Frequency Signal Analysis Part I: Continuous-Time Signals*, Philips J. Res., Vol. 35, 1980, pp. 217-250.

[68] T. A. C. M. Claasen and W. F. G. Meckenbräker, *The Wigner Distribution - A tool for Time-Frequency Signal Analysis Part II: Discrete-signals*, Philips J. Res., Vol. 35, 1980, pp. 276-300.

[69] F. Hlawatsch and G.F. Boudreaux-Bartels, *Linear and Quadratic Time-Frequency Signal Representations*, IEEE Signal Processing Magazine, April 1992, pp. 21-67.

[70] P. J. Loughlin, J. W. Pitton, and L.E. Atlas, *Bilinear Time-Frequency Representations: New Insights and Properties*, IEEE Trans. Signal Processing, Vol. 41, No. 2, Feb. 1993, pp. 750-767.

[71] P. Flandrin, "Maximum Signal Energy Concentration in a Time-Frequency Domain," in *Proc. IEEE 1988 Int. Conf. Acoust., Speech, Signal Processing* (New York, NY), April 11-14, 1988, pp. 2176-2179.

[72] D. L. Jones and T. W. Parks, *A High Resolution Data-Adaptive Time-Frequency Representation*, IEEE Trans. Acoust., Speech, Signal Processing, Vol. 38, No. 12, Dec. 1990, pp. 2127-2135.

[73] D. L. Jones and T. W. Parks, *A Resolution Comparison of Several Time-Frequency Representations*, IEEE Trans. Signal Processing, Vol. 40, No. 2, Feb. 1992, pp. 413-420.

[74] O. Rioul and P. Flandrin, *Time-Scale Energy Distributions: A General Class Extending Wavelet Transforms*, IEEE Trans. Signal Processing, Vol. 40, No. 7, July 1992, pp. 1746-1757.

[75] L.Cohen, *A General Approach for Obtaining Joint Representations in Signal Analysis-Part I: Characteristic Function Operator Method*, IEEE Trans. Signal Processing, Vol. 44, No. 5, May, 1996, pp. 1080-1089.

[76] C. H. M. Turner, *On the Concept of an Instantaneous Spectrum and its relationship to the Autocorrelation*, J. Appl. Phys.,Vol. 25, 1954, pp. 1347-1351.

[77] L. Cohen, *Generalized Phase-Space Distribution Functions*, J. Math. Phys., Vol. 7, No. 5, May 1966, pp. 781-786.

[78] F. Hlawatsch and R. L. Urbanke, *Bilinear Time-Frequency Representations of Signals: The Shift-Scale Invariant Class*, IEEE Trans. Signal Processing, Vol. 42, No.2, Feb. 1994, pp. 357-366.

[79] F. Hlawatsch, *Duality and Classification of Bilinear Time-Frequency Signal Representations*, IEEE Trans. Signal Processing, Vol. 39, No. 7, July 1991, pp. 1564-1574.

[80] L. Cohen, *A General Approach for Obtaining Joint Representations in Signal Analysis - Part II: General Class, Mean and Local Values, and Bandwidth*, IEEE Trans. Signal Processing, Vol. 44, No. 5, May 1996, pp. 1091-1098.

[81] T. A. C. M. Claasen and W. F. G. Mechlenbräker, *The Wigner Distribution - A Tool for Time-Frequency Signal Analysis Part III: Relations with Other Time-Frequency Signal Transformations*, Philips J. Res., Vol. 35, No. 6, 1980, pp. 372-389.

[82] W. J. Williams and J. Jeong, "Reduced Interference Time-Frequency Distributions," in *Time-Frequency Signal Analysis*, B. Boashash, ed., Longman Cheshire, Melbourne, 1992, pp. 74-97.

[83] M. Amin, *Spectral Decomposition of Time-Frequency Distribution Kernels*, IEEE Trans. Signal Processing, Vol. 42, No. 5, May 1994, pp. 1156-1165.

[84] L. Cohen, "What is a Multicomponent Signal?," in *Proc. IEEE 1992 Int. Conf. Acoust. Speech, Signal Processing*, Vol. 5, 1992, pp. 113-116.

[85] H. I. Choi and W.J. Williams, *Improved Time-Frquency Representation of Multicompent Signals using Exponential Kernels*, IEEE Trans. Acoust., Speech, Signal Processing, Vol. 37, June 1989, pp. 861-871.

[86] E. J. Deithorn, *The Generalized Exponential Time-Frequency Distribution*, IEEE Trans. Signal Processing, Vol. 42, No. 5, May 1994, pp. 1028-1037.

[87] Y. Zhao, L. E. Atlas, and R. J. Marks, II, *The Use of Cone-Shaped Kernels for Generalized Time-Frequency Representations of Nonstationary Signals*, IEEE Trans. Acoust., Speech, Signal Processing, Vol. 38, No. 7, July 1990, pp. 1084-1091.

[88] S. Oh and R. J. Marks, II, *Some Properties of the Generalized Time-Frequency Representation with Cone-Shaped Kernel*, IEEE Trans. Signal Processing, Vol. 40, No. 7, July 1992, pp. 1735-1745.

[89] R. N. Czerwinski and D. L. Jones, *An Adaptive Time-Frequency Representation using a Cone-Shaped Kernel*, Proc. IEEE 1993 Int. Conf. Acoust., Speech, Signal Processing, Vol. 4, 1993, pp. 404-407.

[90] J. Jeong and W. J. Williams, *Kernel Design for Reduced Interference Distributions*, IEEE Trans. Signal Processing, Vol. 40, No. 2, Feb. 1992, pp. 402-412.

[91] L. Stanković, *Auto-Term Representation by the Reduced Interference Distributions: A Procedure for Kernel Design*, IEEE Trans. Signal Processing, Vol. 44, No. 6, June 1996, pp. 1557-1563.

[92] Z. Guo, L. Durand, and H. C. Lee, *The Time-Frequency Distributions of Nonstationary Signals Based on a Bessel Kernel*, IEEE Trans. Signal Processing, Vol. 42, No. 7, July 1994, pp. 1700-1707.

[93] R. G. Baranuik and D. L. Jones, *A Signal-Dependent Time-Frequency Representation: Optimal Kernel Design*, IEEE Trans. Signal Processing, Vol . 41, No. 4, April 1993, pp. 1589-1602.

[94] R. G. Baranuik and D. L. Jones, *A Signal-Dependent Time-Frequency Representation: Fast Algorithm for Optimal Kernel Design*, IEEE Trans. Signal Processing, Vol. 42, No. 1, Jan. 1994, pp. 134-145.

[95] G. Jones and B. Boashash, *Generalized Instantaneous Parameters and Window Matching in the Time-Frequency Plane*, IEEE Trans. Signal Processing, Vol. 45, No. 5, May 1997, pp. 1264-1275.

[96] M. G. Amin, G. T. Venkattesan, and J. F. Carroll, *A Constrained Weighted Least Squares Approach for Time-Frequecy Distribution Kernel Design*, IEEE Trans. Signal Processing, Vol. 44, No. 5, May 1996, pp. 1111-1123.

[97] C. H. Page, *Instantaneous Power Spectra*, J. Appl. Phys. , Vol 23, No. 1, Jan., 1952, pp. 103-106.

[98] M. J. Levin, *Instantaneous Spectra and Ambiguity Functions*, IEEE Trans. Information Theory, Vol. IT-10, No. 1, Jan. 1964, pp. 95-97.

[99] A. W. Rihaczek, *Signal Energy Distribution in Time and Frequency*, IEEE Trans. Information Theory, Vol. IT-14, No. 3, May 1968, pp. 369-374.

[100] J. G. Kirkwood, *Quantum Statistics of Almost Classical Ensembles*, Phys. Rev., Vol. 44, 1933, pp. 31-37.

[101] F. Hlawatsch and W. Kozek, *The Wigner Distribution of a Linear Signal Space*, IEEE Trans. Signal Processing, Vol. 41, No. 3, March 1993, pp. 1248-1258.

[102] F. Peyrin and R. Prost, *A Unified Definition for the Discrete-Time, Discrete-Frequency, and Discrete-Time/Frequency Wigner Distributions*, IEEE Trans. Signal Processing, Vol. ASSP-34, No. 4, August 1986, pp. 858-866.

[103] P. M. Woodward, *Probability and Information Theory, with Applications to Radar*, 2nd ed., Pergamon Press, Oxford, 1964.

[104] L. Auslander and R. Tolimieri, *Radar Ambiguity Function and Group Theory*, SIAM J. Math. Anal., Vol. 16, No. 3, May 1985, pp. 577-601.

[105] H. Naparst, *Dense Target Signal Processing*, IEEE Trans. Information Theory, Vol. 37, No. 2, March 1991, pp. 317-327.

[106] L. G. Weiss, *Wavelets and Wideband Correlation Processing*, IEEE Signal Processing Magazine, Jan. 1994, pp. 13-32.

[107] P. Mass, "Wideband Approximation and Wavelet Transform," in *Radar and Sonar, Part* II, Vol. 39, IMA Volumes in Mathematics and its Applications, F. A. Grünbaum, M. Bernfeld, and R. E. Blahut, eds., Springer-Verlag, New York, 1992, pp. 83-88.

[108] P. Moulin, J. A. O'Sullivan and D. L. Snyder, "A Sieve-Constrained Maximum-Likelihood Method for Target Imaging", in *Radar and Sonar, Part* II, Vol.39, IMA Volumes in Mathematics and is Applications, F. G. Grünbaum, M. Bernfeld, and R.E. Blahut, eds., Springer-Verlag, New York, 1992, pp. 95-122.

[109] J. M. Speiser, H. J. Whitehouse, J. C. Allen, "Wideband Time-Frequency Distributions", in *Time-Frequency Signal Analysis*, B. Boashash, ed., Longman Cheshire, 1992, pp. 141-162.

[110] L. K. Montgomery, Jr. and I. S. Reed, *A Generalization of the Gabor-Helstrom Transform*, IEEE Trans. Information Theory, IT-13, April 1967, pp. 344-345.

[111] J. M. Speiser, *Wide-Band Ambiguity Functions*, IEEE Trans. Information Theory, Jan. 1967, pp. 122-123.

[112] R. L. Gassner and G. R. Cooper, *Note on a Generalized Ambiguity Function*, IEEE Trans. Information Theory, Jan. 1967, pp. 126.

[113] L. H. Sibul and E. L. Titlebaum, *Volume Properties for the Wideband Ambiguity Function*, IEEE Trans. Aero. Elect. Systems, Vol. Aes-17, No.1, Jan. 1981. pp. 83-87.

[114] R. Tolimieri and R. S. Orr, *Poisson Summation, Ambiguity Function, and the Theory of Weyl-Heisenberg Frames*, J. Fourier Anal. Appl. Vol. 1, No. 3, 1995, pp. 234-247.

[115] R. De Buda, *An Extension of Green's Condition to Cross-Ambiguity Functions*, IEEE Trans. Information Theory, Vol. IT-13, No. 1, Jan. 1967, pp. 75-81.

[116] J. R. Klauder, *The Design of Radar Signals Having Both High Range Resolution and High Velocity Resolution*, Bell Systems Tech. J., Vol. 39, July 1960, pp. 809-820.

[117] A. Papoulis, *Signal Analysis*, McGraw-Hill, New York, 1977.

[118] L. Auslander and R. Tolimieri, *Characterizing the Radar Ambiguity Functions*, IEEE Trans. Information Theory, Vol. IT-30, No. 6, Nov. 1984, pp. 832-836.

[119] C. E. Cook and M. Bernfeld, *Radar Signals*, Academic Press, New York, 1967.

[120] L. Auslander and R. Tolimieri, *Sampling and Aliasing of the Radar Ambiguity Function*, CUNY, preprint, 1989, pp. 89-91.

[121] R. Tolimieri and S. Winograd, *Computing the Ambiguity Surface*, IEEE Trans. Acoust., Speech, Signal Processing, Vol. ASSP-33, No. 4, Oct. 1985, pp. 1239-1245.

[122] L. Auslander and R. Tolimieri, *Computing Decimated Finite Cross-Ambiguity Functions*, IEEE Trans. Acoust., Speech, Signal Processing, Vol. 36, No. 3, March 1988, pp. 359-363.

[123] A. Kumar, D. R. Fuhrmann, M. Frazier, and B. D. Jawerth, *A New Transform for Time-Frequency Analysis*, IEEE Trans. Signal Processing, Vol. 40, No. 7, July 1992, pp. 1697-1707.

[124] L. B. Almeida, *The Fractional Fourier Transform and Time-Frequency Representations*, IEEE Trans. Signal Processing, Vol. 42, No. 11, Nov. 1994, pp. 3084-3091.

[125] A. J. E. M. Janssen, *Bargmann Transform, Zak Transform, and Coherent States*, J. Math. Phys., Vol. 23, No. 5, May 1982, pp. 720-731.

[126] J. B. Allen and L. R. Rabiner, *A Unified Approach to Short-Time Fourier Analysis and Synthesis*, Proc. IEEE, Vol. 65, No. 11, Nov., 1977, pp. 1558-1564.

[127] M. Boon and J. Zak, *Amplitudes on Von Neumann Lattices*, J. Math. Phys., Vol. 22, No. 5, May 1981, pp. 1090-1099.

[128] I. Daubechies, A. Grossman, and Y. Meyer, *Painless Nonorthogonal Expansions*, J. Math. Phys., Vol. 27, No. 5, May 1986, pp. 1271-1283.

[129] I. Daubechies and A. J. E. M. Janssen, *Two Theorems on Lattice Expansions*, IEEE Trans. Information Theory, Vol. 39, No. 1, Jan. 1993, pp. 3-6.

[130] G. Battle, *Heisenberg Proof of the Balian-Low Theorem*, Lett. Math. Phys., Vol. 15, 1988, pp. 175-177.

[131] I. Daubechies, S. Jaffard, and J. Journè, *A Simple Wilson Orthonormal Basis with Exponential Decay*, SIAM J. Math. Anal., Vol. 22, No. 2, March 1991, pp. 554-572.

[132] L. Auslander and R. Tolimieri, *Abelian Harmonic Analysis, Theta Functions, and Function Algebra on a Nilmanifold*, Springer-Verlag, New York, 1975.

[133] H. Bacry, A. Grossman, and J. Zak, *Proof of Completeness of Lattice States in the kq Representation*, Phys. Rev. B, Vol. 12, No. 4, August, 1975, pp. 1118-1120.

[134] M. Boon, J. Zak, and I. J. Zucker, *Rational Von Neumann Lattices*, J. Math. Phys., Vol. 24, No. 2, Feb. 1983, pp. 316-323.

[135] P. Flandrin, "Wavelets and Related Time-Scale Transforms," in *Advanced Signal-Processing Algorithms, Architectures, and Implementations*, F. T. Luk, ed., Proc. SPIE, Vol. 1348, San Diego, 1990, pp. 2-13.

[136] C. K. Chui, *An Introduction to Wavelets*, Academic Press, New York, 1992.

[137] A. Grossman and J. Morlet, *Decomposition of Hardy Functions into Square Integrable Wavelets of Constant Shape*, SIAM J. Math. Anal., Vol. 15, No. 4, July 1984, pp. 723-736.

[138] O. Rioul and M. Verterli, *Wavelets and Signal Processing*, IEEE Signal Processing Magazine, Oct. 1991, pp. 14-38.

[139] X. Xia and B. W. Bruce, *Vector-Valued Wavelets and Vector Filter Banks*, IEEE Trans. Signal Processing, Vol. 44, No. 3, March 1996, pp. 508-518.

[140] J. Bertrand and P. Bertrand, "Affine Time-Frequency Distributions," in *Time-Frequency Signal Analysis*, B. Boashash, ed., Longman Cheshire, Melbourne, 1992, pp. 118-140.

[141] W. R. Madych, "Some Elementary Properties of Multiresolution Analysis of $L_2(\mathbb{R}^n)$," in *Wavelets – A Tutorial Review in Theory and Application*, C. K. Chui, ed., Academic Press, New York, 1992, pp. 259-294.

[142] S. G. Mallat, *Multiresolution Approximations and Wavelet Orthonormal Bases of* $L_2(\mathbb{R})$, Trans. Amer. Math. Soc., Vol. 315, No. 1, Sept. 1989, pp. 69-87.

[143] S. G. Mallat, *A Theory for Multiresolution Signal Decomposition: The Wavelet Representation*, IEEE Trans. Pattern Anal. Machine Intell., Vol. 11, No. 7, July 1989, pp. 674-693.

[144] O. Rioul, *A Discrete-Time Multiresolution Theory*, IEEE Trans. Signal Processing, Vol. 41, No. 8, Aug. 1993, pp. 2591-2605.

[145] G. Strang, *Wavelets and Dilation Equations: A Brief Introduction*, SIAM Review, Vol. 31, No. 4, Dec. 1989, pp. 614-627.

[146] X. Zhang, L. Tian, and Y. Peng, *From the Wavelet Series to the Discrete Wavelet Transform–The Initialization*, IEEE Trans. Signal Processing, Vol. 44, No. 1, Jan. 1996, pp. 129-133.

[147] P. P. Vaidyanathan, *Multirate Systems and Filter Banks*, Prentice Hall, Englewood Cliffs, 1993.

[148] H. G. Feightinger and K. Gröchenig, "Gabor Wavelets and the Heisenberg Group: Gabor Expansions and the Short-Time Fourier Transform from the Group Theoretic Point of View," in *Wavelets - A Tutorial in Theory and Applications*, C. K. Chui, ed., Academic Press, New York, 1992, pp. 359-397.

[149] A. J. E. M. Janssen, *Weighted Wigner Distributions Vanishing on Lattices*, J. Math. Anal. Appl. , Vol. 80, 1981, pp. 157-167.

[150] M. R. Schoeder and B. S. Atal, *Generalized Short-Time Power Spectra and Autocorrelation Functions*, J. Acoust. Soc. Am., Vol. 34, No. 11, Nov. 1962, pp. 1679-1683.

[151] J. B. Allen, *Short Term Spectral Analysis, Synthesis, and Modification by Discrete Fourier Transform*, IEEE Trans. Acoust., Speech, and Signal Processing, Vol. ASSP-25, No. 3, June 1977, pp. 235-238.

[152] M. R. Portnoff, *Time-Frequency Representation of Digital Signals and Systems Based on Short-Time Fourier Analysis*, IEEE Trans. Acoust., Speech, and Signal Processing, Vol. ASSP-28, No. 1, Feb. 1980, pp. 55-67.

[153] G. Gambardella, *Time Scaling and Short-Time Spectral Analysis*, J. Acoust. Soc. Am., Vol. 44, No. 6, 1968, pp. 1745-1747.

[154] M. J. Bastiaans, *A Sampling Theorem for the Complex Spectrogram, and Gabor's Expansion of a Signal in Gaussian Elementary Signals*, Opt. Eng., Vol. 20, No. 4, July/Aug. 1981, pp. 594-598.

[155] P. B. Yale, *Geometry and Symmetry*, Dover Publications, New York, 1988.

[156] A. K. Brodzik, *The Design of Discrete Gabor Expansion Algorithms and an Efficient Realization of the Gerchberg-Popoulis Algorithm in the Zak Space*, Ph. D. Thesis, The City University of New York, New York, 1995.

[157] J. J. Benedetto, "Gabor Representations and Wavelets," in *Commutative Harmonic Analysis, 1987*, D. Collela, ed., Contemp. Math., Vol. 91, Amer. Math. Soc., Providence, 1989, pp. 9-27.

[158] H. J. Landau and H. O. Pollak, *Prolate Spheroidal Wave Functions, Fourier Analysis and Uncertainty - III: The Dimension of the Space of Essentially Time- and Band-Limited Signals*, Bell Syst. Tech. J., Vol. 413, July 1962, pp. 1295-1336.

[159] S. A. Klein and B. Beutter, *Minimizing and Maximizing the Joint Space-Spatial Frequency Uncertainty of Gabor-Like Functions: Comment*. J. Opt. Soc. Am. A, Vol. 9, No. 2, Feb. 1992, pp. 337-440.

[160] M. Boon and J. Zak, *Coherent States and Lattices Sums*, J. Math. Phys., Vol. 19, No. 11, Nov. 1978, pp. 2308-2311.

[161] M. J. Bastiaans, *Gabor's, Expansion of a Signal into Gaussian Elementary Signals*, Proc. IEEE, Vol. 68, No. 4, April 1980, pp. 538-539.

[162] S. Dharanipragada and K. S. Arun, *Resolution Limits in Signal Recovery*, IEEE Trans. Signal Processing, Vol. 44, No. 3, March 1996, pp. 546-561.

[163] H. J. Landau, *Sampling, Data Transmission, and the Nyquist Rate*, Proc. IEEE, Vol. 55, No. 10, Oct. 1967, pp. 1701-1706.

[164] C. E. Shannon, *Communication in the Presence of Noise*, Proc. IRE, Vol. 37, Jan. 1949, pp. 10-21.

[165] C. E. Shannon, *A Mathematical Theory of Communication*, Bell Syst. Tech. J., Vol. 27, July/Oct., pp. 379-424, 623-657.

[166] A. Guessoum, and R. M. Mersereau, *Fast Algorithms for the Multidimensional Discrete Fourier Transform*, IEEE Trans. Acoust., Speech, Signal Processing, Vol. ASSP-34, No. 4, Aug. 1986, pp. 937-943.

[167] L. Auslander and R. Tolimieri, "On Finite Gabor Expansion of Signals," in *Signal Processing, Part I: Signal Processing Theory*, Springer-Verlag, New York 1990, pp. 13-23.

[168] A. J. E. M. Janssen, *Gabor Representation of Generalized Functions*, J. Math. Anal. Appl., Vol. 83, 1981, pp. 377-394.

[169] H. E. Jensen, T. Hoholdt, and J. Justesen, *Double Series Representation of Bounded Signals*, IEEE Trans. Information Theory, Vol. 34, No. 4, July 1988, pp. 613-624.

[170] N. J. Munch, *Noise Reduction in Tight Weyl-Heisenberg Frames*, IEEE Trans. Information Theory, Vol. 38, No. 2, March 1992, pp. 608-616.

[171] J. Wexler and S. Raz, *Wigner-Space Synthesis of Discrete-Time Periodic Signals*, IEEE Trans. Signal Processing, Vol. 40, No. 8, Aug. 1992, pp. 1997-2006.

[172] X. Xia, *On Characterization of the Optimal Biorthogonal Window Function for Gabor Transform*, IEEE Trans. Signal Processing, Vol. 44, No. 1, Jan. 1996, pp. 133-138.

[173] M. J. Bastiaans, *Gabor's Signal Expansion and Degrees of Freedom of a Signal*, Optica Acta, Vol. 29, No. 9, 1982, pp. 1223-1229.

[174] L. Auslander, C. Buffalano, R. Orr, and R. Tolimieri, "A Comparison of the Gabor and Short-Time Fourier Transforms for Signal Detection and Feature Extraction in Noisy Environments," in *Advanced Signal-Processing Algorithms, Architectures and Implementations*, F. T. Luk, ed., Proc. SPIE, Vol. 1348, San Diego, 1990, pp. 230-240.

[175] A.Weil, *Sur Certains Groupes d'Opérateurs Untaires*, Acta Math., Vol. 111, 1964, pp. 143-211.

[176] J. Zak, "The kq-Representation in the Dynamics of Electrons in Solids," in *Solid State Physics*, H. Ehrenreich, F. Seitz, and D. Turnbull, eds., Academic Press, Vol. 27, New York, 1972, pp. 1-62.

[177] J. W. M. Bergmans and A. J. E. M. Janssen, *Robust Data Equalization, Fractional Tap Spacing and the Zak Transform*, Philips J. Res., Vol. 42, No. 4, 1987, pp. 351-398.

[178] L. Auslander and R. Tolimieri, *Is Computing with the Finite Fourier Transform Pure or Applied Mathematics?*, Bull. Amer. Math. Soc., Vol. 1, No. 6, Nov. 1979, pp. 847-897.

[179] M. An, M. Conner, R. Orr, and R. Tolimieri, *Computation and Meaning of Gabor Coefficients*, CUNY, preprint, 1991.

[180] G. G. Walter, *A Sampling Theorem for Wavelet Subspaces*, IEEE Trans. Information Theory, Vol. 38, No. 2, March 1992, pp. 881-884.

[181] A. J. E. M. Janssen, *The Zak Transform and Sampling Theorems for Wavelet Subspaces*, IEEE Trans. Signal Processing, Vol. 41, No. 12, Dec. 1993, pp. 3360-3364.

[182] I. Gertner and R. Tolimieri, *Multiplicative Zak Transform*, J. Visual Com. Image Rep. Vol. 6, No. 1, March 1995, pp. 89-95.

[183] A. J. E. M. Janssen, *The Zak Transform and Some Counterexamples in Time-Frequency Analysis*, IEEE Trans. Information Theory, Vol. 38, No. 1, Jan. 1992, pp. 168-171.

[184] M. Conner and R. Tolimieri, *Zak Transform as an Adaptive Tool*, CUNY, preprint, 1991.

[185] M. Zibulski and Y. Zeevi, *Oversampling in the Gabor Scheme*, IEEE Trans. Signal Processing, Vol. 41, No. 8, Aug. 1993, pp. 2679-2687.

[186] A. Grossmann, J. Morlet, and T. Paul, *Transforms Associated to Square Integrable Group Representations* I , J. Math. Phys., Vol. 26, No. 10, Oct. 1985, pp. 2473-2479.

[187] B. Torrèsani, *Wavelets Associated with Representation on the Affine Weyl-Heisenberg Group*, J. Math. Phys. Vol. 32, No. 5, May 1991, pp. 1273-1279.

[188] E. W. Aslaksen and J. R. Klauder, *Continuous Representation Theory Using Affine Group*, J. Math. Phys., Vol. 10, No. 12, Dec. 1969, pp. 2267-2275.

[189] Y. M. Kadah and A. H. Tewfik, *Efficient Design of Ultrasound True-Velocity Flow Mapping*, IEEE Eng. Medicine and Biology Magazine, Vol. 15, No. 5, Sept./Oct. 1996, pp. 118-125.

[190] S. Haykin and T. K. Bhattacharya, *Modular Learning Strategy for Signal Detection in a Nonstationary Environment*, IEEE Trans. Signal Processing, Vol. 45, No. 6, June 1997, pp. 1619-1637.

[191] B. Boashash and P. O'Shea, *A Methodology for Detection and Classification of Underwater Acoustic Signals Using Time-Frequency Analysis Techniques*, IEEE Trans. Acoust., Speech, and Signal Processing, Vol. 38, No. 11, Nov. 1990, pp. 1829-1841.

[192] D. B. Malkoff, "Detection and Classification By Neural Networks and Time-Frequency Distributions," in *Time-Frequency Signal Analysis*, B. Boashash, ed., Longman Cheshire, Melbourne, 1992, pp. 324-348.

[193] R. A. Altes, *Detection, Estimation, and Classification with Spectrograms*, J. Acoust. Soc. Am., Vol. 67, 1980, pp. 1232-1246.

[194] M. G. Amin, *Interference Mitigation in Spread Spectrum Communication Systems Using Time-Frequency Distributions*, IEEE Trans. Signal Processing, Vol. 45, No. 1, Jan. 1997, pp. 90-101.

[195] B. Zhang and S. Sato, *A Time-Frequency Distribution of Cohen's Class with a Compound Kernel and its Application to Speech Signal Processing*, IEEE Trans. Signal Processing, Vol. 42, No. 1, Jan. 1994, pp. 54-64.

[196] L. E. Atlas, P. J. Loughlin, and J. W. Pitton, "Signal Analysis with Cone Kernel Time-Frequency Distributions and their Application to Speech," in *Time-Frequency Signal Analysis*, B. Boashash, ed., Longman Cheshire, Melbourne, 1992, pp. 375-387.

[197] R. J. Sclabassi, M. Sun, D. N. Krieger, P. Jasiukaitis, and M. S. Scher, "Time-Frequency Domain Problems in the Neurosciences," in *Time-Fequency Signal Analysis*, B. Boashash, ed., Longman Cheshire, Melbourne, 1992, pp. 498-543.

[198] P. Bonato, G. Gagliati, and M. Knaflitz, *Analysis of Myoelectric Signals Recorded During Dynamic Contractions*, IEEE Eng. Medicine and Biology, Nov./Dec. 1996, pp. 102-111.

[199] W. J. Williams, H. P. Zaveri, and J. C. Sackellares, *Time-Frequency Analysis of Electrophysiology Signals in Epilepsy*, IEEE Eng. Medicine and Biology, March/April 1995, pp. 133-143.

[200] V. X. Afonso and W. J. Tompkins, *Detecting Ventricular Fibrillation: Selecting the Appropriate Time-Frequency Analysis Tool for the Application*, IEEE Eng. Medicine and Biology, March/April 1995, pp. 152-159.

[201] J. C. Wood, A. J. Buda, and D.T. Barry, *Time-Frequency Transforms: A New Approach to First Heart Sound Frequency Analysis*, IEEE Trans. Biomedical Eng., Vol. 38, 1992, pp. 728-739.

[202] G. Cristobal, J. Bescos, and J. Santamaria, *Image Analysis Through the Wigner Distribution Function*, Appl. Opt., Vol. 28, No. 2, Jan. 1989, pp. 262-271.

[203] D. M. Healy, Jr. and J. B. Weaver, *Two Applications of Wavelet Transforms in Magnetic Resonance Imaging*, IEEE Trans. Information Theory, Vol. 38, No. 2, March 1992, pp. 840-860.

[204] W. B. Richardson, Jr., *Applying Wavelets to Mammograms*, IEEE Eng. Medicine and Biology, Sept./Oct. 1995, pp. 551-560.

[205] N. A. Whitmal, J. C. Rutledge, and J. Cohen, *Reducing Correlated Noise in Digital Hearing Aids: A Wavelet-Based Method for Extracting Speech from Background Noise*, IEEE Eng. Medicine and Biology, Sept./Oct. 1996, pp. 88-95.

[206] S. H. Park, W. H. Kwon, O. K. Kwon, and M. Kim, *Short-Time Fourier Analysis via Optimal Harmonic FIR Filters*, IEEE Trans. Signal Processing, Vol. 45, No. 6, June 1997, pp. 1535-1542.

[207] R. R. Bitmead, A. C. Tsoi, and P. J. Parker, *A Kalman Filtering Approach to Short-Time Fourier Analysis*, IEEE Trans. Acoust., Speech, Signal Processing, Vol. ASSP-34, No. 6, Dec. 1986, pp. 1493-1501.

[208] J. S. Lim, *Enhancement and Bandwidth Compression of Noisy Speech*, Proc. IEEE, Vol. 67, Dec. 1979, pp. 1586-1604.

[209] S. Mallat and W. L. Hwang, *Singularity Detection and Processing with Wavelets*, IEEE Trans. Information Theory, Vol. 38, No. 2, March 1992, pp. 617-643.

[210] T. Kalayci and Ö. Özdamar, *Wavelet Preprocessing for Automated Neural Network Detection of EEG Spikes*, IEEE Eng. Medicine and Biology, March/April 1995, pp. 160-166.

[211] J. M. Moser, and J. I. Aunon, *Classification and Detection of Single Evoked Brain Potentials Using Time-Frequency Amplitude Features,* IEEE Trans. Biomedical Eng., Vol. 33, Dec. 1986, pp.1096-1106.

[212] L. R. Rabiner and R. W. Schafer, *Digital Processing of Speech Signals*, Prentice-Hall, Englewood Cliffs, 1978.

[213] M. R. Portnoff, *Short-Time Fourier Analysis of Sampled Speech*, IEEE Trans. Acoust., Speech, Signal Processing, Vol. 29, June 1981, pp. 364-373.

[214] G. Evangelista, *The Coding Gain of Multiplexed Wavelet Transform*, IEEE Trans. Signal Processing, Vol. 44, No. 7, July 1997, pp. 1681-1692.

[215] R. E. Crochiere and L. R. Rabiner, *Multirate Digital Signal Processing*, Prentice-Hall, Englewood Cliffs, 1983.

[216] A. Lewis and G. Knowles, *Image Compression Using 2-D Wavelet Transform*, IEEE Trans. Image Processing, Vol. 1, 1992, pp. 244-250.

[217] R. A. Devore, B. Jawerth, and B. J. Lucier, *Image Compression Through Wavelet Transform Coding*, IEEE Trans. Information Theory, Vol. 38, No. 2, March 1992, pp. 719-746.

[218] M. Akay, *Wavelet Applications in Medicine*, IEEE Spectrum, May 1997, pp. 50-56.

[219] U. Wiklund, M. Akay, and U. Niklasson, *Short-Term Analysis of Heart-Rate Variability by Adapted Wavelet Transforms*, IEEE Eng. Medicine and Biology, Sept./Oct. 1997, pp. 113-118, pp. 138.

[220] A. Figliola and E. Serrano, *Analysis of Physiological Time Series Using Wavelet Transforms*, IEEE Eng. Medicine and Biology, May/June 1997, pp. 74-79.

[221] H. Dickhaus and H. Heinrich, *Classifying Biosignals with Wavelet Networks: A Method of Noninvasive Diagnosis,* IEEE Eng. Medicine and Biology, Sept./Oct. 1996, pp. 103-111.

[222] C. He and J. M. F. Moura, *Robust Detection with the Gap Metric*, IEEE Trans. Signal Processing, Vol. 45, No. 6, June 1997, pp. 1591-1604.

[223] N. Lee and S. C Schwartz, *Robust Transient Signal Detection Using the Oversampled Gabor Representation*, IEEE Trans. Signal Processing, Vol. 43, June 1995, pp. 1498-1502.

[224] B. Friedlander and B. Porat, *Detection of Transient Signals by the Gabor Representation*, IEEE Trans. Acoust., Speech, Signal Processing, Vol. 37, Feb. 1989, pp. 169-180.

[225] B. Friedlander and A. Zeira, *Oversampled Gabor Representation for Transient Signals*, IEEE Trans. Signal Processing, Vol. 43, Sept. 1995, pp. 2088-2094.

[226] A. C. Bovik, N. Gopal, T. Emmoth, and A. Restrepo, *Localized Measurement of Emergent Image Frequencies By Gabor Wavelets*, IEEE Trans. Information Theory, Vol. 38, March 1992, pp. 691-712.

[227] J. G. Daugman, *Complete Discrete 2-D Gabor Transforms by Neural Networks for Image Analysis and Compression*, IEEE Trans. Acoust., Speech, Signal Processing, Vol. ASSP-36, 1988, pp. 1169-1179.

[228] M. Porat and Y. Zeevi, *Localized Texture Processing in Vision: Analysis and Synthesis in the Gaborian Space*, IEEE Trans. Biomedical Eng., Vol. 36, Jan. 1989, pp. 115-129.

[229] M. Porat and Y. Zeevi, *The Generalized Gabor Scheme of Image Representation in Biological and Machine Vision*, IEEE Trans. Pattern Anal. Machine Intell., Vol. 10, July 1988, pp. 452-468.

[230] S. Blanco, S. Kochen, O. A. Rosso, and P. Salgado, *Applying Time-Frequency Analysis to Seizure EEG Activity: A Method to Help Identify the Source of Epileptic Seizures*, IEEE Eng. Medicine and Biology, Jan./Feb. 1997, pp. 64-71.

[231] H. J. Landau, *On the Density of Phase-Space Expansions*, IEEE Trans. Information Theory, Vol. 39, No. 4, July 1993, pp. 1152-1156.

[232] E. I. Jury, *Theory and Application of the z-Transform Method*, John Wiley & Sons, New York, 1964.

[233] A. V. Oppenheim and D. H. Johnson, *Discrete Representation of Signals*, Proc. IEEE, Vol. 60, No. 6, June 1972, pp.681-691.

[234] R. W. Keyes, *Fundamental Limits in Digital Information Processing*, Proc. IEEE, Vol. 69, No. 2, Feb. 1981, pp. 267-278.

[235] S. Pei and M. Yeh, *An Introduction to Discrete Frames*, IEEE Signal Processing Magazine, Nov. 1997, pp. 84-95.

[236] J. M. Morris and Y. Lu, *Discrete Gabor Expansion of Discrete-Time Signals in* $l_2(Z)$ *via Frame Theory*, Signal Processing, Vol. 40, Nov. 1994, pp. 155-181.

[237] M. Zibulski and Y. Y. Zeevi, *Frame Analysis of the Discrete Gabor-Scheme*, IEEE Trans. Signal Processing Vol. 42, No. 4, April 1994, pp. 942-945.

[238] J. M. Morris and Y. Lu, *Generalized Gabor Expansions of Discrete-Time Signals in* $l_2(Z)$ *via Biorthogonal-Like Sequences*, IEEE Trans. Signal Processing, Vol. 44, No. 6, June 1996, pp. 1378-1391.

[239] J. M. Morris and H. Xie, *Fast Algorithms for Generalized Discrete Gabor Expansion*, Signal Processing, Vol. 39, Sept. 1993, pp.317-331.

[240] A. Brodzik and R. Tolimieri, *Generalized Biorthogonal Method for Computing Gabor Coefficients*, CUNY, preprint, 1995.

[241] D. F. Stewart, L. C. Potter, and S. C. Ahalt, *Computationally Attractive Real Gabor Transforms*, IEEE Trans. Signal Processing, Vol. 43, No. 1, Jan. 1995, pp. 77-84.

[242] S. Qian and D. Chen, *Discrete Gabor Transform*, IEEE Trans. Signal Processing, Vol. 41, No. 7, July 1993, pp. 2429-2438.

[243] J. Wexler and S. Raz, *Discrete Gabor Expansions*, Signal Processing, Vol. 21, Nov. 1990, pp. 207-220.

[244] P. Prinz, *Calculating the Dual Gabor Window for General Sampling Sets*, IEEE Trans. Signal Processing ,Vol. 44, No. 8, Aug. 1996, pp. 2078-2082.

[245] S. Qui and H. G. Feichtinger, *Discrete Structures and Optimal Representations*, IEEE Trans. Signal Processing, Vol. 43, No. 10, Oct. 1995, pp. 2258-2268.

[246] T. Strohmer, "Numerical Algorithms for Discrete Gabor Expansions," in *Gabor Analysis and Algorithms*, H. G. Feichtinger and T. Strohmer, eds., Birkhäuser (in press), Boston, 1997, Chapter 8, pp. 1-33.

[247] R. E. Crochiere and L. R. Rabiner, *Interpolation and Decimation of Digital Signals - A Tutorial Review*, Proc. IEEE, Vol. 69, No. 3, March 1981, pp. 300-331.

[248] H. Murakami, *Sampling Rate Conversion Systems Using a New Generalized Form of the Discrete Fourier Transform*, IEEE Trans. Signal Processing, Vol. 43, No. 9, Sept. 1995, pp. 2095-2102.

[249] M. G. Bellanger, G. Bonnerot, and M. Coudreuse, *Digital Filtering by Polyphase Network: Application to Sample-Rate Alteration and Filter Banks*, IEEE Trans. Acoust., Speech, Signal Processing, Vol. ASSP-24, No. 2, April 1976, pp. 109-114.

[250] H. Bölcskei, F. Hlawatsch, and H. G. Feichtinger, "Equivalence of DFT Filter banks and Gabor Expansions," in *Wavelet Applications in Signal and Image Processing* III, *Part* I, Proc. SPIE, Vol. 2569, San Diego, July 1995, pp. 128-139.

[251] Z. Cvetković and M. Vettterli, *Tight Weyl-Heisenberg Frames in* $l_2(Z)$, IEEE Trans. Signal Processing, Vol. 46, No. 5, May 1999, pp. 1256-1259.

[252] L. Auslander, I. Gertner, and R. Tolimieri, "The Finite Zak Transform and Finite Fourier Transform," in *Radar and Sonar, Part* II, Vol. 39, IMA Volumes in Mathematics and its Applications, F. A. Grünbaum, M. Bernfeld, and R.E. Blahut, eds., Springer-Verlag, New York, 1992, pp. 21-35.

[253] C. Heil, *A Discrete Zak Transform*, Tech. Rep. MTR-89W00128, Mitre Corp., Danvers, 1989, pp. 1-13.

[254] H. Bölcskei and F. Hlawatsch, *Discrete Zak transforms, Polyphase Transforms, and Applications*, IEEE Trans. Signal Processing, Vol. 45, No. 4, April 1997, pp. 851-866.

[255] Y. Y. Zeevi and I. Gertner, *The Finite Zak Transform: An Efficient Tool for Image Representation and Analysis*, J. Visual Commun. Image Represent., Vol. 3, No. 1, March 1992, pp. 13-23.

[256] S. Pei and M. Yeh, *Time and Frequency Split Zak Transform for Finite Gabor Expansion*, Signal Processing, Vol. 52, 1996, pp. 323-341.

[257] M. J. Bastiaans and M. C. W. Geilen, *On the Discrete Gabor Transform and the Discrete Zak Transform*, Signal Processing, Vol. 49, 1996, pp. 151-166.

[258] R. S. Orr, *The Order of Computation for Finite Discrete Gabor Transforms*, IEEE Trans. Signal Processing, Vol. 41, No. 1, Jan. 1993, pp. 122-130.

[259] R. S. Orr, *Derivation of the Finite Discrete Gabor Transform*, Signal Processing, Vol. 34, Oct. 1993, pp. 86-97.

[260] M. J. Bastiaans, *On the Sliding Window Representation in Digital Signal Processing*, IEEE Trans. Acoust., Speech, Signal Processing, Vol. ASSP-33, No. 4, Aug. 1985, pp. 868-873.

[261] A. J. E. M. Janssen, *On Rationally Oversampled Weyl-Heisenberg Frames*, Signal Processing, Vol. 47, 1995, pp. 239-245.

[262] L. Auslander, M. An, M. Conner, I. Gertner, and R. Tolimieri, "Fine Structure of the Classical Gabor Approximation," in *Radar and Sonar, Part II*, Vol. 39, IMA Volumes in Mathematics and its Applications, F. A. Grünbaum, M. Bernfeld, and R. E. Blahut, eds., Springer-Verlag, New York, 1992, pp. 11-20.

[263] J. R. O'Hair and B. W. Suter, *The Zak Transform and Decimated Time-Frequency Distributions*, IEEE Trans. Signal Processing, Vol. 44, No. 5, May 1996, pp. 1099-1110.

[264] N. Polyak and W. A. Pearlman, *Filters and Filter Banks for Periodic Signals, the Zak Transform, and Fast Wavelet Decomposition*, IEEE Trans. Signal Processing, Vol. 46, No. 4, April 1998, pp. 857-873.

[265] J. W. Cooley and J. W. Tukey, *An algorithm for Machine Computation of Complex Fourier Series,* Math. Computation, Vol. 19, April 1965, pp. 297-301.

[266] L. Auslander and F. A. Grünbaum, *The Fourier Transform and the Discrete Fourier Transform*, Inverse Problems, Vol. 5, 1989, pp. 149-164.

[267] M. An, C. Lu, and R. Tolimieri, *Weyl-Heisenberg Systems and the Finite Zak Transform*, Submitted for publication.

[268] W. T. Cochran et al, *What is Fast Fourier Transform?,* Proc. IEEE, Vol. 55, Oct. 1967, pp. 1664-1674.

[269] J. R. Deller, Jr., *Tom, Dick, and Mary Discover the DFT,* IEEE Signal Processing Magazine, April 1994, pp. 36-50.

[270] B. P. Lathi, *Linear Systems and Signals,* Cambridge Press, Berkeley, 1992.

[271] A. Jerri, *The Shannon Sampling Theorem—Its Various Extensions and Applications: A Tutorial Review,* Proc. IEEE, Vol. 65, Nov. 1977, pp. 1565-1596.

[272] P. L. Butzer and R. L. Stens, *Sampling Theory for not Neceassarily Band-Limited Functions: A Historical Overview,* SIAM Review, Vol. 34, No. 1, March, 1992, pp. 40-53.

[273] R. J. Marks II, *Introduction to Shannon Sampling and Interpolation Theory,* Springer-Verlag, New York, 1991.

[274] G. M. Swisher, *Introduction to Linear Systems Analysis,* Matrix Publishers, Cleveland, 1976.

[275] G. Bachman, *Elements of Abstract Harmonic Analysis,* Academic Press, New York, 1964.

[276] C. E. Reid and T. B. Passin, *Signal Processing in C,* John Wiley & Sons, New York, 1992.

[277] R. Strichhartz, *A Guide to Distribution Theory and Fourier Transforms,* CRC Press, Boca Raton, 1994.

[278] J. J. Benedetto, *Harmonic Analysis and Applications,* CRC Press, Boca Raton, 1996.

[279] G. P. Tolstov, *Fourier Series,* Translated by R. A. Silverman, Dover Publications, New York, 1976.

[280] A. Papoulis, *The Fourier Integral and Its Applications,* McGraw-Hill, New York, 1962.

[281] J. S. Walker, *Fourier Analysis,* Oxford University Press, Oxford, 1988.

[282] Y. Katznelson, *An Introduction to Harmonic Analysis,* Dover Publications, New York, 1976.

[283] W. Ruden, *Functional Analysis,* 2nd ed., McGraw-Hill, New York, 1991.

[284] H. J. Landau, *Extrapolating a Band-Limited Function from its Samples in a Finite Interval,* IEEE Trans. Information Theory, Vol. IT-32, No. 4, July 1986, pp. 464-470.

[285] P. W. Berg and J. L. McGregor, *Elementary Partial Differential Equations,* Holden-Day, Oakland, 1966.

[286] R. V. Kadison and J. R. Ringrose, *Fundamentals of the Theory of Operator Algebra: Volume I, Elementary Theory*, Academic Press, New York, 1983.

[287] J. W. Cooley et al, *The Fast Fourier Transform and its Applications*, IEEE Trans. Education, Vol. 12, No. 1, March 1969, pp. 27-34.

[288] G. D. Bergland, *A Guided Tour of the Fast Fourier Transform*, IEEE Spectrum, July 1969, pp. 41-51.

[289] P. Kraniauskas, *A Plain Man's Guide to the FFT*, IEEE Signal Processing Magazine, April 1994, pp. 24-35.

[290] S. Winograd, *On Computing the Discrete Fourier Transform*, Math. Comput., Vol 32, No. 141, Jan. 1978, pp. 175-199.

[291] A. K. Jain, *Image Data Compression: Review*, Proc. IEEE, Vol. 69, No. 3, March 1981, pp.349-391.

[292] J. A. Cadzow, *Signal Enhancement — A Composite Property Mapping Algorithm*, IEEE Trans. Acoust. Speech, Signal Processing, Vol. 36, No. 1, Jan. 1988, pp. 49-62.

[293] B. Friedlander and B. Porat, *Adaptive Detection of Transient Signals*, IEEE Trans. Acoust. Speech, Signal Processing, Vol. ASSP-34, No. 6, Dec. 1986, pp. 1410-1418.

[294] B.Friedlander and B. Porat, *Performance Analysis of a Class of Transient Detection Algorithms — A Unified Framework*, IEEE Trans. Signal Processing, Vol. 40, No. 10, Oct. 1992, pp. 2536-2546.

[295] N. Lee and S. C. Schwartz, *Robust Transient Signal Detection Using the Oversampled Gabor Representation*, IEEE Trans. Signal Processing, Vol. 43, No. 6, June 1995, pp. 1498-1502.

[296] B. Friedlander and B. Porat, *Performance Analysis of Transient Detectors Based on a Class of Linear Data Transforms,* IEEE Trans. Information Theory, Vol. 38, No. 2, March 1992, pp. 665-673.

[297] S. Qui, *The Undersampled Discrete Gabor Transform*, IEEE Trans. Signal Processing, Vol. 46, No. 5, May 1998, pp. 1221-1227.

[298] N. Polyak and W. A. Pearlman, *Orthogonalization of Circular Stationary vector Sequences and its Application to the Gabor Decomposition*, IEEE Trans. Signal Processing, Vol. 43, No. 8, Aug. 1995, pp. 1778-1789.

[299] M. Zibulski and Y. Y. Zeevi, *Discrete Multiwindow Gabor-Type Transforms* IEEE Trans. Signal Processing, Vol. 45, No. 6, June 1997, pp.1428-1442.

[300] M. An and R. Tolimieri, *Time-Frequency Representations*, Birkhaüser, Boston, 1997.

IMAGE EVALUATION TEST TARGET (QA-3)

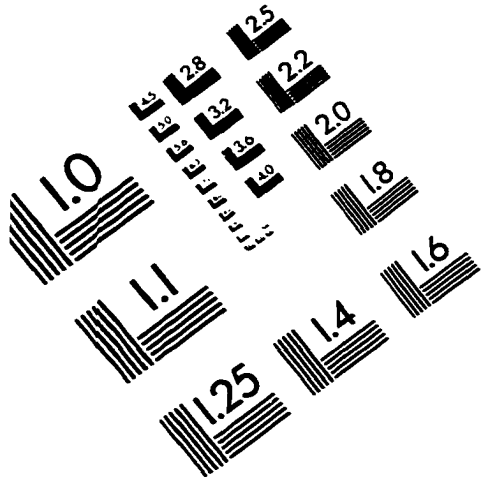

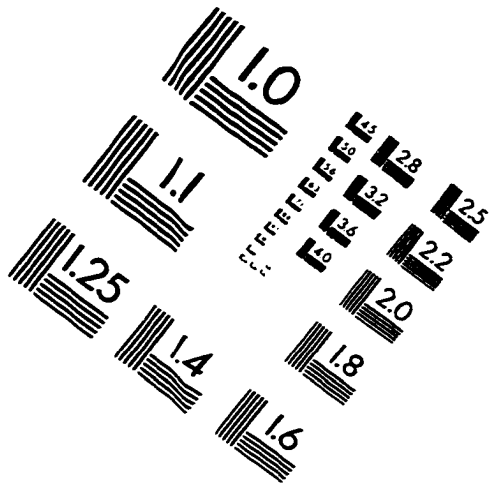

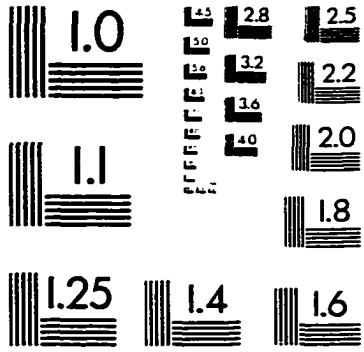

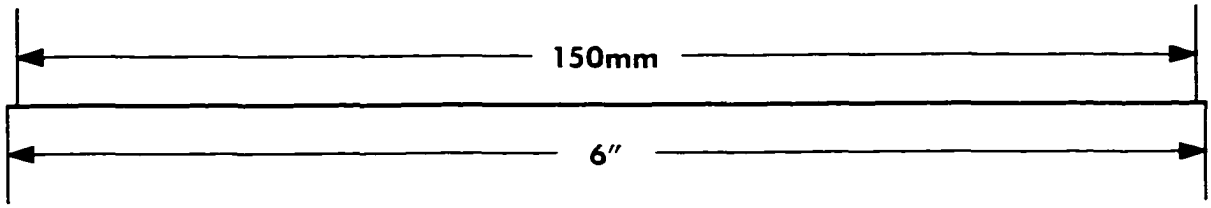

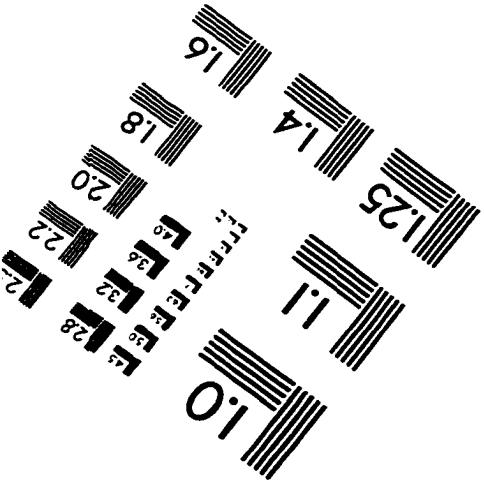

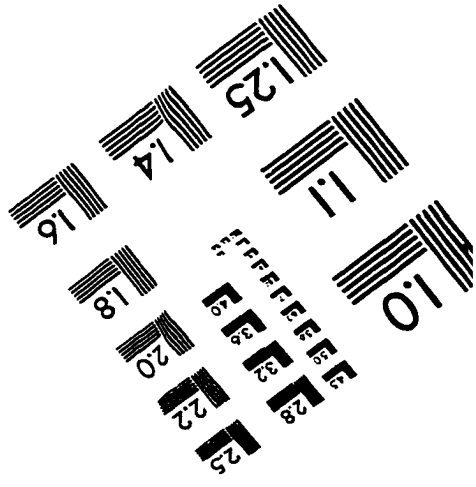

APPLIED IMAGE, Inc
1653 East Main Street
Rochester, NY 14609 USA
Phone: 716/482-0300
Fax: 716/288-5989